Effectiveness of pavement preservation treatments on the structural health of the pavement

by

Md Towhid Ur Rahman

A thesis submitted to the Graduate Faculty of
Auburn University
in partial fulfilment of the
requirements for the Degree of
Masters of Science

Auburn, Alabama
November 18, 2019

Keywords: pavement, preservation, NDT,
falling weight deflectometer

Approved by

Adriana Vargas- Nordcbeck, Chair, Assistant Research Professor, NCAT
David H. Timm, Brasfield and Gorrie Professor, Dept of Civil Engineering
Michael A. Heitzman, Assistant Director, NCAT

ABSTRACT

Pavement preservation treatments are widely applied for surface condition restoration based on different purposes and extent of surface damage. No significant study has been executed on if the preservation treatments provide structural benefits to the pavement layers. There is also remaining scope to investigate if the treatments help the long life of pavement structure, the life extension benefit has not yet been quantified. NCAT at Auburn University has low volume pavement preservation sections at Lee Road 159. At that test location, there are 23 treated sections along with two control sections constructed back in 2012. Along with other surface condition testing, falling weight deflectometer (FWD) deflections are being collected periodically over the years in service. The treatments were subdivided in groups based on the categorical type of the treatments. The center deflections, base damage index, base curvature index, area under pavement profile, backcalculated layer moduli, and required overlay thickness were calculated based on the deflection values over the deflection basin. Statistical and numerical analysis have been performed to investigate if the treatments are providing structural benefits to the pavement layers and the expected extension of life is being predicted from the structural health condition indices mentioned above. In the summary, the study focuses to investigate if the treatments impose any structural benefit to the pavement and how much benefit it can reach to the pavement over the years of service. It was observed from the results that, the preservation treatments are helping to maintain structural soundness of the pavement depending on the type and extent of the treatment application.

ACKNOWLEDGEMENT

The author would extend his thanks to the persons who believed in his ability and extended help to make the work possible. The committee chair and graduate advisor -Dr Adriana Vargas has offered her knowledge and directions to make the study reach to a position where it can be defended. Her mentoring and support made the work more of enjoyment rather than professional liabilities.

The author would thank all the fellow colleagues, professors, engineers and stuffs at National Center for Asphalt Technology (NCAT) who were always there with beautiful smiles with words of hope. Their dedicated and thoughtful inputs made the work more sensible and reliable.

I would love to dedicate my thesis to my parents (Mr. and Mrs. Rahman) and my sister Farhana- who have been missing me in the dinner table for last few years but always supported me with smiling face. I would also thank my friends at Auburn University who always cheered me up and didn't let slow down.

TABLE OF CONTENTS

LIST OF TABLES

LIST OF FIGURES

1 INTRODUCTION

1.1 Background

Pavement surface and underlying layers deteriorate with the wheel surface abrasion action, wheel load and natural forces. If the underlying layers deteriorate, the damage cannot be seen over the surface. Different types of testing can be performed to assess the health of the pavement and measure the damage due to repeated loading or seasonal effects. There are two major types for the testing of pavements: destructive and non-destructive. Destructive testing provides more accurate in-situ condition of the pavement by extracting the cores from the pavement structures, it is not always possible to perform because it may disturb the integrity of the pavement. As an alternative, several non-destructive testing (NDT) methods are available to assess the structural condition of the pavement. Based on the NDT results, specially the falling weight deflectometer deflections, some mechanistic response of the pavement layers can be calculated which can be used to predict the life of pavement. Falling weight deflectometer (FWD) is one of the widely used NDT technologies now a days. There are some established parameters to measure the geometry of the deflection basin created by the impulse loading of FWD load plate. These parameters are deflection basin parameters (DBP).

1.2 Objectives

The objectives of the study were to:

1) Assess the effect of pavement preservation treatments on the structural health of the pavement.

2) Perform a comparative assessment of structural health condition of different pavement layers from different treatment sections in comparison with the untreated "Control" section.
3) Perform a statistical and graphical analysis of the deflection basin parameters as a representation of the structural health of different pavement layers.
4) Estimate the structural requirement of the treated sections based on the required overlay thicknesses.

1.3 Scope of the study

The data and observations presented in this study are part of the National Center for Asphalt Technology (NCAT) Pavement Preservation Group (PG) Study. This research effort is funded by multiple State Departments of Transportation (DOTs), the Federal Highway Administration (FHWA) and the Foundation for Pavement Preservation (FP2 Inc.) and aims at determining the life-extending benefit of various pavement preservation treatments under varying conditions. This thesis focuses on the sections located in a low traffic volume test site in Auburn, Alabama, where treatments have been in service for approximately seven years.

Among other performance indicators, falling weight deflectometer (FWD) testing was performed on a monthly basis to evaluate the structural condition of the pavement. To evaluate the accuracy of the calculated DBPs, the values were compared to the parameters used for the evaluation of the surface condition. For all the comparisons, one of the untreated sections on the test location was chosen as "Control" section.

1.4 Organization of Thesis

The thesis is organized into five chapters. Chapter 2 focuses on the literature review to provide enough background for the present study. Chapter 3 presents the methodology adopted for the present study based on the findings and knowledge base from Chapter 2. Chapter 4 discusses the results of the study and is subdivided based on the type of DBP being graphically compared, statistically analyzed and forecasted. Chapter 5 summarizes the findings from Chapter 4 and provides recommendations for future investigations.

2 LITERATURE REVIEW

This literature review covers the studies aiming to relate the DBPs to the structural condition of the pavement. Pavements over a life cycle go through several minor and major maintenance and rehabilitation activities to restore the pavement condition and rideability. There are several maintenance treatments which can be considered as preservation practices, such as fog seals, slurry seals, chip seals, cape seals, scrub seals, micro surfacing, thinlays etc. The literature review chapter will also cover information on the effectiveness of different preservation techniques. The outcome will be covering the necessary background to perform a study to investigate the effect of pavement preservation treatments over the deflection basin parameters.

2.1 Non-destructive Testing of Pavement: Falling Weight Deflectometer Method

Over the years of pavement research starting from the WASHO Road Test (Highway Research Board, 1954), different methods of measurement have been introduced to measure the surface deflection of pavement tested under measured surface loads. At the point of contact between load plate and pavement surface, the measured deflection is maximum and the depression over the surrounding surface due to the load is called deflection basin. The deflection dissipates with the increase of radial distance from the center unless the pavement layer is too weak to experience permanent deformation due to impact. The mechanics and material characteristics on the underlying layers can be predicted and backcalculated measuring the deflections at regular radial distances from the point of contact (Smith et al. 2017). The diagram shown in **Figure 2-1** is the simplified demonstration of the deflection basin due to loading at

pavement surface. As flexible pavements deflect more under impacts, the deflection basin is a very useful component of non-destructive testing (NDT) of flexible pavements.

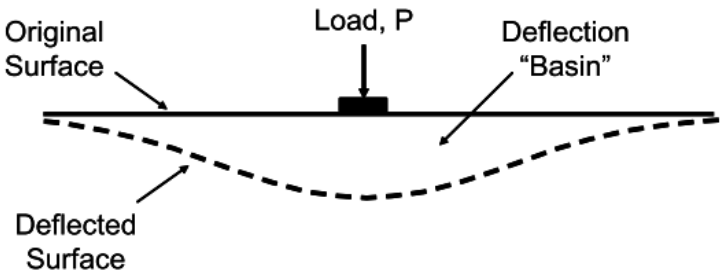

Figure 2-1: Typical pavement Deflection Basin subjected to loading (Smith et al. 2017)

Different agencies and researchers suggested different methods to adopt based on the type and frequency of loading on the pavement surface. They can be broadly classified as: static loading, steady-state loading and impulse loading (Smith et al. 2017). In the early stage of development of the concept of deflection basin, deflection could be measured at a single point under load. With the development of concepts, devices capable to vibrate i.e.- Dynaflect and Road Raters were introduced. These vibrating devices also could provide measured deflection not only on center but also some fixed radial distances from the load. Deflection basin parameters are measured for structural integrity assessment, proper relation with critical response of pavement and in-situ layer strength characteristics measurement (Hossain & Zaniewski, 1991). The Benkelman beam is one of the pioneering devices used for measuring the deflection basin. This device is portable, and the working principal is simple- the lever arm action. The measurement device has a tip which is placed between dual tires of a single axle truck (axle load 18,000 lb.) which remains in contact with the deflected pavement surface. As the vehicle moves, the pavement surface starts to rebound. The deflection of the pavement surface during the loaded condition is then measured. The truck tires are inflated to a tire pressure ranging between 70-80

psi. Despite being inexpensive, the method was eliminated because of the labor and time-consuming procedure. Moreover, the Benkelman beam could only measure a single deflection (the maximum) under the tire loading.

For steady-state loading, a constant vibration is applied to the pavement surface at the point of contact. This method is well accepted and accurate for thinner pavements. Impulse loading is the mostly used method of deflection measurement over the pavement surface due to its capability to capture the deflection basin around the point of contact between load plate and pavement surface (Smith et al. 2017). The impulse loading is the most suitable one to simulate the high volume, high-speed vehicle stream. It is important to note that all the measured deflections from any measuring device need to be temperature corrected. As the loading plate is in contact with the surface of the pavement, the viscoelastic effect can be a prominent source of erroneous prediction if the temperature is not recorded and defections are not corrected. **Figure 2-2** shows the steady-state loading deflection measuring equipment by Dynatest. In this device the load is applied on the loading plate at a sinusoidal pattern. The deflection measuring geophones measure the deflections.

Figure 2-2: Dynaflect (Rijkswaterstaat, 2017)

Falling Weight Deflectometer (FWD) as a means of non-destructive testing (NDT) is adopted by many agencies and researchers for its portability and accuracy to characterize the pavement responses. From the deflections recorded from this test, many condition parameters i.e.- stress, strains, layer moduli, remaining life, equivalent structural numbers etc. can be calculated and predicted. Many studies have been performed on the following topics: prediction of distresses, remaining life of pavement, strength estimation, pavement condition indicators, stress-strains at each layer of pavement and incorporation to mechanistic-empirical (ME) design (Hossain & Zaniewski, 1991). Several mathematical models are developed using deflection basin parameters (DBPs) by means of finite element (FE) modeling and artificial neural network (ANN) based interfaces. **Figure 2-3** is the schematic of the measurement and instrumentations associated with FWD non-destructive testing.

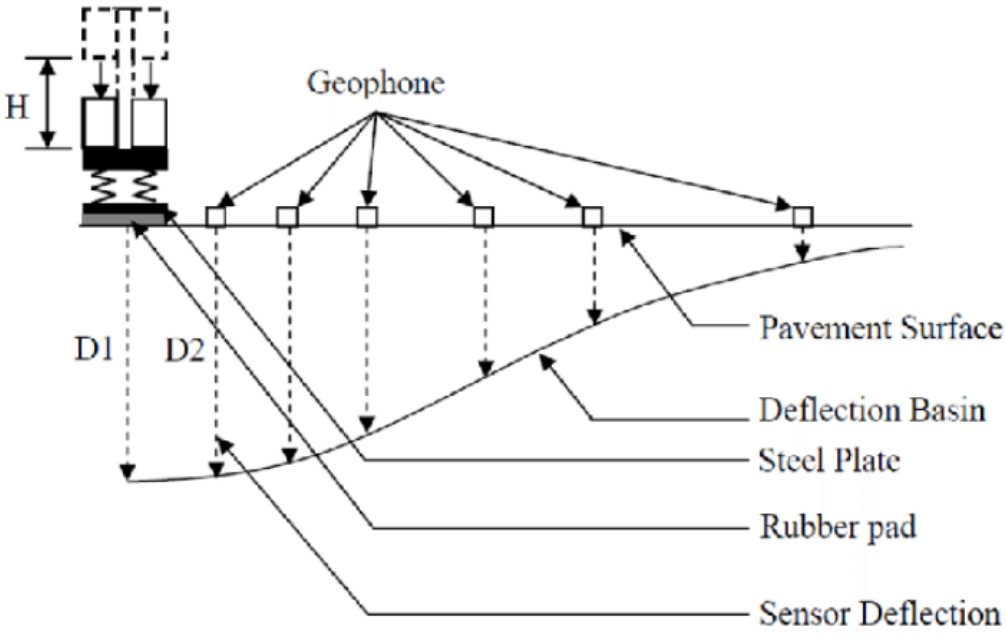

Figure 2-3: Schematic of FWD Testing using impulse loading mechanism (Kavussi et al. 2017)

2.2 Errors in FWD Data

There are several error conditions that could be encountered while measuring the deflections from FWD geophones. They can be listed as follows (Schmalzer, 2006):

- Roll-off: Error recorded when the deflection sensor doesn't return to zero due to weak pavement surface resulting from permanent deformation while impulse loading, poor contact between load plate and pavement surface, deflection is higher than geophone capacity etc.
- Nondecreasing Deflections: Errors recorded when the geophone deflection values don't decrease with the increment of the distance from point of loading. Possible reasons are-

presence of cracking, very high magnitude of impulse loading or very weak pavement resulting to permanent deformation after impulse loading.

- Overflow: Errors recorded when measured deflection exceeds the capacity of geophones.

Besides these errors, there are some other sources such as load variation, deflection variation, etc. All the errors can be subjected to double check and procedures for the elimination of error is provided in the manual (Schmalzer, 2006).

The deflections from the FWD devices can be used to estimate the layer moduli of the underlying pavement layers. Several methodologies have been developed to backcalculate the layer moduli. Indeed, all the methodologies might incorporate some errors which can be eliminated through mathematical modeling or computations. Hoffman et al. (1982), Thompson et al. (1985), Jung et al. (1992), and Irwin (1989) discussed different methodologies to backcalculate the layer modulus from the deflection basin measured during FWD testing. Some of the shortcomings discussed in the literature are- thin layers, adjacent layers of similar modulus, large modular ratios and degree of bonding. Irwin (1989) used the root mean square (RMS) error to eliminate the errors from the backcalculated moduli. The objective of the study was to find a method to calculate the layer moduli eliminating the effect of errors encountered during testing. MODCOMP 2 software at that time could backcalculate up to 15 layers while the software could backcalculate up to 8 surface deflections at different load levels. Through an iterative process, starting with some "seed" moduli- this software could calculate up to a tolerance on the order of 0.1%. The Root Mean Square (RMS) error was used to quantify the accuracy by enhanced goodness of the fit. Equation [1] shows the calculation of RMS Error.

$$RMS\ Error, \% = \left[\frac{1}{n}\sum_{i=1}^{n} D_i^2\right] \quad [1]$$

Where,

n= number of measured deflections,

D_i= 100(d_c-d_m)/d_m=error of the calculated deflection at radius i,%

d_c= calculated deflection at radius i

d_m= measured deflection at radius i

2.3 Effect of Temperature on Measured Deflection

Because asphalt is a viscoelastic material, the pavement responses to loading are variable at different air and surface temperatures. Moreover, flexible pavements are comprised of several underlying layers and the temperature gradient of the underlying layers can also contribute to the seasonal variation of pavement responses. The DBP values are also affected by seasonal variations. To eliminate the seasonal effect on the DBP parameters, several correction factors are suggested by different studies. Y R Kim et al. (2000) and Seo et al. (2009) recommends from their study that the asphalt layer on top is more sensitive to seasonal changes and temperature cycles compared to base layer and subgrade layers. This is why the Strategic Highway Research Program (SHRP 1993) proposed the temperature correction of the deflections measured at the standard temperature of 68ºF. Asphalt is a visco-elastic material which means the material strength property of asphalt mix is temperature dependent. In FWD tests, the measured peak deflection at the center of the load plate has the most dominant effect of the temperature cycles.

Figure 2-4 shows the seasonal effect on the maximum deflection over the year at different months.

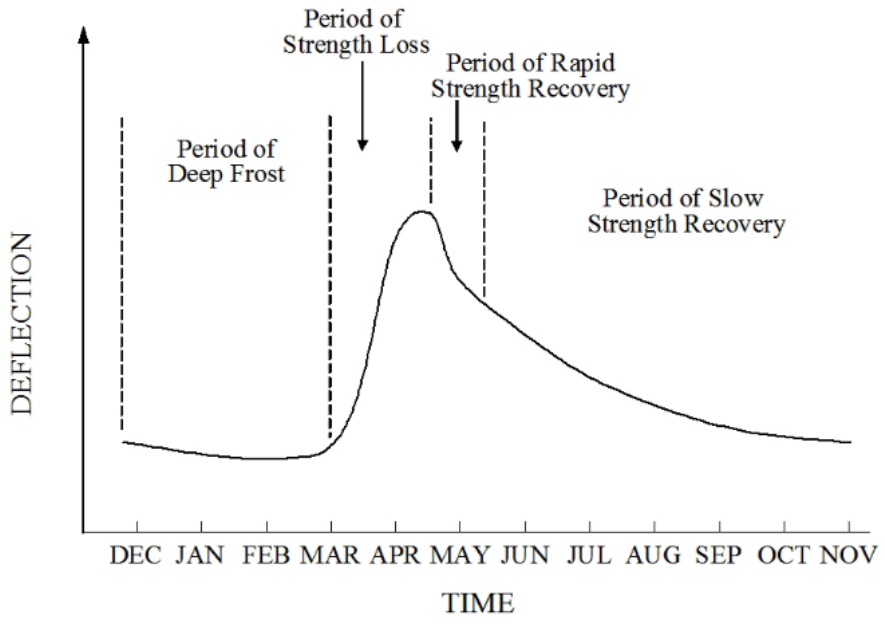

Figure 2-4: Seasonal effects on pavement deflection (Data from MnRoad) (Kim and Park 2002)

Kim et al. (1993) discussed the relationship between temperature corrected maximum deflection and pavement mid-depth temperatures. Though the measured AC temperatures were similar for the same location at different time of the day, the measured deflections were significantly different. The study accounts for different heating and cooling cycles which has effect on the temperature gradient. As a result, the measured deflections might not be the same at the different time of the day even if the surface temperature are the same. The same study showed the measured changes of temperatures at different depths of pavement at different hours of the day. The temperature correction factors were plotted against different mid-depth

temperatures (importantly different seasons) and it was found that they have a non-linear relationship. The temperature correction factors for wheel paths and center of the lane were reported significantly different.

Park et al. (2007) demonstrated the difference between surface and mid-depth pavement temperature at different hours of the day. As seen in **Figure 2.5**, data from 8:04 AM shows the surface temperature is lower than the mid-depth temperature while at 12:00 PM the surface temperature increased around 43°F while the mid-depth temperature increased around 7°F. Again, at 3:00 PM the surface temperature is lower than the temperature of pavement at a depth of 2 inches from the surface. The plot is a good representation of how pavement temperatures change at different times of the day.

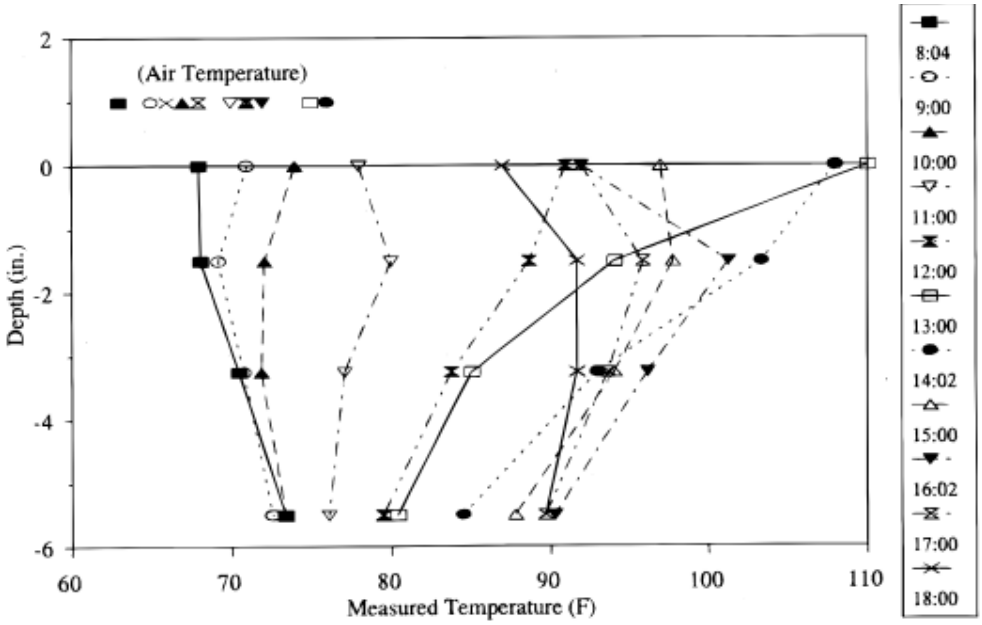

Figure 2-5: Temperature Changes Monitored on US-70 Sections (Kim et al. 1993)

The study also published the surface deflections along with different mid-depth temperatures of the AC layer. The trends and regression coefficients from the study show proper

relationship between pavement temperatures and recorded maximum deflection at the surface of the pavement in **Figure 2-6** (Kim et al. 1993).

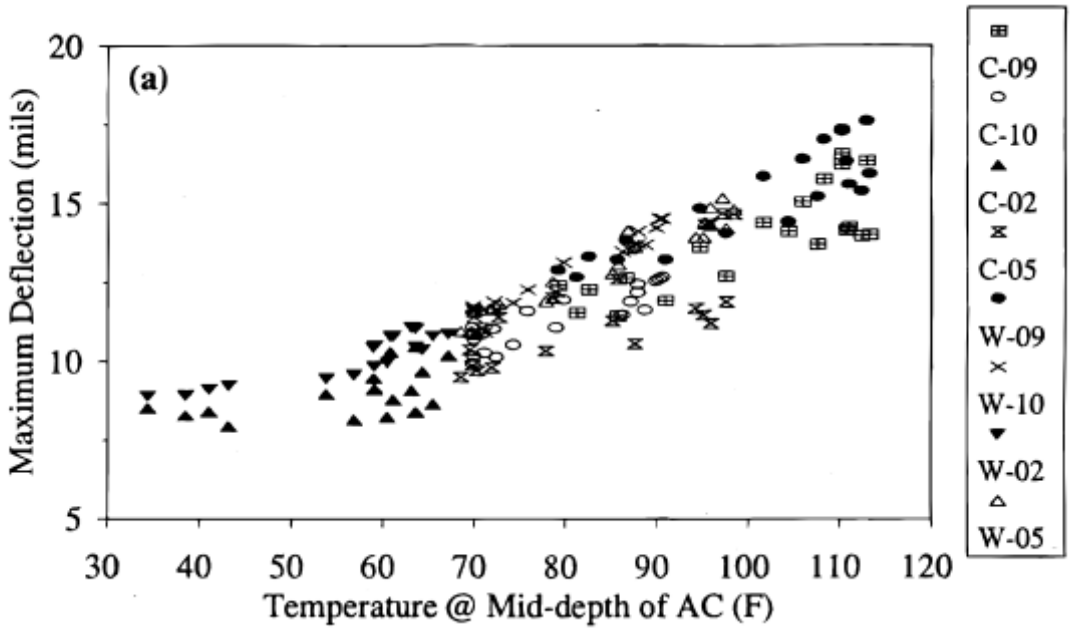

Figure 2-6: Maximum Deflection vs Mid-Depth Temperature for US-70 (Kim et al. 1993)

From the literature reviewed, in can be concluded that the daily air temperature and surface temperature influence the DBPs. The structural properties and stresses and strains of the pavement layers should be corrected based on the temperature correction factors (Xu et al. 2002).

2.4 Effect of Stiff Layers

Studies show that the presence of hard bedrock or a stiff layer affects the measurement of the deflection basin, thus the backcalculated moduli results are inaccurate and erroneous. The depth of stiffer layers within 12m (39ft) from the top of the surface has minor or no effect on the deflection values. Considering the subgrade to be semi-elastic half-space, several regression equations have been derived to find the depth of the stiff layer. This method follows the offset of

inverse deflection for various AC layer thicknesses to calculate regression coefficients (Pierce et al. 2009). Pierce et al. (2017) suggest detecting the presence of subgrade with a parameter called "Deflection Ratio". The Deflection Ratio is the ratio of dynamic deflection to static deflection measured by FWD testing. By this method, the author suggests the effect of bedrock is more evident in the dynamic loading scenario. For the softest subgrade conditions, the difference between dynamic deflections and static deflections are distinguishable while the stiffest layers in shallow depth have equal impression over both types of loading. It was suggested the offset time in the time-deflection record after the first impulse can be a more effective method of measuring stiff layer depth under the subgrade (Roesset et al. 1995). The following sets of regression equations are suggested by the authors for calculating bedrock or stiff layer depth for different thicknesses of AC (Pierce et al. 2017). Equation [2-5] show the relationships between the DBPs and depth of bedrock.

$$\frac{1}{B} = 0.0362 - 0.3242\,(r_0) + 10.2717(r_0^3) - 0.0037\,(BCI) \quad [2]$$

$$\frac{1}{B} = 0.0065 - 0.1652\,(r_0) + 5.4290(r_0^2) + 11.0026(r_0^3) - 0.0037\,(BDI) \quad [3]$$

$$\frac{1}{B} = 0.0413 - 0.9929\,(r_0) + 0.0012(SCI) + 0.0063(BDI) - 0.0078(BCI) \quad [4]$$

$$\frac{1}{B} = 0.0409 - 0.5669\,(r_0) + 3.0137\,(r_0^2) + 0.0033(BDI) - 0.0665\,\log(BCI) \quad [5]$$

Where,

B = Depth to rigid layer, measured from pavement surface (ft).

$r_0 = \frac{1}{r}$ intercept

Base Curvature Index, BCI = $D_{24} - D_{36}$

Base Damage Index, BDI = $D_{12} - D_{24}$

Surface Curvature Index, SCI = $D_0 - D_{12}$

Where, D_{xx} = Deflection measured at the xx -in radial distance from the center of the loading plate in inches.

The analysis method suggested by Pierce et al. (2017) requires the definitions of the stiffness of the bedrock between 700 to 6,900 MPa with a specified thickness of subgrade above the stiff layer. Another way of backcalculation suggests that, if the depth of stiff layer is not determined, a set of trial depths can be plugged in to observe if reasonable results are obtained.

Figure 2-7 demonstrates the series deflections at different sensors after the first impact. It is apparent that the sensors spaced at different radial distances measure equal deflections except for the first impact. The damped natural period (Td) is the time difference between the peak deflections after the first impact. A previous work on characterization of the bedrock based on the time histories at different sensors suggested a methodology to use the velocity of shear wave to determine the depth of bedrock. The natural period (T_d) is the time difference between free vibrations after the impact of FWD load plate is applied. Using the damped natural period (T_d) values, the depth of subgrade stiff layer can be calculated with a set of equations based on the

surface layer condition, saturation of subgrade and overall stiffness of the bedrock (Roesset et al.1995).

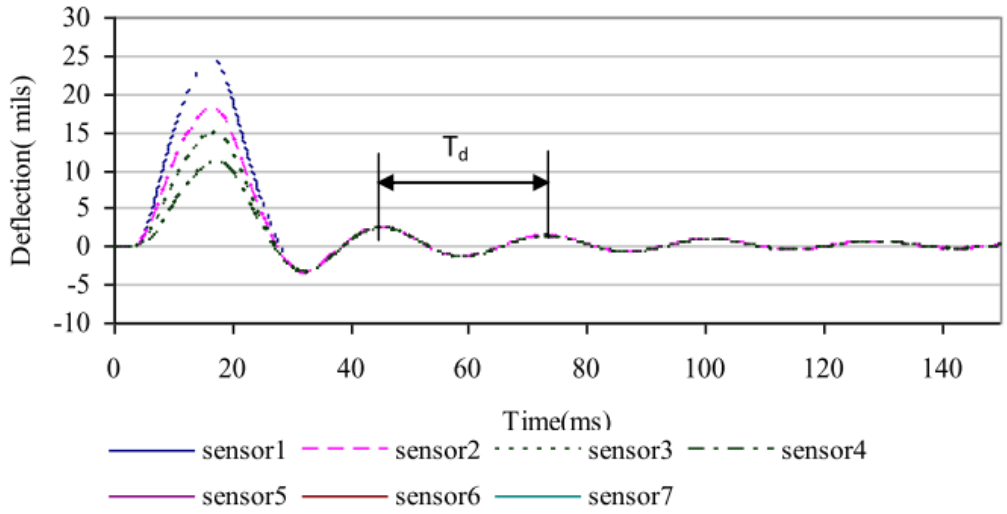

Figure 2-7: Illustration of natural period, Td, from sensor deflection time histories (Chatti, Ji, and Harichandran 2004)

2.5 FWD Testing on Distressed Pavements

Cracking, rutting and stripping are the major distresses on asphalt pavement surfaces. The crack openings promote moisture infiltration and saturated base layers may provide erroneous deflections when tested. Rutting and stripping create an irregular surface, which might result in a seating error. Several studies have been performed to observe the FWD testing responses on distressed pavements.

According to Boussinesq's and Odemark's method- the effective modulus of surface deflection and subgrade deflections are observed. PROBE, a modeling program, was used for the study to measure a weighted average of the properties of the underlying layers. This computer program requires the mechanistic responses of the pavement to estimate the structural integrity

of the layers. This program measures the structural integrity based on the two moduli (a) effective modulus calculated from measured deflection, (b) effective modulus of subgrade reaction. The effective modulus trend shows erroneous pattern due to distresses from a disturbed, cracked, uneven or broken pavement. The study found that the deflection reading and the effective modulus at the distant sensors (or deflection measuring devices) are less interrupted than the ones in close vicinity of the loading plate. Thus, the tail modulus function was introduced to estimate the correct modulus. One of the observations was that the stiffening effect close to the load plate is higher than the surrounding. In other words, the effective modulus of the pavement is higher at the location close to the loading plate which reduces along the radial distances from the center of the load plate. The computer-generated moduli from ELSYM5 show a trend of horizontal asymptote with a level of subgrade modulus. The modulus calculated from the real data does not show any asymptote but rather a positively sloped line or curve (Jung & Stolle, 1992). **Figure 2-8** shows the concept of the effective moduli and tail moduli as the function of radial distance from the center of the loading plate. E_x and E_{mx} are referenced as the effective modulus and the tail modulus function respectively. The tail modulus at the larger radial distance tend to create a linear trend rather than a horizontal asymptote from theoretical values.

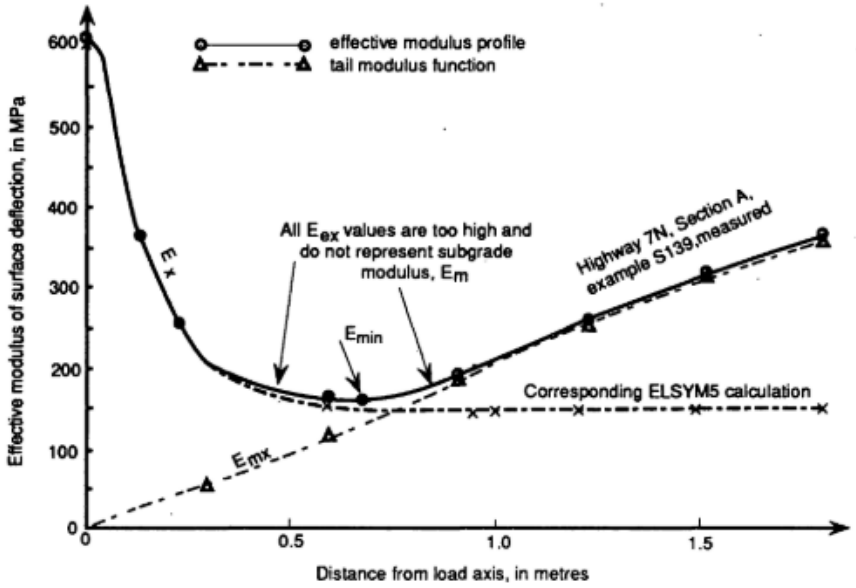

Figure 2-8: Effective Modulus of surface deflection (Jung and Stolle 1992)

2.6 Deflection Basin Parameters for Benchmarking of Structural Condition

For project level rehabilitation decisions, mechanistic design procedures with multi-layer linear elastic theories and backcalculation procedures are followed. Horak (2007) considered a semi-mechanistic, semi-empirical analysis technique using FWD deflection basin parameters. This method helps users to consider relative structural condition of the pavement without detailed as-built data. Influence of deflection basin spreads up to 1m to 2m radial distance from the center of loading. The size and shape of the deflection basin depends on the structure, properties of materials, magnitude of loading, size of contact area, duration of impulse/loading, temperature etc. (Horak 2007).

Horak (2007) divided the deflection basin in three zones: Zone 1(positive curvature), Zone 2 (curvature inflection), and Zone 3 (reverse curvature). Zones are divided along with

different radial distance from the center of load plate. **Figure 2-9** shows zones of the deflection basin.

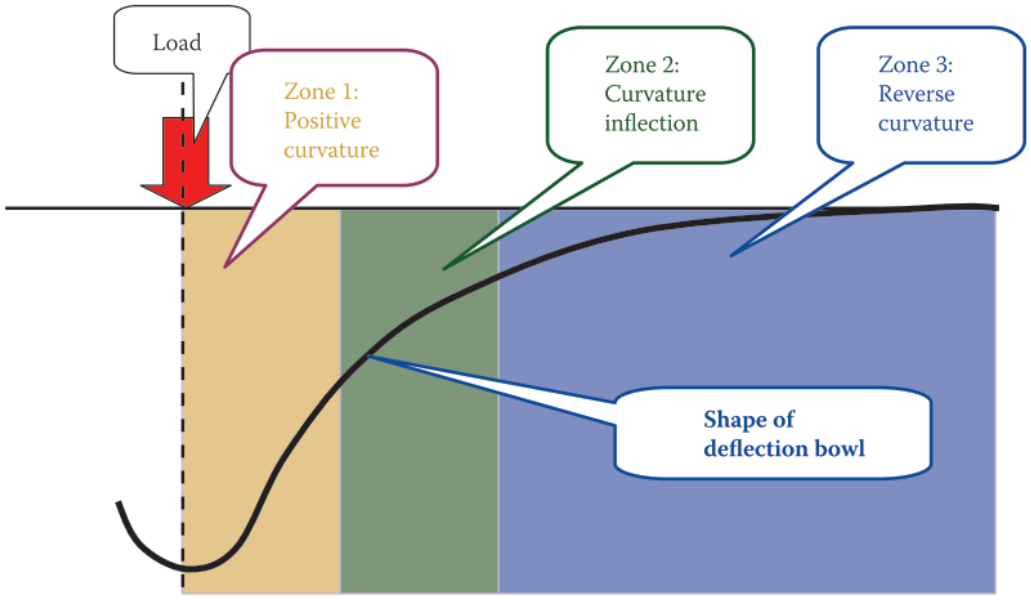

Figure 2-9: Curvature Zones in Deflection Basin (Horak 2008)

For the benchmarking purpose by Horak (2007), the following deflection basin parameters were considered: Maximum Deflection (D_0), Radius of Curvature (RoC), Base Layer Index (BLI) or SCI, Middle Layer Index (MLI) or BCI, Lower Layer Index (LLI) or BDI. Indices correlate to the condition of the zones as shown in Table 2-1.

Table 2-1: Deflection Basin Parameters and Influence Zones (Horak 2008)

Deflection Basin Parameter	Zone Correlated to
Maximum Deflection	1,2 and 3
Radius of Curvature	1
Base Layer Index/ Surface Curvature Index	1

Middle Layer Index/ Base Curvature Index	2
Lower Layer Index/ Base Damage Index	3

The deflection basin parameters were classified among different condition ratings (Sound, Warning and Severe) based on the individual values provided in Table 2-2.

Table 2-2: Deflection Bowl/Basin Parameter Structural Condition Criteria for Various Pavement Types (Horak 2008)

	Structural Condition Rating	Deflection Basin Parameter				
		Do (μm)	RoC (m)	BLI (μm)	MLI (μm)	LLI (μm)
Granular Base	Sound	<500	>100	<200	<100	<50
	Warning	500-700	50-100	200-400	100-200	50-100
	Severe	>750	<50	>400	>200	>100
Cementitious Base	Sound	<200	>150	<100	<50	<40
	Warning	200-400	80-150	100-300	50-100	40-80
	Severe	>400	<80	>300	>100	>80
Bituminous Base	Sound	<400	>250	<200	<100	<50
	Warning	400-600	100-250	200-400	100-150	50-80
	Severe	>600	<100	>400	>150	>80

Though all the layers underneath the loading plate contribute to the deflection, the subgrade layer contributes between 60%-80% of the measured deflection at the center of the load plate (Huang, 2004; Ullidtz, 1987). The influence of the load spreads along the stress bulb in an angle of 45° with the surface of the pavement. Therefore, it is important to record the deflections up to a considerable radial distance from the center of the load (usually 72 in.). The concept of surface modulus (SM) is reintroduced here which is the weighted mean modulus of the layers

considered in the half-space under the surface deflection (Ullidtz, 1987). Equation [6]-[7] show the equations to calculate surface moduli at different radial distances.

$$SM_0 = 2\sigma_0(1-\mu^2)(a/d_0) \quad [6]$$

$$SM_r = \sigma_0(1-\mu^2)\left(\frac{a^2}{r * d_{(r)}}\right) \quad [7]$$

Where,

SM_0= Surface Modulus at the center of the loading plate, r=0 (psi)

SM_r= Surface Modulus at the radial distance r from the center of the loading plate (psi)

σ_0= Stress at the bottom of the loading plate or contact stress (psi)

μ= Poisson's ratio; for AC=0.35

a= Radius of loading plate (in)

$d_{(r)}$= Deflection measured at the radial distance r (in)

Based on the surface modulus differential criteria, the subgrade responses can be classified as follows: stress softening (>20 MPa), linear elastic (20 to -20 MPa) , stress stiffening (<-20 MPa) (Horak 2008).

2.7 Base Damage Index (BDI)

Base Damage Index (BDI) is the measurement to represent the base layer condition. The mechanistic design procedure targets the horizontal strain at the top of base layer to prevent bottom-up fatigue cracking (BUFC), thus the structural condition assessment is very important. Again, the base layer also helps to spread the wheel load to the bottom surfaces. Therefore, the

modulus of elasticity of the base layer is also important to model. Equation [8] shows the equation for BDI calculation.

$$BDI = D_{12} - D_{24} \quad [8]$$

Where,

D_{12} = deflection at 12 in radial distance from the center of load (mils)

D_{24} = deflection at 24 in radial distance from the center of load (mils)

Kheradmandi and Modarres (2018) developed a model correlating the BDI and deflection at base layer. The thicknesses of AC, base layer and stresses under the loading plate were also the variables in the correlation equation. The study found that the BDI, layer thicknesses and stress yield a linear relationship with the log of the deflection. The study suggests the following correlation Equation [9] to measure the deflection at the top of base layer:

$$\log \delta_{base} = 1.691 \log BDI + 1.377 \log H_{ac} - 0.674 \log \sigma + 0.002 H_{base} - 0.29 \quad [9]$$
$$R^2 = 0.97$$

Where,

δ_{base}= Deflection of base layer (μm)

σ= Applied stress in FWD test (kPa)

BDI= Base Damage Index (mils)

H_{ac}= Thickness of AC layer (in)

H_{base} = Thickness of Base layer (in)

Kheradmandi et al. (2018) shows the linear relationship between base layer deflection and calculated BDI. The study found more correlation between base deflection and BDI. Xu et al. (2002) also considers the relationship between the strain at the bottom of AC layer and calculated BDI. The study developed a correlation equation between log of AC layer strain and SCI, BDI, layer thicknesses. The R^2 values for full-depth base and aggregate base were 0.987 and 0.992 respectively in Equation [10].

$$\log \in_{AC} = 0.5492 \ \log SCI + 0.3850 \log BDI + 0.7812 \log H_{ac} - 0.0017 \ H_{ac} + 1.735$$
$$R^2 = 0.992 \quad [10]$$

Where,

$\in_{AC}$= Strain at AC layer (μm/ μm)

SCI= Surface Curvature Index (mils)

BDI= Base Damage Index (mils)

H_{ac}= Thickness of AC layer (in)

H_{base} = Thickness of Base layer (in)

The microstrain under the AC layer vs the BDI values correlated well for both aggregate base AC and full-depth pavements (Xu et al.2007). A linear relationship was found between log of AC microstrain and BDI for full-depth pavements (**Figure 2-10**) and aggregate base pavements (**Figure 2-11**).

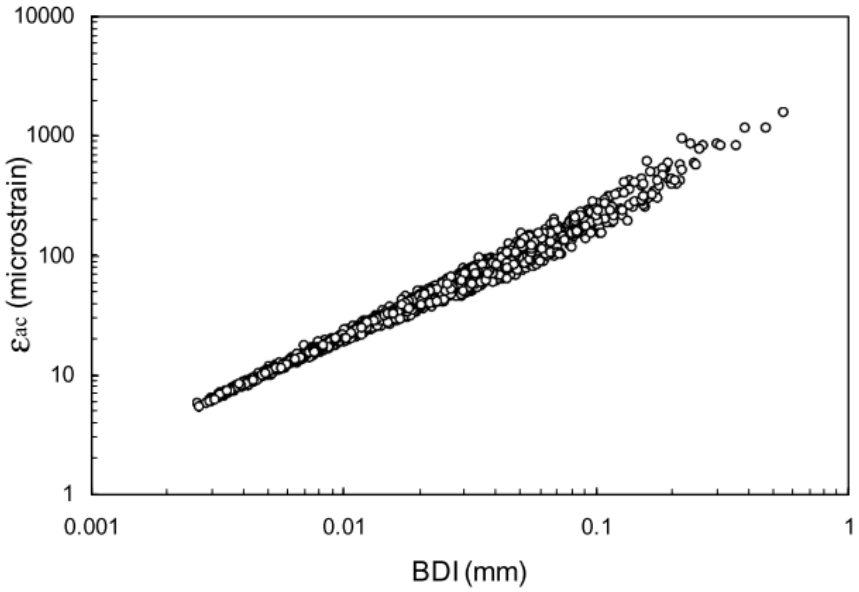

Figure 2-10: AC microstrain vs BDI for Full-Depth pavement (Xu et al.2007)

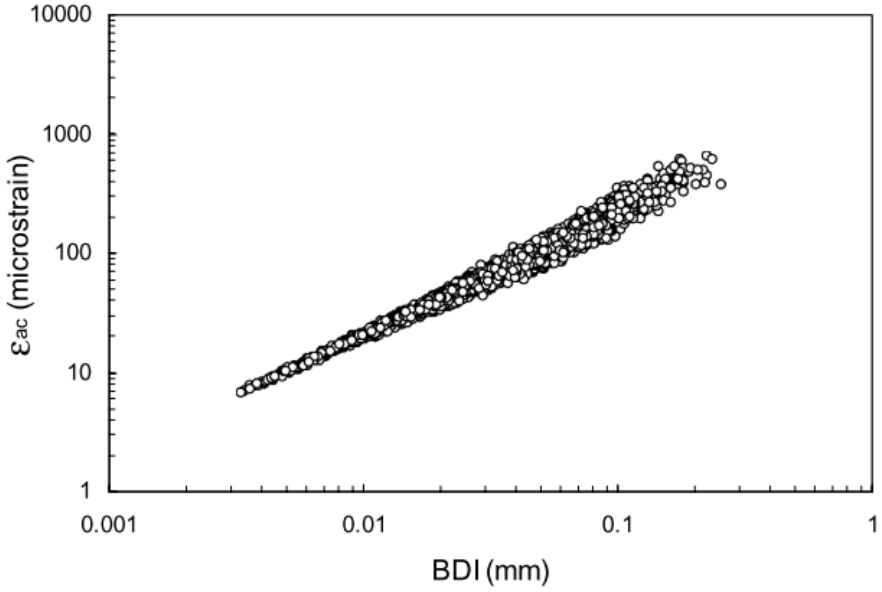

Figure 2-11: AC microstrain vs BDI for aggregate bases (Xu et al.2007)

2.8 Surface Curvature Index (SCI)

Surface Curvature Index (SCI) indicates the change of deflection from the maximum deflection (under the center of the loading plate) to the recorded deflections at variable distances from the center of the loading plate. The SCI values provide an overview of the overall stiffness condition of the underlying layers. Studies show that, up to a certain thickness, the AC moduli is linearly related to the SCI values in a logarithmic scale (Xu et al. 2001). The SCI is calculated using the following equation:

$$SCI_i = D_0 - D_i \quad [11]$$

Where:

SCI_i= Surface Curvature Index (mils)

D_0 = Deflection recorded at the center of the loading plate (mils)

D_i = Deflection recorded at the distance i from the location of D_0 (mils)

Further studies developed a numerical relationship between AC layer modulus and SCI for both full-depth and aggregate base pavements. When the AC layer is strong, it is also found that the subgrade or the stiff layer has minor or no effect on the SCI value. For full-depth AC pavements (thickness usually greater than 150 mm) there is negligible effect of lower layer on the SCI value. For aggregate bases, there is an effect of base layer on the AC layer modulus, so the Base Damage Index (BDI) is also added to the regression equation [12] and [13] (Xu et al. 2007).

$$\log(E_{ac}) = -1.0831*\log(SCI) - 2.6210*\log(H_{ac}) + 0.0019*H_{ac} + 8.0889$$

$R^2 = 0.994$; SEE=0.028 [12]

$$\log(E_{ac}) = -1.7718*\log(SCI) + 0.8395*\log(BDI) - 2.5124*\log(H_{ac}) + 0.0030*H_{ac} + 7.7696$$

$R^2 = 0.975$; SEE=0.089 [13]

where,

E_{ac} = Modulus of Elasticity of asphalt concrete surface layer (psi)

H_{AC} = Thickness of the AC layer (in)

SCI= Surface Curvature Index (mils)

BDI= Base Damage Index (mils)

SEE= Standard estimate of error for the model

The calculated AC Layer Modulus (E_{ac}) shows a linear relationship with SCI, where the moduli decrease with the increase of the SCI value. The study simulated different thicknesses of AC layer to observe the above relationship for the case of both full-depth asphalt and aggregate base pavements.

From **Figure 2-12** and **Figure 2-13**, it is observed that the plot is converging towards the higher SCI from the lower SCIs. Compared to the full-depth pavement response in (Xu et al. 2007), it can be noted that, for aggregate bases, there is a combined effect of aggregate base and AC layer thickness on the AC layer modulus.

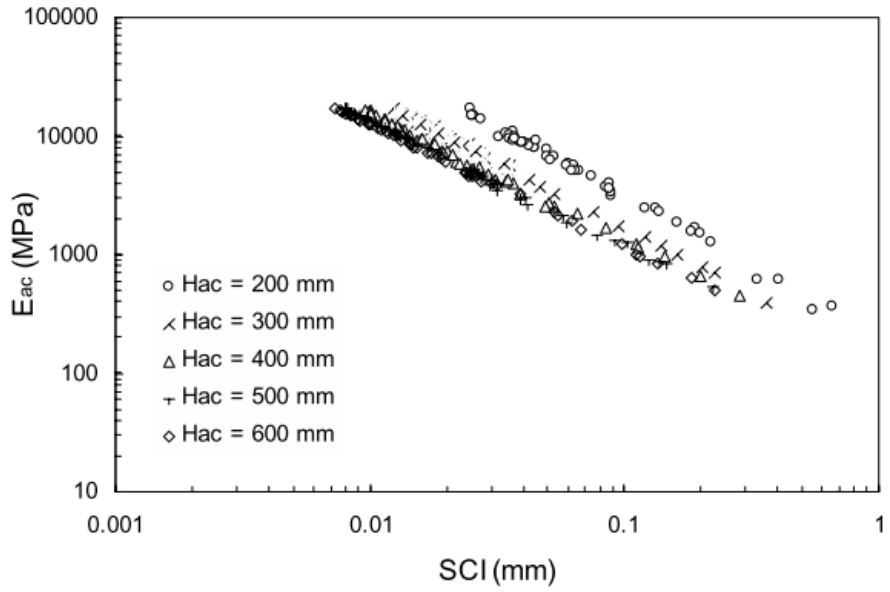

Figure 2-12: Eac vs SCI for various Hac for Full-Depth Pavements (Xu et al. 2007).

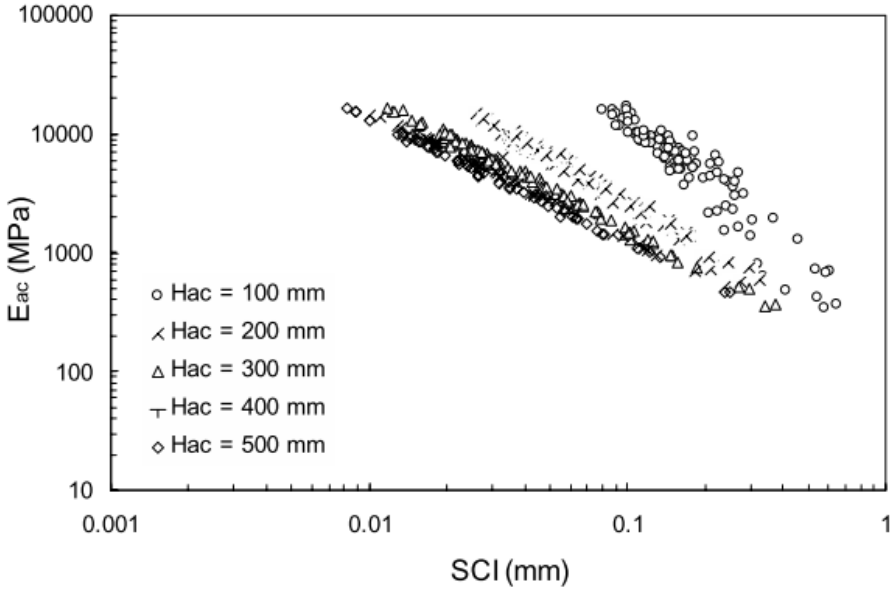

Figure 2-13: Eac vs SCI for various Hac for Aggregate Base Pavements (Xu et al. 2007)

2.9 AREA and AUPP

In 1982, an approach with non-linear material properties was introduced where ILLI-PAVE was used as a tool to interpret the deflection basin parameters by developing algorithms and nomographs for ease of overlay design. ILLI-PAVE is a static finite element computer program for the analysis of materials with stress-dependent properties. In a separate study by IDOT and the University of Illinois, the Benkelman Beam, Road Rater (RR) and Falling Weight Deflectometer were compared to analyze the most efficient and accurate device to simulate real traffic conditions and record the pavement responses. The FWD was found to be the fittest. Alongside identifying the accurate device of deflection testing, to characterize the deflection basin, the following parameters were introduced: AREA of deflection basin, shape factors- F1 and F2 (Hoffman & Thompson, 1982). The shape factor F_2 has correlation with BDI and $E_{sg.}$ Lee et al. (1998) developed a nomograph to portrait shape-factor (F_2) and base damage index (BDI) at variable subgrade modulus values for both intact and cracked AC pavements. The same study also suggested a relationship between center deflection, AREA, AC layer thickness and subgrade modulus of elasticity in a two-layer system shown in **Figure 2-14**.

$$AREA = 6\left[1 + \left(2 * \frac{D_{12}}{D_0}\right) + \left(2 * \frac{D_{24}}{D_0}\right) + \frac{D_{36}}{D_0}\right] \quad [14]$$

$$F_1 = \frac{D_0 - D_{24}}{D_{12}} \quad [15]$$

$$F_2 = \frac{D_{12} - D_{36}}{D_{24}} \quad [16]$$

Where,

D_{12}= deflection recorded at 12 in. from the center of load plate (mil)

D_{24}= deflection recorded at 24 in. from the center of load plate (mil)

D_{36}= deflection recorded at 36 in. from the center of load plate (mil)

D_0= deflection recorded at the center of load plate (mil)

F_1,F_2= Shape Factor

The deflection basin area calculation require data from the first 4 sensors of the FWD. In the study, the sensors are spaced at equal distance (12" c/c). The AREA of the deflection basin varies from 11in to 36in while stiffer pavements have larger areas. The RR deflections were converted to equivalent FWD deflections using correlation coefficients. The RR deflections at 8 kips magnitude with a frequency of 15 Hz were selected for the conversion. The conversion coefficients are shown in Table 2-3, where FWD variable equals $A + (B \times BR)$.

Table 2-3: Correlation Coefficients between RR and FWD Deflections (Hoffman and Thompson 1982)

FWD Variable	A	B	R^2	SSE	Mean FWD Value	Mean RR
D_0	-3.40	1.21	0.94	3.23	24.19	22.85
D_1	1.68	0.72	0.92	1.13	12.24	14.62
D_2	3.98	0.27	0.54	0.64	6.57	9.71
D_3	2.69	0.25	0.48	0.55	4.56	7.52
AREA	-7.59	1.19	0.95	1.14	18.88	22.17
F_1	-0.15	1.73	0.93	0.19	1.29	0.84
F_2	0.03	1.57	0.72	0.26	1.16	0.72

Kim et al. showed the relationship between AREA and center deflection is a function of AC layer thickness (H_{ac}), AC layer modulus (E_{ac}) and Subgrade Modulus (E_{sg}). For the backcalculation of AC layer modulus, this relationship is valid for two-layer systems. Lee et al. (1998) developed a method to detect the condition of the AC layer if the layer is cracked or not. Thus, the F2-AREA relationship at 225 mm (8.85 in.) AC thicknesses, variable base thickness and infinite subgrade thickness develop an envelope between cracked and intact AC layer. For the three-layer systems, the thickness and modulus for the base layer are required for the estimation of the AC layer modulus. The relationship among center deflection, AREA, thickness of AC layer and modulus of elasticity of subgrade is shown in **Figure 2-14**.

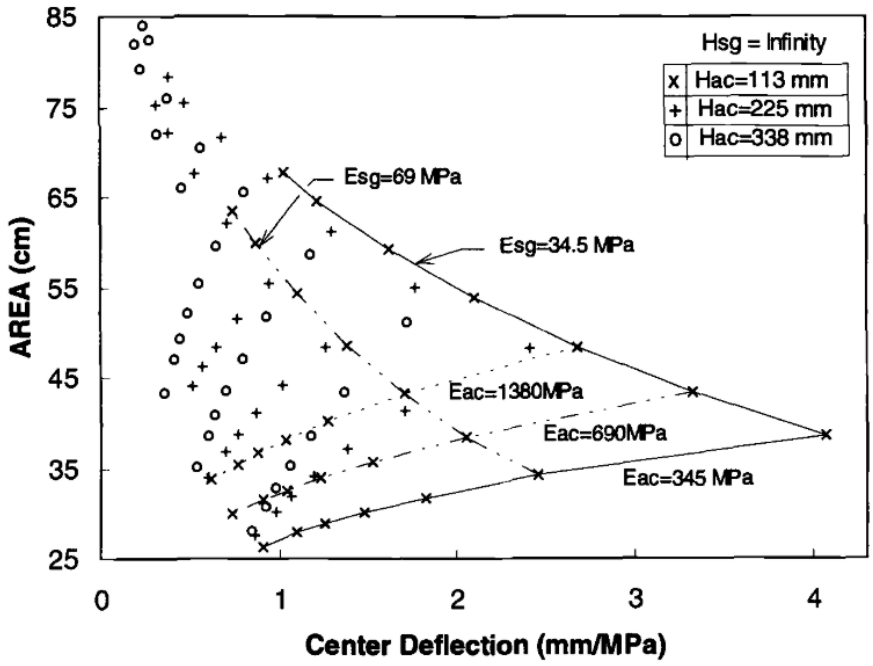

Figure 2-14: Relationship among Center Deflection, AREA, AC layer thickness and Subgrade Modulus for 2 -layer systems (Kim et al. 2000)

Y R Kim et al. (2000) introduced another parameter, Area Under Pavement Profile (AUPP), which can be used to predict tensile strain at the bottom of AC layer. The information

has been validated by MnROAD test section observations (M R Thompson, 1989; Marshall R Thompson & Elliott, 1985). The equation for AUPP is shown in equation [17]. The study also proposes a set of equations for measuring tensile strain at the bottom of the AC as in equations [18] and [19].

$$AUPP = \frac{1}{2}(5D_0 - 2D_{12} - 2D_{24} - D_{36}) \quad [17]$$

$$\log(\varepsilon_{ac}) = 1.024 \log(\text{AUPP}) + 1.001 \quad [18]$$

$$\log(\varepsilon_{ac}) = 0.821 \log(\text{AUPP}) + 1.210 \quad [19]$$

Where,

D_{12}= deflection recorded at 12 in. from the center of load plate (mil)

D_{24}= deflection recorded at 24 in. from the center of load plate (mil)

D_{36}= deflection recorded at 36 in. from the center of load plate (mil)

D_0= deflection recorded at the center of load plate (mil)

ε_{ac}= tensile strain at the bottom of the AC layer

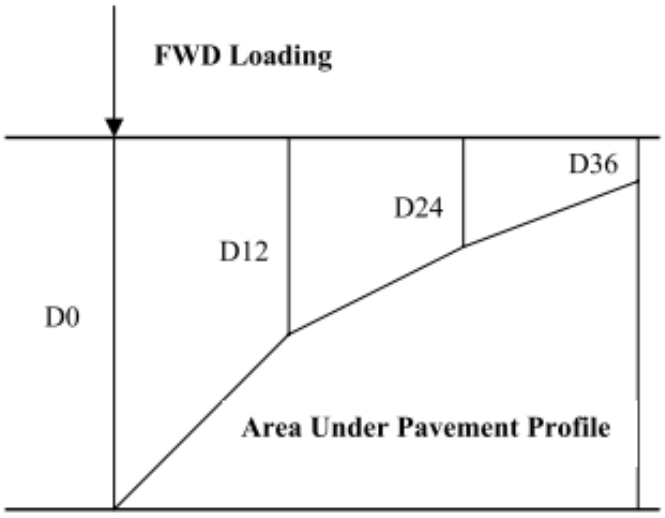

Figure 2-15: Area Under Pavement Profile (Y Richard Kim and Park 2002)

Equation [18] and [19] are respectively for full-depth asphalt and aggregate base pavements for the prediction of tensile strain at the bottom of the AC layer. As shown **in Figure 2-15**, AUPP is a geometric parameter of the deflection basin, the type of subgrade doesn't have any effect over the strains predicted using the equations (Kim and Park 2002).

2.10 DBP Values Implementation in Pavement Condition Assessment

Several studies have been conducted on the relationship between pavement condition and deflection basin parameters. For the pavement condition assessment, rutting and fatigue cracking are the most common assessment parameters and are widely studied. Talvik and Aavik (2009) suggested a methodology involving SCI, BDI and BCI to calculate equivalent pavement modulus to predict pavement condition. The secondary objective was to develop limit values of the DBPs against different types of pavement failures. The SCI and BDI have a strong relationship with the equivalent pavement modulus (E_{eq}) while the BCI does not show any distinguishable relationship with E_{eq} (Talvik and Aavik 2009).

Partial Defect Sum (PDS) was introduced by Talvik et al. (2009) to represent the pavement condition by the measurement of length of longitudinal cracks and extent of alligator cracking along the width of the pavement. The study shows the absence of relationship between SCI and PDS with an R^2 value less than 0.1. Rut depth also showed indifferent response to the change of SCI. The response of the E_{eq} towards varied BDI for both distressed pavements and intact pavement sections. The R^2 value for pavement without surface defect and with surface defect pavement were 0.74 and 0.68, respectively, which signify a proper relationship between E_{eq} and BDI (see **Figure 2-16**). Another aspect of the study was the limiting values for the deflection basin parameters based on the minimum required effective pavement modulus (E_{eq}). Equation [20] shows the parameters for the modeling of the limiting BDP values (Talvik and Aavik 2009).

$$y = a_0 x^{a1} \quad [20]$$

Where,

x= minimum E_{eq} in MPa

y= Deflection Basin Parameter (SCI,BDI,BCI)

a_0, a_1=correlation constants

For the interest of the present study, only few parameters for calculating the limiting values for BDI, BCI and SCI are provided in Table 2-4.

Table 2-4: Values of Constants for calculation of max allowable deflection basin parameter values (Talvik 2007)

Type of pavement	Deflection Basin Parameter	Values of Constant		R^2
		a_0	a_1	
AC Pavement on top of existing pavement	SCI	1795660	-1.70	0.83
	BDI	1265966	-1.74	0.78
	BCI	51220	-1.36	0.68
AC Pavement on Crushed Stone	SCI	498577	-1.45	0.87
	BDI	10645	-0.84	0.21
	BCI	51984	-1.31	0.61

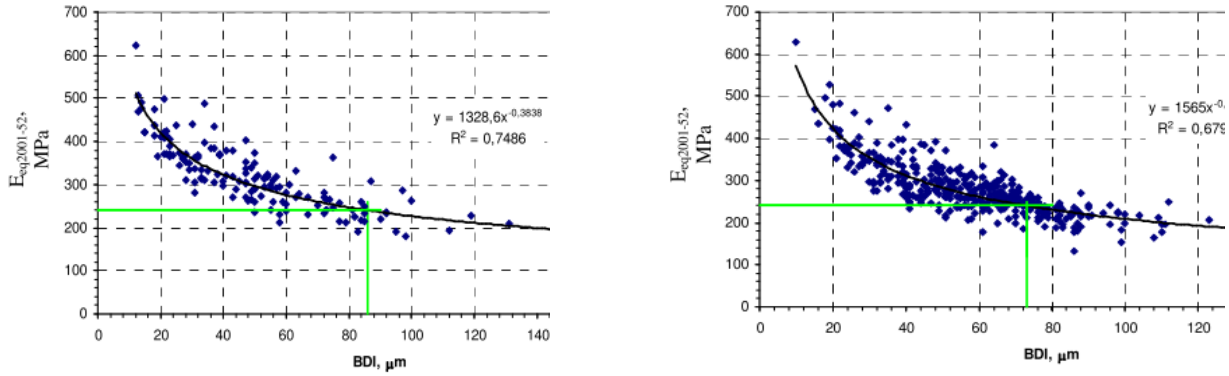

Figure 2-16: Relationship between Eeq and BDI for pavements without surface defects (left) and with surface defects (right) (Tavik and Aavik 2009)

Horak et al. (2014) studied the correlation between effective structural number (SN_{eff}) of the pavement and deflection basin parameters. The concept of the modified structural number is also correlated with empirical values collected from test section and conventional structural number derived from AASHTO 1993 equations. The study claims that the AASHTO 1993 equations are based on the maximum deflection under the load calculated from the Benkelman beam. The other deflections at different radial distances are not considered in this method. Incorporation of the deflection measured at surrounding surface with the effective structural number requires modification to the AASHTO 1993 equation. Another anomality was that the traditional AASHTO 1993 method doesn't cover varieties of combination of pavement layers, only the sections considered in the AASHO road test in the 1950's. A detailed and extensive study outcome was a modified regression equation for the calculation of effective (SN_{eff}).

$$SN_{eff} = e^{5.12} BLI^{0.31} AUPP^{-0.78} \quad [21]$$

Where,

SN_{eff} = Effective SN at the time of measurement of FWD deflection

BLI = Base Layer Index (also known as SCI)

AUPP= Area Under Pavement Profile

For project level management, another terminology found in many literatures was the Structural Condition Index (SCI). This numerical parameter allows quick assessment and PMS decision making and is defined as shown in Equation [22].

$$SCI = \frac{SN_{eff}}{SN_{req}} \quad [22]$$

Where,

SCI = Structural Condition Index

SN_{eff} = Effective Structural Number at the time of FWD testing

SN_{req} = Required Structural Number needed for 20 years traffic based on known parameters

Zhanmin et al. (2011) suggested a three-tiered condition rating system based on SCI, according to the following criteria: a) sound condition or green for SCI above 1 , b) warning or amber condition for SCI between 0.75 and 1, c) severe or red condition for SCI below 0.75. Still, one drawback for this method is that the numbers cannot describe the extent and type of distress of the pavement sections in the network (Horak et al. 2015).

Structural number or effective structural number consists of two components: structural contribution of subgrade and contribution from the upper layers on top of the subgrade (Ullidtz 1987; Parkman 2000). This is why the contribution of subgrade to the effective structural number has been characterized based on subgrade in-situ properties (Rohde & Van Wijk, 1996; Watanatada, 1987). The estimation of the structural number contribution by the subgrade (SNSG) based on the CBR value of the subgrade can be obtained from Equation [23].

$$SNSG = 3.51(\log_{10} CBR) - 0.85(\log_{10} CBR)^2 - 1.43 \quad [23]$$

Where,

SNSG = Structural Number Contribution by subgrade

CBR = California Bearing Ration number of the subgrade

Kim et al. (2013) developed a variety of options to select pavement types and estimate the Structural Number (SN) with a non-linear regression equation with eight coefficients. In this methodology, a database of 1,194,514 combinations of pavement structures have been modeled via NETFWD and have been classified in 4 different pavement management information system (PMIS) Classes. NETFWD is a methodology developed by Murphy to assess structural condition of pavements based on existing PMIS database. Table 2-5 is the summary of the structural geometry and strength of the pavement layers along with the number of the sections covered within the study. This table provides with the sense of accuracy that the

Table 2-5: PMIS Classes from NETFWD Data (Kim et al. 2013)

PMIS Class	Number of Structures	Surface		Base		Subgrade	
		Thickness (in.)	Modulus (ksi)	Thickness (in.)	Modulus (ksi)	Thickness (in.)	Modulus (ksi)
Type 4	567159	6-12	20-1250	4-18	15-500	60-720	4-45
Type 5	390663	2.5-5.5	50-1250	6-18	10-500	60-720	4-45
Type 6	161188	1.5-2	50-1250	4-18	5-500	60-720	4-45
Type 10	75054	1-2	50-1250	4-18	4-500	60-720	4-45

After mathematical modelling, the non-linear regression in Equation 24 was derived using the DBPs and structural parameters. The k_i's are the coefficients with PMIS type based values described in the literature (Kim et al. 2013). The equation was developed by the TxDOT to benefit the PMIS by achieving more accurate structural number for the pavement sections

within the network. Among the road types of the PMIS classes shown in Table 2-5, the pavements with AC thickness less than 5.5 in, showed proper correlation between estimated SN from Equation [24].

$$SN=k_1 SIP^{k2} HP^{k3}+k_4(1+r_0)^{k5}+k_6 SCI^{k7} BDI^{k8} \quad [24]$$

Where,

SN = Structural Number

Hp =Total Pavement Thickness (in)

SIP = D_0-$D_{1.5Hp}$ (mils)

$k_1, k_2, k_3, k_4, k_5, k_6, k_7, k_8$ = Regression coefficients.

From the above paragraphs discussed it can be summarized that the deflection basin parameters (DBPs) can be used as a very effective method to quantify the structural health of the pavement. It is also important to cross validate the observations with other correlating parameters to reach a more accurate observation. Yet, the requirement of destructive testing cannot be undermined by all non-destructive testing.

2.11 Preservation Review

With time, the pavement surface and underlying structure deteriorate due to the traffic, moisture and oxidation. Within the design life, the pavement goes through several cycles of maintenance and rehabilitation procedures to restore the pavement serviceability. Pavement preservation is “a proactive, planned strategy applied in a timely manner to extend the life of the pavement” (Chan et al. 2011). The effectiveness of a preservation treatment is dependent upon the following: right treatment, right time, and right condition of the pavement. Some of the treatments target the cease of moisture penetration to prevent stripping and other moisture related structural issues. Some other treatments focus on the restoration of the serviceability and skid resistance. Establishment of program guidelines, determination of maintenance needs, framework development, development of analysis procedure and initiation of feedback mechanism, are the major steps for preventive maintenance program. Rutting, cracking, bleeding, roughness and weathering are the major distresses that can be addressed with crack sealing, fog seals, chip seals, thinlays, thin-cold mix (slurry seals, cape seals, Micro surfacing), etc. (Hicks et al. 1999). Table 2-6 demonstrates the common distress types and the appropriate treatments.

Table 2-6: Treatments for various distresses (Hicks,et al. 1999)

Types of Distresses/ Properties	Crack Seal	Fog Seal	Micro-surfacing	Slurry Seal	Cape Seal	Chip Seal	Thin Overlay	Milling
Roughness								
Non-Stability Related			×		×		×	×
Stability Related							×	
Rutting			×	×	×		×	
Fatigue Cracking								
Cracking	×	×	×	×	×	×	×	
Bleeding			×			×		×
Raveling		×	×	×	×	×		

A standardized pavement life cycle can compare the extension of life if the pavement is treated for preservation. A simplified pavement condition index (PCI) vs pavement life curve shows how much the life is extended and how much economic the treatments are at the end of life, as seen in **Figure 2-17**.

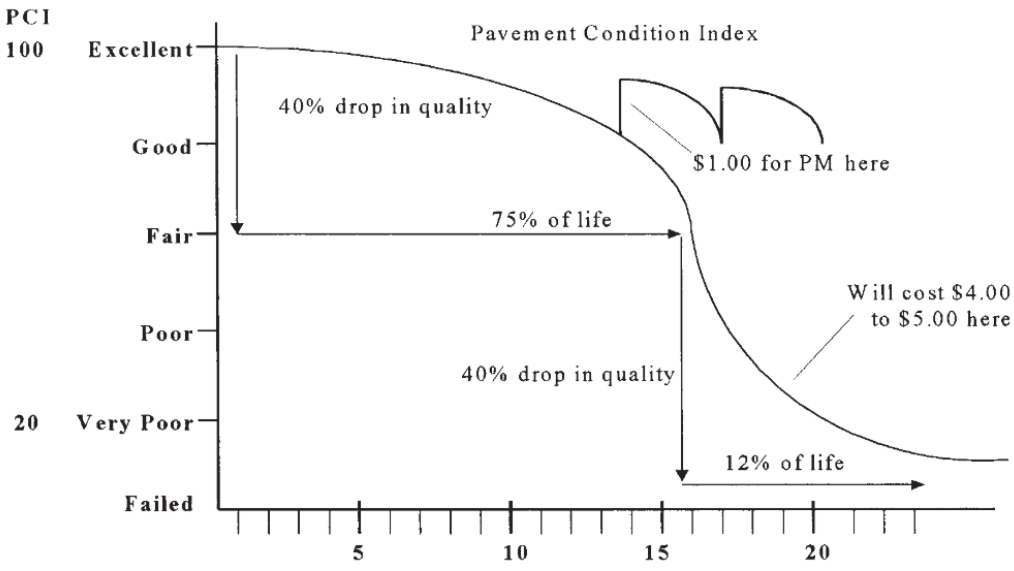

Figure 2-17: Pavement Life Cycle and the effect of Preservation Methods (Hickset al. 1999)

Labi & Sinha (2003) focused on the short-term effectiveness of the treatments and introduced the following terms: deterioration reduction level (DRL), performance jump (PJ) and deterioration of rate reduction (DRR). DRL is the measurement of the increase of the pavement condition between spaced out points in time due to the treatment. The performance jump (PJ) is the difference between Pavement Condition Rating (PCR) just before and after the treatment. The deterioration rate reduction (DRR) is the measurement of the PCR slope compared to the untreated PCR slopes. The treated sections DRR show a mild slope where the untreated sections show a steep slope with time or traffic. The DRL concept schematic is shown in **Figure 2-18**. ΔC_1 is the deterioration between a specified time and just after maintenance, ΔC_2 is the deterioration between just before maintenance and a specified time after maintenance, ΔC_3 is the deterioration between 2 specified time where the maintenance occurs.

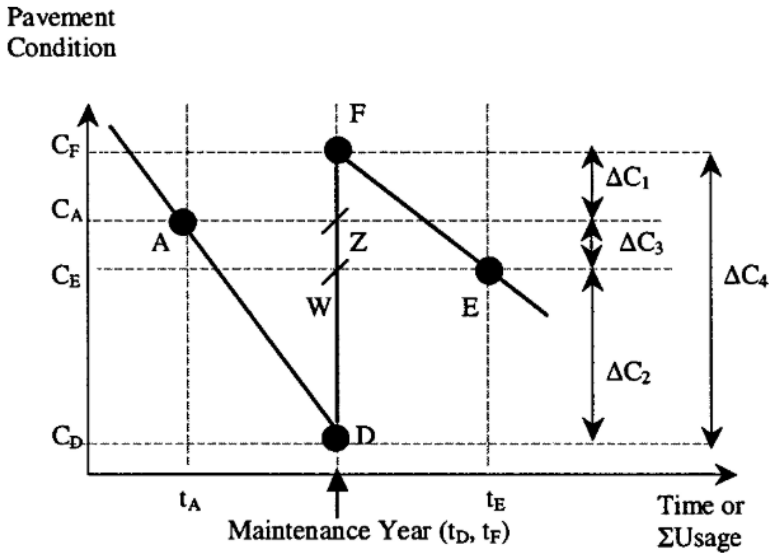

Figure 2-18: Illustration of deterioration reduction level concept (Labi and Sinha 2003)

Zubeck et al. (2012) studied the effectiveness of the treatments in cold regions and compared the common types of treatments service life as per literature and survey. This study also indicated some of the treatments are unsuitable for hauling and may suffer from complications during application due to extreme cold situations. Additional frost action, winter traction and ice removal actions also reduce the life expectancy of the treatments (Zubecket al. 2012). Table 2-7 shows the comparative service life of the treatments from Canadian cold regions.

Table 2-7: Treatment life for cold regions (Zubeck et al. 2012)

Treatment	Service Life (Years)	
	Literature	Survey
Crack Sealing	3-8	3.4
Fog Sealing	-	3.4
Chip Sealing	3-10	5.6
Slurry Seals	3-5	4.6
Micro surfacing	3-9	6.0
Thinlays	5-12	6.8

Performance evaluation measures two major components: (a) life expectancy of the treatment, and (b) the time effect over the treatment performance. Eltahan et al. (1999) used data collected from the LTPP SPS-3 experiment to perform survival analysis. In survival analysis the failure criteria are fixed, and the survival time is examined until the values fall to failure criteria. A standard failure curve is shown in **Figure 2-19**. The SPS-3 study recorded the performance data until some of the sections reach the poor condition after 6 to 8 years of service. The Kaplan-Meier method was used to perform the survival analysis on the SPS-3 censored data. Based on the initial condition (pre-treatment) the sections were ranked and grouped. Each group based on the rank and number of sections received a probability of failure at a given time. The estimated probabilities were plotted against different survival times and compared to the control section.

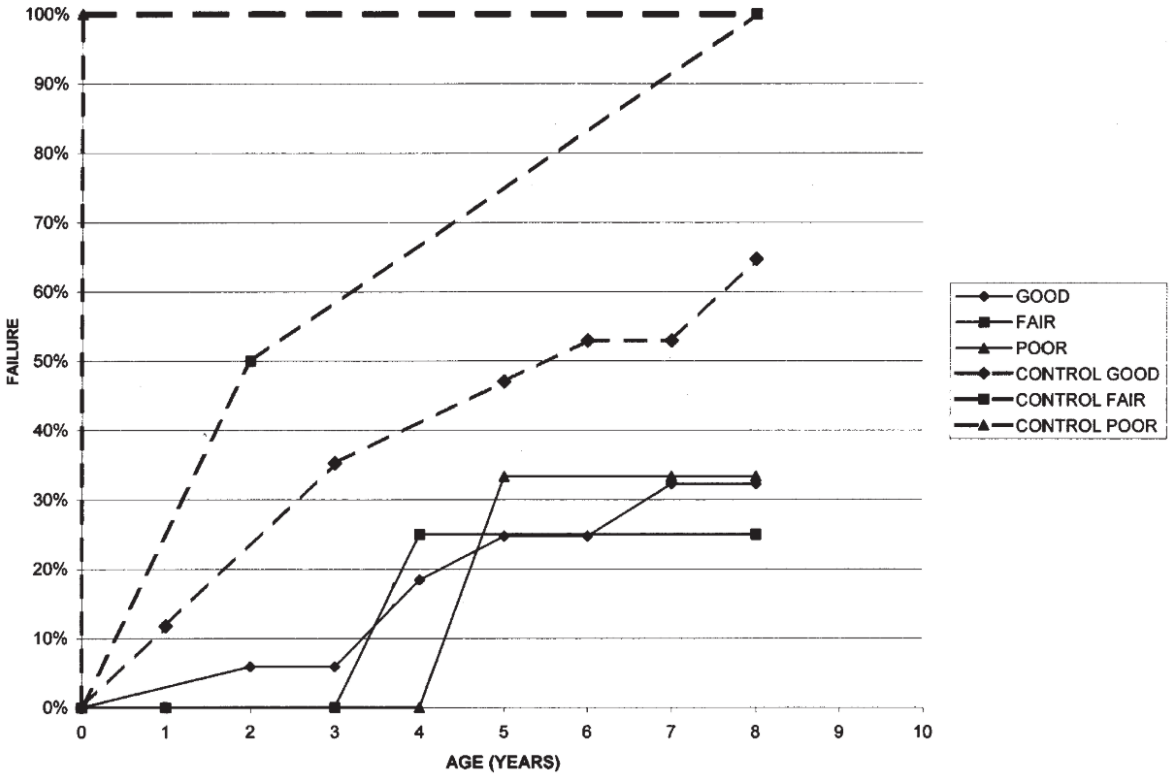

Figure 2-19: Failure Curves for chip seals (Eltahan et al. 1999)

Cuelho et al. (2006) summarized the expected life of several treatments found in different sources. The cost for each type of treatment is also listed in the same literature. The study summarizes the following (Cuelho, Mokawa, & Akin, 2006):

- Thin overlays perform well structurally (mostly impact on SCI and RI values). Some improvement on surface rating have been observed but didn't significantly reduce the extent of distresses subjected to (Johnson, et al. 2007; Wade, M., R. DeSombre 2001).
- The chip seals addresses cracking, bleeding, raveling, oxidation and frictional resistance. From additional layering, the life of the treatment increases (5 year for single layer and 7 year for double layer). Still mixed proposals are suggested by studies (Jahren et al. 2003; Wade, M., R. DeSombre, 2001).

- Micro surfacing creates less disruption to traffic and users. Also reported for less aggregate loss. Initially address rutting but for longer life, it was not effective. Another drawback is that the treatment requires full mixed design based on location and traffic (Johnsonet al. 2007; Labiet al. 2007; Wade, M., R. DeSombre 2001).
- Fog seal is the least expensive and initially protect pavement from accelerated oxidation, but no structural influence found. Suggested that fog seals can be applied over newly applied chip seals (Bolander, 2005; Hicks et al. 1999).
- Cape seals offer longer pavement life. Simply defined by some authors, cape seal is the combination of slurry seal over chip seal (Bolander, 2005).
- Scrub seals are polymer modified emulsion chip seals followed by broom-scrubbing. Seals cracks more than 1/8" wide (Bolander, 2005; Wade, M., R. DeSombre, 2001).

The same study also suggests a set of treatments along with the expected life and cost of treatments. The summary table is shown in Table 2-8:

Table 2-8: Summary of the presrvation treatment life and costs (Cuelho et al. 2006)

Preventive Maintenance Treatment	Treatment Life (years)			Cost per Lane Mile (12- ft width)
	Min	Average	Max	
Crack Sealing	2	4.4	10	$5,300
Thin Overlay	2	8.4	12	$14,600
Chip Seal (Single)	1	5.9	12	$7,800
Chip Seal (Double)	4	7.3	15	$12,600
Micro surfacing	4	7.4	24	$12,600
Cold In-Place Recycling	5	10.6	20	$17,700
Ultrathin Friction Course	7	9.8	12	$31,100
Fog Seal	1	2.2	4	$2,200
Slurry Seal	1	4.8	10	$6,600
Cape Seal	6	9.8	15	$16,700
Scrub Seal	1	3.7	8	$5,800

Vargas-Nordcbeck (2018) studied the performance of chip seals based on the percentage of area cracked, IRI, mean texture depth (MTD) and rut depth. For the 4.5 years long service life of chip seal treatments the following observation was made by the author: performance of the treatment depends on the initial condition of the pavement when the treatments were applied. Those sections in good or fair condition tend to remain in the good or fair condition for a longer time. The same study also concludes that treated sections with chip seals perform better than the untreated sections (Vargas-Nordcbeck, 2018).

Hall et al. (2002) reported that roughness, rutting and fatigue cracking issues can be addressed by thin overlay, chip seals (standalone or combinations) and slurry seal treatment. Crack sealing didn't show any long-term significant effect over IRI, rutting and cracking. The

rest of the treatments have no, or minor effect based on the statistical analysis performed in the study.

Arabali et al. (2017) designed a new method for the non-technical decision makers for the general aviation. Thus, this method applies also for the flexible pavements in different climate regions and traffic level. This method uses an online based tool that contains a database of different pavements and runways at different climatic regions. A benefit-to-cost-ratio analysis is performed to suggest alternatives for the decision makers. The summary of the study came up with 2 decision matrices for National and Regional airports followed by Local and Basic airports. The climatic regions are selected based on the type of airport and the freeze-thaw cycle. The matrix provides with the preservation alternative(s) based on the type and extent of the distresses for varied climatic zones. The study also includes a general guideline for the preservation treatments based on the unit cost of treatment at any referenced year and the expected life of the treatment applied. Table 2-9 is the summary of the treatment alternatives and expected life for each treatment.

Table 2-9: Unit Cost and Expected Treatment Life Comparison, (Arabali et al. 2017)

Treatment name	Relative cost	Unit cost for reference year 2015 ($)	Unit	Expected life (years)
Do Nothing	0	0	-	-
Crack seal or fill	$	0.33-4.92	m	Crack seal: 2.9; crack fill: 4.1
Rejuvenator	$	0.30-0.60	m^2	
Fog or coal tar seal	$	0.30-0.60	m^2	Fog Seal: 3.1; Coal tar seal: 4.9~5.0
Slurry Seal or Micro surfacing	$$	0.90-4.92	m^2	5.0
Chip or cape seal	$$	1.80-4.80	m^2	Chip seal: 5.7; Cape Seal: 6.2
AC Overlay or Mill +Overlay	$$$	w/o milling: 2.40-7.20 w/ milling: 6.00-12.00	m^2	AC Overlay: 11.4; Mill+ Overlay: 14.6
Patch or reconstruction	$$$	538	m^2	5.3
Rehab or reconstruct	$$$$	90	m^2	Variable

Peshkin et al. (2011) recommended a guideline for the pavement preservation techniques for the high-traffic-volume roadways. The guideline was developed based on the survey reports from the agencies. The guideline is the reflection of the agency experience over the years followed by current practices based on existing literatures in 2011. The decisions from the guideline convey many interacting factors i.e.- project selection, materials availability and quality, contractor capabilities, practices and the ambient condition during construction. The study subdivided the overall maintenance and rehabilitation activities as the following types: 1. Pavement Preservation, 2. Pavement Maintenance, 3. Minor Rehabilitation, 4. Routine

Maintenance, 5. Corrective Maintenance, 6. Major Rehabilitation, 7. Reconstruction. **Figure 2-20** is the summary of the process involved in selecting the required selection of preservation treatment. The final choice of decision from the process is then verified through a cost-benefit analysis which allows the user to achieve the most effective treatment at lowest cost. The whole process of selection requires detailed report of the functional and structural condition of the project or network. The historical condition data along with the geometric data, helps the users to choose if any major rehabilitation or reconstruction is warranted. The feasibility and practicality of the output depends on the availability of the historical data.

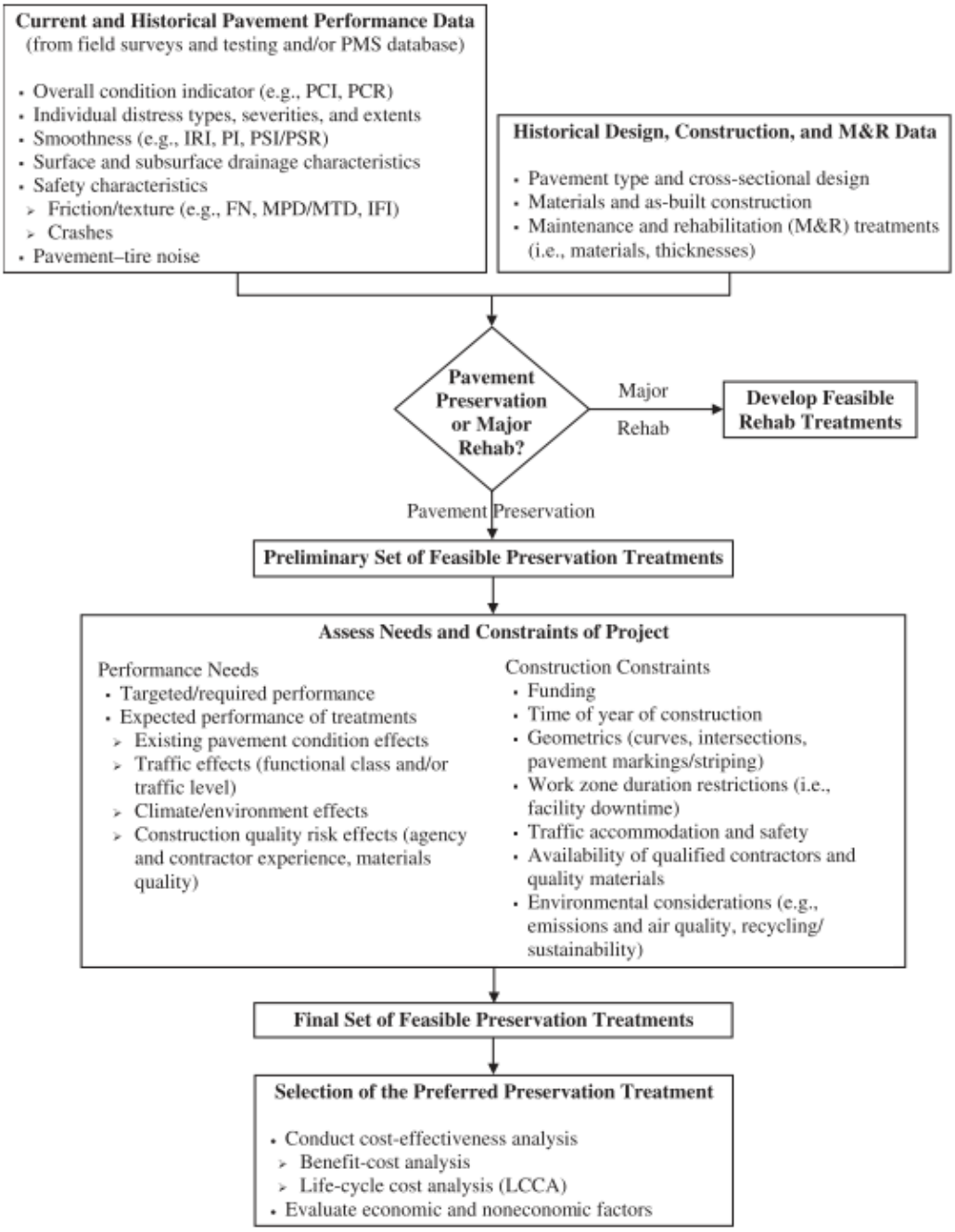

Figure 2-20: Process of selecting preferred treatments for high-traffic-volume-roads

(Peshkin et al. 2011)

2.12 Summary

From the studies covered in the literature review, it has been found that each of the preservation techniques can delay different types of distresses at different extent. Micro surfacing, thinlays and chip seals are the treatments which have major effect on the life and performance of the pavement. Fog seals, slurry seals, cape seals, scrub seals are some of the treatments which help to treat minor cracks and surface distresses. These individual treatments or combination of treatments restore the deteriorated surface rating or pavement condition index (PCI). The literature on the treatments mostly covers the following component of the pavement surface: roughness, cracking, rutting, IRI, mean texture depth etc. No structural evaluation has been recorded on the performance of different treatments. Falling weight Deflectometer is one of the most common non-destructive testing devices in network level management system. After several generations of testing, the impulse loading from the deflectometer has been found the most accurate to help prediction of the mechanistic and strength parameters of the underlying component layers of the pavement. There have been several studies to relate the DBPs with the mechanistic responses of the pavement. There has been no study to observe the effectiveness of the treatments over the DBPs and the mechanistic responses under the loads. Therefore, the present study on the influence of different treatments over the pavement structure is conducted to investigate if the treatments also contribute to the structure of the pavement and longer service life.

3 METHODOLOGY

The methodology chapter discusses the construction data of the treatment sections scrutinized followed by the testing information and data processing. The National Center for Asphalt Technology at Auburn University has two preservation treatment sites in Alabama, the Lee Road 159 and US-280 sections. Preservation treatments were applied to full-scale test sections in 2012 and 2015, respectively. Routine testing of the sections is performed to observe the performance of the treatments. Along with rutting, roughness, friction and crack measurement; falling weight deflectometer (FWD) testing is also performed to investigate the structural condition of the pavement. In this study, the treatment sections from Lee Road 159 site is analyzed as there was considerable duration of time elapsed in service to study performance trend and perform complex statistical modeling. Moreover, common treatments applied in both locations at Alabama are shortlisted for the present study. The data collected from FWD testing are used to measure the deflection basin parameters and backcalculate layer moduli. Measured deflections were temperature corrected and standardized to 9,000 lb. loads to calculate the deflection basin parameters. The FWD files collected from the Dynatest device were used for the backcalculation with ELMOD 6.0 software. For the statistical analysis of the deflection basins and backcalculated moduli, the Statistical Analysis Software (SAS) tool was selected for the study. Finally, the measured parameters of the treated sections are compared to the parameters of the control/untreated sections to measure the extent of structural benefit the treatments are providing to the life of the pavement.

3.1 NCAT's Pavement Preservation Group Study

The Pavement Preservation Group (PG) study at NCAT has both low-volume and high-volume traffic test sections in Alabama. Lee Road 159 in Auburn serves as the low volume setting and highway US-280 is the high-volume traffic route near Opelika, AL. Since the Lee Road 159 sections have been in service for a longer period, the present study mainly focuses on the low-volume traffic route. Lee Road 159 is a two-lane dead-end county road that provides access to a quarry and asphalt plant. The half- mile section is subdivided into 25 treatment sections each 100ft long covering both traffic lanes (inbound: into to the quarry and asphalt plant; outbound: away from the quarry and asphalt plant). 23 sections received treatment and 2 control sections were left untreated. At the time of treatment, the road surface was 14 years old with an average AC thickness of 5.5 inches over a crushed aggregate base of 6 inches average thickness. No further maintenance and rehabilitation works have been performed in the elapsed service life of the treatment sections. To this date, approximately 1 million ESALs have been applied on the outbound lane of the test sections. **Figure 3-1** shows the aerial view of the Lee Road 159 test site.

Figure 3-1: Location and Overview of Lee Road 159 Sections (Vargas-Nordcbeck, 2018)

The high traffic volume PG study sections lies over the westbound direction over the outer lane of highway US 280. There are 46 total 0.1-mile-long sections, including 6 control sections and 6 empty sections. The remaining 34 sections are either standalone treatments or combinations of treatments. The treatments were applied in the summer of 2015 based on the existing condition of the pavement. The control sections were chosen based on the comparative criteria of both high and low cracking, rutting, texture and IRI readings. Moreover, there are 11 segments of the road which were found in the Long-Term Pavement Performance (LTPP) database that helped to extract structural information about the sections. Collected data from cores, LTPP database and construction records show a frequent variability of the layer thicknesses of the underlying layers of the pavement. The segment of the road under study has an accumulated 2.2 million ESALs over the last 4 years of service as of 2019. **Figure 3-2** shows the aerial view of the US-280 test site in Opelika, AL.

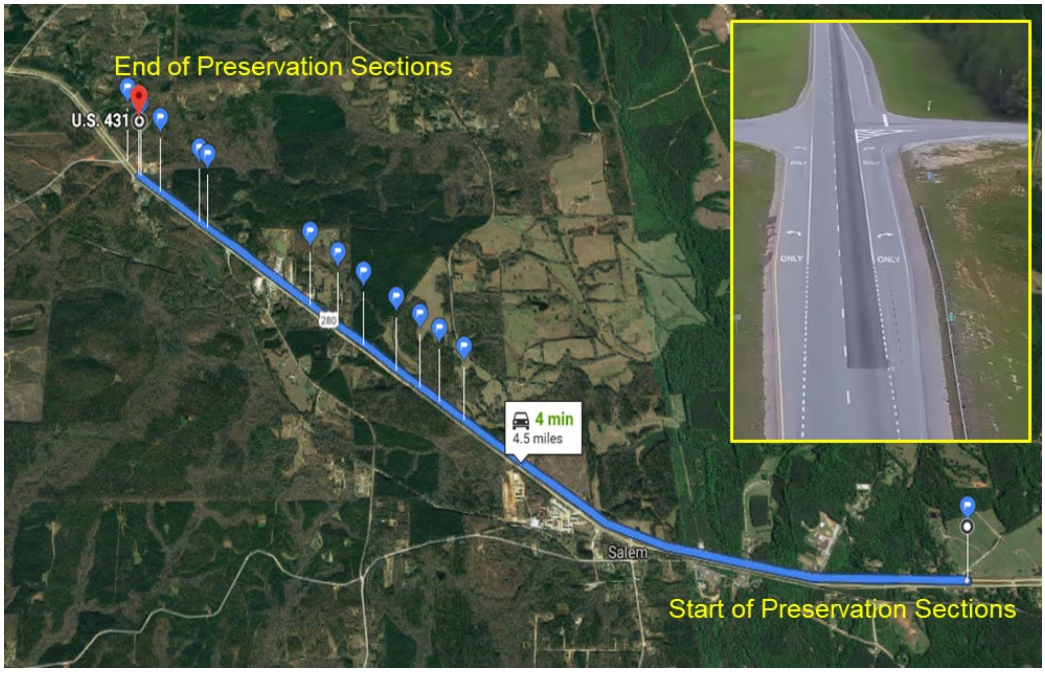

Figure 3-2: Location and Overview of US 280 Sections with LTPP Database points

In this study, the treatments which are common for Lee Road 159 and US-280 are being selected for study. The US-280 preservation sections selected for study also have variability over the layer thicknesses. The layer thicknesses for the selected sections are shown in **Figure 3-3**. The estimation of the layer thicknesses for all the sections are based on the following: core drilling, construction history, GPR data and comparison of the FWD deflections at pretreatment condition. For Lee Road 159, the drilled cores show a limited variability in the measured AC thickness and crushed aggregate base (CAB) which led to the estimation of 5.5 in of AC and 6 in CAB. As homogeneous as built pavement structure is assumed for all the treatment sections, so the layer thicknesses are not varied for the sections within Lee Road 159. The core extraction results along with lift thicknesses at different locations are shown in APPENDIX A.

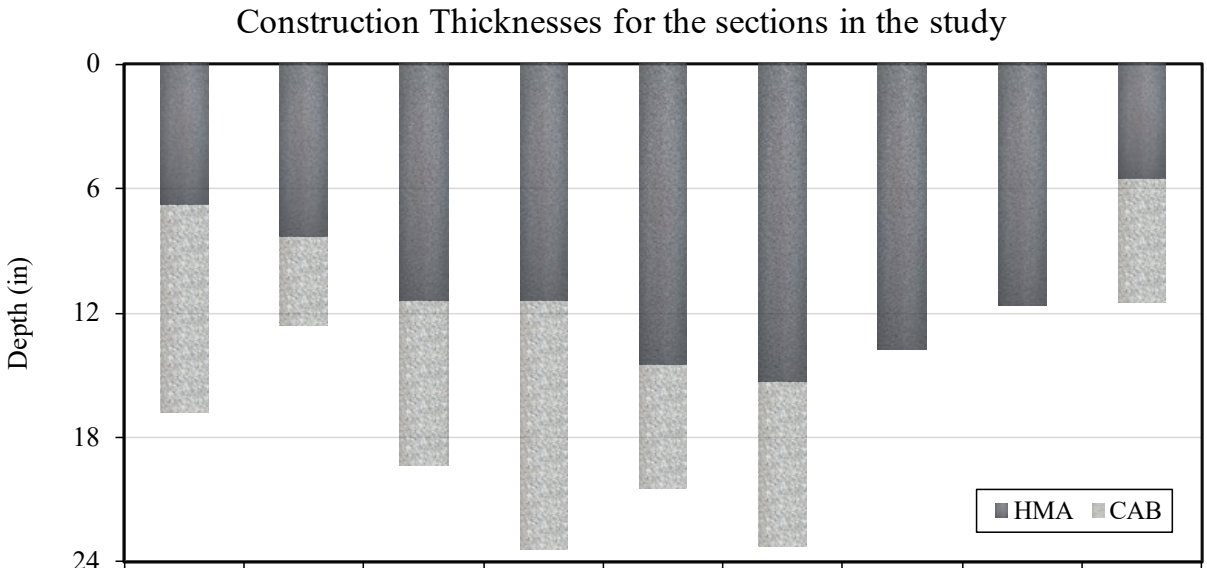

	Sec: 6-8,11-18,36	Sec: 20-25	Sec: 26	Sec: 27,28	Sec: 29	Sec: 40	Sec: 45	Sec: 46	Lee Road 159- All
CAB	10	4.3	8	12	6	8			6
HMA	6.75	8.3	11.4	11.4	14.5	15.3	13.8	11.6	5.5

Figure 3-3: Layer Thicknesses for the pavement sections within the study

3.2 Field Data Collection

On Lee Road 159, FWD testing is performed on a monthly basis. The locations for FWD testing were randomly selected before the test cycle started. Arrangement and drop locations are shown in APPENDIX B. The FWD test is performed on the same locations on each test date. FWD data are collected over both lanes (inbound and outbound) and both wheel paths (inner and outer). Since 2018, as there was no significant change in the parameters being tested, the testing frequency was changed from each month to each quarter.

Testing on highway US 280 requires lane closures due to its route type and traffic level. Thus, to reduce user cost and ensure uninterrupted traffic, the lane closures on US 280 are performed on a

quarterly basis. There are three preselected designated locations spaced at equal distances for FWD testing within each 0.1-mile-long segment.

3.3 Deflection Data

The testing equipment and procedure followed the ASTM D4694, ASTM D 4695 and AASHTO T 295 standards. A Dynatest 8000 model FWD device is used by NCAT at Auburn University for deflection testing. Load magnitudes of 6-kip, 9-kip and 12-kip were applied with a plate radius of 5.91 inches and three replicates were obtained for each load magnitude. Though FHWA also recommends application of 16-kip load but for the present test site does not observe this high speed and high traffic load. Moreover, this high magnitude of load could induce damage to the existing pavement layers. The standard specification requires the variation between the replicates of the load magnitude should be within 3% of tolerance of the target magnitude of load intended to be applied. In the warmup session, the variability was checked before the start of every session. Any deviation causing high variability was addressed by adjusting drop height, cleaning the track or checking the spring and pads (ASTM, 2015). In detailed project level testing, spacing between the locations of consecutive testing are required between 25 ft to 250 ft at one stretch of road (ASTM, 2008). A set of geophones are arranged to measure the deflection basin around the point of load or the center of the load plate. In this study, a total of 9 geophones are located at 0, 8, 12, 18, 24, 36, 48, 60, and 72-in. spacing from the center of load plate.

Figure 3-4 demonstrates the arrangement and spacing of the geophones used in FWD testing in the present study. The geophones used in this study report up to ±0.01 mil accuracy where the minimum resolution for deflection measurement is ±0.04 mils (ASTM, 2015).

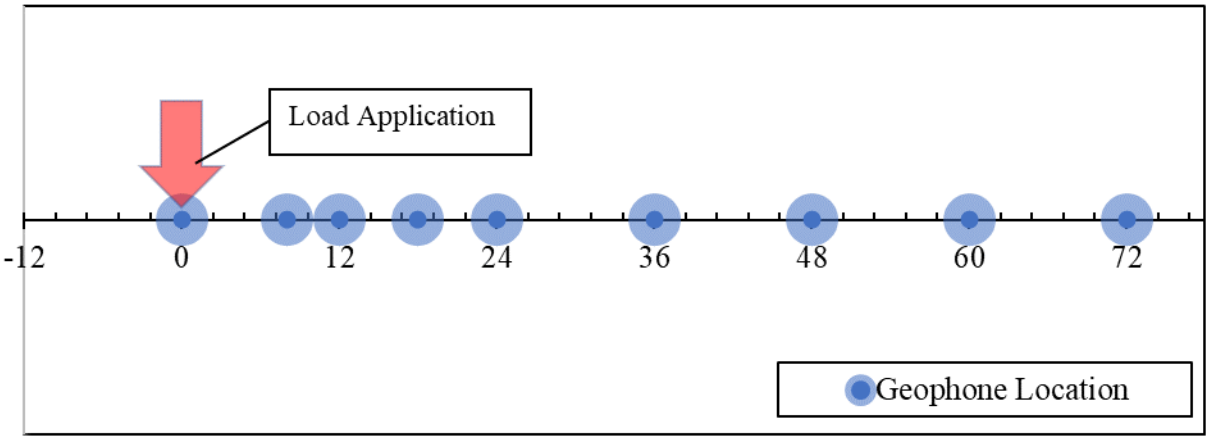

Figure 3-4: Geophone Locations for FWD Testing

3.3.1 Elimination of Outliers

The first step in the data processing involves elimination of outlier values. The outliers can be caused by several reasons, such as seating error, presence of cracking on the surface or irregularities, cleanliness of surface, deflections beyond mechanical limit etc. (Huang, 2004). The collected deflection files were stored in a database. The errors could be classified within 2 major types:

1. Zero deflection reading under load plate been recorded. The possible reasons can be explained by a seating error and systematic errors as per FHWA.
2. Measured deflection at larger radial distance from the load plate is higher than measured deflection at a point closer to the center of load. These type of readings lead to erroneous backcalculated modulus (Smith et al. 2017).

A schematic diagram of the shape for the deflection basins with errors types 1 and 2 along with correct deflections are shown in **Figure 3-5**.

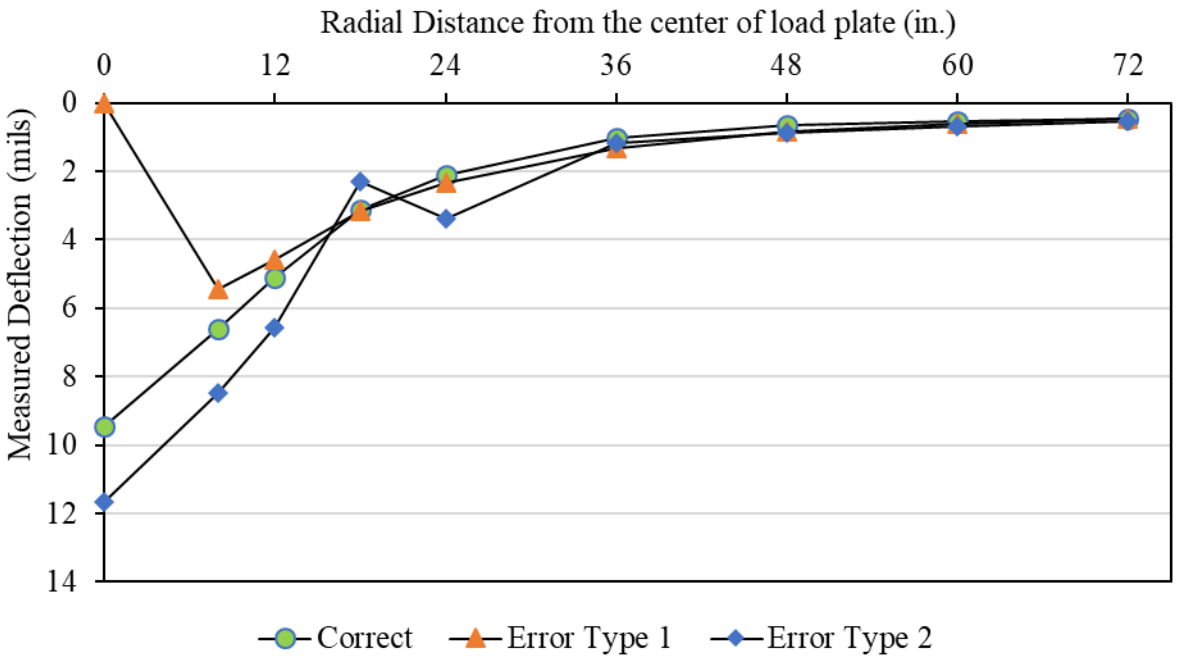

Figure 3-5: Types of Errors that was filtered as outliers

The drops with irregular deflections which fall into Type 1 or Type 2 errors were discarded automatically and not included in the deflection basin parameters (DBPs) and backcalculation procedure. All other noises and random errors cannot be eliminated but were reduced by averaging out all the deflections within a set of standard drops at multiple magnitudes and standardizing the deflections to 9-kip load deflections. As a result, all the sets drops at multiple magnitudes at a single location at a single day are aggregated to one single drop of 9-kip magnitude. Load Correction

Due to the viscoelastic behavior of asphalt, mix designs, non-uniform support condition etc., the deflections measured in different loading conditions don't exhibit a linear relationship.

To achieve a test load close to the design load of 18-kip single axle load or 9-kip wheel load, all the deflections at different load magnitudes were standardized to a 9-kip (40 KN) load (Smith et al. 2017). To address this issue, all the deflections within a set of load magnitudes along with replicates were used to develop a linear regression equation. **Figure 3-6** shows an example of the linear relationship between measured deflections at different radial distances and applied load. The R^2 values are close to unity and the regression equations are used to measure a standardized deflection at a specific radial distance accounting for all the magnitude of loads at that radial distance within that set of testing.

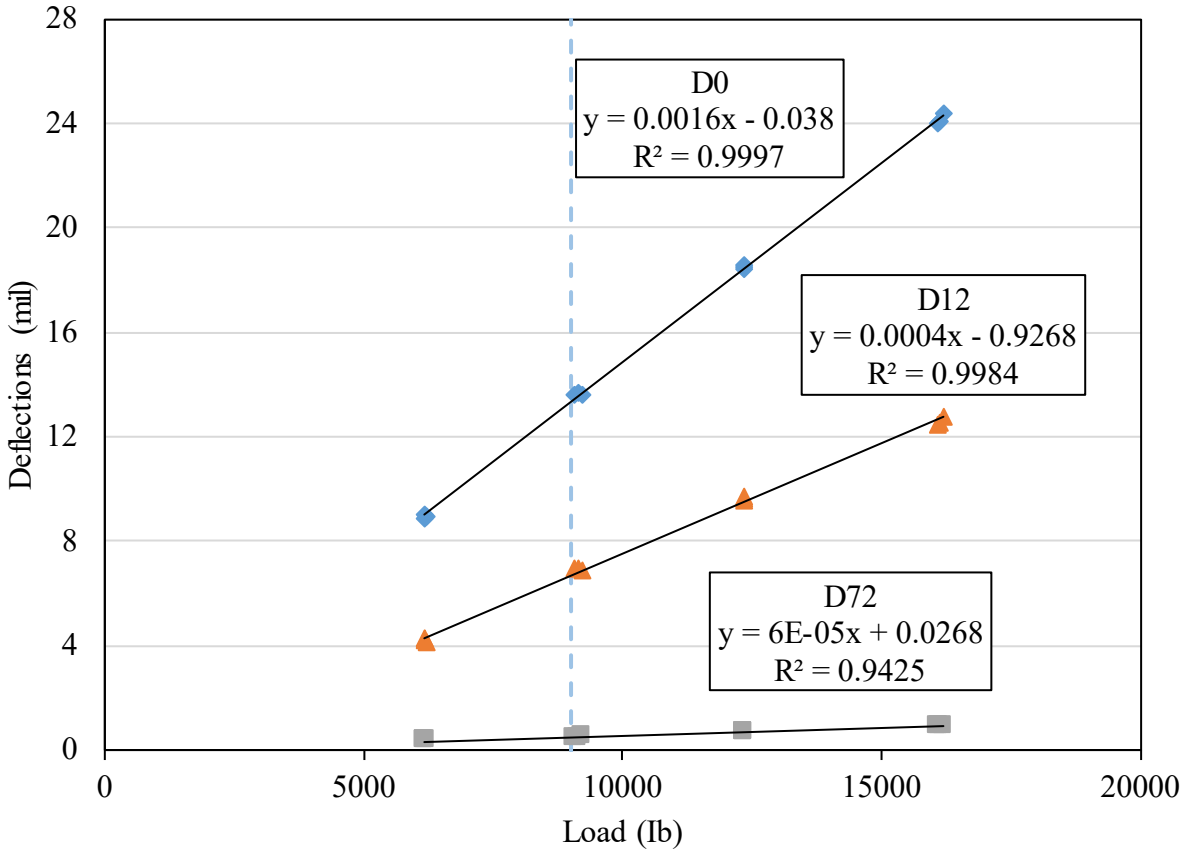

Figure 3-6: Linear Regression lines for deflections vs load relationship from a set of drops

At each testing location, a set of nine regression equations (for D_1- D_9) from a set of 3 drops was developed to measure the deflections at the standard 9-kip wheel load. In the initial stage of research, a 16-kip load was applied to the pavement surface which was found to be overstressing the pavement layer. Again, the test sections were in a low traffic low speed traffic location, it was decided not to apply 16-kip load anymore. The R^2 values signify that there is a strong correlation between measured deflection on a same date on same test location and magnitude of applied loads irrespective of the radial distance of the sensor from the center of the load plate.

3.3.2 Temperature Correction

Temperature and seasonal effects affect the behavior of the asphalt concrete (AC) modulus. Different temperatures at different seasons would cause variation in the elastic modulus of the AC, base and subgrade. **Figure 3-7** shows an example of the relationship between pavement temperature and deflections at distances of 0, 18 and 72 in. from the center of the load plate. The data points were collected on the same test location over a one-year cycle to capture a wide range of temperatures and observe the effect of temperature over the measured deflections at various radial distances. There is scatter among the data points which is due to variability of load magnitude and the conditions among test dates.

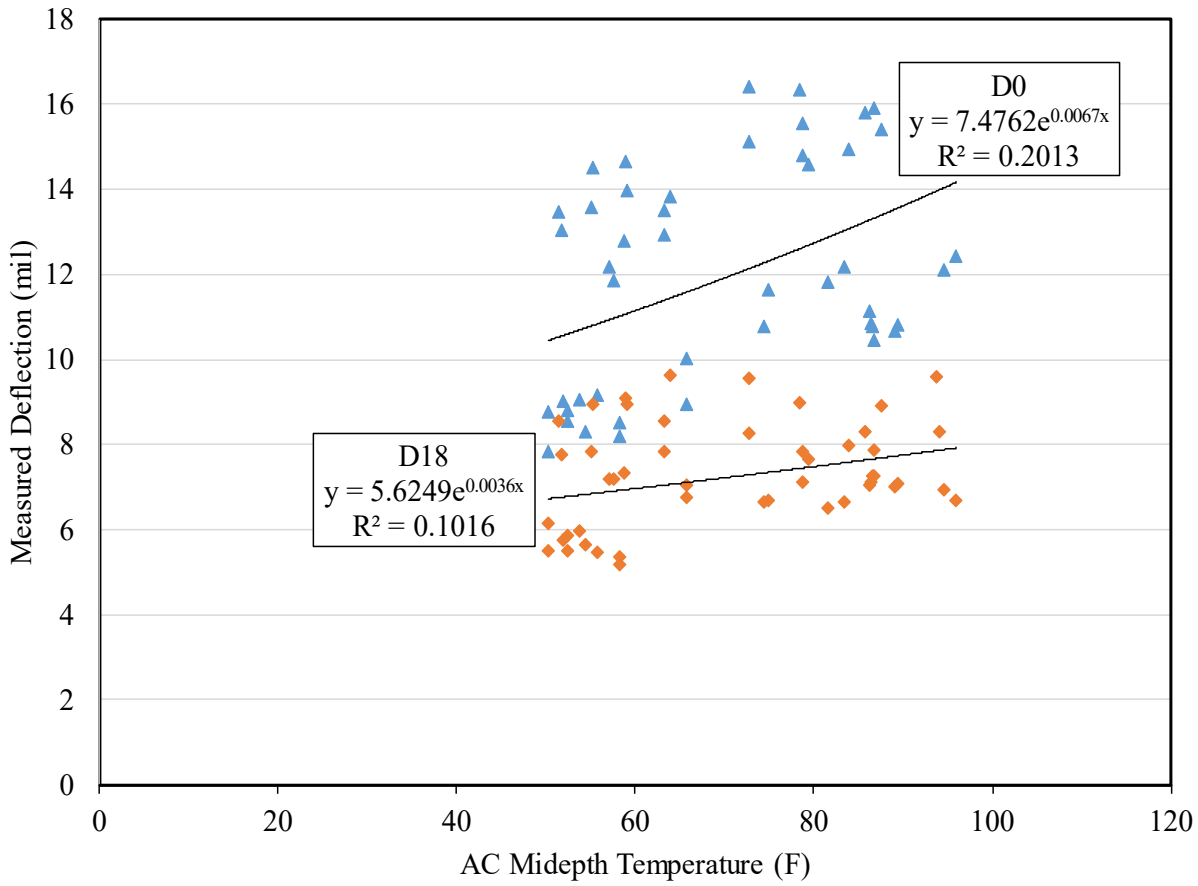

Figure 3-7: Load Corrected Deflections at different pavement mid-depth temperatures

An exponential regression model was used to determine the relationship between asphalt concrete mid-depth temperature according to BELLS3 equation and measured load corrected deflections. The R^2-values were observed to understand the sensitivity of the deflections to the seasonal temperature cycles. The data presented in **Figure 3-7** are the data points over the year of 2015 in the outbound lane on a section treated with chip seal and crack sealing. Thus, the deflection values also have the seasonal effect, damage due to wheel loads and testing variability incorporated within. The literature review concludes the deflections closer to the load plate are representative of the characteristics of all the underlying layers where the deflections at distant radial distance (D_{60} or D_{72}) are representative of the characteristics of the subgrade. The base and

subgrade layers are less sensitive to temperature while the asphalt layer is more susceptible to temperature changes. Literature shows the practice of temperature correction of the deflection ranging from D_0 to D_{36} (Vrtis, 2017). In the dataset, it was found that the deflections are showing proper correlation with temperature up to D_{60} or D_{72}, so the measured deflections at all the radial distances were corrected to temperature. All the deflections were standardized to 68º F in accordance with the procedure mentioned in AASHTO 1993 Design Guide (AASHTO, 1993; SHRP, 1993). The temperature correction factors were collected based on Equation [25] developed for a 5.5 in. AC layer thickness.

$$T(t) = -0.0074 \times T_d + 1.5183 \quad [25]$$

$$T(t) = \frac{d_{temperature\ corrected}}{d_{measured}} \quad [26]$$

Where,

$T(t)$= Temperature Correction Factor

T_d= Estimated AC mid-depth temperature according to BELLS3 equation (ºF)

$d_{temperature\ corrected}$ = Temperature corrected deflection (mil)

$d_{measured}$= Measured deflection at given AC temperature (mil)

After the temperature correction at 68º F of the measured deflections, the corrected deflections in **Figure 3-8** show the reduced R^2 values for the exponential regression equations for the temperature corrected deflection and estimated mid-depth AC temperatures from the measured

air temperature and surface temperature. It can be concluded that the temperature correction at 68º F eliminated the temperature effect from the dataset. The temperature correction was performed for all the offsets within the dataset to assure the homogeneity and same correction for all the deflection measurement on the dataset.

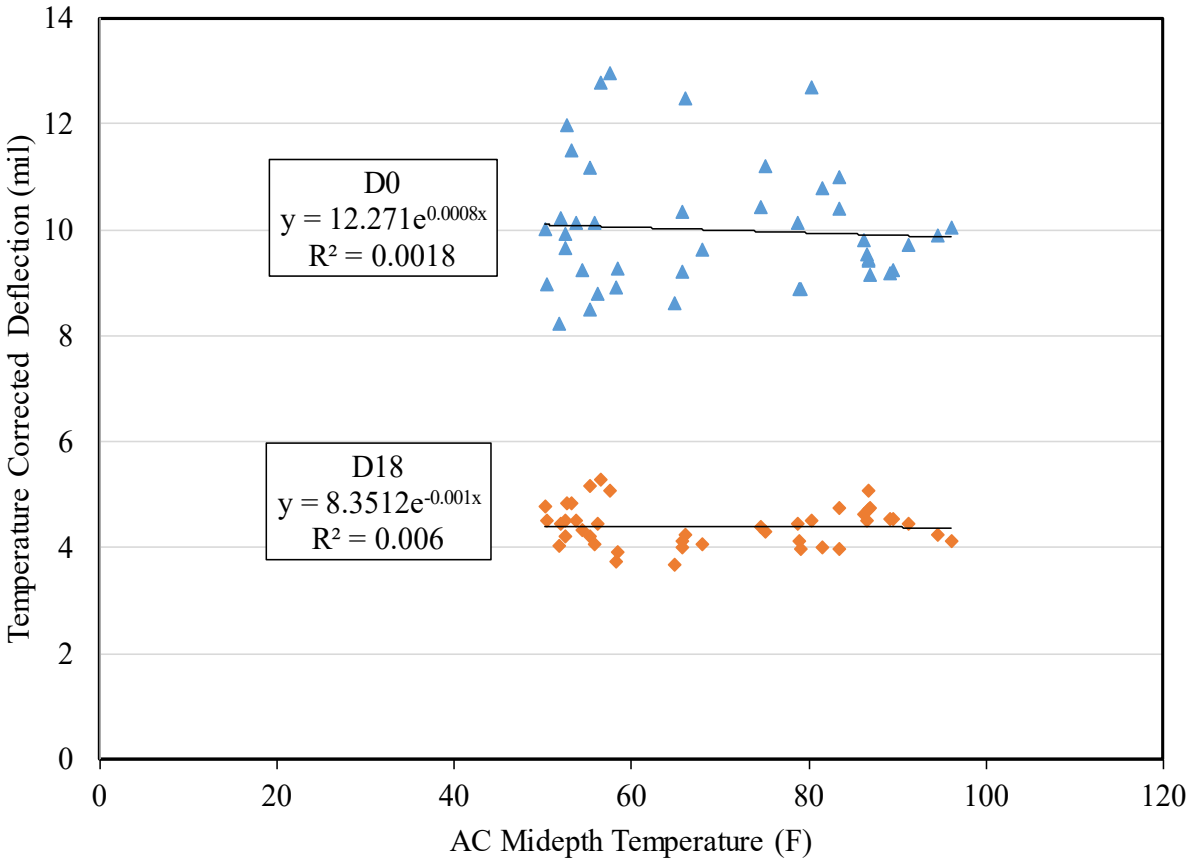

Figure 3-8: Load and Temperature Corrected Deflections vs Temperature

3.4 Statistical analysis

The statistical analysis of the collected data was performed using Statistical Analysis Software (SAS). For this study, several of the statistical procedures were performed: numerical analysis of

the collected data to generate basic statistical models, Analysis of Variance (ANOVA), time series mixed modeling, and time series forecast.

3.4.1 Analysis of Variance (ANOVA)

Paired t-test is one of the statistical testing for the analysis of outputs in pairs. But in pavement research, there are a lot of factors that affect the outputs. In this study, there are several sections where the same treatment was applied multiple times or combination of two or three different types of treatments were applied. For this reason, analysis of variance was found to be more effective in this instance. Moreover, several pairs of all levels of factors enhances the probability of Type-1 error in the output results. The ANOVA procedure can process different levels of a single factor or treatment. If y_{ij} is an entry for j-th replicate at i-th level of factor. For each level of factor there would be *n* observations. Thus, for total a levels of factors the total number of entries will be $N = a \times n$. The experimental model can be written as Equation [27].

$$y_{ij} = \mu_i + \epsilon_{ij} \quad [27]$$

Where,

$i = 1,2,3, \ldots a$= Level of factors

$j = 1,2,3, \ldots n$= Number of replicates or repetitions at each treatment level

$\mu_i =$ Mean of the i-th level of factor

$\epsilon_{ij} =$ Random error at i-th level of factor at j-th replicate

The random error ϵ_{ij} incorporates all random error as source variability, measurements, uncontrolled factors etc. The μ_i or the mean for i-th level of treatment might have an effect based on the specific level of treatment which may vary from μ_{i+1}. Thus, another parameter treatment

effect is introduced. Equation [27] is explained as means model where there is another equation developed as the effects model shown in Equation [28].

$$y_{ij} = \mu + \tau_i + \epsilon_{ij} \quad [28]$$

Where,

$i = 1,2,3, \ldots a$= Level of factors

$j = 1,2,3, \ldots n$= Number of replicates or repetitions at each treatment level

$\mu =$ Overall mean for all measurements at all levels and replicates

$\tau_i =$ Treatment effect for the i-th level of treatment

$\epsilon_{ij} =$ Random error at i-th level of factor at j-th replicate

In this study, the ANOVA for the deflection basin parameters or backcalculated moduli were analyzed based on fixed effect modeling. It was considered that all treatment types and repeated applications have fixed effect over the observations which is donated by τ_i. The total corrected sum of squares (SS_T) is a measurement of overall variability of the data with $an - 1$degrees of freedom. Equation [29] shows the equation for SS_T calculation and equation [31] shows the sum of squares due to errors (SS_E) calculation. The degrees of freedom for SS_E is $n(a-1)$ or $N - a$. $SS_{Treatment}$ is the measurement of sum of squares between treatments with a degree of freedom $a - 1$.

$$SS_{Treatment} = SS_T - SS_E \quad [29]$$

$$SS_T = \sum_{i=1}^{a}\sum_{j=1}^{n}(y_{ij} - \bar{y}_{..})^2 = \sum_{i=1}^{a}\sum_{j=1}^{n}[(\bar{y}_{i.} - \bar{y}_{..}) + (y_{ij} - \bar{y}_{i.})]^2 \quad [30]$$

$$SS_E = \sum_{i=1}^{a}\sum_{j=1}^{n}(y_{ij} - \bar{y}_{i.})^2 \quad [31]$$

Where,

SS_T = Total corrected sum of squares of the overall data

SS_E = Sum of squares due to errors due to treatments

$SS_{Treatment}$ = Sum of squares of differences

y_{ij} = observation at i-th level of treatment at j-th replicate

$\bar{y}_{i.}$ = Mean of the j-th observation at i-th level of treatment

$\bar{y}_{..}$ = Overall mean of the data

The null hypothesis has been adopted for the calculation which involves calculation of mean of sum of squares for treatments and errors. Equation [32] shows the steps to calculate the F_0 value. Cochran's theorem for null hypothesis implies that if the null hypothesis of no difference in treatments is true, the F_0 value lies within the F distribution with $a - 1$ and $N - a$ degrees of freedom. To reject the null hypothesis, which is that the treatment means are equal, the following statement should be true: $F_0 > F_{\alpha,\alpha-1,N-a}$ (Montgomery, 2013).

$$F_0 = \frac{SS_{Treatment}/(a-1)}{SS_E/(N-a)} = \frac{MS_{Treatment}}{MS_E} \quad [32]$$

3.4.2 Linear Mixed Effects Model

Linear mixed effect modeling is one of the most popular statistical models for longitudinal data analysis. The mixed models aim at observing the change in response over the period of study alongside investigating the factors that impede the influence. These modeling protocols are more sensitive as the data collected over the same treated sections might appear positively correlated and the random effects are heterogeneous in manner. The linear mixed model accounts for both the correlation and heterogeneity. The longitudinal data convey the following parameters- the mean response over time and the covariance among repeated measures. To achieve a good fit model for longitudinal data the tasks to be performed are: (1) choice of a covariance model that provides a good fit to the variance and covariance, (2) fitting a linear regression model that fits well to the mean of the outcome variable.

The linear mixed effect modelling considers both fixed effect and random effect. The fixed effect incorporates the mean response of all the population group. As an example, the measure of damage caused by the vehicle wheels, aging and in situ subgrade condition are the fixed effects that are common for all the treatment sections. The subject-specific effects are considered random effects which incorporates the changes in observation due to the type of treatment. Linear regressive models are used to model the mean response.

$$E(Y_{ij}) = \mu_{ij} = \beta_1 + \beta_2 t_{ij} = \beta_1 X_{ij1} + \beta_2 X_{ij2} + \beta_3 X_{ij3} + \cdots + \beta_p X_{ijp} \quad [33]$$

Where,

$\beta_1, \beta_2, \beta_3 \ldots . \beta_p =$ Regression coefficients

$X_{ij1} = 1, X_{ij2} = t_{ij}$

$X_{ij3} =$ Treatment Indicator

$X_{ij4} = t_{ij} \times$ Treatment Indicator

To address the random subject effect in the dataset, the covariance modelling is performed among the repeated measures. This is assumed that all the observation has an "underlying level of response" for all the time instances as in example a minimum measurement for all the deflections. Thus, the subject effect is considered to random effect and the equation [33] changes to Equation [34].

$$Y_{ij} = \beta_1 + \beta_2 X_{ij2} + \beta_3 X_{ij3} + \cdots + \beta_p X_{ijp} + b_i + \varepsilon_{ij} \qquad [34]$$

Where,

$b_i =$ Subject effect

$\varepsilon_{ij} =$ Within- subject measurement error

Furthermore, it is assumed that b_i and ε_{ij} are mutually independent with fulfilled normality assumptions. The Equation [34] can be represented as the linear mixed effect model for longitudinal data. There are few more complicated modeling of variances and covariances which were not required to cover for the present study (Fitzmaurice, Laird, & Ware, 2011).

3.4.3 Performance Forecast

Literature suggests many forecasting models where autoregressive moving average (ARMA) or autoregressive integrated moving average (ARIMA) models are very common. The generic form of the model is ARIMA (p, d, q) where p stands for the autoregressive (AR) order, d stands for difference order (I) and q stands for the moving average (MA) order. The basic difference between ARMA and ARIMA is the stationarity of the data. If the data are stationary, the difference order (I) is 0 and the ARIMA turns into ARMA model. If the model is ARIMA (1,0,0) it can be written as AR (1) model in simple notation. In a similar fashion, if the model is ARIMA (0, 0, 1), the model can be denoted as MA (1) model. If the ARIMA model fits in to seasonal ARIMA model the generic model is written as ARIMA (p, d, q) × (P, D, Q) model.

From the white noise data, if the residuals have higher correlation with a trend or seasonality, the data are not considered stationary. The Box- Jenkin's method for ARIMA models requires the data to be stationary. Therefore, the differencing process is performed to make the data stationary. The ARMA model comprises of two approaches to handle univariate time series- autoregressive (AR) models and moving average (MA) models. AR model is the linear regression model correlating the present data to one or more previous data on the same series. The general model for AR can be simply written as Equation [36].

$$X_t = \delta + \phi_1 X_{t-1} + \phi_2 X_{t-2} + \cdots + \phi_p X_{t-1} + A_t \quad [35]$$

$$\delta = \left(1 - \sum_{i=1}^{p} \phi_i\right)\mu \quad [36]$$

Where,

X_t = The times series

A_t = White noise

μ = The process means.

$p =$ The order of autoregression model

Another common model for time series analysis is the moving average model which correlates the white noise or random shocks to the observations of the study. Fitting MA regression is more challenging than AR where the random shocks within the observations in the past are carried over to the future readings. Moreover, it is quite troublesome to fit the error terms in a non-linear regression model. The generic model for moving average (MA) estimate can be written as Equation [37].

$$X_t = \mu + A_t - \theta_1 A_{t-1} - \theta_2 A_{t-2} - \cdots - \theta_p A_{t-q} \qquad [37]$$

Where,

X_t = The times series

A_t = White noise

μ = The process means

$q =$ The order of moving average model

As in the MA modeling, means from the iterative non-linear method is used rather linear least square for AR models- makes the interpretation less obvious than the AR modeling. The

prediction model adopted in this study predicts forecast values considering moving average (MA) modeling. Autocorrelation factor (ACF) and partial autocorrelation factor (PACF) are very useful for selecting the order of the models. The ACF and PACF values and patterns suggests a user if there is needed to design the forecast model with MA model alone or both the AR and MA model together.

Finally, the Box- Jenkins model is adopted for the time series analysis and forecasting of the parameters. There are few steps for developing a Box- Jenkins timeseries model: (1) Model Identification, (2) Model Estimation, and (3) Model Validation. The model can be applicable if the data are stationary. If not, then the data should be made stationary by differencing of the data. In some cases, the series mean is subtracted from the dataset being analyzed. This develops a series with a mean of zero. This model allows to develop models incorporating seasonality over the AR and MA models (Box & Jenkins, 1994).

3.5 Required Overlay Thickness Calculation

In the present study, required overlay thickness has been calculated as a part of quantification of the structural requirement of the pavement sections over the months elapsed in service. The AASHTO 1993 provides a set of equations to measure the composite pavement modulus (E_p) from the measured FWD deflections. Trial and error process up to 25 iterations for each drop was performed to estimate the representative composite pavement modulus. The equation to measure center deflection from the composite pavement modulus is shown as Equation [38]. The effective structural number of the pavement structural number was computed based on the correlation equation shown in Equation [39].

$$d_0 = 1.5\,pa\left\{\frac{1}{M_R\sqrt{1+\left(\frac{D}{a}\sqrt[3]{\frac{E_p}{M_R}}\right)^2}}+\frac{\left[1-\frac{1}{\sqrt{1+\left(\frac{D}{a}\right)^2}}\right]}{E_P}\right\} \quad [38]$$

Where,

P = Load on the load plate (lbs.)

a = Radius of the load plate (in)

D = Total thickness of the pavement on top of subgrade (in)

E_p = Composite pavement modulus (psi)

M_R = Modulus of resilience of the subgrade (psi)

$$SN_{eff} = 0.0045D\sqrt[3]{E_p} \quad [39]$$

Where,

SN_{eff} = Effective structural number

E_p = Composite pavement modulus (psi)

Using Equation [39], the calculated effective structural number of the treated sections were collected over the duration of the analysis period. The required overlay thickness is measured based on the difference between effective structural number and required structural number. The required structural number was calculated for each individual drop at each location

over the analysis period. The AASHTO 1993 Design equation for required structural number is calculated using Equation [40]. Alike the composite pavement modulus calculation in this study, the calculation of the required SN also involves trial and error process up to 7 iterations.

$$\log_{10}(W_{18}) = Z_R \times S_0 + 9.36 \times \log_{10}(SN+1) - 0.20 + \frac{\log_{10}\left[\frac{\Delta PSI}{4.2-1.5}\right]}{0.40 + \frac{1094}{(SN+1)^{5.19}}} + 2.32 \times \log_{10}(M_R) - 8.07 \quad [40]$$

Where,

W_{18} = Accumulated future ESALs over the life of the pavement

S_0 = Overall Standard Deviation

R = Design Reliability

ΔPSI = Design Serviceability Loss

Z_R = Standard Normal Deviate

P_t = Terminal Serviceability

For the present study, the future ESAL was projected for 20 years of design life with 5% traffic growth, 80% directional distribution, 80% Truck traffic- resulting to a future ESAL of 3.4 million ESALs. The other parameters and their values used in Equation [40] to calculate the required SN are tabulated in Table 3-1.

Table 3-1: Values of the parameters used in SNreq calculation

Parameters	Values
W_{18}	3.40E+06 ESALs
log (W_{18})	6.53E+00
R	90%
Z_R	-1.28164
S_0	0.45
P_t	2.0
ΔPSI	2.2

The required overlay thickness at each month was calculated using the difference between the computed required SN and computed effective SN, divided by the structural coefficient of the overlay material. Equation [41] shows the equation to calculate the required overlay thickness of a pavement.

$$D_{OL} = \frac{SN_{required} - SN_{effective}}{a_1} \quad [41]$$

Where,

D_{OL} = Required overlay thickness (in)

$SN_{required}$ = Required Structural Number

$SN_{effective}$ = Effective Structural Number

a_1 = Structural Co-efficient of the overlay material (=0.44)

The required overlay thickness over the years of analysis for all the treatment sections were collected and separate cumulative distribution function (CDF) were prepared for each year to compare the structural need of the treatment sections over the elapsed years of service. Each of the CDF curve includes around 5400 data points representing the overlay thickness requirement measured at 19 treated sections, 8 drop locations, 3 load magnitudes and 12 months of testing each year.

3.6 Summary

It can be concluded from the methodology that there are structured processes for outlier detection, elimination of outliers and cleaning up the dataset for analysis which was explained in Section 3.3. The statistical analysis methods were selected to represent the most accurate and sensible outputs based on the suitability of the dataset being studied. As the dataset is mostly the same repeated observation over time, there was enough suitability of the linear mixed model and ARIMA modeling of the data as per the literature review. The statistical analysis models are explained in Section 3.4. Finally, quantification of the structural deficit was performed by computing required overlay thickness over the elapsed service life within the analysis period. The outputs provide the shift of the structural requirement along with the ranking of the overall structural health of preservation sections as a whole.

4 RESULTS

The National Center for Asphalt Technology (NCAT) has two pavement preservation sites in Auburn, Alabama. For the analysis and results, the low traffic volume treatment sections located at Lee Road 159 were found to be the eligible candidates for the present study. Availability of data over 7 years and more accurately recorded ESALs are the two major reasons that qualify Lee Road 159 for the study. Treatments were sub-grouped among the following five major types: Standalone Treatments, Chip Seals, Micro surfacing, Thinlays and Combination of Treatments. Table 4-1 shows the treatments, the section ID, and the assigned group for analysis.

The study results were compared with the control section within the same group assigned. The high cracking control section (L4) was assigned as "Untreated" or "Control" for the study. The collected cores from Lee Road 159 and GPR results help the study considering that all the sections within the test location are similar in geometry as explained in Section 3.1. Thus, the comparison of the structural performance does not require other subdivisions based on the layer thicknesses, structural properties of each layer and age of the pavement. Based on the literature review the following parameters are selected for the analysis: Central Deflection under the load plate (D_0), Base Damage Index (BDI), Base Curvature Index (BCI), Area Under Pavement Profile (AUPP), Required Overlay thickness (D_{OL}) and backcalculated layer modulus of the surface course (E_{AC}). The parameters were tested for statistical significance (P-value test) followed by the forecasting of the parameter using the ARIMA models.

Table 4-1: Treatments and Treatment Groups Shortlisted

Treatment Name	Section ID	Groups
Control section with high cracking	L4	Control or Untreated
Rejuvenating fog seal	L1	Standalone
Crack sealing only	L5	Standalone
FiberMat chip seal	L2	Chip Seals Group
Chip seal	L6	Chip Seals Group
Chip seal w/ crack sealing	L7	Chip Seals Group
Triple layer chip seal	L8	Chip Seals Group
Double layer chip seal	L9	Chip Seals Group
Scrub seal	L16	Chip Seals Group
Single layer micro surface	L11	Micro surfacing Group
Single layer micro surface w/ crack sealing	L12	Micro surfacing Group
Double layer micro surface	L13	Micro surfacing Group
Cape seal	L10	Combinations Group
FiberMat Cape seal	L14	Combinations Group
Scrub Cape seal	L15	Combinations Group
Thinlay on FiberMat chip seal	L18	Combinations Group
Thinlay	L19	Thinlay Group
Polymer modified thinlay	L21	Thinlay Group
Ultra-thin bonded thinlay	L22	Thinlay Group

4.1 Center Deflection Under Loading Plate (D_0)

Center Deflection under loading plate is the preliminary point of investigation in this study. Though the deflection value does not represent a specific layer, rather represents the overall structural health of the pavement. The magnitude of the center deflection provides the overall structural health of the pavement; thus, it can be marked as the starting point of the result analysis. Higher deflections are an indication of a weaker pavement structure when assumed that all the pavement sections being compared are of equal thicknesses underneath the surface layer. All the deflections mentioned in the sections are standardized to 9,000 lb. load deflection and temperatures are normalized to 68ºF using AASHTO 1993 set of equations for the non-destructive testing with falling weight reflectometer.

4.1.1 Standalone Group Results

The standalone group includes of the rejuvenating fog seal and crack sealing. All the surface treatments were applied in as-is condition of the pavement without prior maintenance works except surface preparations. For the thinlay group, the top of AC layer was milled off before construction of the thinlay. The group results show how effective the individual treatment practices are to sustain the structural condition of the pavement.

All the measured center deflection over all the treatment groups were tested for the fittest distribution type. Most of the treated section mean center deflection over time showed Weibull distribution except the single layer chip seal treated sections which are normally distributed. The generalized Weibull distribution function can be demonstrated as Equation 42. The details of the distributions and fitting information are provided in APPENDIX C.

$$f(t) = \frac{\beta}{\eta}\left(\frac{t-\gamma}{\eta}\right)^{\beta-1} e^{-\left(\frac{t-\gamma}{\eta}\right)^{\beta}} \quad [42]$$

Where,

$$f(t) > 0, t \geq \gamma, \beta > 0, \eta > 0, -\infty < \gamma < +\infty$$

$\eta = Scale\ Parameter$

$\beta = Shape\ Parameter$

$\gamma = Location\ Parameter$

Table 4-2 shows the summary statistics for the standalone group treatments along with the control section. The mean and summary statistics of the center deflections measured over the 77 months of post application service are tabulated. The crack seal shows a higher deflection mean than the control section while the standard deviation and coefficient of variation is also higher than the control section. The coefficient of variation (COV), which is the statistical measurement of the variability of the data shows that the crack seal and control sections yield 33.1% and 26%, respectively. Fog seal treated sections shows lower COV values which means the collected center deflections for those treatment sections have lower variability over the service period.

Table 4-2: Summary Statistics of the D_0 values for the standalone treatments group

Treatment	Mean	Std Dev	Min	Max	N	COV
Fog Seal	15.7	2.1	11.0	22.6	521	13.2
Crack Seal	17.6	5.8	4.9	35.6	518	33.1
Control	16.0	4.2	8.1	33.3	519	26.0

The load standardized and temperature corrected center deflection values collected over the time elapsed are plotted within bar charts and the trends were observed. In the present study, there are few definitions of terminology are required. They are pretreatment, posttreatment and present. The summary of the definition of the terms are provided in Table 4-3.

Table 4-3: Definition of terminology marking time stamps

Term	Time	Point of Time
Pretreatment	August 2012	Pretreatment FWD testing results
Posttreatment	January 2013	FWD testing at 76K Cum ESALs on Outbound lane, 5 months apart
Present	May 2019	Most recent testing at 1.1M Cum ESALs on Outbound lane,77 months

The pretreatment, posttreatment and present values for the standalone treatment group are plotted in **Figure 4-1**. A paired t-test at 95% confidence level was performed to assess the significance of the differences between the pretreatment and posttreatment values. The p-values of the paired t-test results are shown in APPENDIX D.

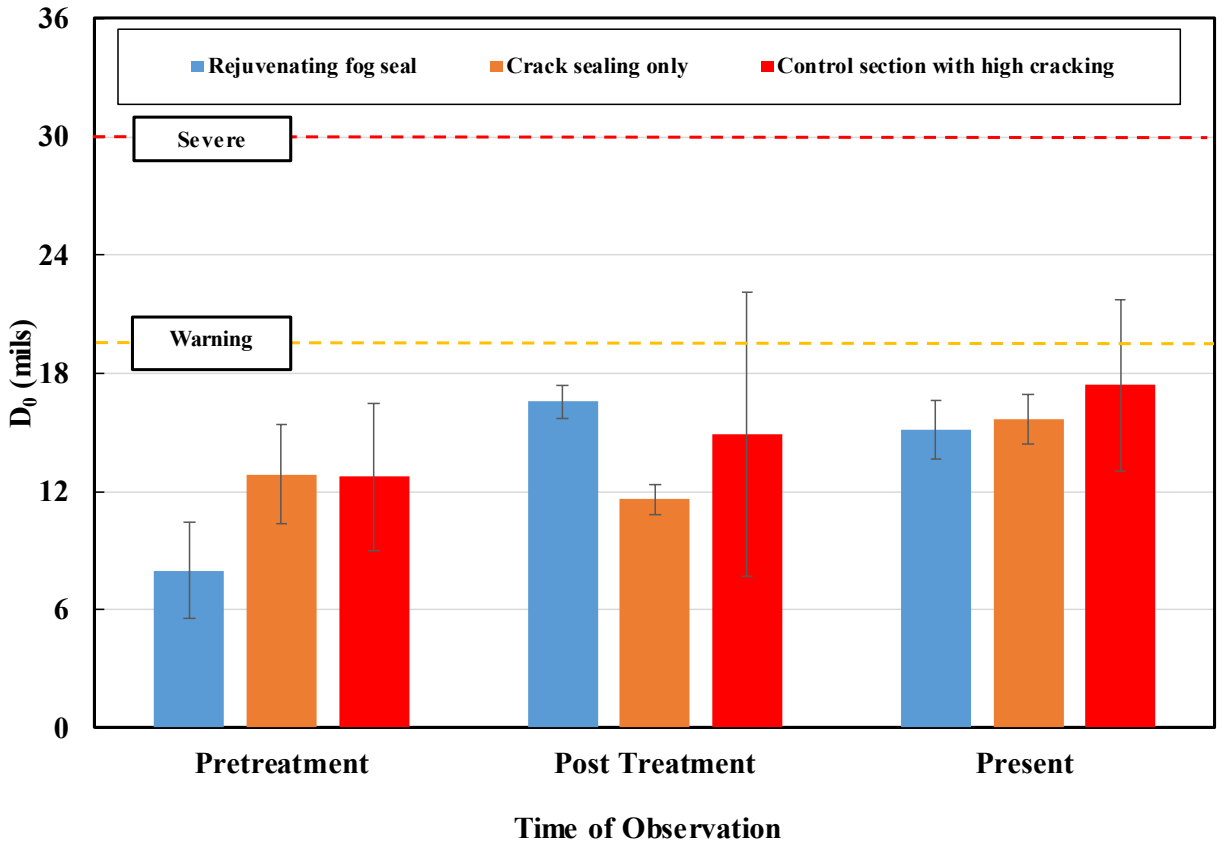

Figure 4-1: Center deflection values at different times for different treatments within standalone treatment group

The pretreatment deflections were measured during the summer of 2012 while the first drops at post treatment condition were measured in the spring of 2013. The consecutive deflections from pre-treatment and posttreatment condition are measured 5 months apart. There was significant interval of time between measurements to observe a drop of mean center

deflection. At present condition, all the treatments show the center deflection below the FHWA designated warning limit for center deflections (≥ 20 mils). The treated sections show rise in the deflection at the present condition yet, all the values are lower than the untreated control section center deflection value.

The load standardized and temperature corrected deflections for different treatments over the elapsed service life to this date are shown in **Figure 4-2**. Exponential smoothing (damping factor =0.1) of the curve was performed to reduce the seasonality and reduce the sum of square error (SSE) value. The results show that crack sealing have higher center deflection than the fog seal and control section.

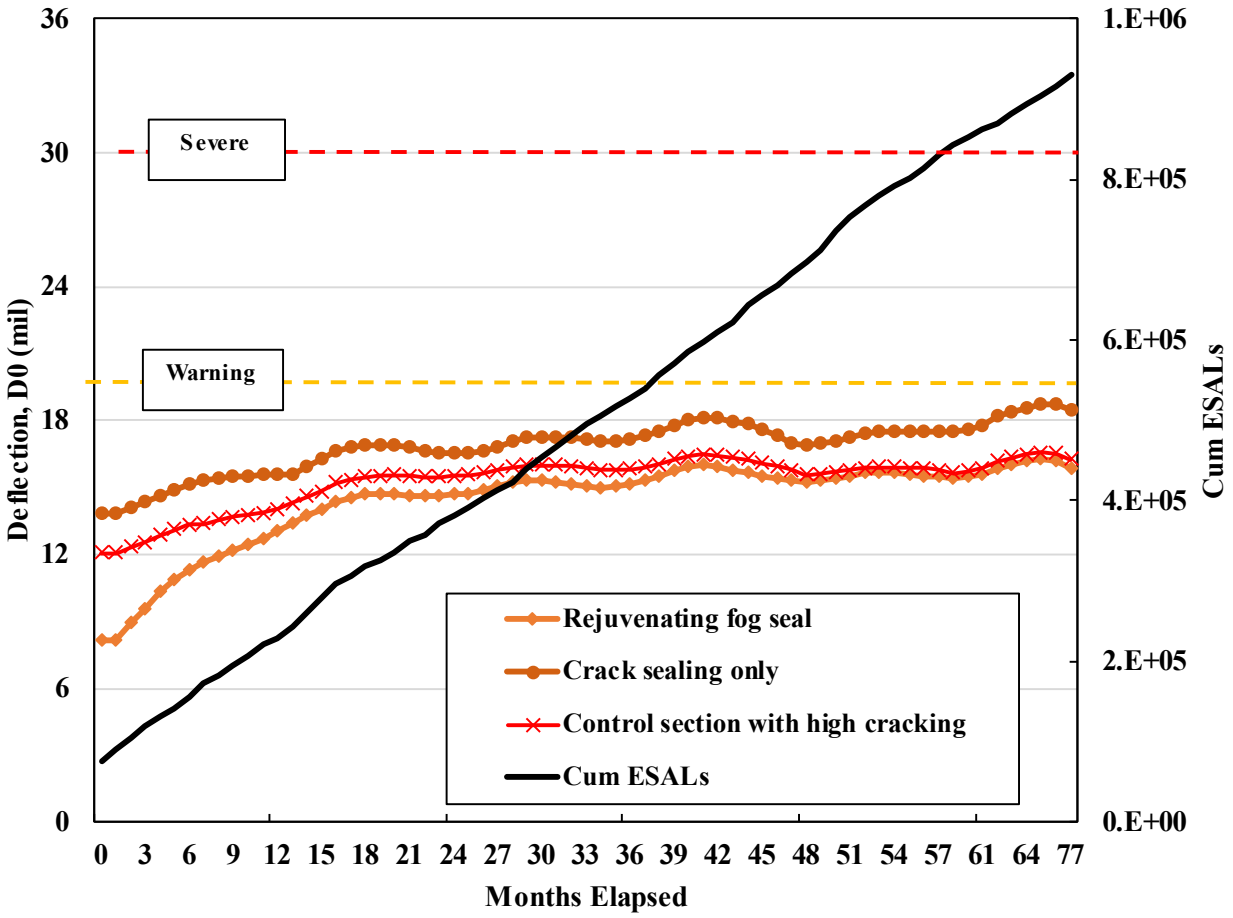

Figure 4-2: Center Deflection over the elapsed service life for standalone treatment group

The data points for all sections in **Figure 4-2**, including the control, are below the FHWA designated warning limit (≥20 mils). It is anticipated that more seasonal cycles and accumulated damage by traffic ESALs can show more significant differences between treated and untreated sections.

4.1.2 Chip Seal Group Results

The FiberMat chip seal, single layer chip seal, double layer chip seal, triple layer chip seal, scrub seal and chip seal with crack seal are the treatments included in this group. The

summary statistics of the chip seal group center deflections over 77 months of elapsed service life are presented in Table 4-4.

Table 4-4: Summary Statistics of the D_0 values for the chip seal group

Treatment	Mean	Std Dev	Min	Max	N	COV
FiberMat chip seal	13.2	3.7	5.6	21.2	521	28.4
Single layer chip seal	13.5	2.9	4.0	22.1	519	21.6
Chip seal w/ crack seal	13.7	3.7	6.7	22.1	515	26.9
Double layer chip seal	12.9	2.4	7.9	18.8	517	19.0
Triple layer chip seal	12.9	3.2	4.9	20.6	516	24.8
Scrub Seal	14.9	3.2	7.9	23.7	516	21.3
Control	16.0	4.2	8.1	33.3	519	26.0

The mean center deflection values for the treated sections are lower than the control section. It is observed that the mean center deflection for double and triple layer chip seals are in the lowest order of recorded center deflections within the chip seal group. This suggests multiple applications are helping the treated sections maintain their structural integrity. The coefficient of variation for the FiberMat chip seal and chip seal with crack seal are 28.4% and 26.9% respectively, which are greater than the control section COV. Thus, the FiberMat chip seal and chip seal with crack sealing show more variability in the mean center deflection than the control section. The scrub seal treated sections show higher mean center deflections than the rest of the chip seal sections within the group. The COV of the mean deflection of the scrub seal treated sections also indicate lower variability of the mean center deflection of the treatment section.

The mean center deflections for different treatments within chip seal group treatment sections at different times are shown in **Figure 4-3**.

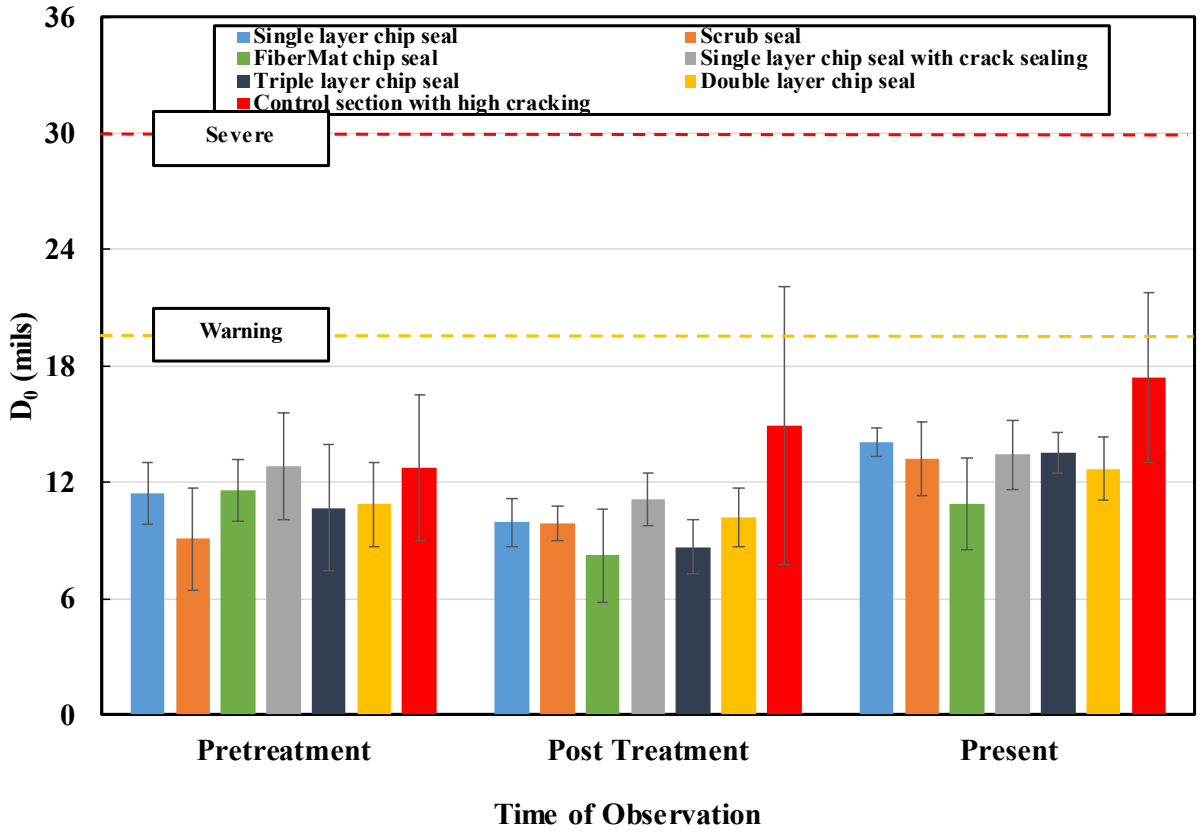

Figure 4-3: Center deflection values at different time for different treatments within chip seal group

The results in **Figure 4-3** show that the mean center deflection had immediate change after the treatments were applied at the posttreatment condition. The mean deflection for the FiberMat and triple layer chip seals show a very significant drop in the center deflection value due to the application of treatment. At the present condition, at 77 months of service after the treatments were applied, the chip seal group treatments mean center deflection values are lower than the control section.

The load standardized and temperature corrected center deflections for different treatment sections within chip seal group over the timeline are shown in **Figure 4-4**. The yearly data were smoothed using the second order exponential smoothing method to minimize the sum of square error (SSE). It can be observed that the mean center deflection of the treated sections is always lower than the control section mean center deflection over the 77 months of service.

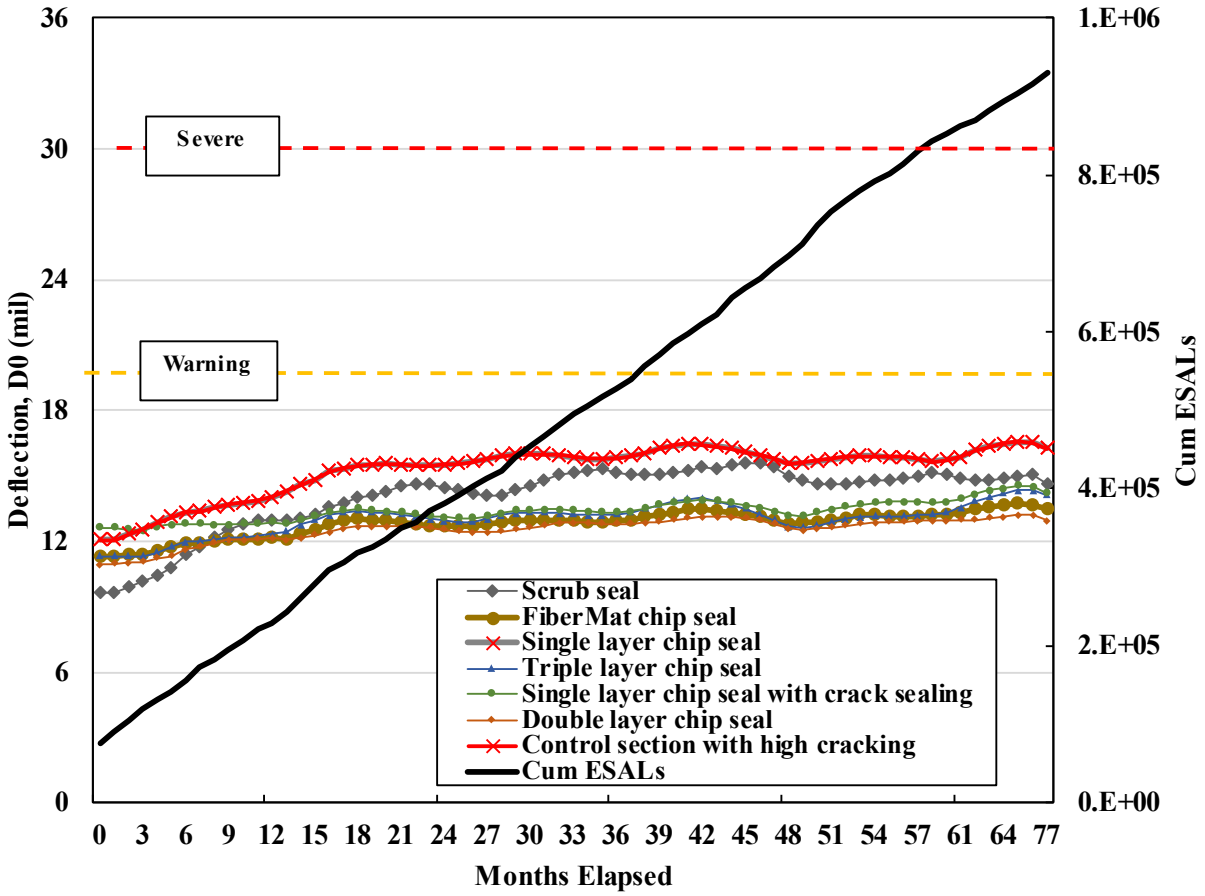

Figure 4-4: Center Deflection over the elapsed service life for the chip seal group

4.1.3 Micro Surfacing Group Results

The micro surfacing group includes single layer micro surfacing, micro surfacing with crack sealing and double layer micro surfacing. The center deflections were load standardized and temperature corrected before the analysis as mentioned in the methodology.

Table 4-5 shows the summary statistics of the center deflections of the treated sections within the micro surfacing group. The mean center deflections for different treated sections are compared to the mean center deflections of the control section. The mean center deflection was lowest for single layer micro surfacing followed by single layer micro surfacing with crack sealing. The double layer micro surfacing mean center deflection is higher than the control section which indicates a weaker structural health than the control section. The possible explanation could be the mean center deflection in the pre-treatment condition was higher than the control section. The coefficient of variation (COV) for all the treated sections are lower than control section indicating a lower variability in the measured means.

Table 4-5: Summary statistics of the D_0 values for the Micro surfacing group

Treatment	Mean	Std Dev	Min	Max	N	COV
Single layer Micro surfacing	13.2	2.1	7.8	19.3	520	16.1
Single layer Micro surfacing w/ crack seal	14.7	1.9	10.3	19.5	518	12.7
Double layer Micro surfacing	17.9	3.4	10.7	36.8	519	18.8
Control	16.0	4.2	8.1	33.3	519	26.0

Figure 4-5 indicates the bar plots of the mean center deflections of different micro surfacing treated sections at different times. It can be observed that the center deflections did not show any immediate effect after treatment application. At present date after 77 elapsed months of service, the center deflection for single layer micro surfacing and micro surfacing with crack sealing treated sections are lower than the control section, while the double layer micro surfacing does not show a significant difference with the control section. It is important to note that the measured center deflection in pretreatment condition for the double layer micro surfacing and micro surfacing with crack sealing were higher than the control section while in the present scenario, the both treated sections yield lower center deflections than the control section.

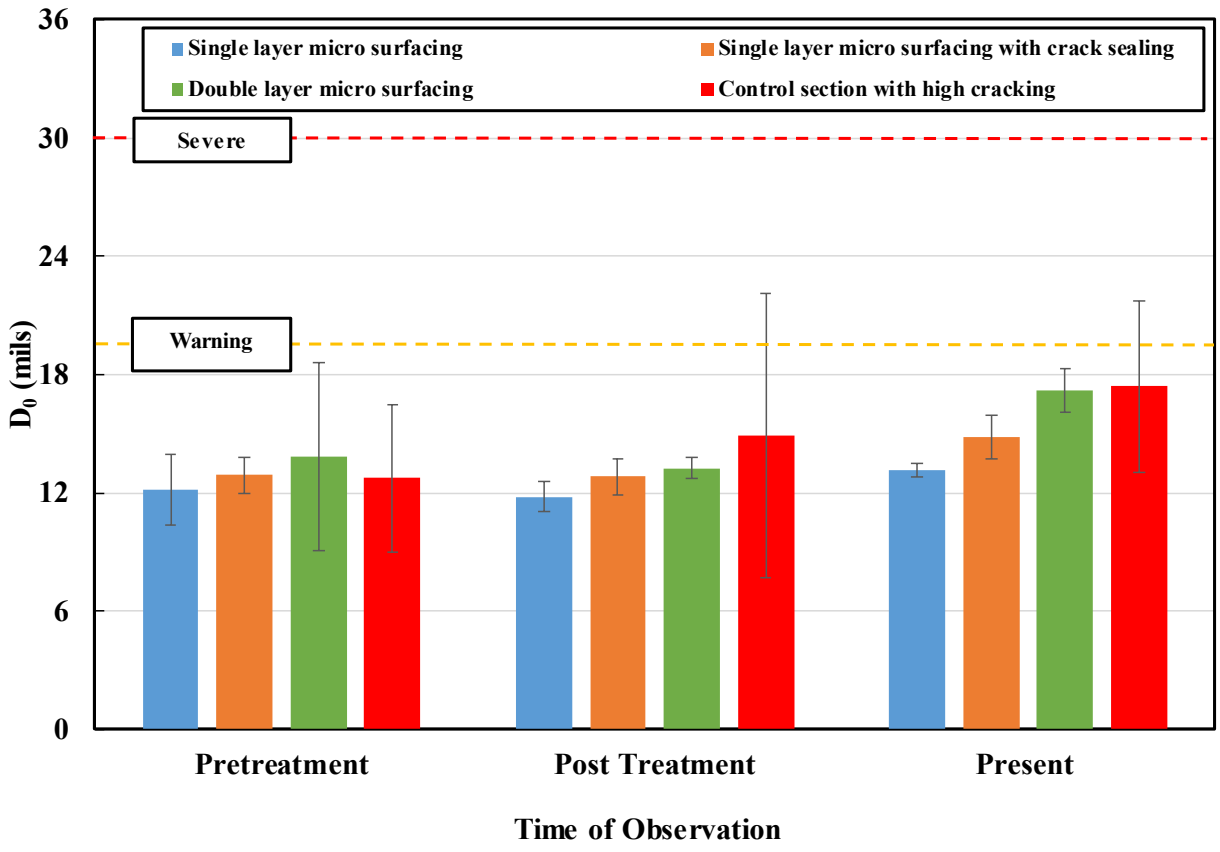

Figure 4-5: Center deflection values at different times for different treatments within Micro surfacing group

Figure 4-6 shows the comparative center deflections over the elapsed service life of 77 months. The center deflections for single layer micro surfacing and micro surfacing with crack sealing did not show significant change over time. The center deflection for was all the sections within micro surfacing were higher than the control section which has remained higher over the 77 months of post-construction service except the section treated with double layer micro surfacing. After 4 months of service, the mean center deflection of the double layer micro surfacing treated section were higher than the control section which remained higher for the rest of the analysis period.

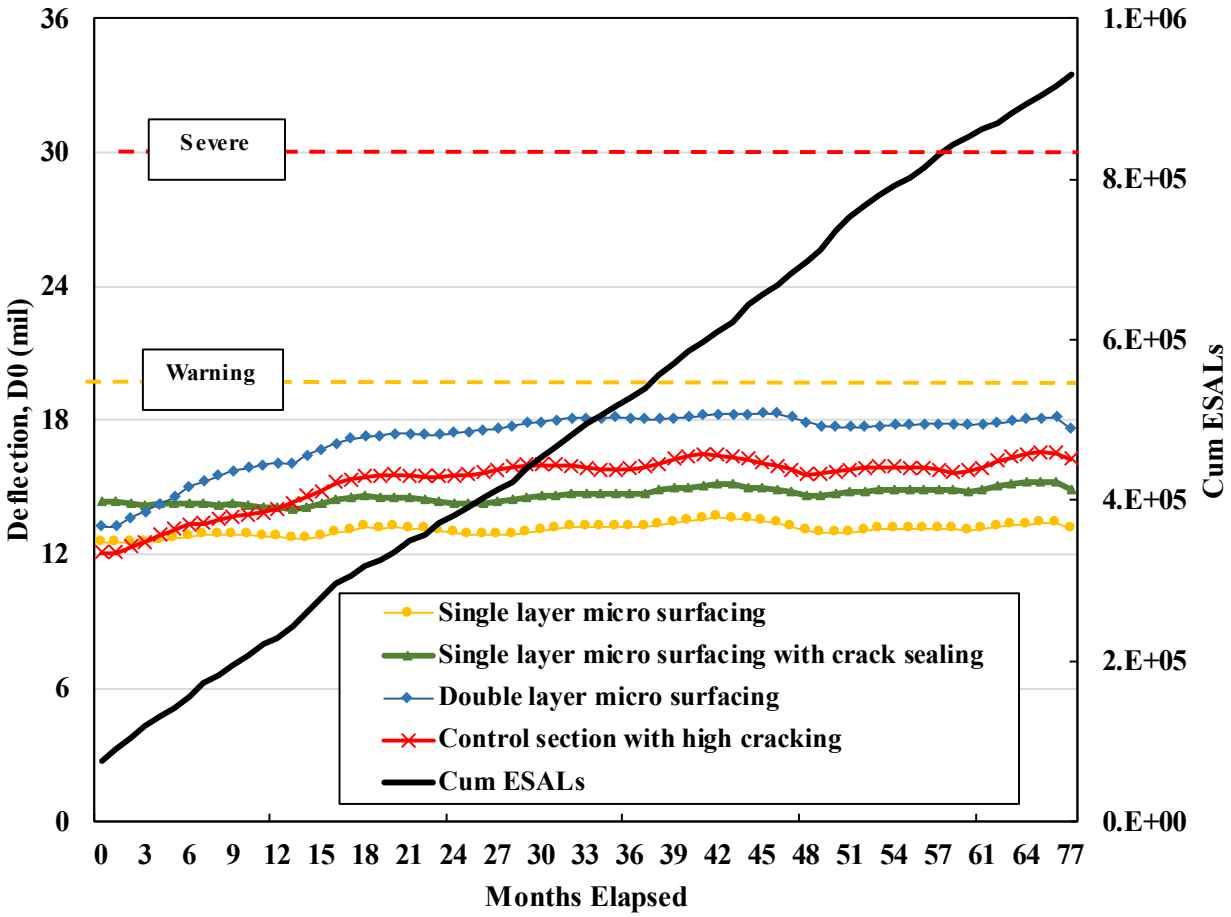

Figure 4-6: Center Deflection over the elapsed service life for Micro surfacing group

4.1.4 Combinations Group Results

Cape seal, FiberMat cape seal and scrub cape seal are applications of a chip seal followed by a micro surface are considered combination treatments. Thinlay on FiberMat chip seal treatment is also considered within the combination group as the thinlay is applied on the FiberMat chip seal coating. Table 4-6 shows the summary statistics of the center deflection values for the sections within combination group. All the treated sections mean center deflections show lower value than the control section. The COV values for the center deflections for treated sections are lower than the control section implying lower variability of the mean center deflection values.

Table 4-6: Summary statistics of the center deflection values for the combination group

Treatment	Mean	Std Dev	Min	Max	N	COV
Cape seal	11.2	2.2	6.7	17.0	516	19.7
FiberMat Cape seal	12.2	2.2	6.2	19.1	520	18.4
Scrub Cape seal	13.5	2.4	6.8	19.3	520	17.5
Thinlay on FiberMat	11.5	1.7	6.6	15.6	516	15.1
Control	16.0	4.2	8.1	33.3	519	26.0

The average center deflection for different treatments are shown in **Figure 4-7** at pretreatment, posttreatment and present time. The data indicate a drop in the mean center deflection within 5 months after application of treatment. At the present time, the mean center deflections are lower than the control section and are below what the FHWA designated as the warning threshold of 20 mils. The combination group treatments applied on the treated sections

tend to maintain the overall structural strength of the pavement as indicated by the mean center deflection values. Cape seal, scrub cape seal, FiberMat cape seal and thinlay on FiberMat treated sections follow a similar trend at different point of observations. After 77 months of elapsed service, the mean deflection values of the treated sections did not show significant increase compared to the control section.

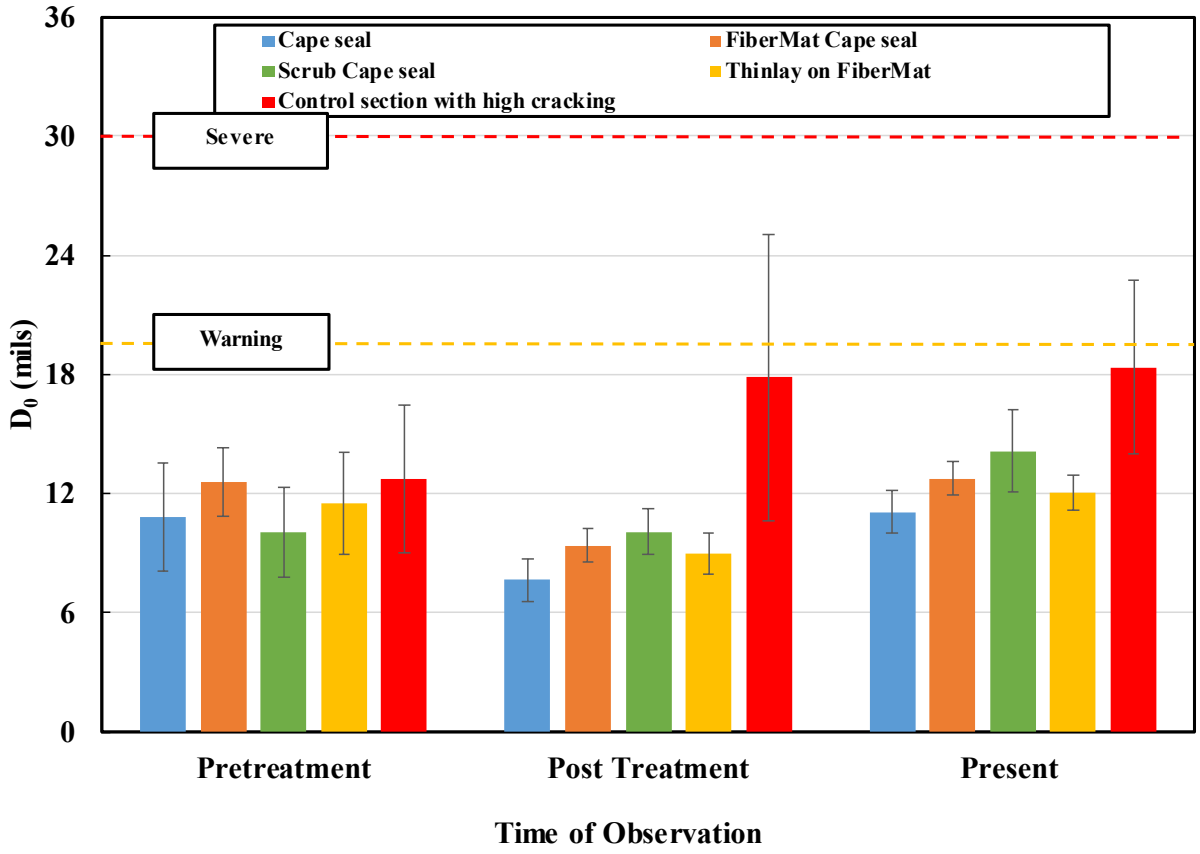

Figure 4-7: Center deflections for different treatments at different times within combination group

Figure 4-8 shows the trend of the mean center deflection over the elapsed service life of 77 months of the sections within combination group. FiberMat cape seal treated sections had higher center deflection than the control section at the beginning but within 3 months after the application of treatment, the control section center deflection surpassed the mean center deflection of FiberMat cape seal. At 77 months of service age, all the combination treatments are helping the pavement structure to be within the "good" condition range.

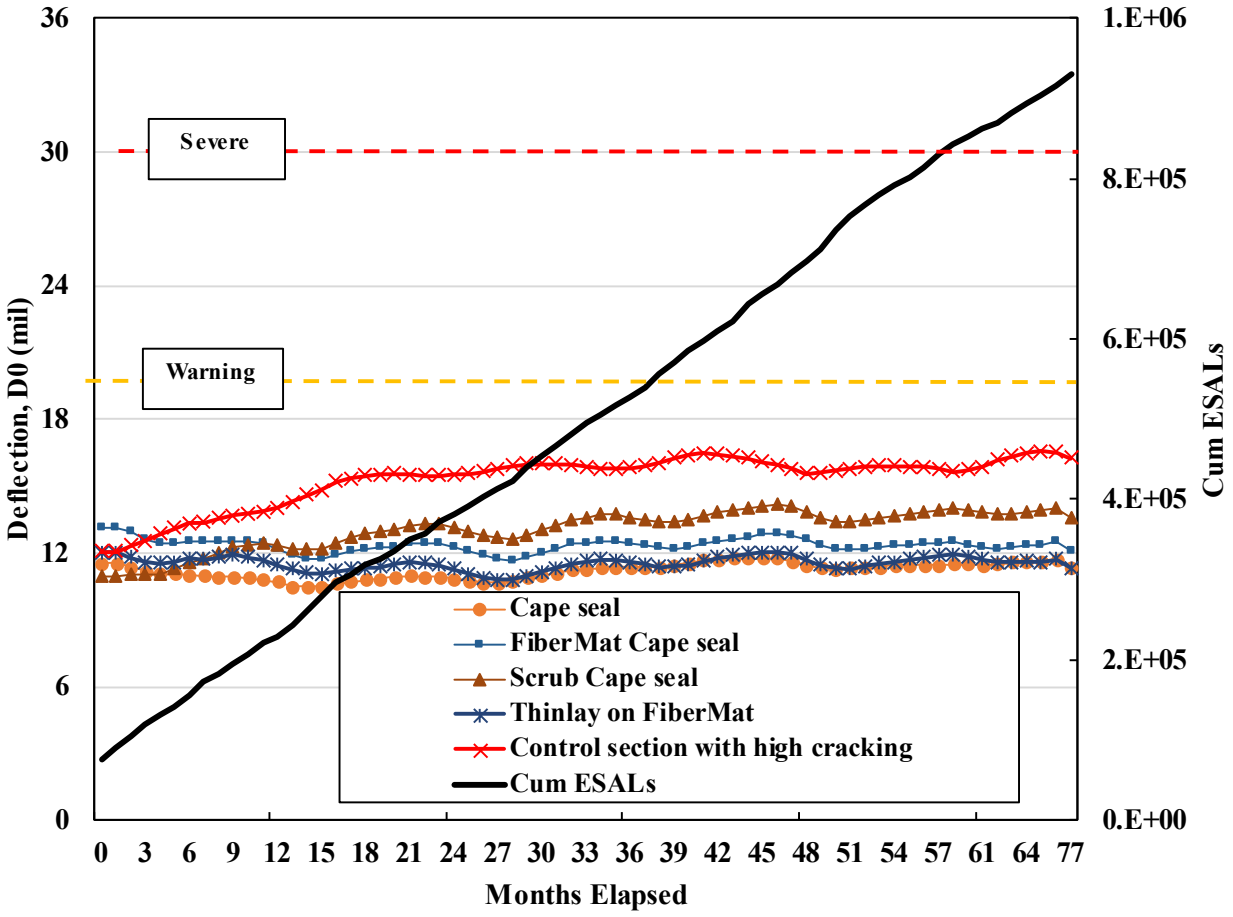

Figure 4-8: Center Deflection over the elapsed service life for combination treatment group

4.1.5 Thinlays Group Results

The thinlay group includes the following treatments: virgin thinlay, polymer-modified virgin thinlay and ultra-thin bonded wearing course thinlay. In all cases, an additional thickness of 0.75 in. of asphalt mix was applied on top of the existing asphalt concrete layer. These uniform and thin overlays are considered non-structural because they do not add structural capacity to the pavement.

Table 4-7 shows the summary statistics of the mean center deflection of the sections treated with thinlays. The mean center deflection of the thinlay treated sections are lower than the mean center deflection of the control section though ultra-thin bonded wearing course sections indicate higher mean deflection than the rest of the treatment sections within thinlay group. The COV of the mean center deflection values of the treated sections are lower than the control section which imply lower variability of the mean center deflection values form the treated sections.

Table 4-7: Summary Statistics of the D0 values for the thinlay group

Treatment	Mean	Std Dev	Min	Max	N	COV
Thinlay	12.3	1.5	7.8	16.0	522	12.4
Polymer Thinlay	12.9	2.2	8.1	18.5	521	17.0
Ultra-Thin Bonded Wearing Course	14.4	3.1	7.6	23.6	517	21.7
Control	16.0	4.2	8.1	33.3	519	26.0

Figure 4-9 shows the mean center deflections of different treated sections in the thinlay group at pretreatment, posttreatment and present time. The mean center deflection in pretreatment condition for all the sections were higher than that of the control section. After construction, the mean center deflections dropped as per measurement performed after 5 months of posttreatment service. At the present time, the mean center deflections for the treated sections are below the center deflection of the control section, and all values at present time are below the FHWA designated warning threshold of 20 mils.

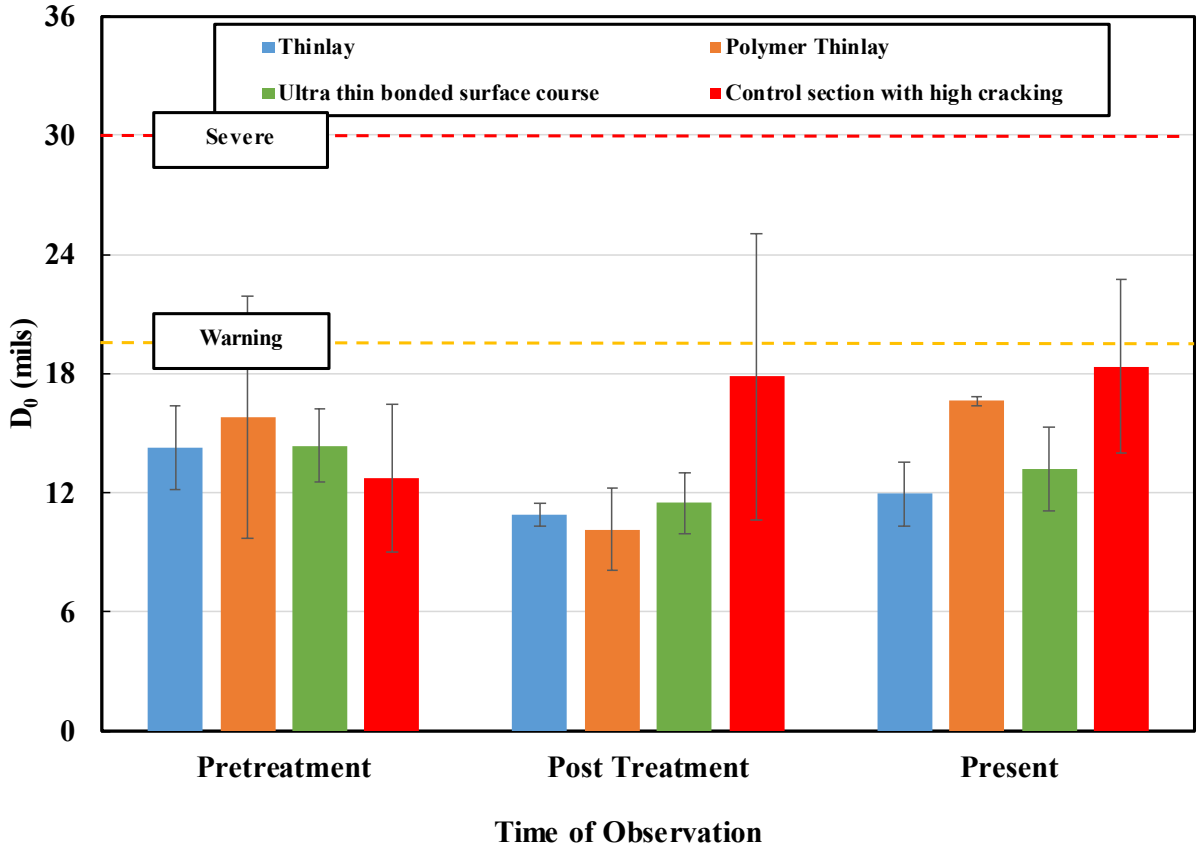

Figure 4-9: D_0 values for different treatments at different times within thinlay group

Figure 4-10 shows the trend of the mean center deflection of the treated section over the elapsed 77 months of service life within the thinlay group. At the beginning of the post-application life, the mean center deflections of all the treated sections within the thinlay group were higher than the control section. As the service life elapsed, the mean center deflection of the treated sections decreased, and the mean center deflection of the control section was higher than the treated sections within 12 months of service.

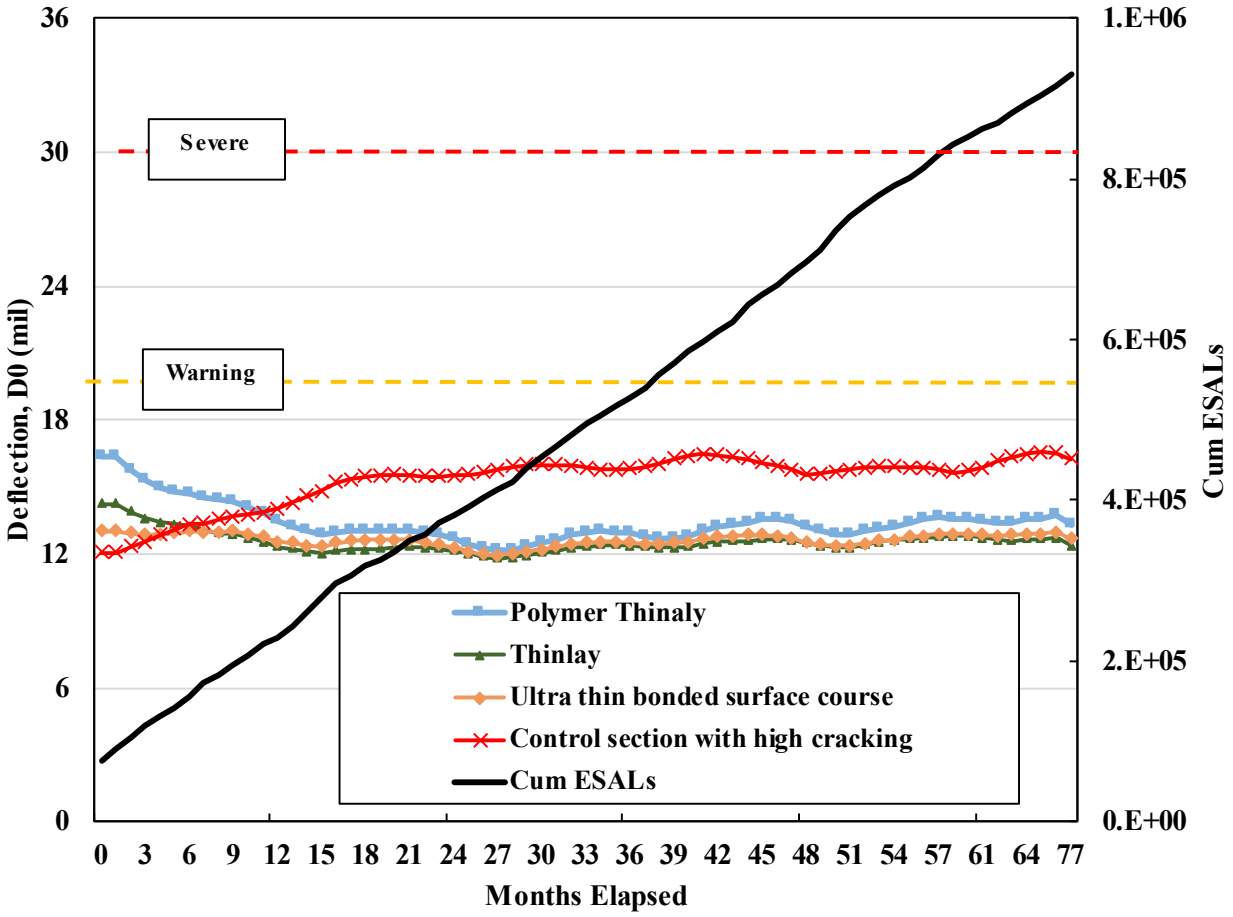

Figure 4-10: Center deflection values over the elapsed service life for thinlay group

4.1.6 Effect of thickness variability on the D_0 results

Detailed information on the as-built thicknesses of the pavement layers is not available on Lee Road 159. Instead, existing pavement structure information was obtained from construction records and a limited number of cores and assumed to be uniform throughout the length of the project. However, it is known that AC layer thickness can vary due to error in the paver screed, location of paving, paving pattern, variation due to elevation, surface condition of the pavement, asphalt mix temperature, amount of water applied during rolling, roller speed, type of roller etc. (Engineers, 2000). The AC thickness can affect the structural performance of the pavement and stress-strain magnitudes. To validate the results from this research, a sensitivity analysis was performed to evaluate the varying AC and base layer thicknesses on the resulting pavement deflections using layered elastic analysis. The software WESLEA was used to simulate pavement deflections in a pavement structure with fixed moduli values while varying the thicknesses of the AC and base layers. The moduli inputs were selected based on the backcalculation results from the test location at 68ºF. The inputs are tabulated in Table 4-8.

Table 4-8: WESLEA simulation structural inputs

Layer	Modulus (psi)	Poisson	Thickness (in)	Slip
AC	583,000	0.35	5.0 to 6.0	No-Slip
Base	80,000	0.40	5.5 to 6.5	No-Slip
Subgrade	30,000	0.45	Infinite	-

The sensitivity analysis was carried out in two parts. First, the AC thicknesses were varied from 5 to 6 inches in 0.1 inch increments while keeping the base thickness constant at 6.0 in). Similarly, the base thickness was varied from 5.5 to 6.5 inches in 0.1 inch increments while

holding the AC thickness constant at 5.5 in. These ranges were selected to reflect the values observed from the cores. The deflections were simulated at 0, 12, 24 and 36 inches from the center of the load, which are the radial distances used for structural evaluation in this research.

The mean center deflection (D_0) results from varying AC thicknesses indicate that a change of 0.5 in of AC thickness results in up to 5% change in the center deflection. **Figure 4-11** shows the percent change plots for deflection values for different AC thickness along with the radial distances. It is observed that the thickness sensitivity is highest at the center for the loading plate decreases as the radial distances form the center of the loading plate increase.

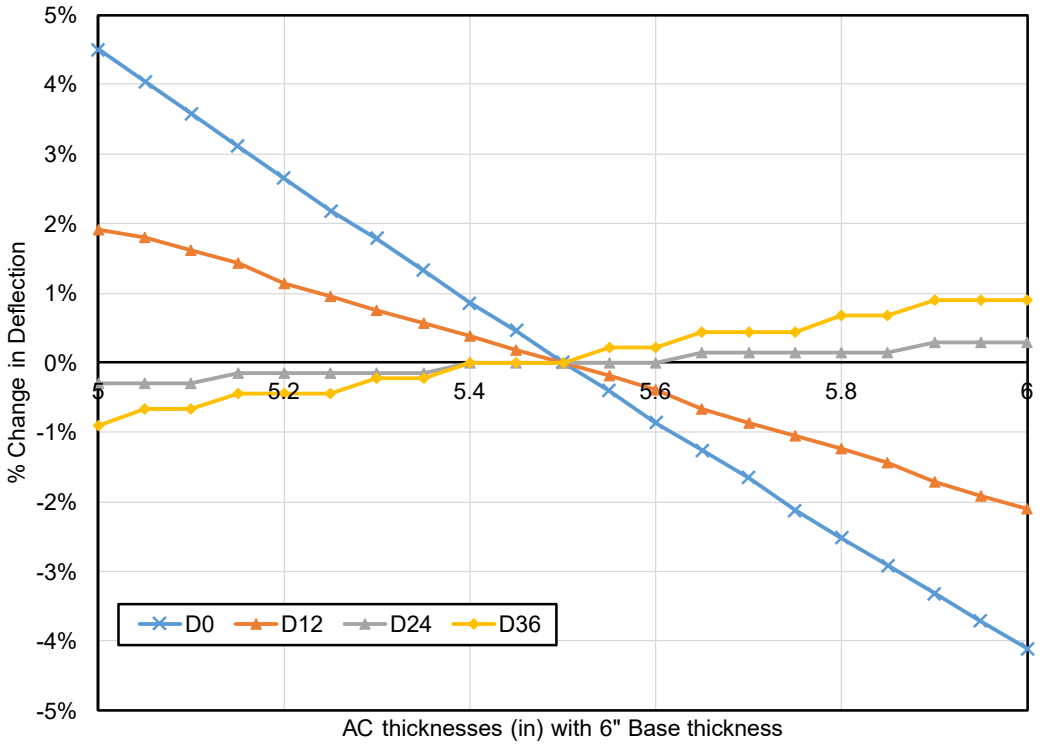

Figure 4-11: Percent Change in Deflections with variable AC thicknesses (6 in. Base Constant)

Another approach was adopted to observe at which AC thickness, the mean center deflection value reaches the warning zone when all the remaining factors remain unchanged. Thus, a variable AC thickness from 1.0 to 10.0 in. were simulated to observe the change in deflections. The analysis was set up such that D_0 was 16 mils for an AC thickness of 5.5 in to match typical values observed. **Figure 4-12** shows the variation in deflection values for different radial distances. It can be observed that the thickness of the AC layer would have to be reduced to 2.5 in to reach the FHWA designated warning threshold taken that all other parameters i.e.- base thickness, layer moduli etc. remains unchanged. This means the AC thickness would have to vary 3.0 from the assumed average value, which is unlikely within the 0.5 mile length of the project.

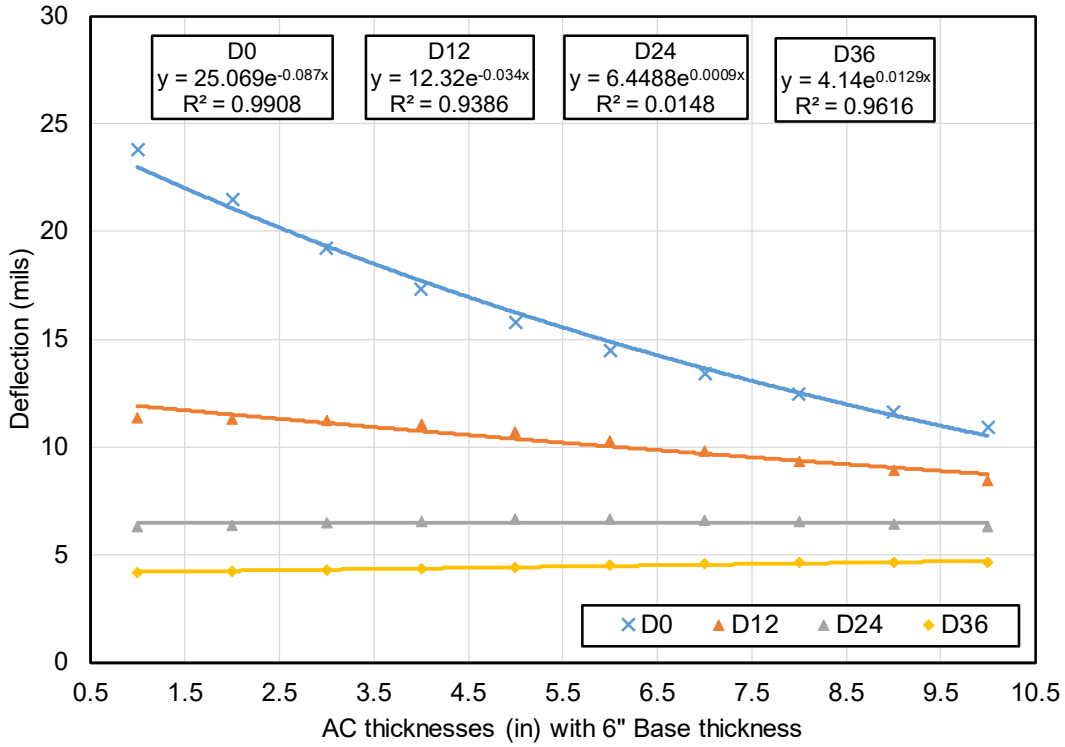

Figure 4-12: AC thickness sensitivity of the deflections with fixed 6 in base thickness

Figure 4-13 shows the changes in deflections for a variable base layer thickness. and constant AC thickness. A change of mean center deflection of approximately 1% was observed with 0.5 in. variation of the base thickness.

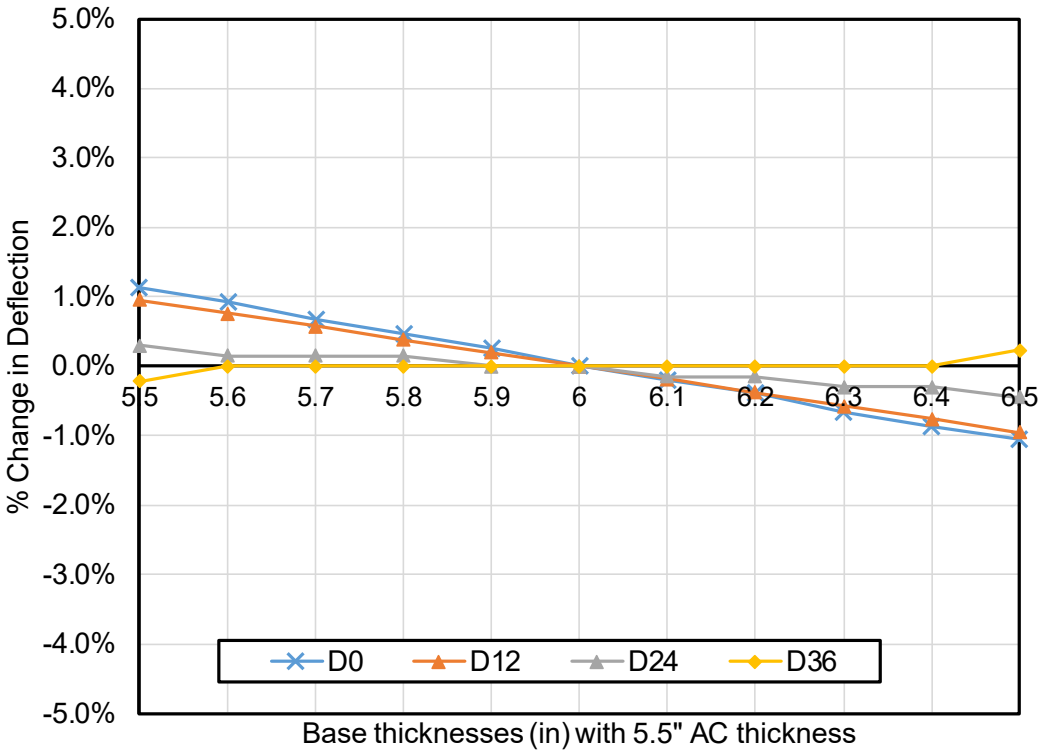

Figure 4-13: % Change of Deflections with variable Base thicknesses (5.5 in AC Constant)

From the results presented above, it can be concluded that although variations in layer thickness may be present as a natural result of the construction process, these variations are not expected to significantly alter the results obtained using an assumed reasonable average value and the way test sections compare to the untreated control sections.

4.2 Base Damage Index (BDI)

From the literature review it was found that the base damage index (BDI) represents the structural condition of the base layer of the pavement structure. Studies also found that the BDI value can be correlated to the backcalculated layer moduli, stress-strain at the AC layer, and other structural index parameters which are mentioned in the literature review. In the following paragraphs the BDI values for the treated sections within each treatment group will be analyzed to investigate the contribution of the treatments. The deflections within the study were all load standardized to 9,000 lb. and temperature corrected to 68ºF, thus the BDI values presented in numbers, plots and curves are load standardized and temperature corrected, too.

4.2.1 Standalone Group Results

Table 4-9 shows the summary statistics of the BDI parameter measured over 77 months of post-application service for different treatments within the standalone treatments group. Crack seal and fog seal show higher mean BDI than the control section. The COV of BDI values for the crack seal treated section (40.4%) is higher than the control section COV (36%) which indicate higher variability of the measured deflections over the 77 months of elapsed service life.

Table 4-9: Summary statistics of the BDI values for the standalone treatment group

Treatment	Mean	Std Dev	Min	Max	N	COV
Fog Seal	5.1	0.9	3.3	7.7	521	17.4
Crack Seal	5.7	2.3	0.9	13.3	518	40.4
Control	5.0	1.8	2.3	13.0	519	36.0

BDI values for different standalone treatment sections at pretreatment, posttreatment and present time are shown in **Figure 4-14**. From the bar charts, it is observed that the BDI values for the treated sections change right after the treatment is applied. At the present condition at 77 months of service, the BDI values for the treated sections are below the FHWA designated warning limit (≥8 mils). Crack seal treated sections show a drop of BDI value within 5 months after treatment application, while the rejuvenating fog seal shows an increase in BDI value at posttreatment condition. At the present condition, all the treatments in the standalone treatment group show lower BDI value than the control section as shown in **Figure 4-14**.

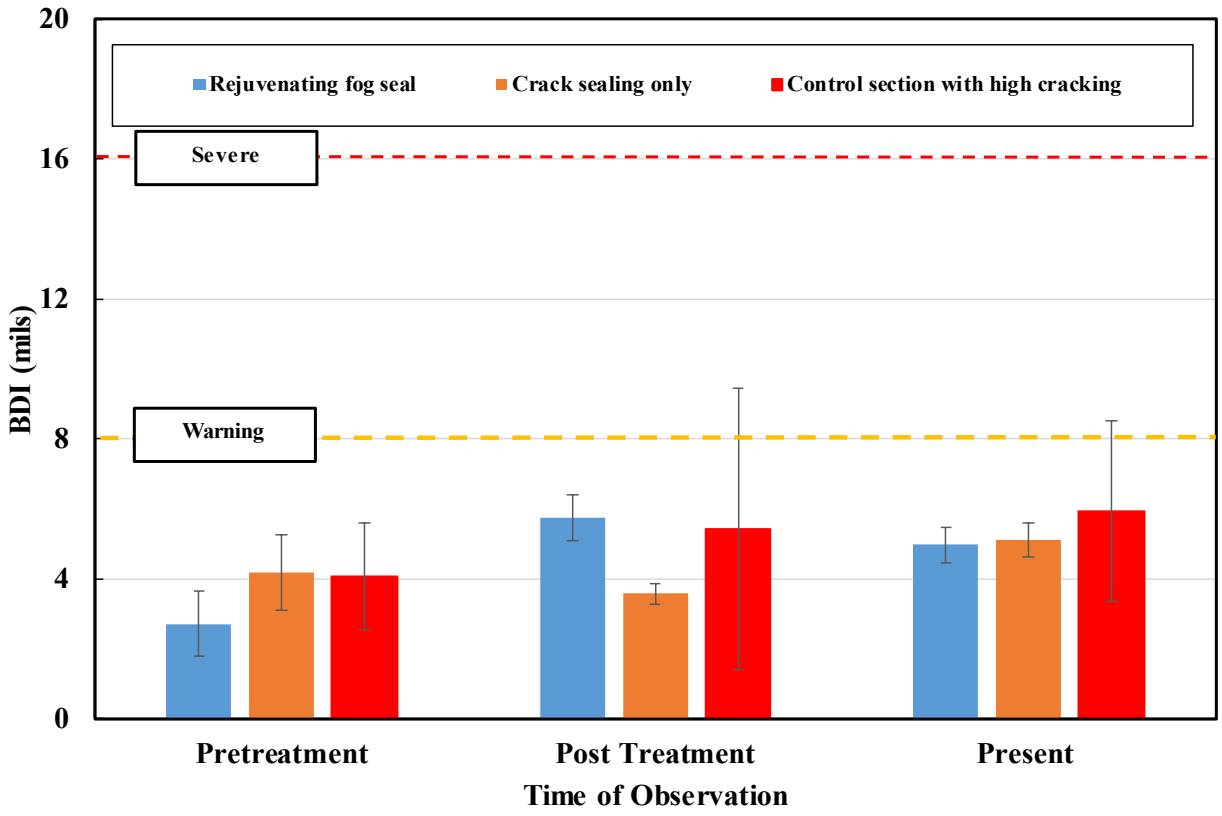

Figure 4-14: BDI values for different treatments at different times within standalone group

As damage at any specific layer of pavement is considered irreversible and time dependent, the BDI values were investigated in a manner that considers time as a variable too. The time series mixed modeling was found in the literature to be one of the most efficient procedures to investigate the time effect, treatment effect or the combined interaction effect (time *treatment). The mean center deflection was not modeled in the similar fashion as the center deflection reflects the overall structural condition rather than a specific layer. Even after temperature correction, the mean deflections indicate certain degree of seasonality that might be related to other factors such as moisture in the pavement structure. To avoid the seasonal effect on the model variables, mean center deflections are not considered for timeseries mixed modeling. The BDI values for the inbound and outbound direction to and from the rock quarry were separated and a mixed modeling procedure was performed with time, treatment and combined interaction variable. The treatment effect is considered if any difference within the means of the BDI values for two different sections are observed due to the application of the treatment. The time effect is considered if there is significant difference between the two pair of mean BDI values over a brief duration of observation or time length the null hypothesis for the mixed model claims the mean of the observations are equal. In other words, there is no time effect or no treatment effect or no time ×treatment interaction effect. The null hypothesis is rejected, and the effects are considered significant if the p-value lies out of the confidence interval. For the present study, the null hypothesis is tested at 95% confidence interval which makes to reject the null hypothesis if p-values is less than or equal to 5% or 0.05.The time series mixed modeling is performed based on the assumption that there is no compound effect. As found from the literature, the D_0 values signify all the layers under the surface, so the changes in the mean center deflection is yet a complex outcome of changes at any underlying layer of the

pavement. This is why, to minimize the effect of other layers, only location-based deflection basin parameters are selected for the time series mixed effect modeling. Table 4-10 shows the p-values for different treatments derived from time series mixed models.

Table 4-10: p-values for time series mixed modeling for BDI values of treatments

Treatment Applied	Inbound lane to the quarry			Outbound lane from quarry		
	Treatment	Time	Combined	Treatment	Time	Combined
Rejuvenating Fog Seal	0.0894	<.0001	<.0001	0.7326	0.0035	0.0013
Crack Sealing	0.0048	0.0137	0.7196	0.0014	0.0031	0.0057

The p-values smaller than 0.05 are considered significant for an effect. The crack sealing shows both time and treatment effect significant on both lanes where, the BDI values for fog seal show very strong time and combined interaction effect (time*treatment).

Figure 4-15 shows the BDI trends for different treatments over the elapsed 77 months. At the post treatment condition, the BDI value for crack seal treated sections were higher than the control section. The rejuvenating fog seal did not improve the base layer significantly and the BDI value is always equal to the BDI values of the control section after 15 months of service. All the treatment sections including the control section BDI values stayed below the FHWA warning zone limit (≥8 mils) until the present date.

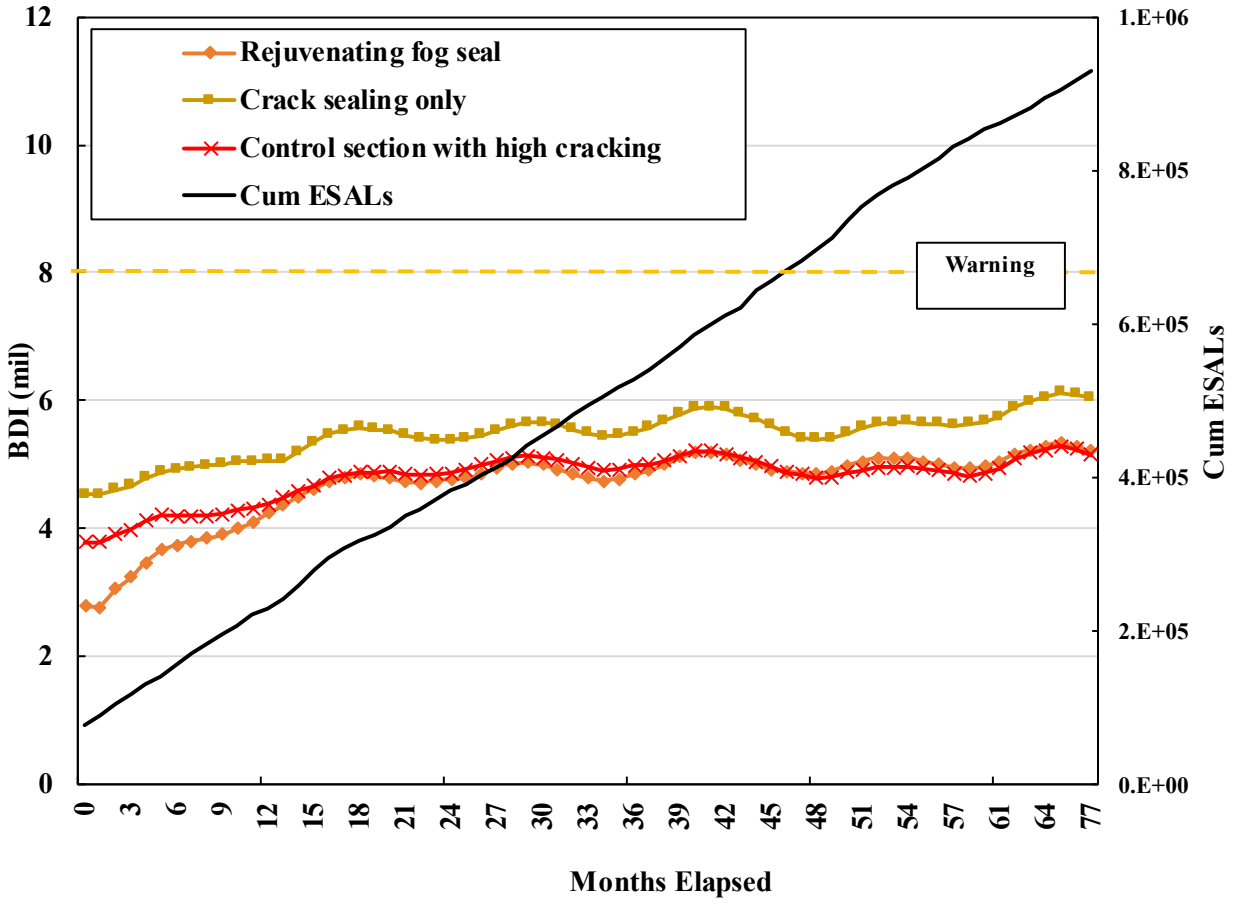

Figure 4-15: BDI values over the elapsed service life for standalone treatment group

To predict the future performance of the base layer, the Autoregressive Integrated Moving average (ARIMA) model was used as a forecasting tool for the present study. The BDI values up to 48 months were used to train the software interface to predict lag and patterns via autocorrelation function (ACF), partial autocorrelation function (PACF). Thus, the forecast was performed with (P, D, Q) = (0,1,1) model. Where, P= autoregressive order, D= integration or stationarity, Q= moving average order. **Figure 4-16** shows the forecast BDI values of different treatment sections within standalone treatment group. The forecast values indicate that the control section BDI values exceed the FHWA BDI "Warning" threshold of 8 mils by 80 months of service while the treated sections reach the threshold at 120 months of service or later. The ranges of confidence and comparison with observed data are shown in APPENDIX E . In the present study, observed BDI values up to 48 months were used to teach the model to determine the autoregressive order, differencing and moving average orders. After the parameters were determined, the projected values up to 120 months of service and 95% confidence intervals were determined for each forecast value. This was observed from the dataset that, the observed BDI values after 48 months for the treatment sections lie within the 95% confidence limit of the projected forecast. Indeed, the ARIMA models are not much accurate to sense seasonal cycles and implement in the model intelligently, yet the plots in APPENDIX E were capable to provide some degree of confidence.

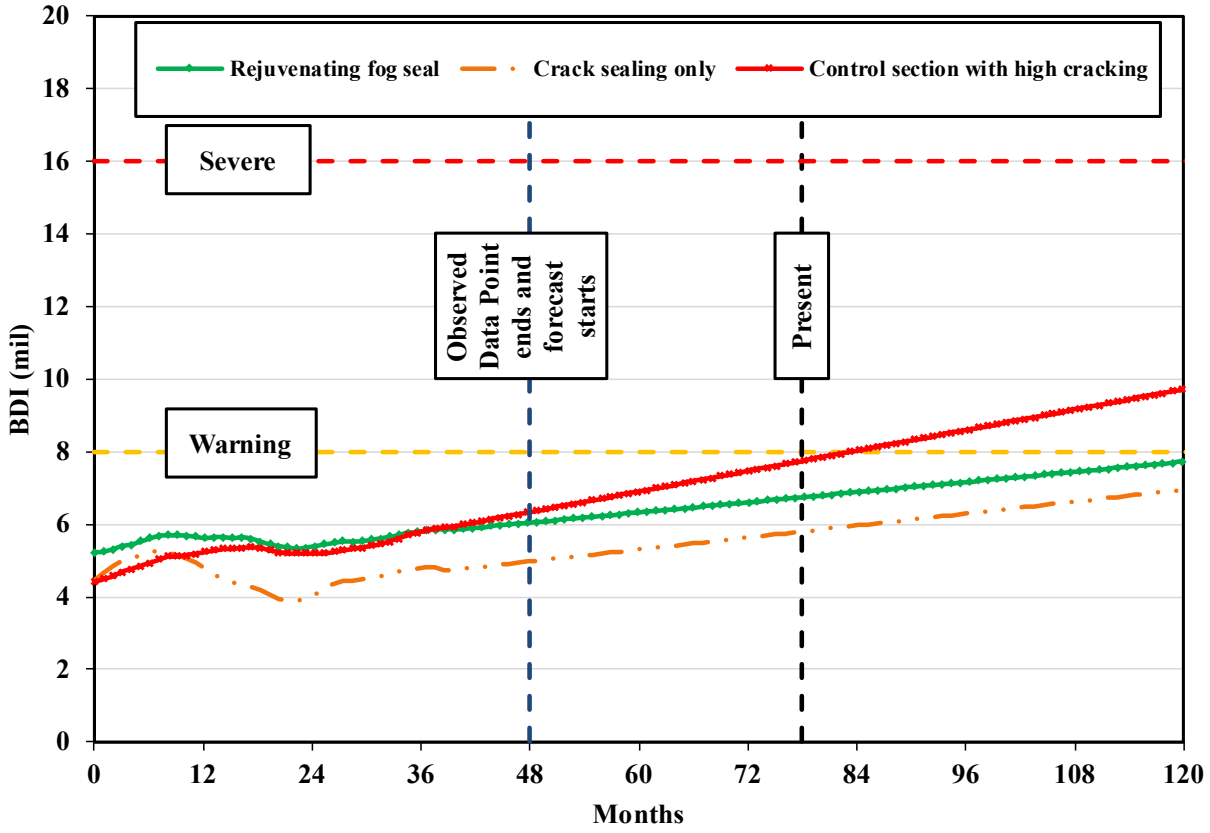

Figure 4-16: Forecast of the BDI values for standalone treatment group

4.2.2 Chip Seal Group Results

The BDI values form the chip seal treated sections over elapsed service life of 77 months were analyzed to obtain summary statistics shown in Table 4-11.

Table 4-11: Summary statistics of the BDI values for the chip seal group

Treatment	Mean	Std Dev	Min	Max	N	COV, %
FiberMat Chip Seal	4.02	1.29	1.4	6.9	521	32.0
Single Layer Chip Seal	4.28	1.20	0.8	7.8	519	28.0
Chip Seal w/ crack seal	4.26	1.34	1.8	7.6	515	31.5
Double Layer chip Seal	3.93	0.75	2.0	6.2	517	19.1
Triple layer chip seal	3.80	1.11	0.7	7.1	516	29.2
Scrub Seal	4.50	1.23	2.3	8.0	516	27.2
Control	5.03	1.81	2.3	13.0	519	36.0

Table 4-11 shows that the mean BDI values for the treated sections are lower than the control section mean BDI value over time. The coefficient of variation (COV) of the BDI values for the treated sections was lower than the control section, which means less variability of the BDI values within the treated sections. Multiple application of chip seal i.e.- double layer chip seal and triple layer chip seal show significantly lower magnitude of BDI values compared to the single layer application.

Figure 4-17 shows the mean BDI values for different treated sections at pretreatment, posttreatment and present condition. The BDI values dropped after treatment application and the variability of the BDI measurements also was reduced significantly, resulting in decreased standard deviation. Along with the control section, the treated sections BDI values are below the FHWA designated warning threshold of 8 mils.

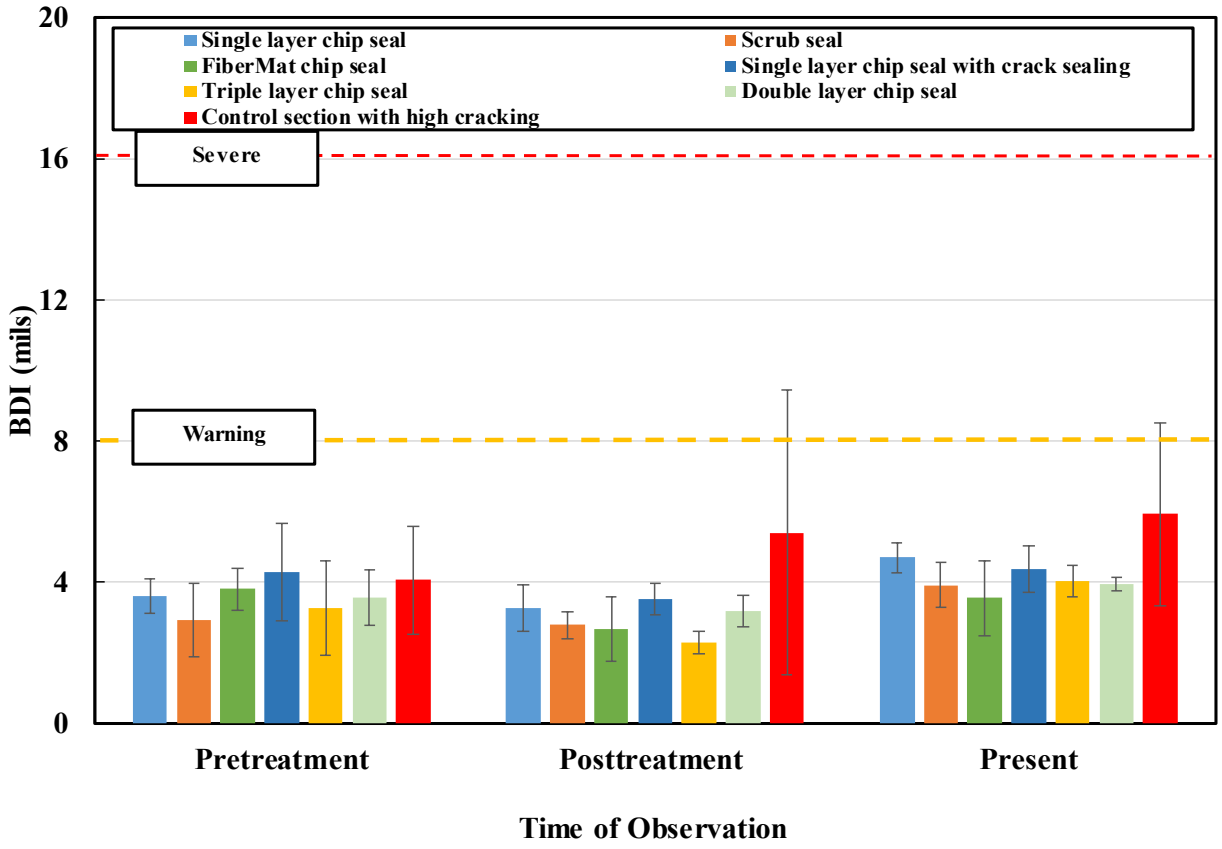

Figure 4-17: BDI values for different treatments at different times within chip seal group

Table 4-12 shows the time series mixed modeling results of the BDI values of the sections within chip seal group. BDI values from single layer chip seal and single layer chip seal with crack sealing show significance of treatment, time and combined interaction (treatment*time) effect on the base layer in both lanes. FiberMat chip seals show time and

treatment effect on the BDI values only in the outbound lane. BDI values from triple layer chip seal treated sections indicate significant time effect in both lanes. Scrub seal treated section BDI values indicate significance of time and combined interaction effect in both lanes of traffic. BDI values from double layer chip seal treated sections did not meet convergence in the inbound lane. The possible reasons are inadequate data, high number of outliers etc. BDI values from the same treatment in the outbound lane indicate significance of time.

Table 4-12: p-values for time series mixed modeling for BDI values of treatments

Treatment Applied	Inbound lane to the quarry			Outbound lane from quarry		
	Treatment	Time	Combined	Treatment	Time	Combined
FiberMat chip seal	0.146	0.1203	0.9078	0.0006	0.0021	0.1569
Single layer chip seal	0.0006	<0.0001	0.0035	0.3286	0.0004	0.0065
Single layer chip seal with crack sealing	0.0053	0.0045	0.0387	0.038	0.0176	0.0045
Triple layer chip seal	0.157	<0.0001	0.0721	0.1418	<0.0001	0.007
Scrub Seal	0.213	0.0005	0.0058	0.285	0.0024	0.0303
Double layer chip seal	Did not meet convergence			0.1997	0.0002	0.5764

Figure 4-18 shows the comparison of mean BDI values of the treated sections to the control section over the elapsed 77 months of service. The untreated control section has mean BDI higher than the treated section mean BDI values. After 77 months of service, the treated section mean BDI values are lower than the FHWA designated warning threshold of 8 mils. Throughout the elapsed service life, all the treated sections BDI values show a trend of similar magnitudes over the elapsed service life.

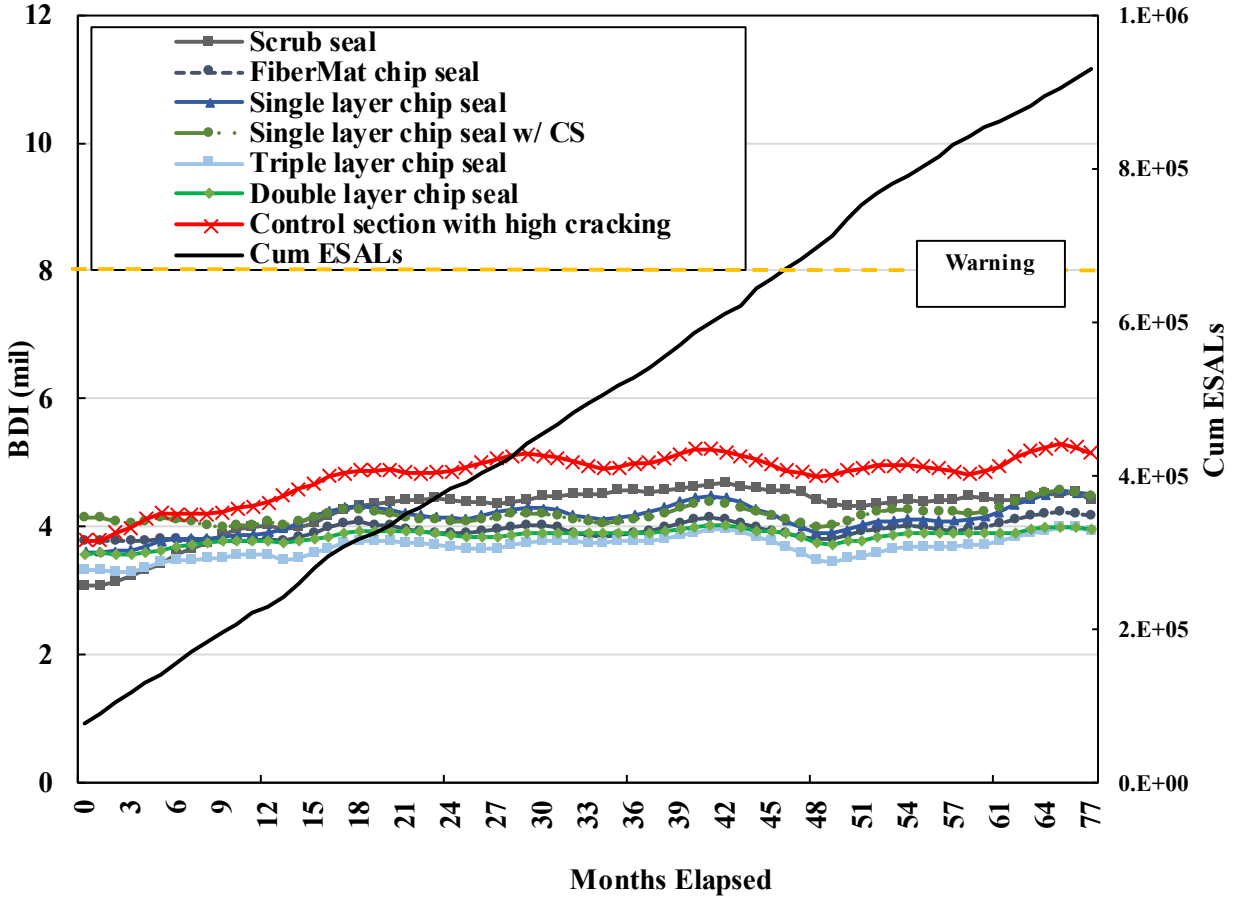

Figure 4-18: BDI values over the elapsed service life for chip seal group

Figure 4-19 shows the forecast of the BDI values for different treatment sections using ARIMA modeling. The prediction model results show that the control section BDI values would reach the warning threshold within approximately 82 months of service. The predicted BDI values for single layer chip seal treated sections show that, the BDI values would reach the warning zone after 90 months of service after application. The remaining chip seal treated sections are expected to remain under the FHWA warning threshold until 120 months of service.

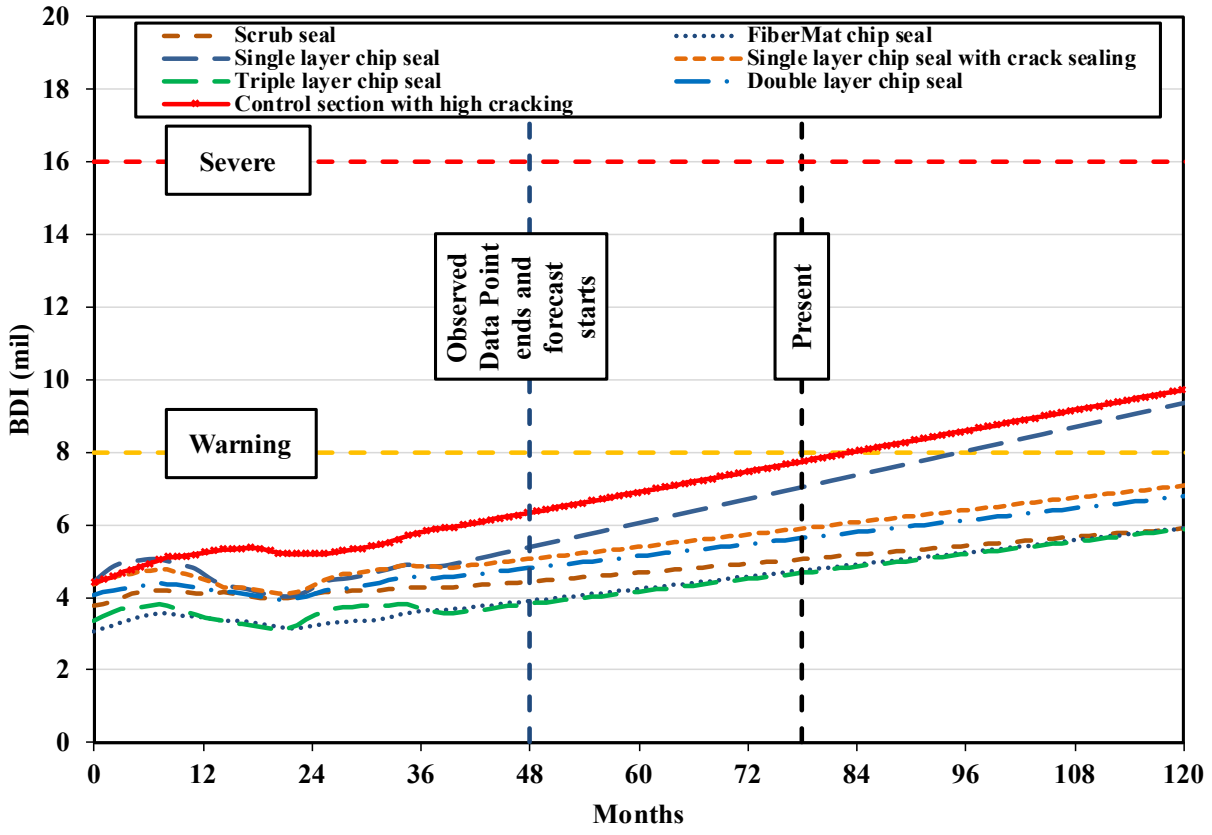

Figure 4-19: Forecast of the BDI values for chip seal group

4.2.3 Micro surfacing Group Results

Table 4-13 shows the summary statistics of the BDI values over the 77 months of elapsed service life from micro surfacing treated sections compared to the control section. This is apparent that the mean BDI value for double layer micro surfacing treated section is higher than the control section. The coefficient of variation (COV) for the BDI value of the treated sections is lower than that of the control section which indicates lower variability within the calculated BDI values from the treated sections.

Table 4-13: Summary statistics of the BDI values for the Micro surfacing group

Treatment	Mean	Std Dev	Min	Max	N	COV
Single layer micro surfacing	4.16	0.7	2.1	6.4	520	17.4
Single layer micro surfacing with crack sealing	4.56	0.6	3.4	6.3	518	13.9
Double layer micro surfacing	5.55	1.2	2.9	12.4	519	21.4
Control	5.03	1.8	2.3	13.0	519	36.0

Figure 4-20 indicate the mean BDI values of the micro surfacing treated sections at different times. The BDI values of the treated sections did not show any significant change after the treatment was applied. At present time, the mean BDI values of the treated sections are lower than the control section with lower variability except the mean BDI value for double layer micro surfacing is close in magnitude to the mean BDI of the control section.

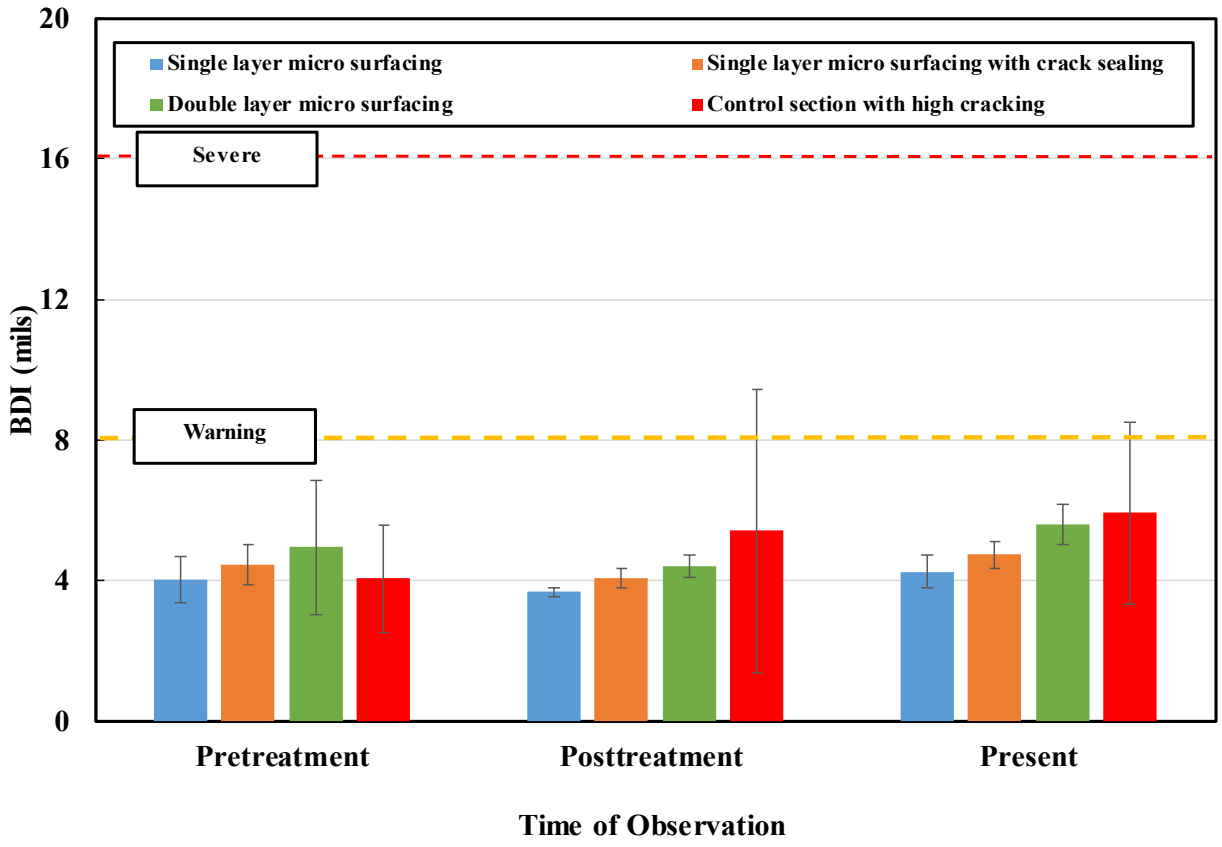

Figure 4-20: BDI values for different treatments at different times within Micro surfacing group

Table 4-14 shows the results of the time series mixed modeling p-values of the BDI values from the micro surfacing treated sections. Results show that all the treatments in each lane exhibit significance of time effect over the BDI values. The mixed modeling results indicate there is very significant time effect over the BDI values from all the treated sections in both lanes. In the inbound lane, the BDI values from single layer micro surfacing and double layer micro surfacing treated sections show very significant treatment effect while the same sections in the outbound lane indicate strong combined effect over the BDI values.

Table 4-14: p-values for time series mixed modeling for BDI values of treatments

Treatment Applied	Inbound lane to the quarry			Outbound lane from quarry		
	Treatment	Time	Combined	Treatment	Time	Combined
Single layer micro surfacing	<0.0001	0.0002	0.2097	0.2189	<0.0001	<0.0001
Single layer micro surfacing with crack sealing	0.3422	<0.0001	0.2881	0.1704	<0.0001	0.6991
Double layer micro surfacing	<0.0001	<0.0001	0.0486	0.566	<0.0001	0.0002

Figure 4-21 shows the BDI trend over the time for the micro surfacing treated sections. At the posttreatment condition the BDI values of the treated sections were higher than the control section. After 15 months of service, the BDI values of the control section exceeded the BDI values of all the treatment sections except double layer micro surfacing. BDI values of the double layer micro surfacing section were higher than the control section at the posttreatment condition which consistently remained higher over the elapsed service life of 77 months to the present date. The single layer micro surfacing and micro surfacing with crack sealing treated sections did not show any significant change in BDI over elapsed service life. All the mean BDI values have been lower than the FHWA designated warning threshold of 8 mils.

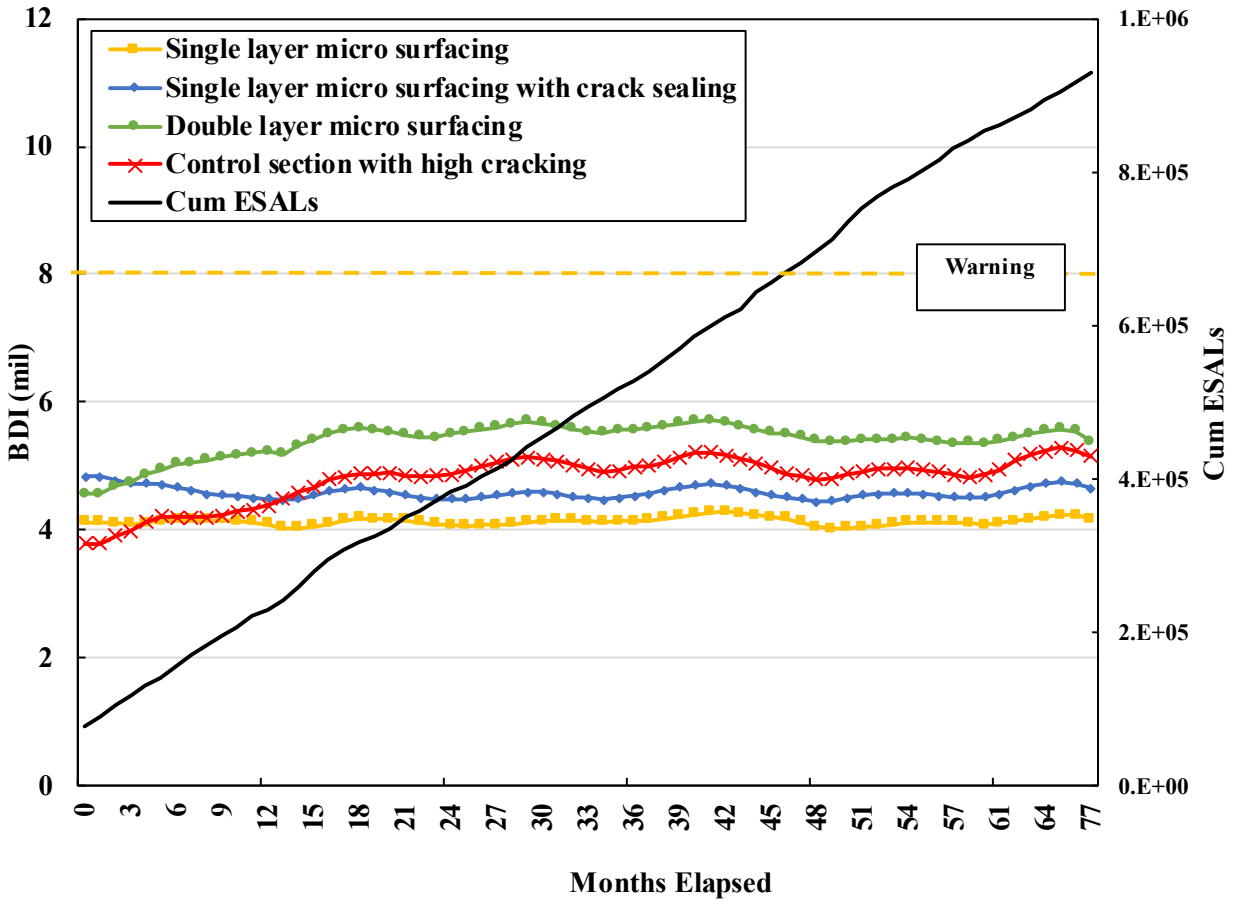

Figure 4-21: BDI values over the elapsed service life for Micro surfacing group

Figure 4-22 shows the performance prediction curves for the BDI values of the micro surfacing treated sections. The observed BDI values for double layer micro surfacing and single layer micro surfacing with crack sealing show higher magnitude of BDI compared to single layer micro surfacing. Predicted BDI values for microsurfacing treatment group do not reach the warning zone until 120 months of service.

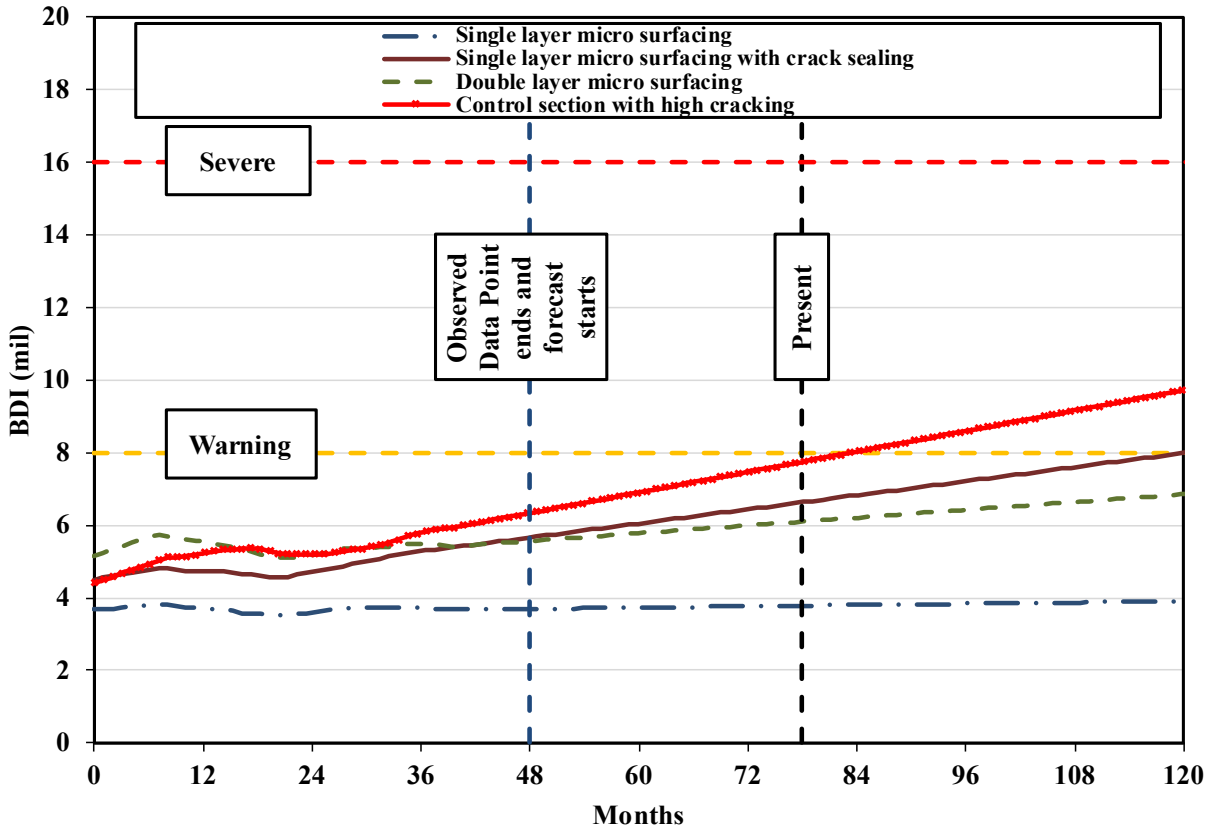

Figure 4-22: Forecast of the BDI values for Micro surfacing group

4.2.4 Combinations Group Results

Table 4-15 shows the summary statistics of the BDI values from treated sections within combination group. The mean BDI values for the treated sections are lower than the control section. Coefficient of variation (COV) values of the BDI values from the treated sections also indicate lower variability than that of the control section.

Table 4-15: Summary statistics of the BDI values for the combination group

Treatments	Mean	Std Dev	Min	Max	N	COV
Cape seal	3.38	0.72	2.0	5.4	516	21.4
FiberMat Cape seal	3.45	0.66	1.8	5.5	520	19.0
Scrub Cape seal	4.01	0.76	1.9	6.2	520	18.9
Thinlay on FiberMat	3.26	0.54	1.9	4.9	521	16.65
Control	5.03	1.81	2.3	13.0	519	36.0

Figure 4-23 indicate the BDI values of the cape seal treated sections at pretreatment, posttreatment and present condition. The mean BDI values indicate a decrease of values of the treated sections within 5 months of post construction service. At present time, after 77 months of service, the BDI values of the treated sections are significantly lower than the mean BDI value of the control section.

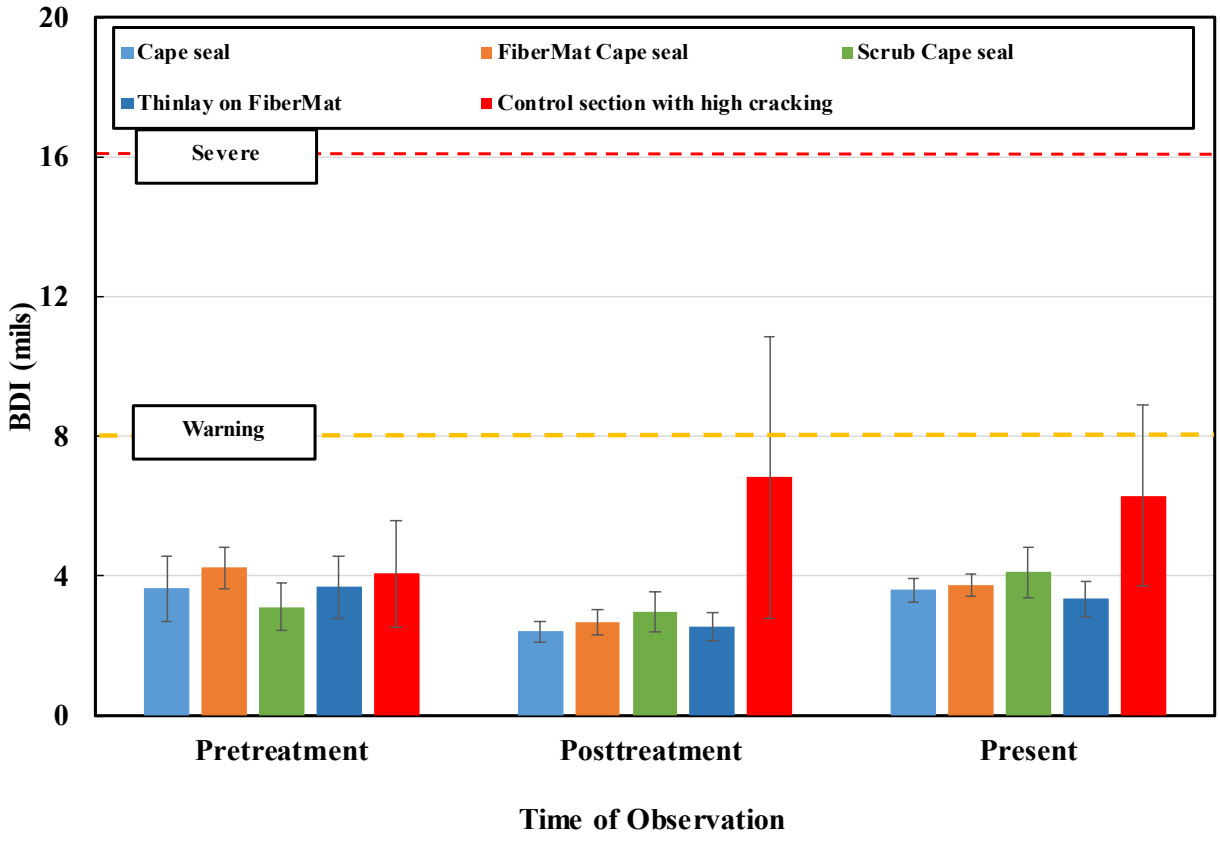

Figure 4-23: BDI values for different treatments at different times within combinations group

Table 4-16 shows the p-values for each treatment section from time series mixed modeling. The results shows that, all the effects are significant for the BDI values from scrub cape seal and thinlay on FiberMat chip seal treated section from the inbound lane. This was also observed that, all the effects are significant for the BDI values from cape seal and thinlay on FiberMat chip seal treated section from the outbound lane. In the inbound direction, the BDI values from the FiberMat cape seal treated section show time effect while the treatment effect was found significant over the BDI values from the outbound lane. BDI values from the sections treated with scrub cape seals in the outbound lane did not converge. The possible reasons could be- limited number of data points or presence of outliers.

Table 4-16: p-values for time series mixed modeling for BDI values of treatments

Treatment Applied	Inbound lane to the quarry			Outbound lane from quarry		
	Treatment	Time	Combined	Treatment	Time	Combined
Cape seal	0.0006	<0.0001	0.4463	<0.0001	0.0007	0.036
FiberMat Cape seal	0.1327	0.0006	0.461	0.0348	0.2229	0.4045
Scrub Cape seal	0.0114	<0.0001	<0.0001	Did not meet convergence		
Thinlay on FiberMat	<0.0001	<0.0001	0.0038	<0.0001	0.0003	0.0005

Figure 4-24 shows the trend of the mean BDI values of the treated sections within the combination group. The BDI value of the FiberMat cape seal treated section was higher than the control section but with time, the mean BDI decreased. The man BDI values of the treated sections are lower than the control section all over the elapsed service life of 77 months after applications of treatment. The mean BDI values of the treated sections have always been below the FHWA designated warning threshold of 8 mils.

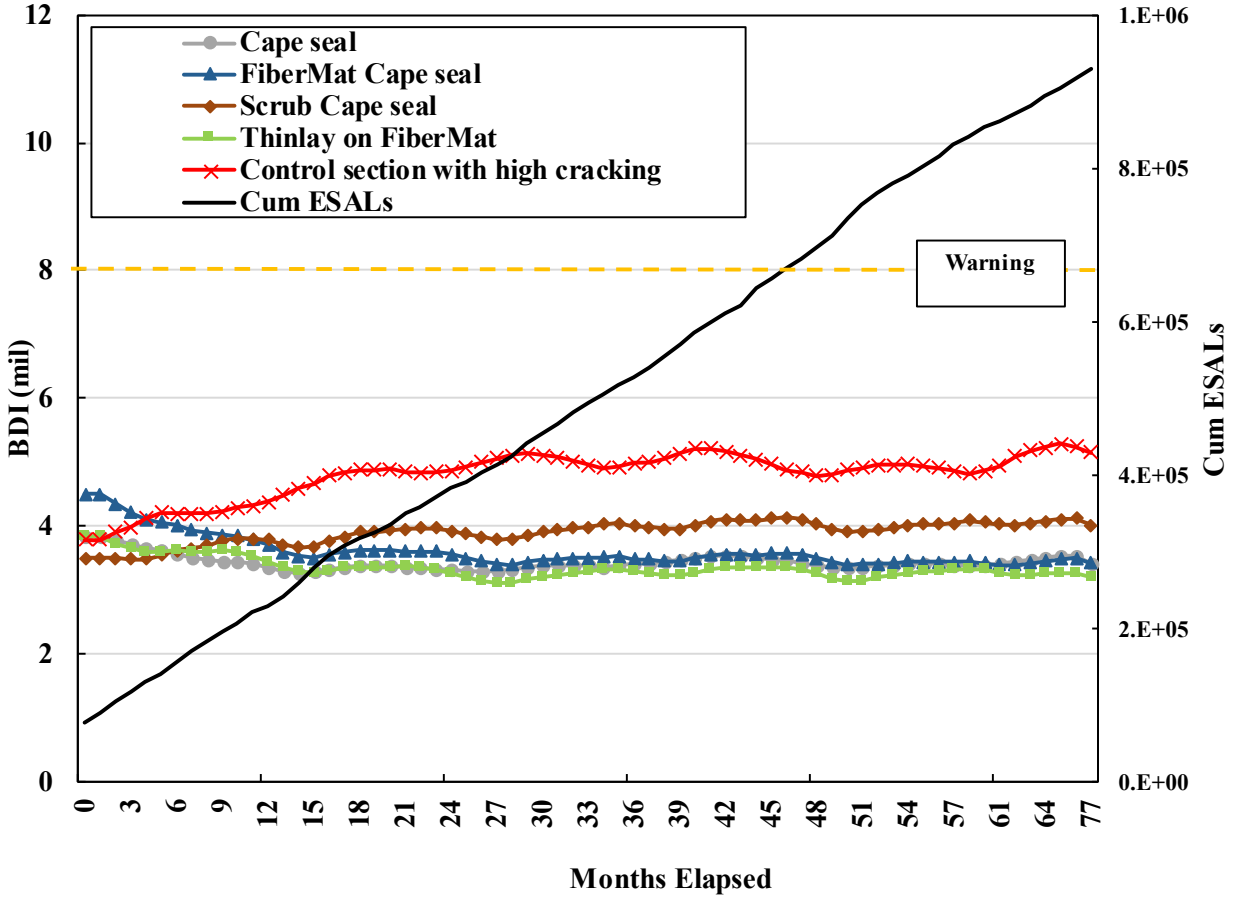

Figure 4-24: BDI values over the elapsed service life for combination group

Figure 4-25 shows the forecast of the BDI values for each treated section within the combination group. The forecast values indicate that the BDI values for the treated sections remain lower than the control section. The BDI value of the control section is forecasted to reach the FHWA designated warning region after 84 months of service, while the forecasted BDI values for the treated sections do not reach the warning zone until 120 months of post application service.

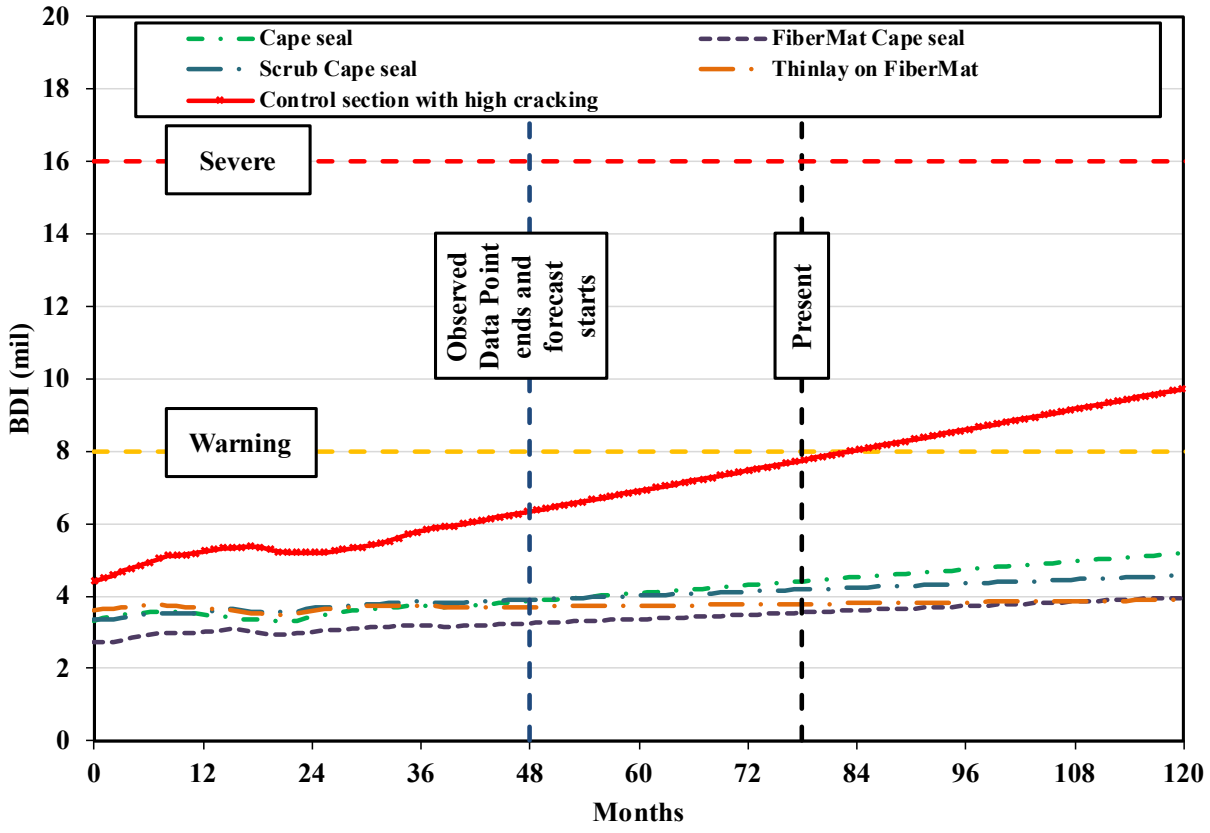

Figure 4-25: Forecast of the BDI values for combination group

4.2.5 Thinlays Groups Results

Table 4-17 shows the summary statistics of the BDI values of the treated sections within thinlay group. The results indicate that the mean BDI value of the treated sections are lower than the mean BDI of the control section. The coefficient of variation, which is the measurement of the variability of the data, shows that the mean deflections from the treated sections are lower than the control section (COV=35.97%).

Table 4-17: Summary statistics of the BDI values for the thinlay group

Treatment	Mean	Std Dev	Min	Max	N	COV
Thinlay	3.49	0.53	2.4	4.8	522	15.27
Polymer Thinlay	3.83	0.76	2.2	5.9	521	19.73
Ultra-Thin Bonded Wearing Course	4.18	1.14	2.1	8.0	517	27.26
Control	5.03	1.81	2.3	13.0	519	35.97

Figure 4-26 shows the mean BDI values of different treated sections within the thinlay group at different times. A drop in BDI after treatment application can be observed within 5 months of posttreatment service. The standard deviation of the BDI values also went lower in magnitude in the posttreatment condition than that of the control section. At present time, the BDI values of the treated sections are significantly lower than that of the control section. BDI values from the thinlay treated sections were lower than the FHWA designated Warning threshold of 8 mils.

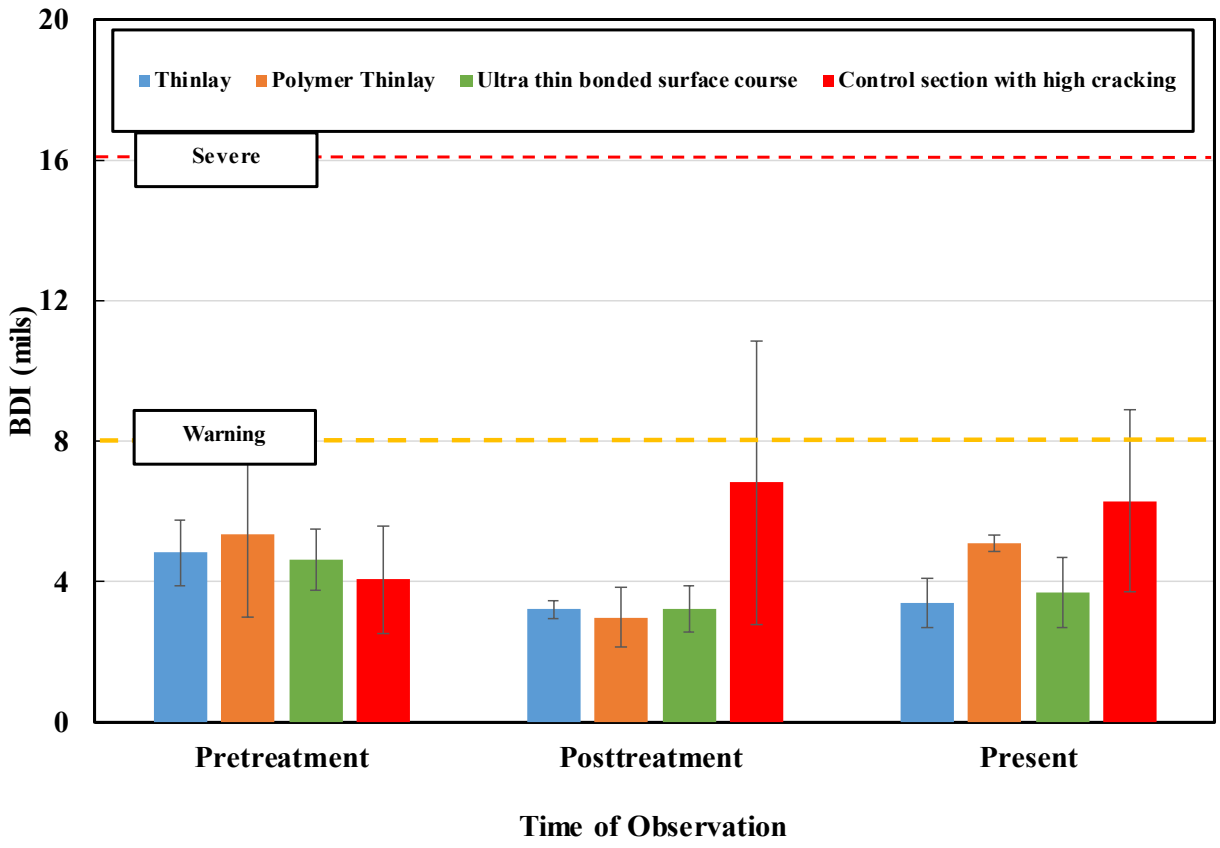

Figure 4-26: BDI values for different treatments at different times within thinlay group

Table 4-18 shows the results from the time series mixed model of the BDI values of the treated sections within thinlay group. The p-values obtained indicate that there are treatment, time and combined effects over all the treated sections mean BDI value in both lanes except thinlays in the inbound lane. The p-values for the ultra-thin bonded wearing course in the outbound lane did not converge in the mixed model. The possible reasons could be- limited data points or presence of excess number of outliers within the dataset.

Table 4-18: p-values for time series mixed modeling for BDI values of treatments

Treatment Applied	Inbound lane to the quarry			Outbound lane from quarry		
	Treatment	Time	Combined	Treatment	Time	Combined
Thinlay	0.0011	<0.0001	0.1584	<0.0001	0.012	<0.0001
Polymer Thinlay	<0.0001	<0.0001	0.0059	0.0005	0.001	0.0342
Bonded Ultra Thinlay	<0.0001	<0.0001	<0.0001	Did not meet convergence		

Figure 4-27 shows the trend of the BDI values of the thinlay treated sections over 77 months of elapsed service life after construction. In the posttreatment condition, the BDI values of the treated sections were higher than the control section. The mean BDI value of the control section exceeded the mean BDI of the treated sections by 12 months of posttreatment service. The mean BDI values did not show significant change over the 77 months of posttreatment service.

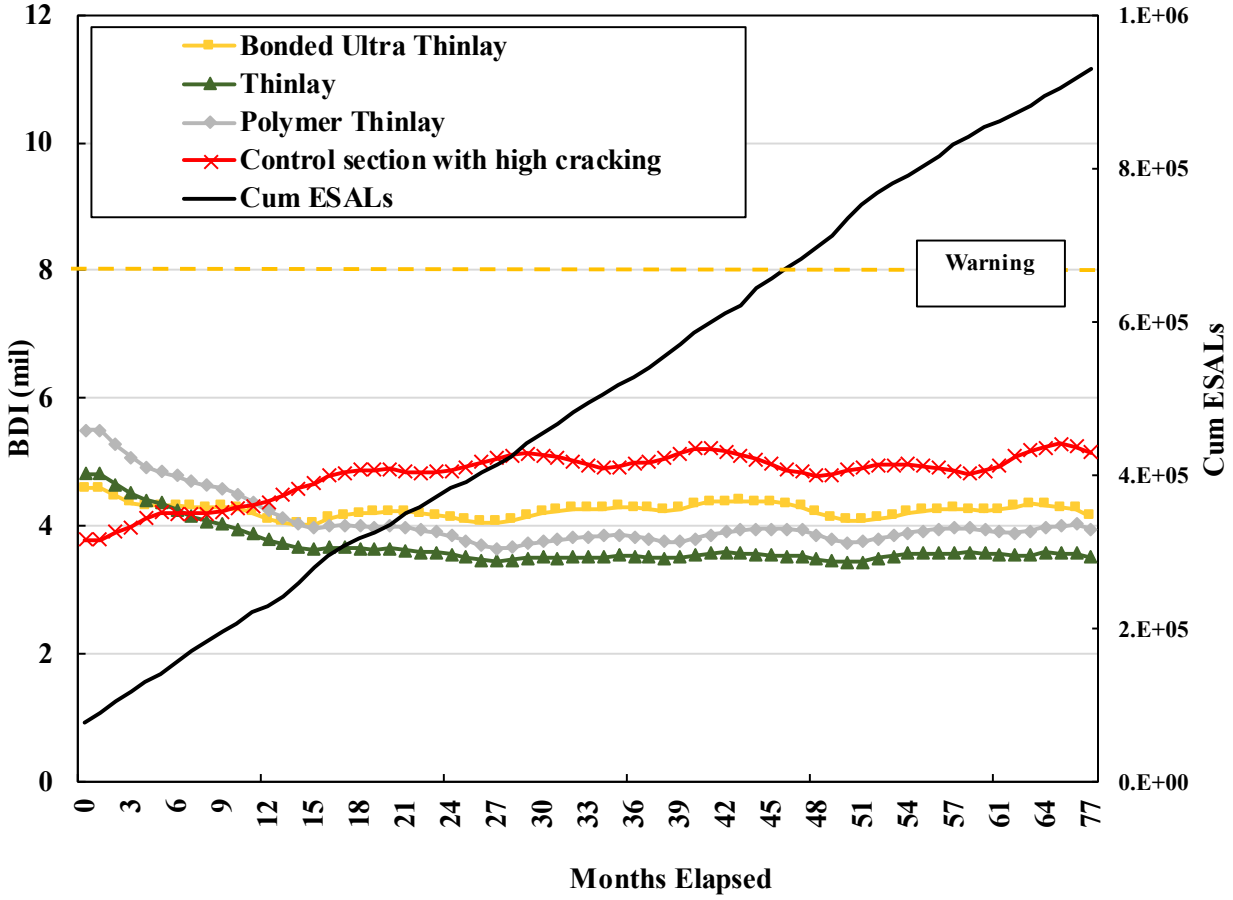

Figure 4-27: BDI values over the elapsed service life for thinlays group

Figure 4-28 shows the forecast BDI values for the treated sections within the thinlays group compared to that of the control section. The forecast BDI values for the sections treated with thinlay and polymer modified thinlay do not increase significantly over the forecast period. The forecast BDI values for the ultra-thin bonded thinlay treated section indicate a prediction of higher mean BDI value than the control section. Forecast values also indicate that the mean BDI values for ultra-thin bonded thinlay would reach the warning threshold (≥8 mils) before the control section but the present recorded values indicate a better performance than the forecast.

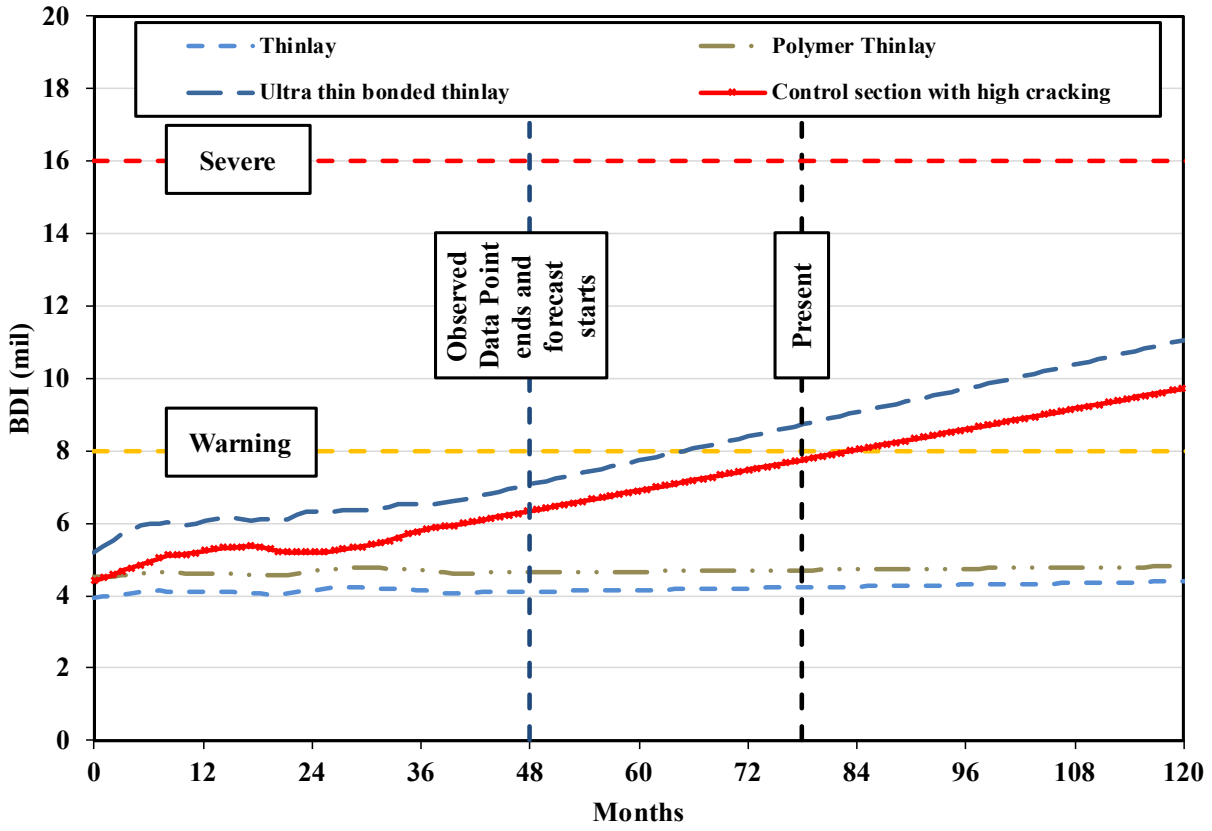

Figure 4-28: Forecast of the BDI values for thinlay group

4.3 Base Curvature Index (BCI)

Literatures claim base curvature index (BCI) represents the structural health of the subgrade layer. Studies found correlation of the BCI values with the layer moduli, stress-strain at the top of subgrade, rutting susceptibility, cracking- which are discussed in the literature review. The BCI values are also discussed in the same fashion as center deflection and BDI values in the previous paragraphs. As mentioned in the literature, the subgrade is less or somewhat not responsive to the temperature changes due to seasonal cycles. Thus, the BCI values are presented without considering seasonal effects on the subgrade.

4.3.1 Standalone Group Results

Table 4-19 shows the summary statistics of the BCI parameter for different treatment within standalone treatment group. Crack sealing and fog seal treatment sections show higher mean value than the control section. The COV of BCI values from crack seal treated section was higher than the COV of the BCI values from the control section, indicating more variability.

Table 4-19: Summary statistics of the BCI values for the standalone treatment group

Treatment	Mean	Std Dev	Min	Max	N	COV
Fog Seal	1.8	0.5	0.6	3.5	521	29.6
Crack Sealing	2.1	0.9	0.3	5.1	518	43.4
Control	1.6	0.5	0.6	3.6	519	33.8

.

The recorded BCI values for the standalone groups are shown at pretreatment, posttreatment and present condition in **Figure 4-29**. It is observed from the bar charts that, the fog seals show an increase in the BCI value while crack seal shows a decrease in the BCI value after the treatment. At present time, the mean BCI values for rejuvenating fog seal and crack seal are somewhat equal to the control section. The present BCI value for all the treatment sections in the standalone group are below the FHWA warning threshold of 4 mils.

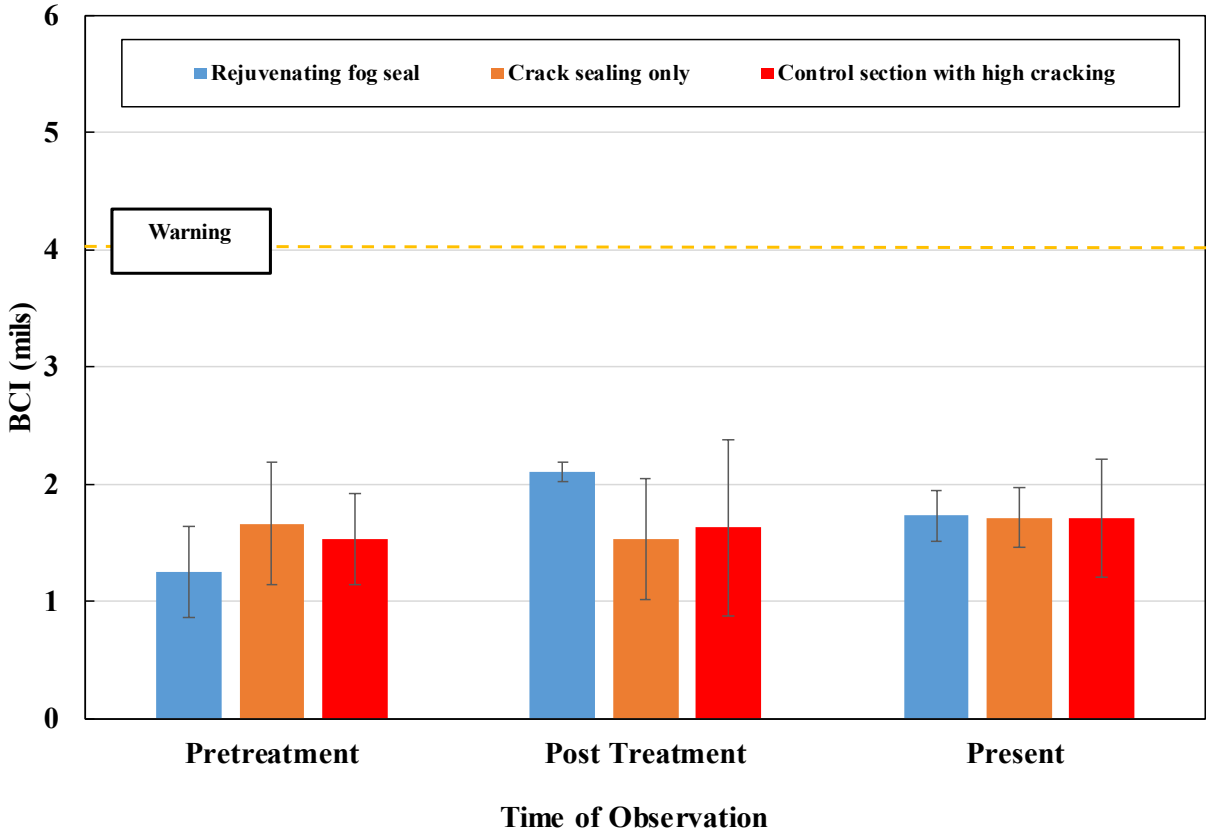

Figure 4-29: BCI values for treatments at different times within standalone group

To observe the influence of the treatment over the subgrade, the BCI values for different treatments were tested with timeseries mixed modeling and the p-value at 95% confidence interval were extracted. Table 4-20 shows the calculated p-values from time series mixed modeling of the BCI values. It was observed that all the effects are significant over the BCI values from the following sections: crack seal in the inbound lane and fog seal in the outbound lane. BCI values from fog seal treated section in the inbound lane showed significant treatment effect. BCI values from the crack seal treated section did not converge in the outbound direction. The reason for this is that there are other significant effect(s) that were not considered in the model. Larger datasets with more effects can aid to find the unidentified effect.

Table 4-20: p-values for time series mixed modeling for BCI values of treatments

Treatment Applied	Inbound lane to the quarry			Outbound lane to the quarry		
	Treatment	Time	Combined	Treatment	Time	Combined
Rejuvenating Fog seal	<u>≤0.0001</u>	0.1091	0.2353	<u>≤0.0001</u>	<u>0.0004</u>	<u>0.0012</u>
Crack seal	<u>≤0.0001</u>	<u>0.0405</u>	<u>0.0077</u>	Did not meet convergence		

Figure 4-30 shows the BCI values for different treatments along the service life elapsed after the application of treatment. The crack sealing sections always showed higher BCI values than fog seal and control sections. The BCI values for the fog seal treated section was lower than the control section while with time the BCI value increased and reached the same magnitude as the control section at present. Yet, all the BCI values for treated sections along with control section were lower than the FHWA designated warning zone threshold of 4 mils.

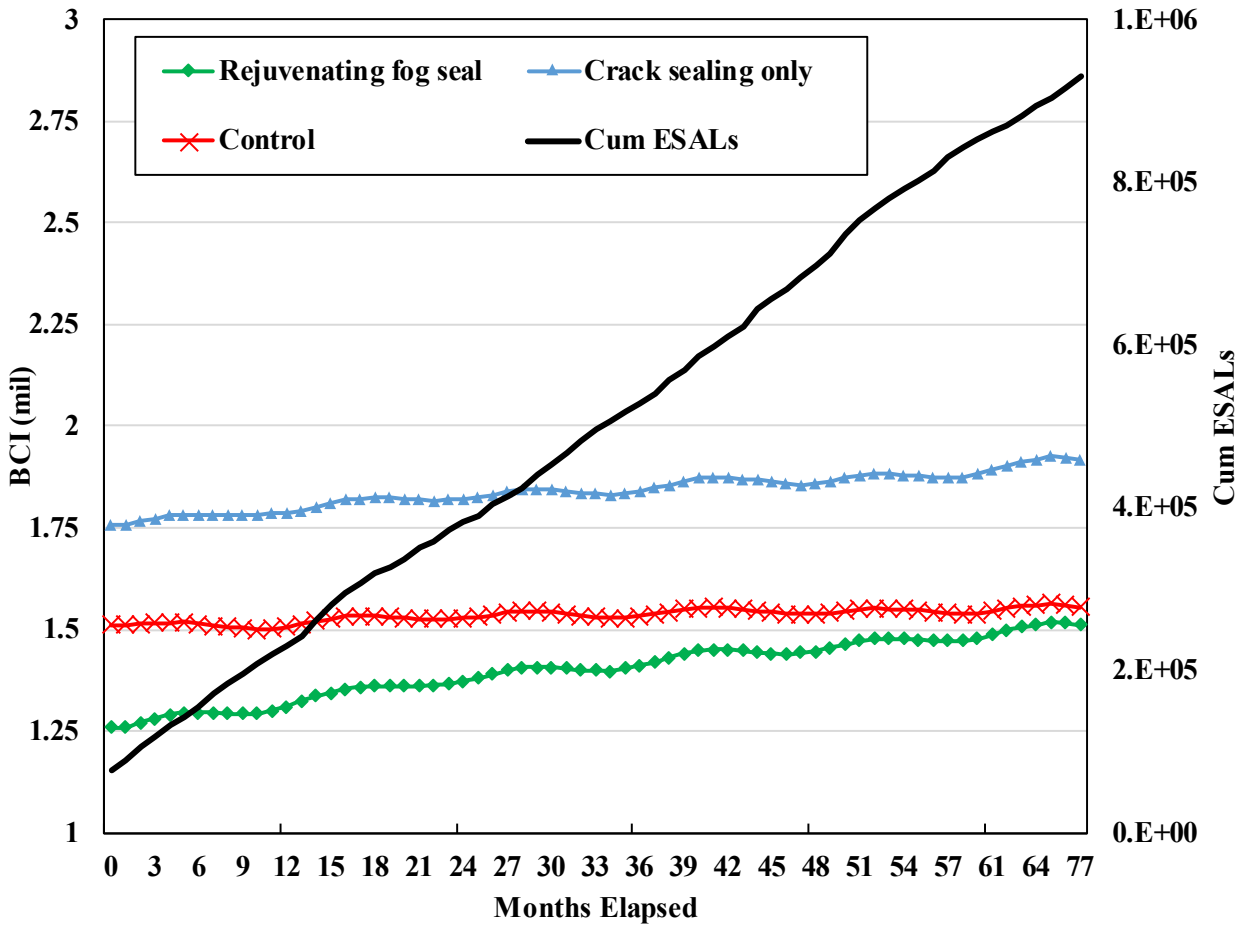

Figure 4-30: BCI values over the elapsed service life for standalone treatment group

Figure 4-31 shows the forecast of the BCI value using ARIMA modeling. The predicted values show that the BCI value for the control section does not reach the Warning limit (≥4 mils) within 120 months from the beginning of the analysis period. None of the mean BCI forecast value from the treatment section reach the warning zone after up to 120 months of posttreatment service life.

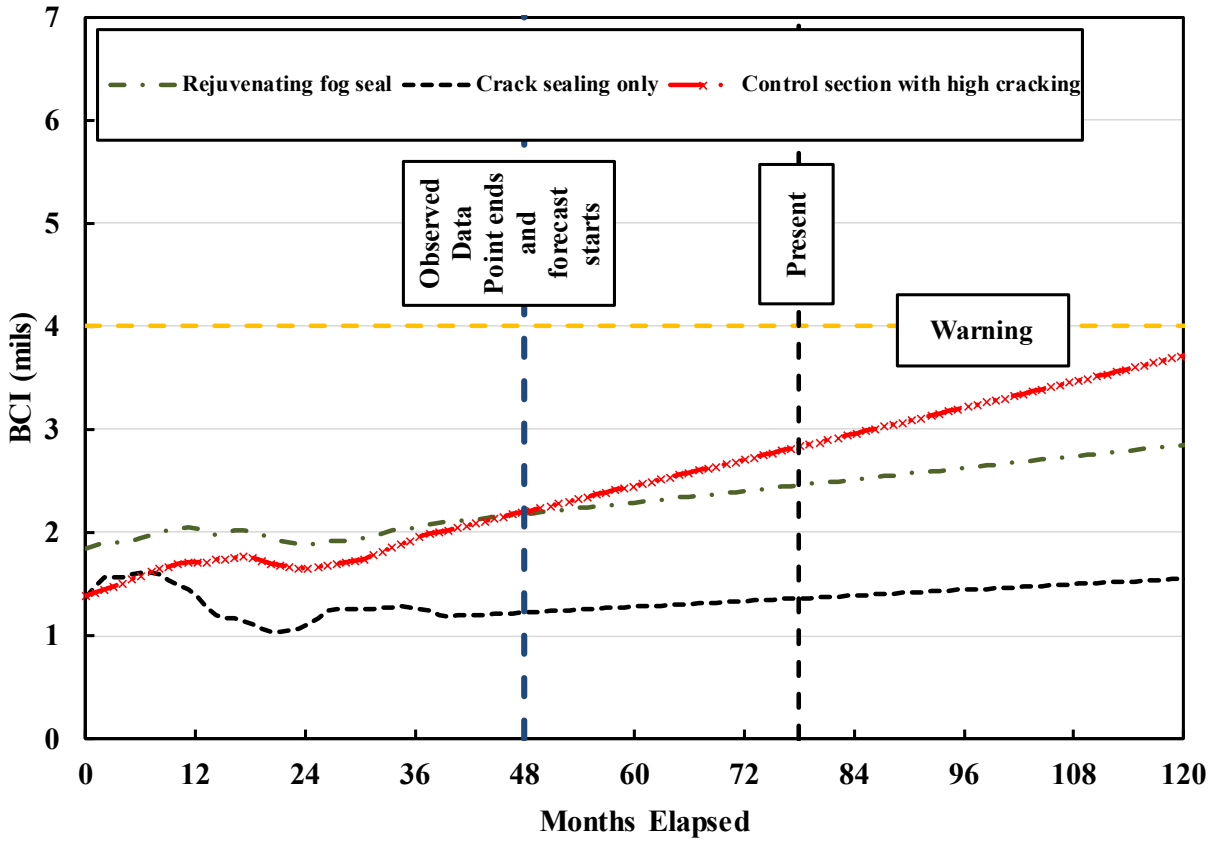

Figure 4-31: Forecast of the BCI values for standalone treatment group

4.3.2 Chip Seal Group Results

Table 4-21 shows the summary statistics of the BCI values of the treated sections within the chip seal group compared to the control section. The mean BCI value for the treated sections are lower than the mean BCI value of the control section. COV values indicate that, BCI values of the treated sections within the chip seal group show higher variability than the control section, except for the double layer chip seal section.

Table 4-21: Summary statistics of the BCI values for the chip seal group

Treatment	Mean	Std Dev	Min	Max	N	COV
FiberMat chip seal	1.46	0.49	0.6	3.3	521	33.51
Chip seal	1.58	0.59	0.2	3.6	519	37.25
Chip seal w/ crack sealing	1.47	0.50	0.6	3.3	515	34.38
Triple layer chip seal	1.42	0.49	0.2	2.9	516	34.58
Double layer chip seal	1.54	0.42	0.6	3.2	517	27.21
Scrub Seal	1.49	0.48	0.5	3.0	516	32.1
Control	1.60	0.54	0.6	3.6	519	33.8

Figure 4-32 shows the mean BCI values for different sections within the chip seal group compared to the mean BCI of the control section at the following times: pretreatment, posttreatment and present. The values indicate that there was a drop in the mean BCI value of the treated section at post treatment condition, except for the single layer chip seal. At present time the FiberMat chip seal, chip seal with crack seal, scrub seal, double layer chip seal and triple layer chip seal treated sections have mean BCI values lower than control section. The same sections also have less variability in BCI measurement which is indicated by decreased standard deviation.

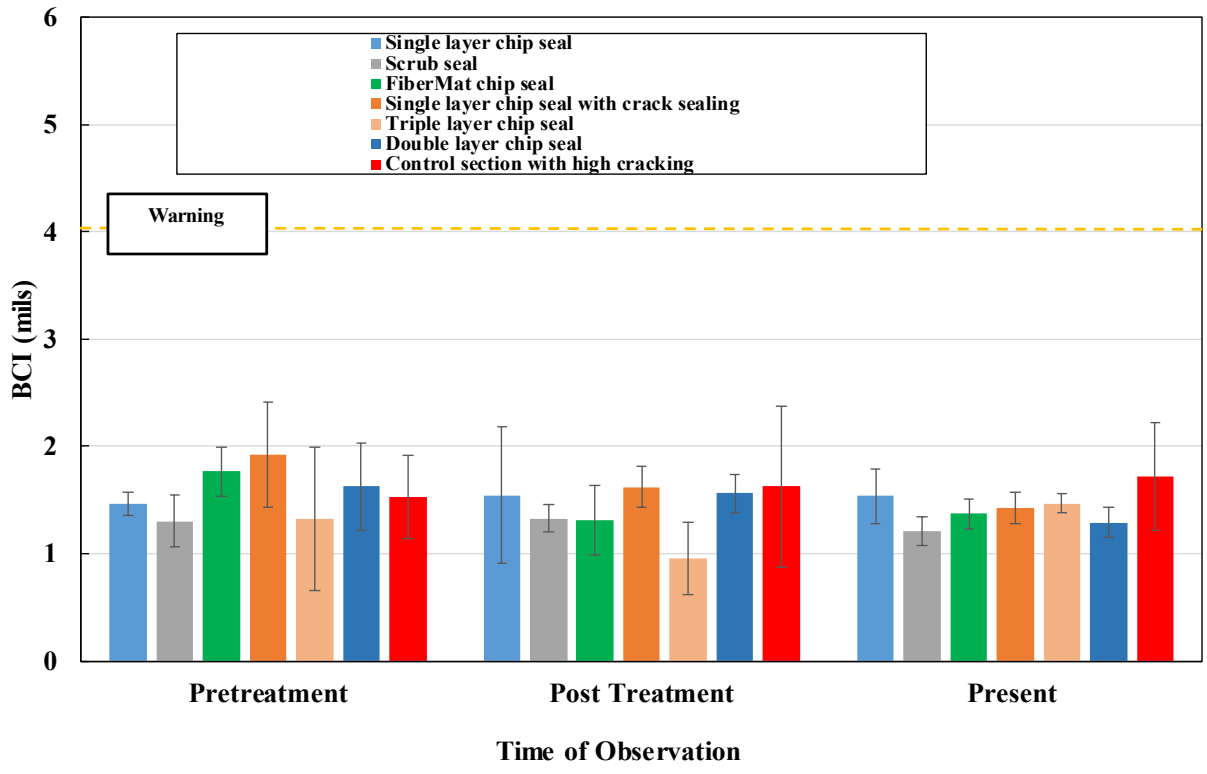

Figure 4-32: BCI values over the elapsed service life for chip seal group

Table 4-22 shows the p-values from the time series mixed model of the BCI values from the treated sections within chip seal group. In the outbound lane it was observed that there is significant time and combined interaction effect over the mean BCI values of all the treated sections, except for the scrub seal. FiberMat chip seal, scrub seal and single layer chip seal with crack sealing treated sections indicate only treatment effect is significant over the measured BCI values in the outbound lane. In the inbound lane, the BCI values from the triple layer chip seal indicate significance of treatment, time and combined interaction effect over the BCI values. In the same lane, single layer chip seal with crack sealing, scrub seal, double layer chip seal and triple layer chip seal indicate significant combined interaction effect over the BCI values.

Table 4-22: p-values for time series mixed modeling for BCI values of treatments

Treatment	Inbound lane to the quarry			Outbound lane from quarry		
	Treatment	Time	Combined	Treatment	Time	Combined
FiberMat chip seal	0.0078	<0.0001	0.5939	<0.0001	<0.0001	0.0002
Single layer chip seal	Did not meet convergence			0.4394	<.0001	<.0001
Single layer chip seal w/ Crack Seal	0.2106	0.8104	0.001	0.0006	<.0001	<.0001
Triple layer chip seal	0.0014	<.0001	<.0001	0.305	<.0001	<.0001
Double layer chip seal	0.2123	0.3745	0.0442	0.1458	<.0001	0.0049
Scrub Seal	0.4444	<0.0001	<0.0001	0.0333	0.0825	0.1782

Figure 4-33 shows the BCI values over the elapsed service life of chip seal treated sections compared to that of the control section. The trends show that there was no significant change in the BCI value for all the treated sections. Single layer chip seal with crack seal, FiberMat chip seal and double layer chip seal treated sections had higher BCI values compared to the control section initially after construction which tend to remain higher until the present time. The single layer chip seal, triple layer chip seal and scrub seal treated sections showed lower BCI values than the control section at the beginning of the analysis period which tend to remain lower over the elapsed 77 months of service life.

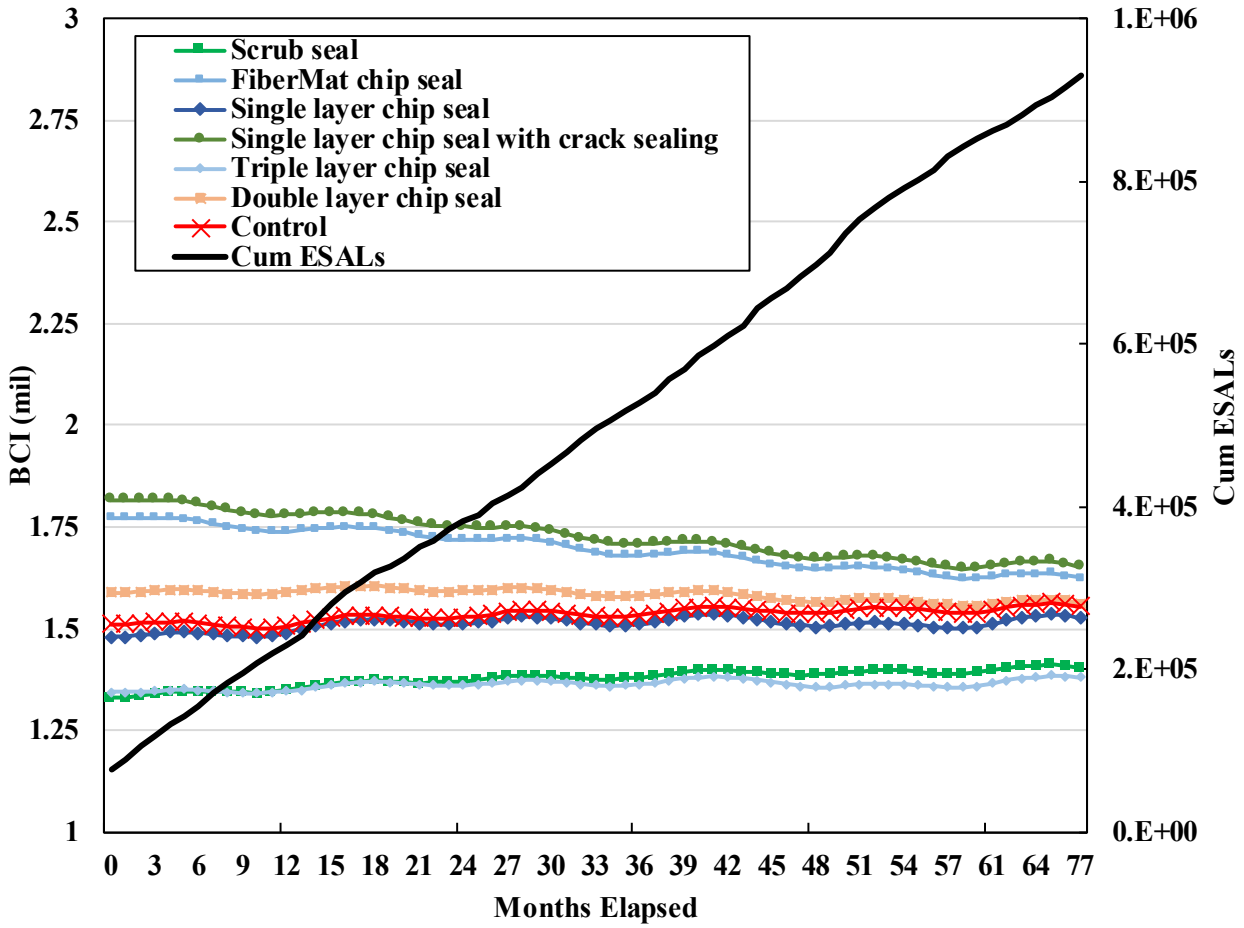

Figure 4-33: BCI values over the elapsed service life for chip seal group

Figure 4-34 shows the forecast of the BCI values for each of the treated sections compared to the control section. The forecast values indicate that the BCI value for single layer chip seal and triple layer chip seal section indicate higher tendency to reach the warning while the BCI values of the control section are most likely to reach the waning threshold at 130 months of service. Any of the BCI values from the treated sections do not seem to reach the warning threshold within 120 months of service according to the observed values and forecast model.

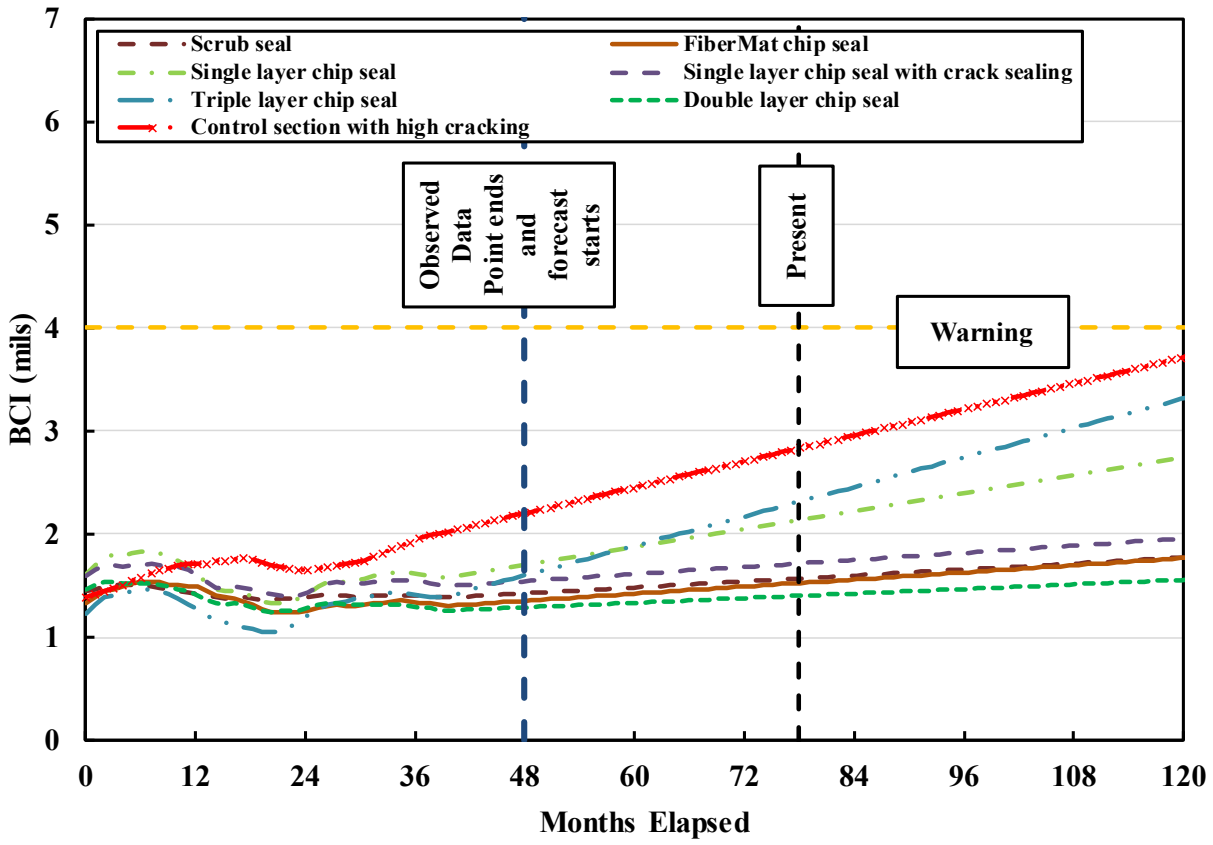

Figure 4-34: Forecast of the BCI values for chip seal group

4.3.3 Micro surfacing Group Results

Table 4-23 shows the summary statistics of the BCI values from the sections within the micro surfacing group. The mean BCI values from the treated sections are lower than that of the control section. Coefficient of variation (COV) values indicate higher variability in BCI values from the single layer micro surfacing with crack sealing and double layer micro surfacing treated sections (35.3% and 38.2% respectively) compared to the control section (33.8%).

Table 4-23: Summary statistics of the BCI values for the Micro surfacing group

Treatment	Mean	Std Dev	Min	Max	N	COV
Single layer micro surface	1.56	0.43	0.5	2.5	520	27.2
Single layer micro surface w/ crack sealing	1.46	0.52	0.6	4.3	518	35.3
Double layer micro surface	1.42	0.54	0.5	4.0	519	38.2
Control	1.60	0.54	0.6	3.6	519	33.8

Figure 4-35 shows mean BCI values for different treated sections within micro surfacing group at various points in time. The mean BCI for the treated sections before treatment application were higher than that of the control section. The mean BCI values did not show any significant change after construction except reduction of variability of BCI values for the section treated with double layer micro surfacing. At the present condition, the mean BCI values are lower than the measured mean BCI of the control section.

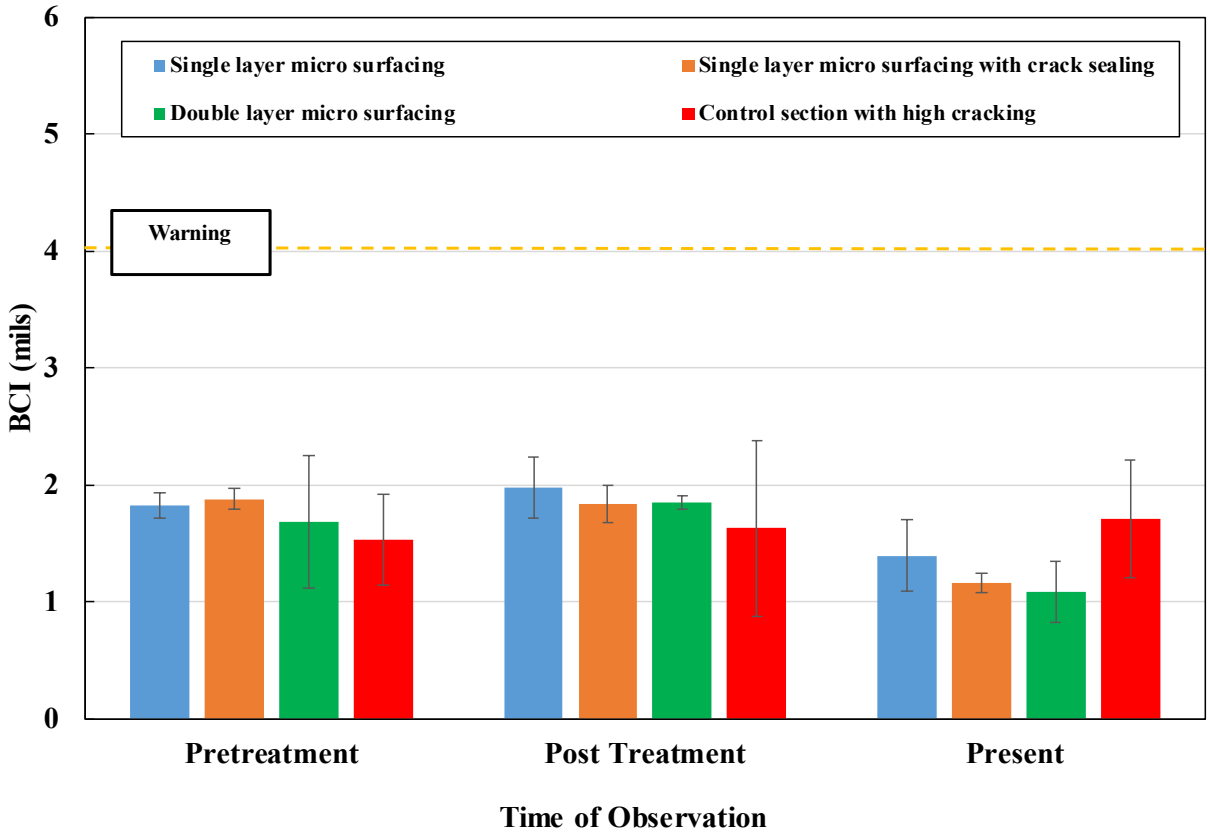

Figure 4-35: BCI values for different treatments at different times within Micro surfacing group

Table 4-24 shows the results of the time series mixed modeling on the BCI values from the treated sections within the micro surfacing group. Results indicate that BCI values from sections with single layer micro surfacing have significant treatment, time and combined effect on both lanes. The other two treatments did not show any strong significant effect of treatment, time or combined interaction effect. Single layer micro surfacing with crack sealing and double layer crack seal BCI values did not converge in the outbound and inbound lane, respectively. The reasons could be inadequate data, presence of high number of outliers in the dataset or presence of any other significant effect which is not yet identified in the model.

Table 4-24: p-values for time series mixed modeling for BCI values of treatments

Treatment	Inbound lane to the quarry			Outbound lane from quarry		
	Treatment	Time	Combined	Treatment	Time	Combined
Single layer micro surfacing	0.0081	0.0004	0.1861	0.005	<.0001	0.0306
Single layer micro surfacing w/ CS	0.4917	0.4311	0.0065	Did not meet convergence		
Double layer micro surfacing	Did not meet convergence			0.002	0.5085	0.3739

Figure 4-36 shows the trend of the BCI values over the elapsed service life of the treated sections within the micro surfacing group compared to the control section. The BCI values of the sections treated with single layer micro surfacing and micro surfacing with crack sealing showed gradual decrease over the time, yet the magnitude was higher than the control section over the 77 months of posttreatment service. The mean BCI value of the double layer micro surfacing treated sections did not show any significant change. At 50 months of elapsed service life, the mean BCI value of the control section exceeds the mean BCI of the double layer chip seal treated section.

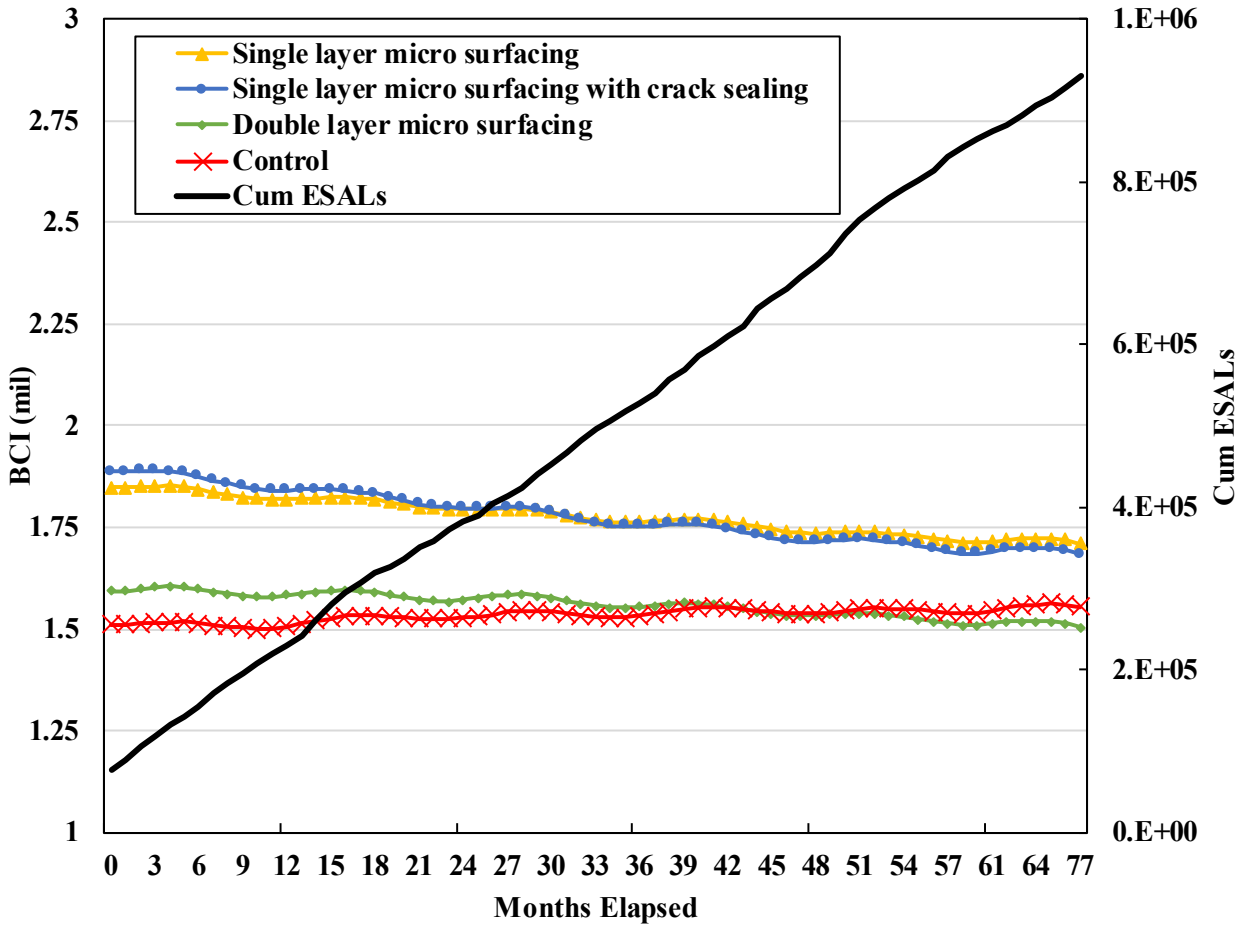

Figure 4-36: BCI values over the elapsed service life for micro surfacing group

Figure 4-37 show the forecast of the BCI values of the treated sections within the micro surfacing group compared to the forecast BCI value of the control section. The forecast values indicate that the BCI values for single layer micro surfacing and double layer micro surfacing values decrease with time, while the values increase with time for the sections treated with single layer micro surfacing with crack sealing. It was also observed that the forecast BCI values do not reach the warning threshold of BCI value designated by FHWA (≥4mils).

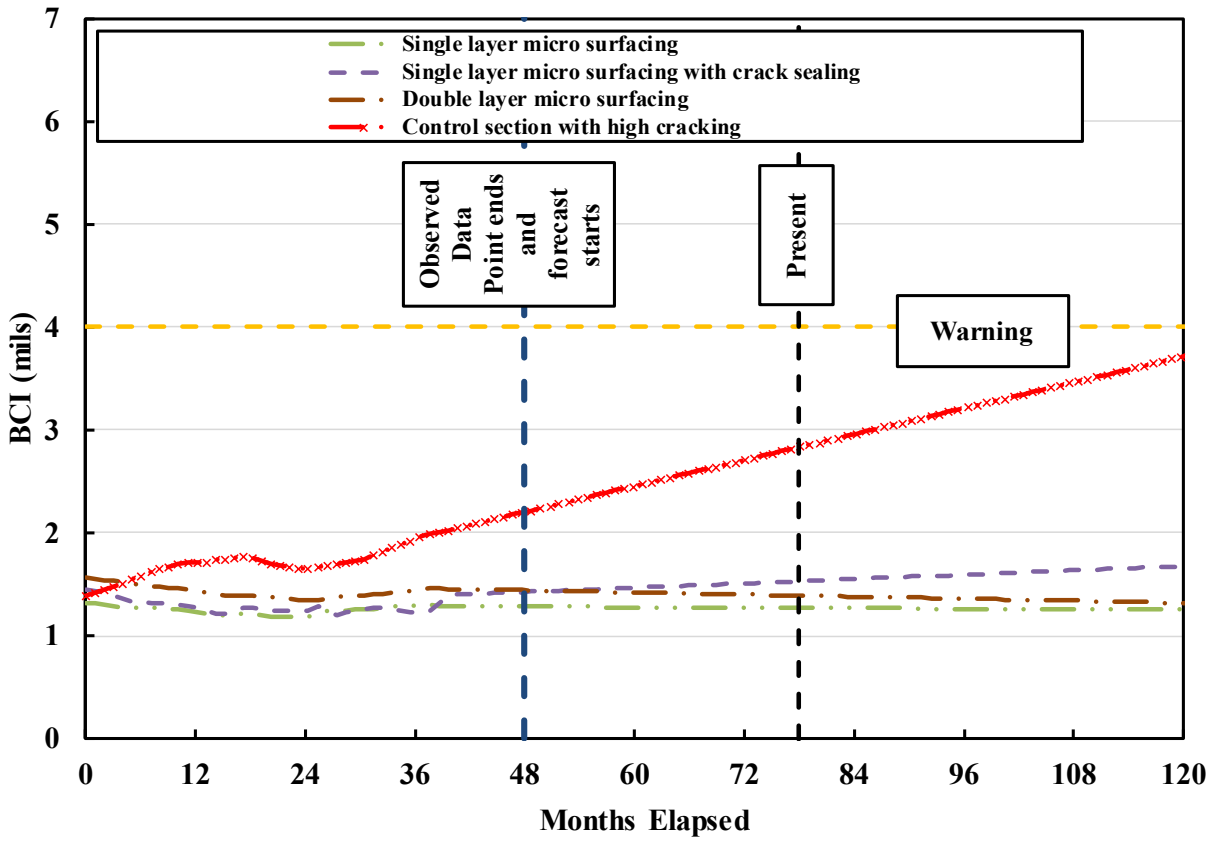

Figure 4-37: Forecast of the BCI values for Micro surfacing group

4.3.4 Combinations Group Results

Table 4-25 shows the summary statistics of the BCI values of the treated sections within the combination group compared to the control section. The mean BCI value of the treated sections are significantly lower than the control section. Coefficient of variation (COV) values for the cape seal and FiberMat cape seal treated sections are close in magnitude to the COV of the control section (33.8%). Among the treatments in the combination group, cape seal and FiberMat cape seal indicate higher variability in BCI values than the rest of the treated sections.

Table 4-25: Summary statistics of the BCI values for the combination group

Treatment	Mean	Std Dev	Min	Max	N	COV
Cape seal	1.03	0.32	0.3	2.0	516	30.5
FiberMat Cape seal	1.16	0.36	0.5	2.1	520	31.0
Scrub Cape seal	1.38	0.37	0.6	2.7	520	26.4
Thinlay on FiberMat	1.25	0.29	0.6	2.0	521	23.6
Control	1.60	0.54	0.6	3.6	519	33.8

Figure 4-38 shows the mean BCI values of the sections treated within the combination group compared to the control section at pretreatment, posttreatment and present time. The bar chart indicates that the mean BCI of the sections treated with cape seal and FiberMat cape seal experience decrease in magnitude after treatment application, while the rest of the treated sections do not show any significant change in BCI values. The present values indicate that the mean BCI values of the treated sections decrease with time, which is the indication that the treatments may be helping with improvement of the subgrade.

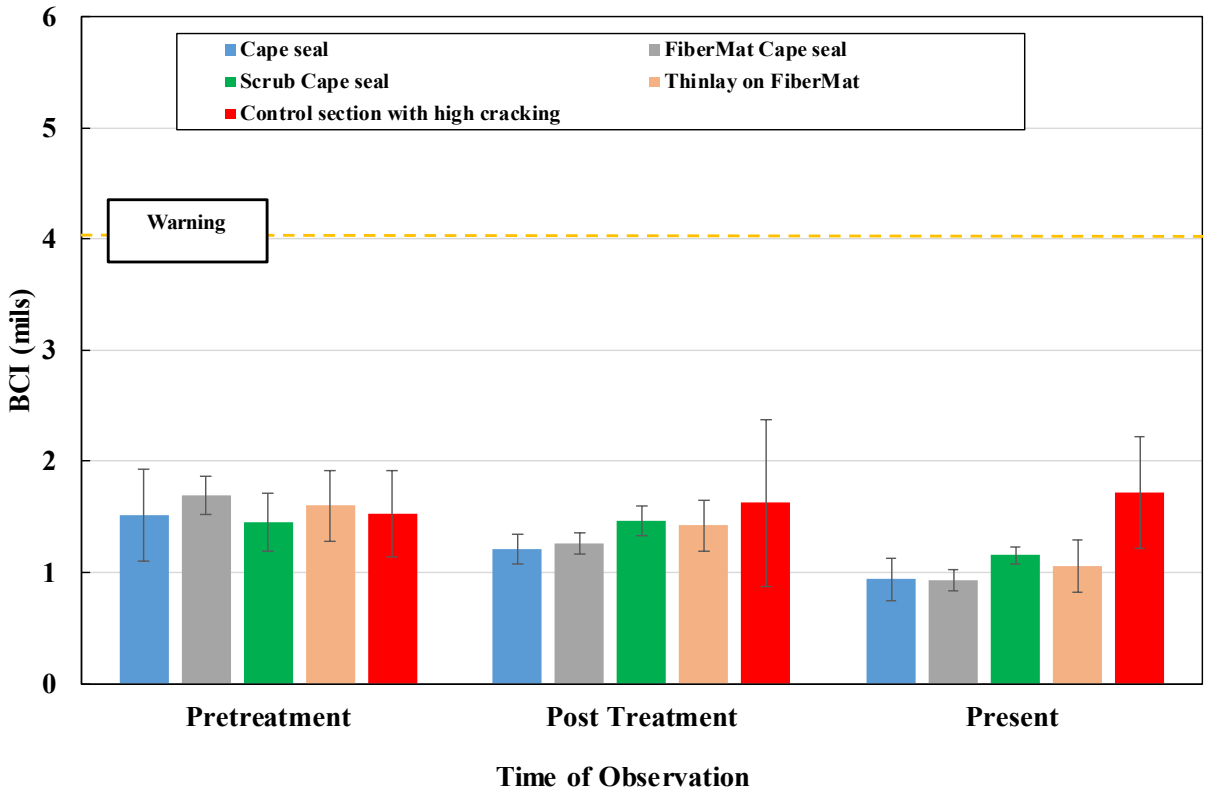

Figure 4-38: BCI values for different treatments at different times within combination group

Time series mixed modeling was performed to analyze the effect of the time, treatment and combined interaction effect on the BCI values from the treated sections. Table 4-26 shows the result of the time series mixed modeling on the BCI values within the combination group. The BCI values in the inbound lane show significance of time effect while in the outbound lane the significance of treatment effect is observed over all the treated sections. BCI values from the sections treated with FiberMat cape seal and cape seal show significance of all effects (treatment, time and combination) in both lanes within the study. Scrub cape seal treated section BCI values show significant time effect in the inbound lane while in the outbound lane the treatment effect is very significant. In the outbound lane, the sections treated with thinlay on FiberMat did not converge. The reasons for the failure to converge could be inadequate data, presence of outliers or any unidentified effect which might be significant.

Table 4-26: p-values for time series mixed modeling for BCI values of treatments

Treatment	Inbound lane to the quarry			Outbound lane from quarry		
	Treatment	Time	Combined	Treatment	Time	Combined
Cape seal	0.0187	<.0001	0.0053	<.0001	<.0001	<.0001
FiberMat Cape seal	<.0001	0.0045	<.0001	<.0001	<.0001	<.0001
Scrub Cape seal	0.0508	0.0006	0.1353	<.0001	0.5573	0.0539
Thinlay on FiberMat	<.0001	0.0126	0.3694	Did not meet convergence		

Figure 4-39 shows the trend of the BCI values over the elapsed 77 months of post application service life of the treated sections within combination group. The BCI value trends were smoothed off using moving average (MA) method with a damping factor of 0.1. The BCI values form the FiberMat cape seal, thinlay on FiberMat and cape seal treated sections show a decreasing trend over the time while the BCI values of the scrub seal treated sections do not change significantly over time. Over the elapsed service period, none of the treated sections had a BCI value over the warning threshold of BCI value designated by FHWA.

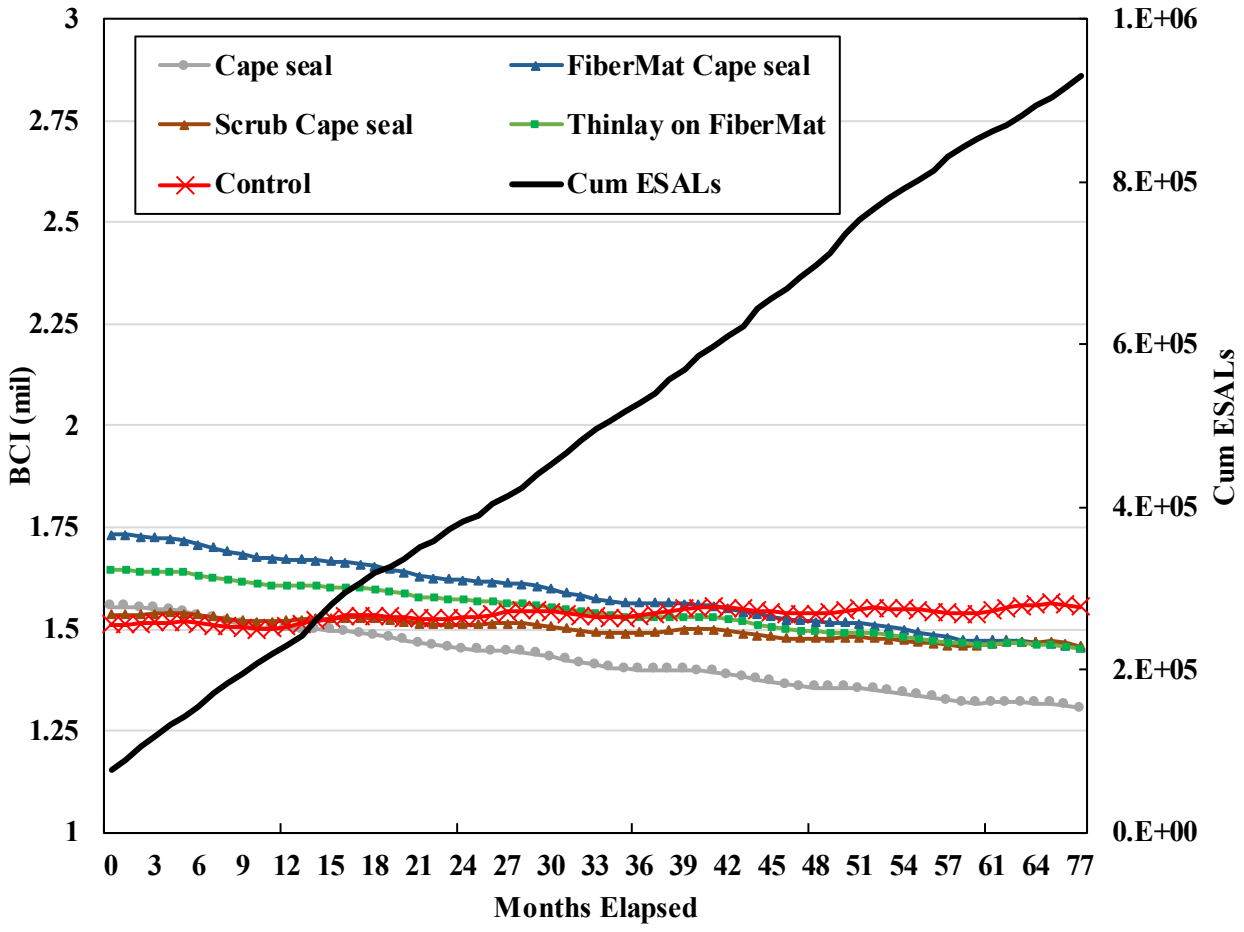

Figure 4-39: BCI values over the elapsed service life for combination group

Figure 4-40 shows the forecast of the BCI values for the treated sections within combination groups using seasonal ARIMA model. The BCI values indicate that, none of the forecast BCI value from the treated section reach the warning threshold at the 120 months of forecast.

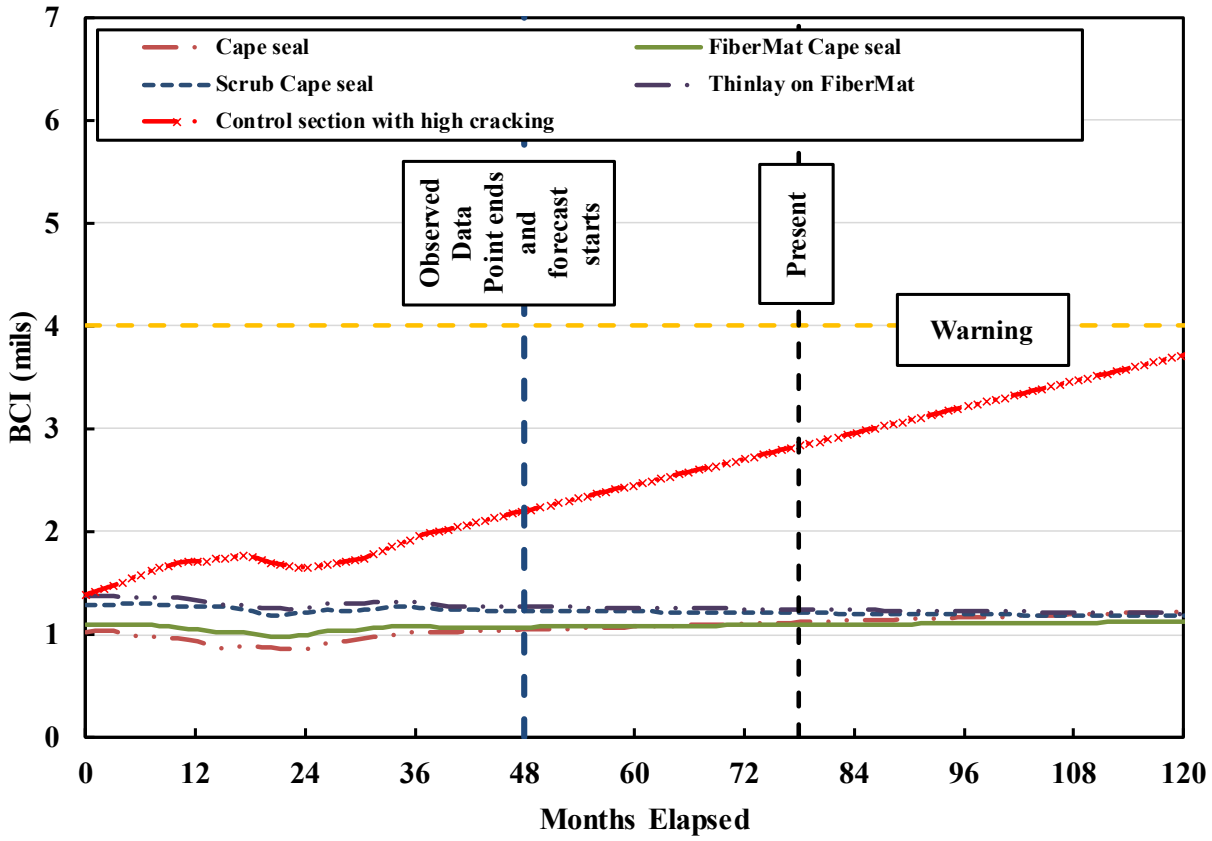

Figure 4-40: Forecast of the BCI values for combination group

4.3.5 Thinlays Group Result

Table 4-27 shows the summary statistics of the BCI values from the treated sections within the thinlay group along with the control section. The mean BCI values from the sections within the thinlay group indicate lower value than the mean BCI from the control section but they can be put in the same order of magnitude. The COV results indicate that the BCI values from the treated sections exhibit less variability than the control section.

Table 4-27: Summary statistics of the BCI values for the thinlays group

Treatment	Mean	Std Dev	Min	Max	N	COV
Thinlay	1.34	0.35	0.7	2.2	522	26.1
Polymer Thinlay	1.47	0.35	0.8	2.9	521	23.9
Ultra-Thin Bonded Wearing Course	1.45	0.41	0.6	2.7	517	28.1
Control	1.60	0.54	0.6	3.6	519	33.8

Figure 4-41 shows the mean BCI values for different treatment sections within the thinlay group compared to the control section at various times. All the treatment sections within the thinlay group had higher BCI values than the control section in pretreatment condition. In the posttreatment condition, the mean BCI values of the treatment sections show a drop in BCI value with decreased standard deviations. At present condition the mean BCI from all treatment sections within thinlays group exhibit lower BCI value than the control section with lesser variability in the measurements.

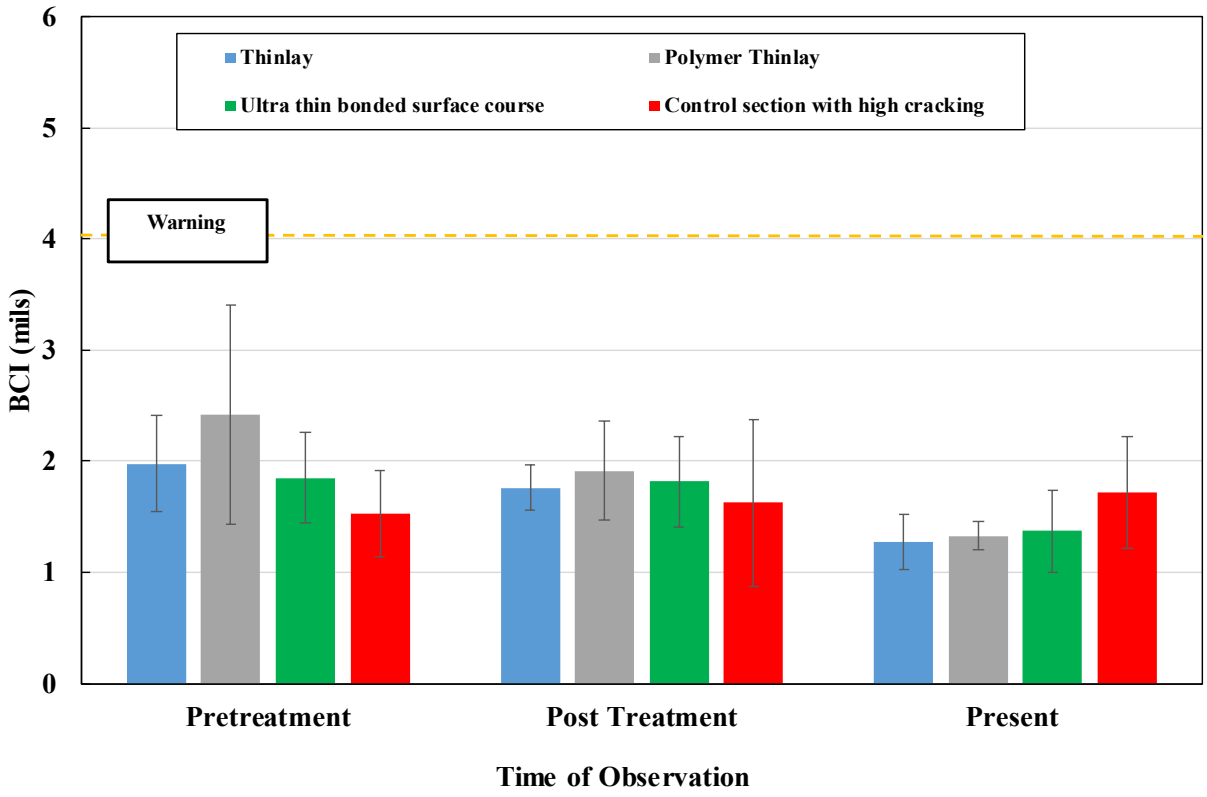

Figure 4-41: BCI values for different treatments at different times within thinlays group

Table 4-28 shows the results of the time series mixed modeling of the BCI values compared to the BCI values of the control section. The p-values from the sections treated with thinlay and polymer modified thinlay indicate that there is effect of treatment, time and combination in both lanes. In the inbound lane, significance of treatment and time were observed on the BCI values from polymer modified thinlay sections. The ultra-thin bonded surface wearing course shows strong significance of treatment and time effect on the BCI values in the inbound lane. In the outbound lane, the BCI values from ultra-thin bonded thinlay sections did not converge.

Table 4-28: p-values for time series mixed modeling for BCI values of treatments

Treatment	Inbound lane to the quarry			Outbound lane from quarry		
	Treatment	Time	Combined	Treatment	Time	Combined
Thinlay	0.0007	<.0001	<.0001	0.0011	0.5531	0.0005
Polymer Thinlay	<.0001	<.0001	<.0001	0.0014	<.0001	0.0029
Ultra-thin bonded surface course	<.0001	<.0001	0.6047	Did not meet convergence		

Figure 4-42 shows the trend of the BCI values of different treated sections within the thinlay group compared to control section over the elapsed 77 months of posttreatment service. It was observed that the mean BCI values of the treated sections decrease with time, while the value increases for the control section. This can be taken as an indication of improvement to the subgrade induced by the thinlays.

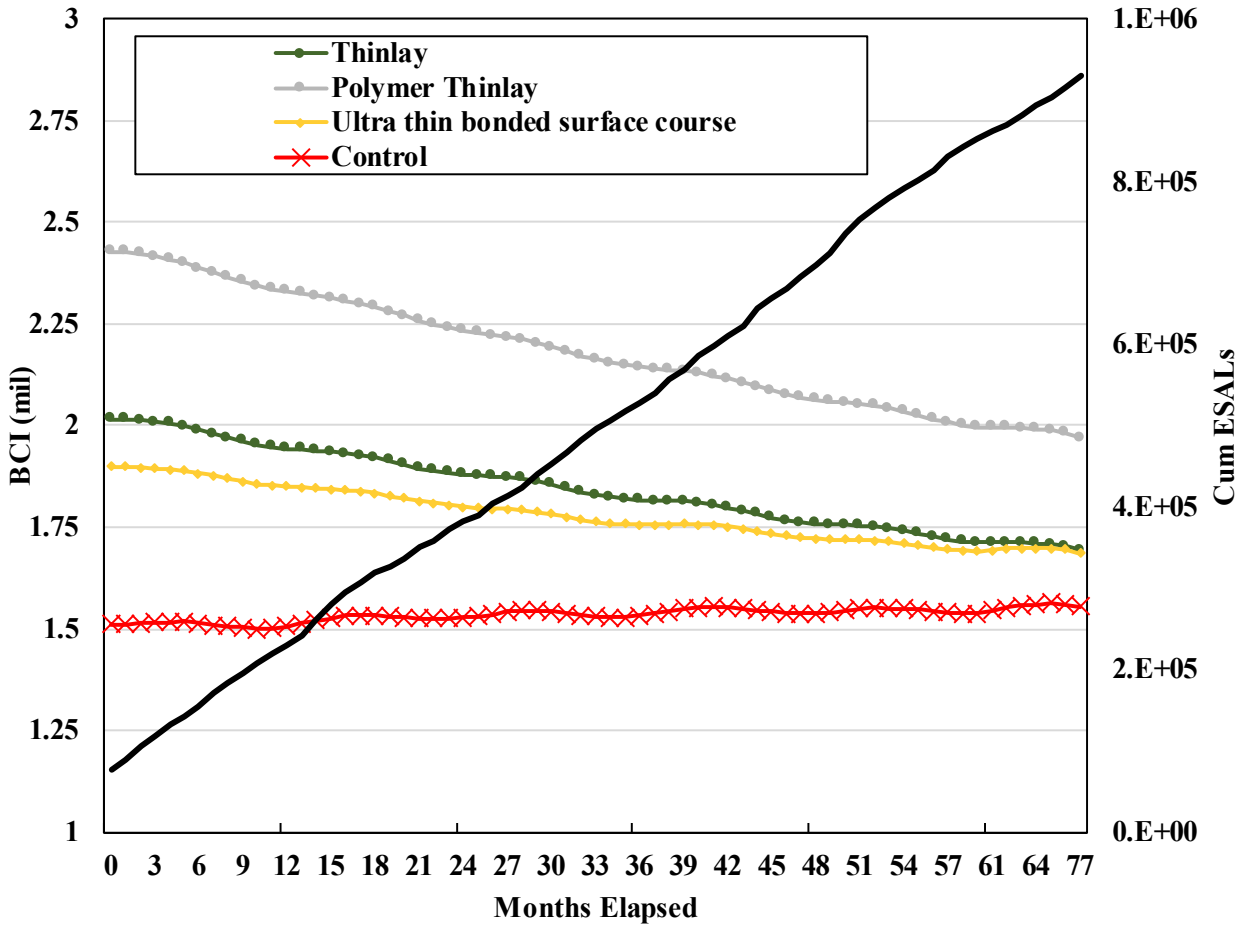

Figure 4-42: BCI values over the elapsed service life for thinlay group

Figure 4-43 shows the forecast of the BCI values for different treated sections within the thinlay group compared to control section. It was observed that, the mean BCI of the thinlay on FiberMat, thinlay and polymer modified thinlay, decrease over time or show insignificant changes over the forecast period of 120 months. BCI values from ultra-thin wearing course section indicate a slight increase over the forecast period but none of the forecast values from any treatment section reach the warning threshold for BCI (≥4 mils).

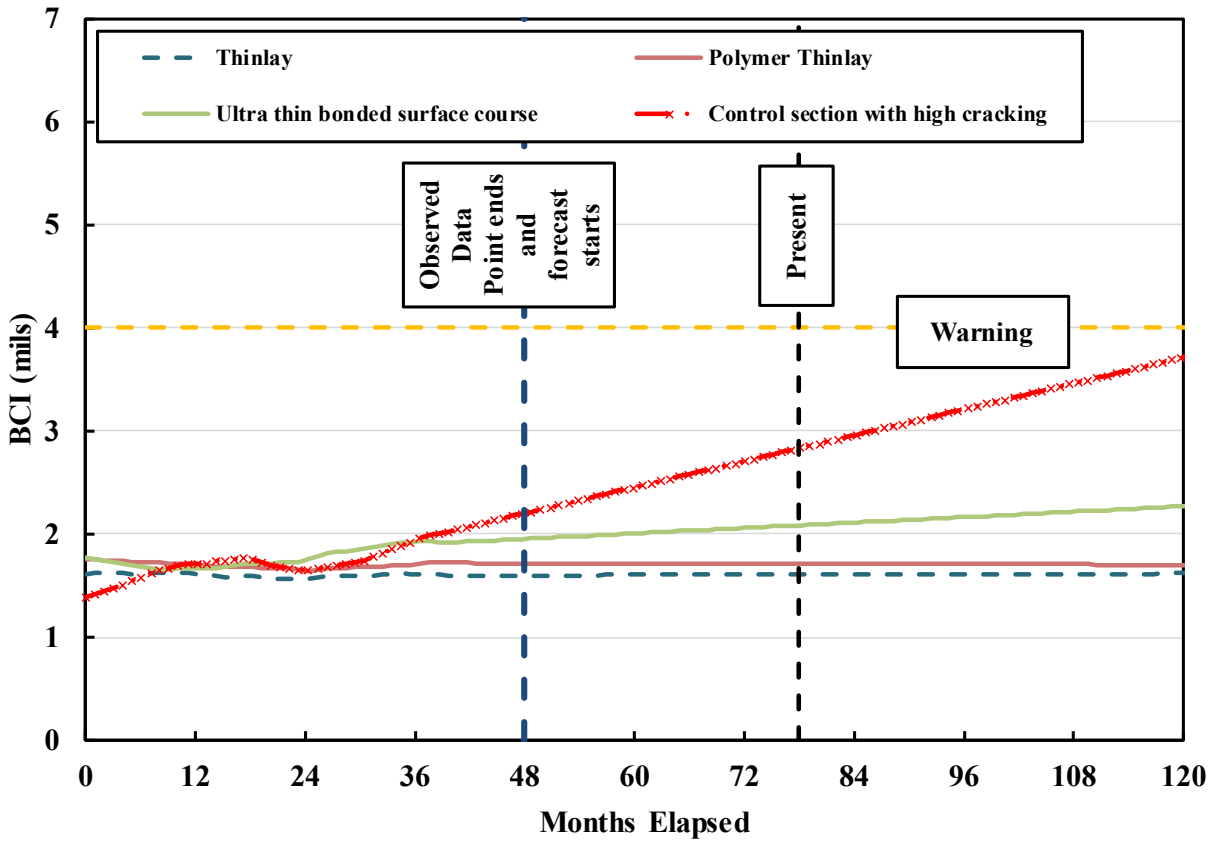

Figure 4-43: Forecast of the BCI values for thinlay group

4.4 Area Under Pavement Profile (AUPP)

Literature mentions area under pavement profile (AUPP) as a useful parameter to measure the overall structural health of the pavement, strain at the bottom of AC layer and layer moduli for AC and base. In the next paragraphs the summary statistics, bar charts, trends, forecast of AUPP values and percent changes in strain at the bottom layer of AC layer are shown for the treatment groups. The evaluation of AUPP values are very important in the study as there is no measured strain at the bottom of AC layer, while AUPP provides with the most accurate estimation of the AC tensile strain as discussed in the literature.

4.4.1 Standalone Group Results

Table 4-29 shows the summary statistics of the AUPP parameters for the treated sections within the standalone treatment group. The mean AUPP values for all the treated sections are like the control section mean AUPP. The standard deviation and COV for AUPP are also close for both treated and control sections.

Table 4-29: Summary statistics of the AUPP values for the standalone treatment group

Treatment	Mean	Std Dev	Min	Max	N	COV
Fog Seal	6.7	0.3	6.2	7.5	521	4.1
Crack Seal	6.8	0.3	6.0	7.9	518	5.1
Control	6.8	0.3	6.2	7.6	519	3.9

The mean AUPP values for the sections within the standalone treatment groups and the control section are shown at pretreatment, posttreatment and present time in **Figure 4-44**. The plots show that the mean AUPP value for the rejuvenating fog seal section decrease after treatment was applied, while the mean AUPP of the crack seal treated section increases at posttreatment condition. At the present time, the mean AUPP values for treated sections are similar in magnitude to the mean AUPP values of the control section.

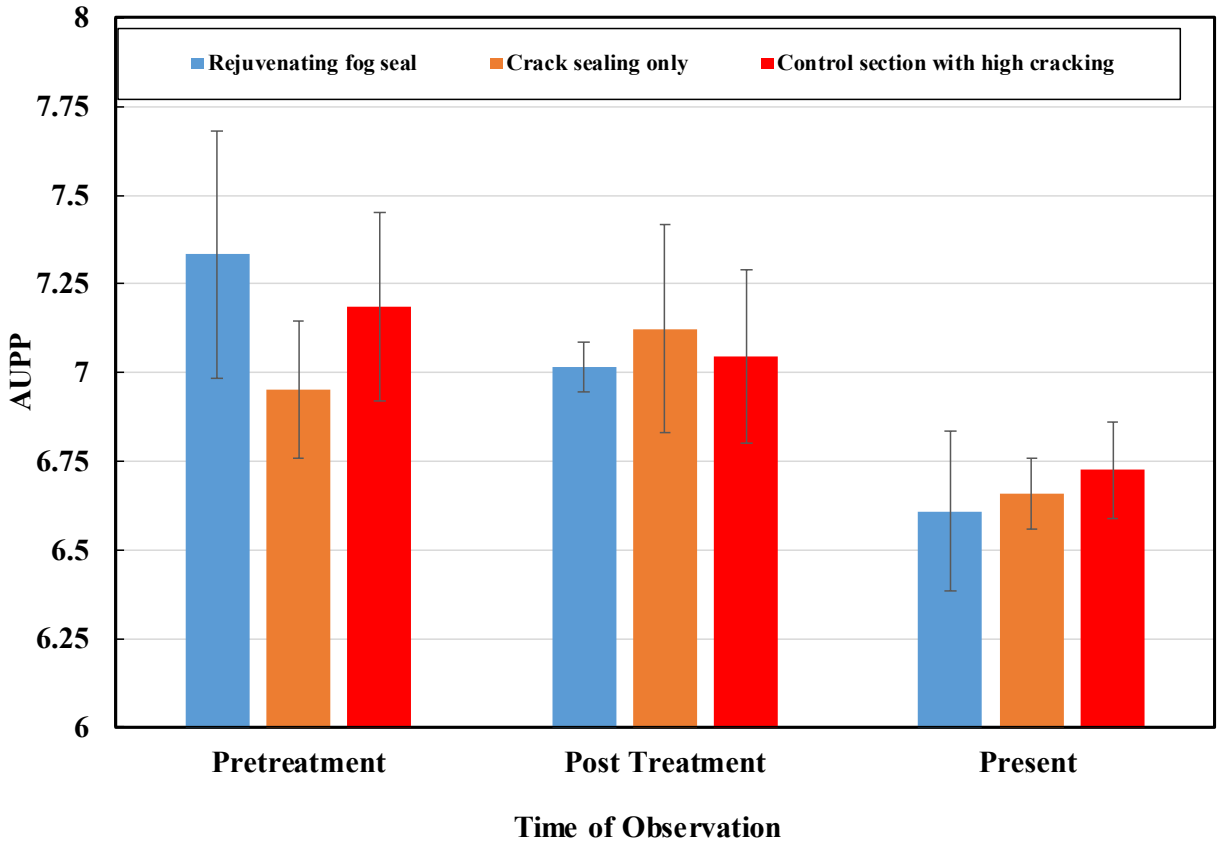

Figure 4-44: AUPP Values for treatments at different times within standalone group

Figure 4-45 shows the trend of the AUPP values for the sections within the standalone treatment group compared to the control section. Both sections within standalone treatment sections exhibit a reduced AUPP value over the elapsed 77 months of posttreatment service life. The gradient of reduction of AUPP value for rejuvenating fog seal section indicates the pavement section is showing an increased stiffness. Compared to the rejuvenating fog seal, the AUPP values from crack seal sections follow a more similar trend as control section.

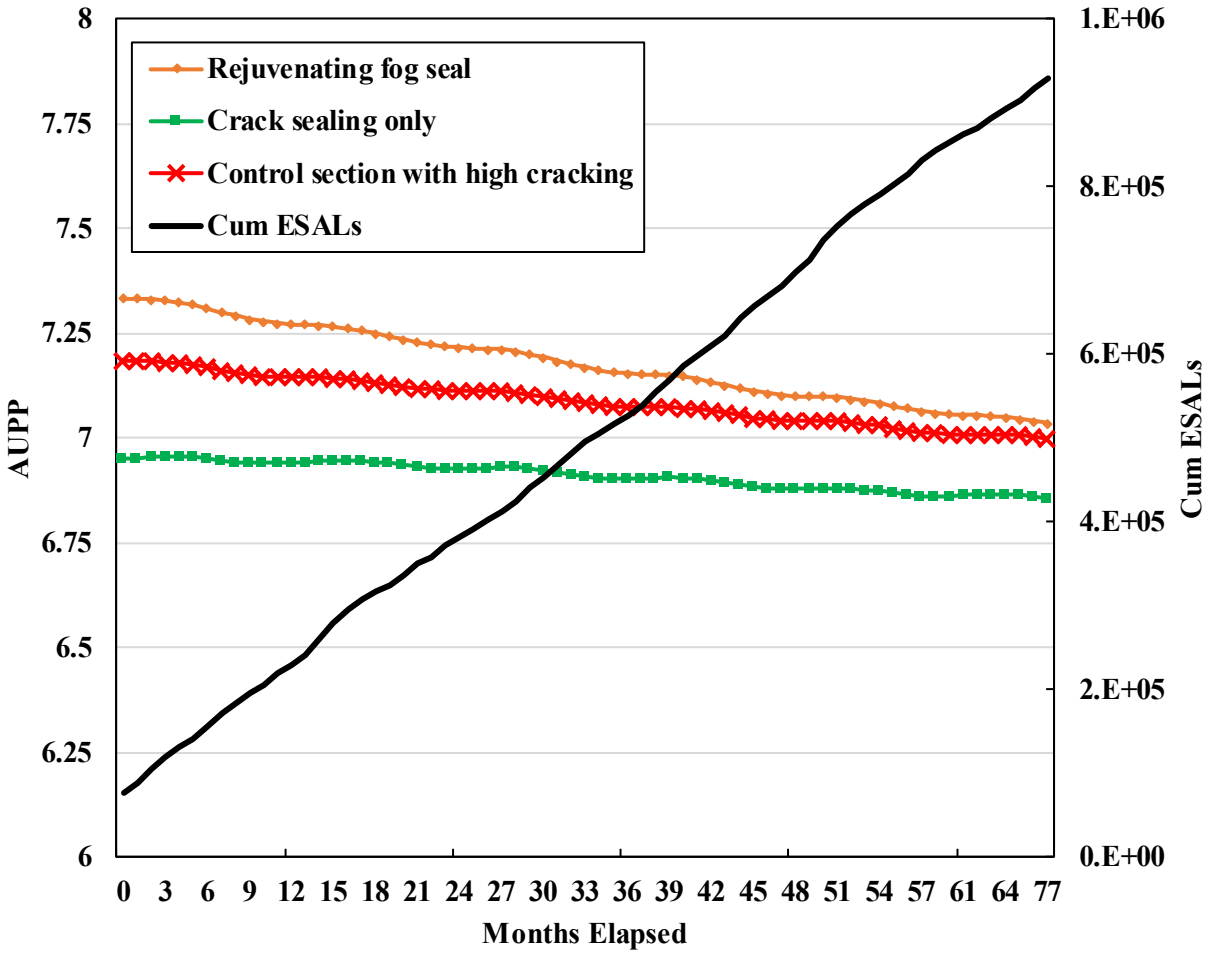

Figure 4-45: AUPP values over the elapsed service life for standalone group

Unlike the BDI and BCI parameters discussed in sections 4.2 and 4.3 respectively, the AUPP values were not selected for forecast as the changes in the observed values did not show

any significant change over time. This resulted in the statistical software being unable to detect and present a reliable estimate for the forecast AUPP values. From the sections onwards, the forecast AUPP values are not presented in this study.

4.4.2 Chip Seal Group Results

The summary statistics of the AUPP values of the chip seal group sections are shown in Table 4-30. The mean AUPP values for the treated sections are not significantly different from the control section. the COV results indicate that AUPP values for all the treated sections within chip seal group have higher variability than the control section.

Table 4-30: Summary statistics of the AUPP values for the chip seal group

Treatment	Mean	Std Dev	Min	Max	N	COV
FiberMat chip seal	6.8	0.5	6.0	8.3	521	7.0
Chip seal	6.7	0.3	6.0	7.6	519	4.8
Chip seal w/ crack sealing	6.7	0.3	6.0	7.7	515	4.8
Triple layer chip seal	6.8	0.3	5.8	7.6	516	4.7
Double layer chip seal	6.8	0.4	6.0	7.8	517	5.6
Scrub Seal	6.6	0.3	6.0	7.5	516	5.1
Control	6.8	0.3	6.2	7.6	519	3.9

Figure 4-46 shows the mean AUPP values for the treated sections within the chip seal group at various times. There was an increase in the mean AUPP value after treatments were applied. The variability of the AUPP values is also observed by increased standard deviation in the posttreatment condition. At present time, the AUPP value for the treated sections are lower than the control section, with the exception of the FiberMat chip seal.

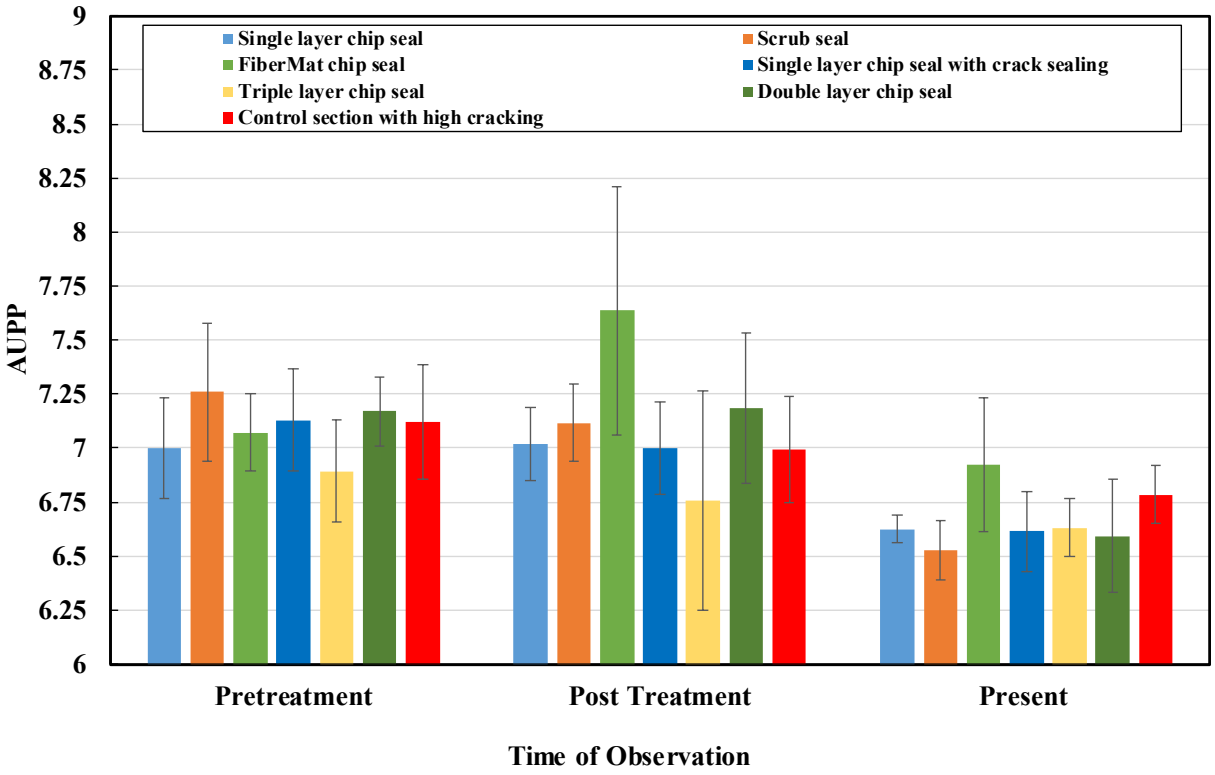

Figure 4-46: AUPP values for different treatments at different times within chip seal group

Figure 4-47 shows the trend of the AUPP values over the post application elapsed service life of the treatment section. The trends show that the mean AUPP values of the sections within the chip seal group follow a similar decreasing trend. Decrease in AUPP values signify increased stiffness of the pavement structure.

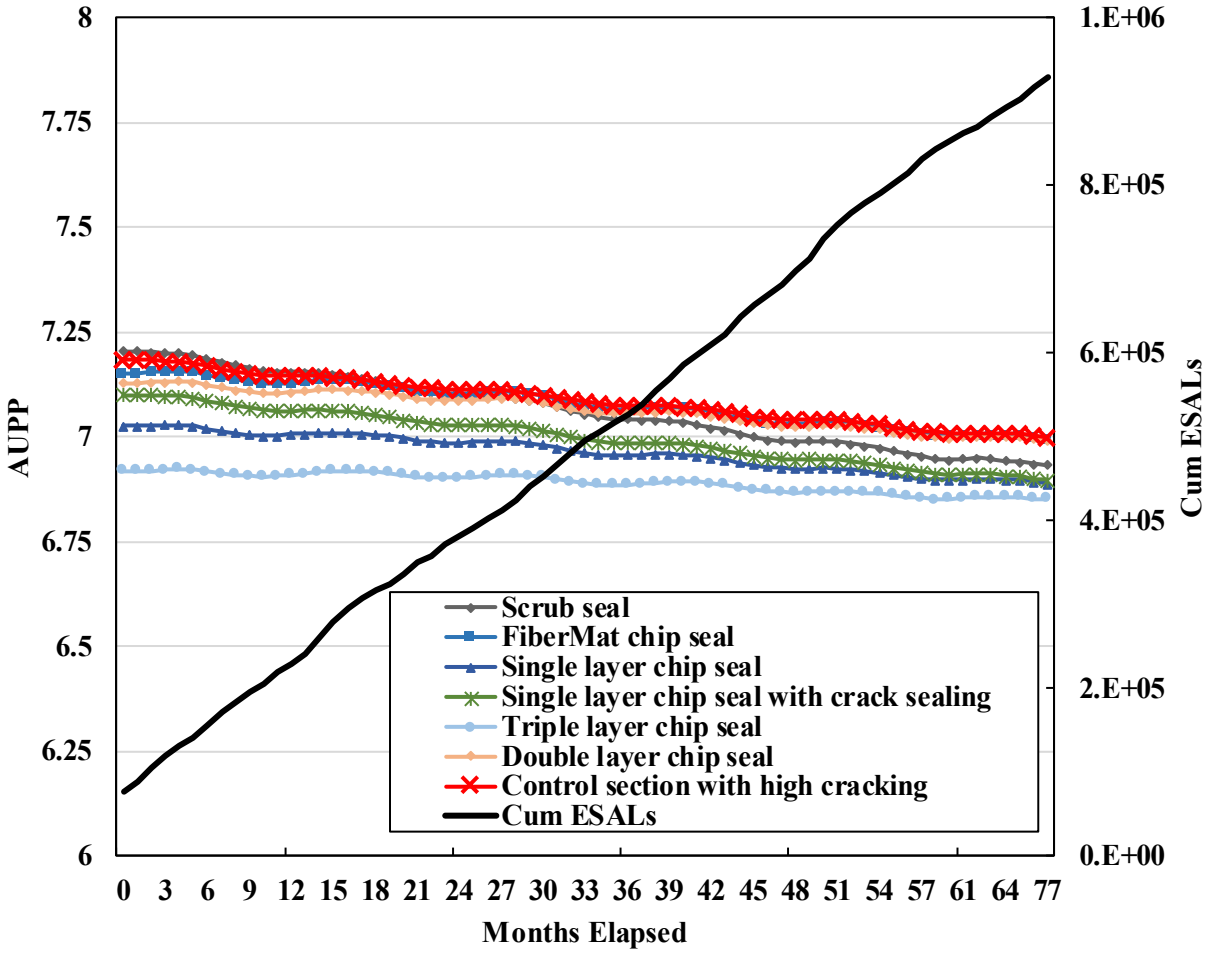

Figure 4-47: AUPP values over the elapsed service life for chip seal group

4.4.3 Micro surfacing Group Results

The summary statistics of the AUPP values from the micro surfacing group is presented in Table 4-31. The results indicate the mean AUPP values for the single layer micro surfacing with crack sealing and double layer micro surfacing are lower than the control section, while the mean AUPP from the single layer micro surfacing section was not significantly different to the control section mean AUPP. COV values for the single layer micro surfacing and single layer micro surfacing with crack sealing treated sections are higher than the control section, which indicates higher degree of variability within the measured AUPP values.

Table 4-31: Summary statistics of the AUPP values for the Micro surfacing group

Treatment	Mean	Std Dev	Min	Max	N	COV
Single layer micro surface	6.8	0.4	6.2	8.0	520	5.4
Single layer micro surface w/ CS	6.6	0.3	5.9	7.3	518	4.6
Double layer micro surface	6.4	0.2	5.9	7.0	519	3.8
Control	6.8	0.3	6.2	7.6	519	3.9

Figure 4-48 shows the mean AUPP values for the sections within the micro surfacing group compared to the control section at pretreatment, posttreatment and present time. The application of micro surfacing did not have any immediate effect over the mean AUPP of the treated sections except for a decrease of variability within the observed AUPP values. At present time, the mean AUPP of the treated sections are lower than the control section.

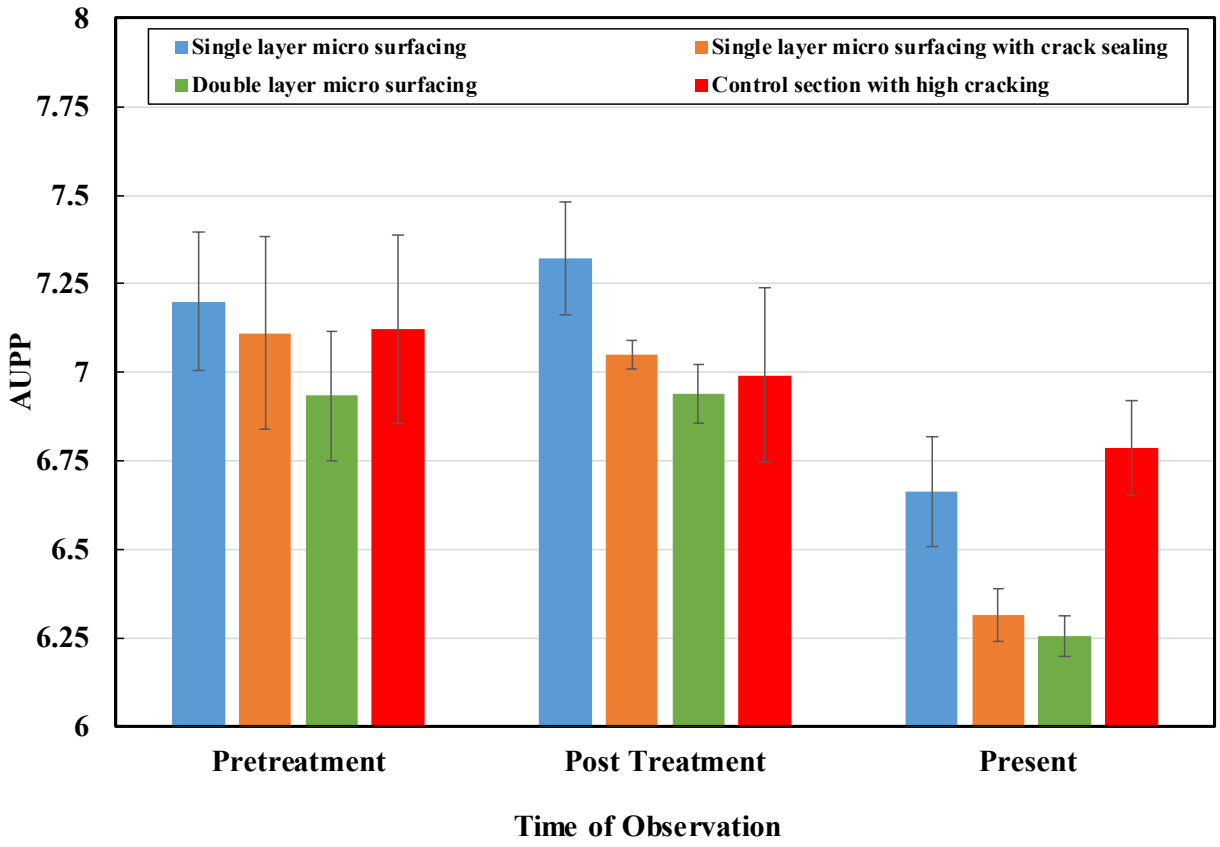

Figure 4-48: AUPP values for different treatments at different times within micro surfacing group

Figure 4-49 shows the trend of the AUPP values form different treated sections within micro surfacing group over the elapsed 77 months of post treatment service. The AUPP trend for single layer micro surfacing is similar to the control section while the other treatments follow a different band for AUPP values. Compared to single layer micro surfacing with crack sealing and double layer micro surfacing, the AUPP values from double layer micro surfacing sections decreased faster.

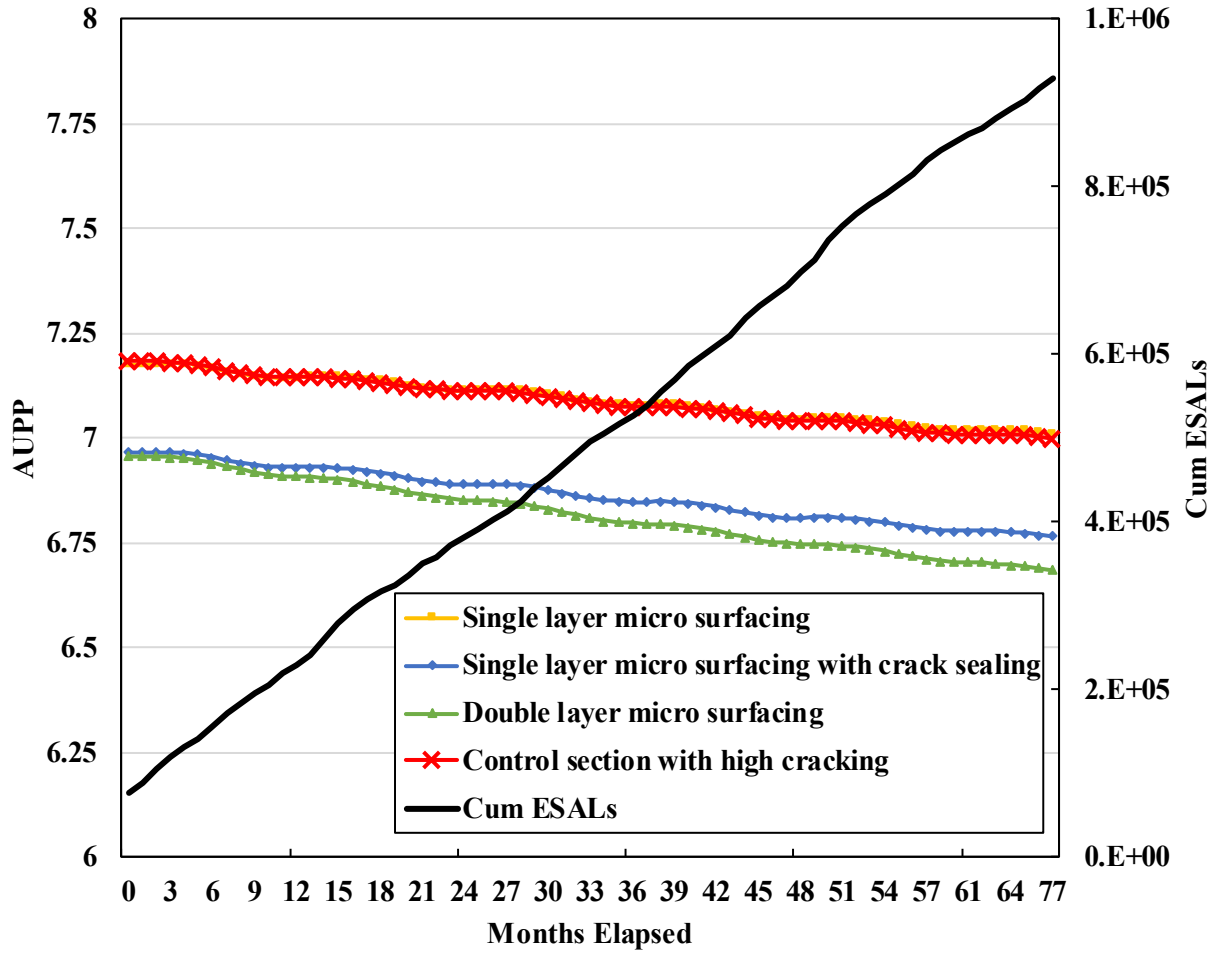

Figure 4-49: AUPP values over the elapsed service life for micro surfacing group

4.4.4 Combinations Group Results

The summary statistics for the combinations group are shown in Table 4-32. The results show that the mean AUPP values for the treated sections are lower than the control section mean AUPP value. Yet, the AUPP values from treated sections exhibit a higher degree of variability than the control section.

Table 4-32: Summary statistics of the AUPP values for the combination group

Treatment	Mean	Std Dev	Min	Max	N	COV
Cape seal	6.6	0.3	6.0	7.4	516	4.8
FiberMat Cape seal	6.7	0.4	6.0	7.7	520	5.8
Scrub Cape seal	6.7	0.4	6.0	7.7	520	5.4
Thinlay on FiberMat	6.8	0.4	6.1	7.9	521	5.5
Control	6.8	0.3	6.2	7.6	519	3.9

Figure 4-50 shows the mean AUPP values of the sections within combination group at various times. The mean AUPP values show an increase after treatment application. Unlike the micro surfacing group results, the variability of the AUPP values in the posttreatment condition did not change significantly due to treatment application. At present condition, the mean AUPP values of the treated sections are lower than the control section with no significant change in the standard deviation.

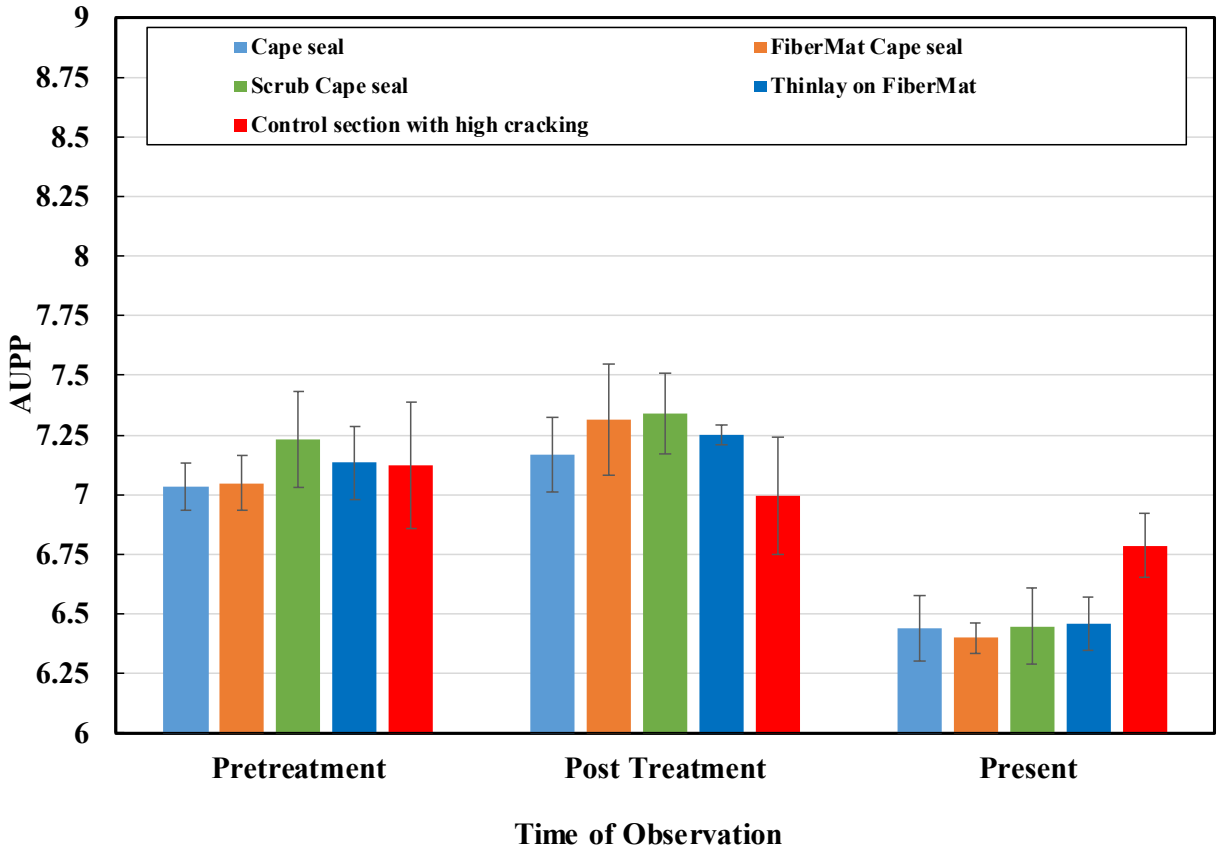

Figure 4-50: AUPP values for different treatments at different times within combination group

Figure 4-51 shows the trend of the AUPP values over the 77 months of elapsed service life. All the treated sections show a uniform rate of decrease in the AUPP value similar to the control section. Cape seal and FiberMat cape seal treated sections show faster decrease in AUPP values compared to the scrub cape seal or thinlay on FiberMat.

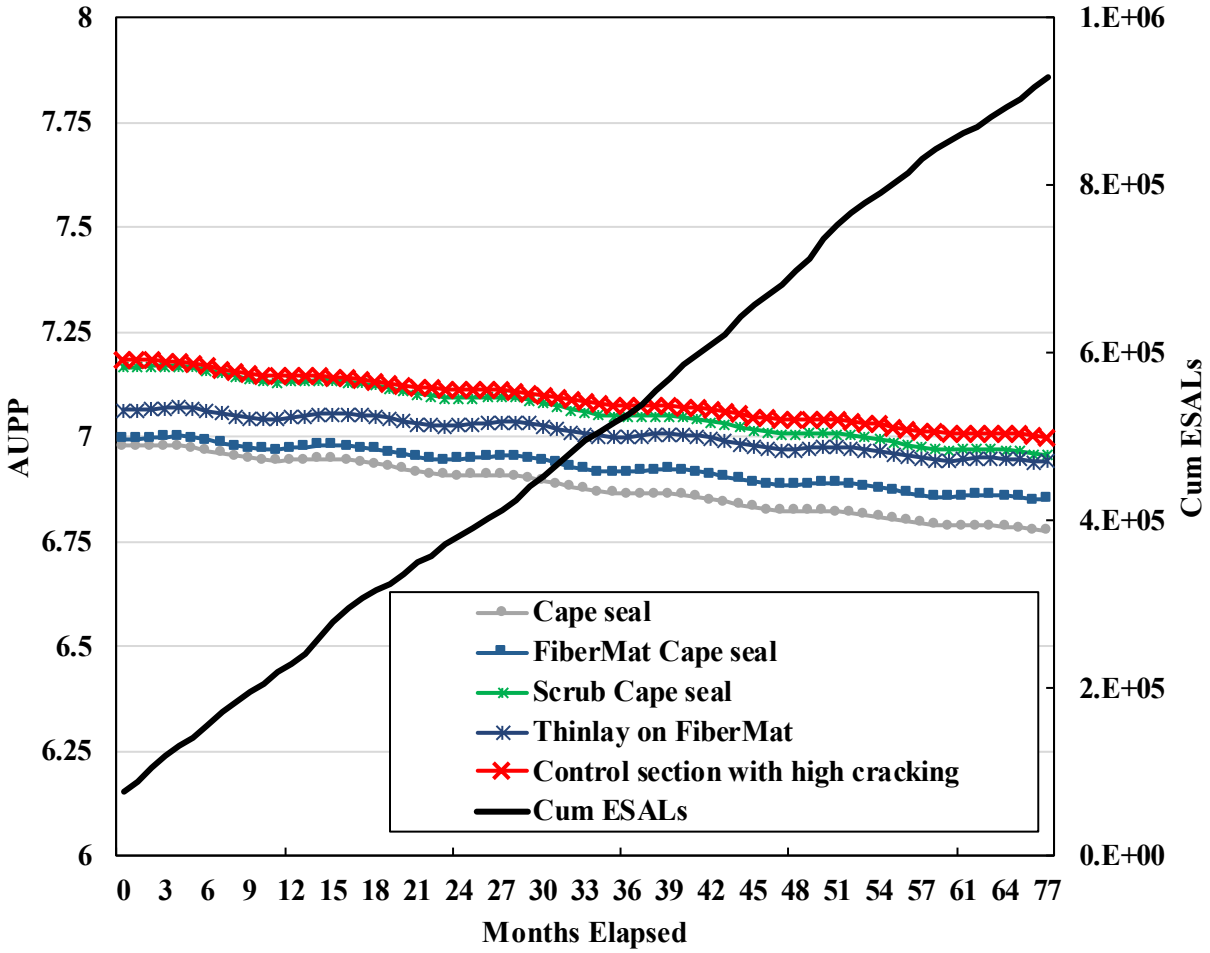

Figure 4-51: AUPP values over the elapsed service life for combination group

4.4.5 Thinlays Group Results

Table 4-33 shows the summary statistics of the AUPP values of the sections from thinlay group. The mean values of the AUPP are all similar to the control section mean AUPP. However, the COV results indicate higher variability in the treated sections compared to the control.

Table 4-33: Summary statistics of the AUPP values for the thinlay group

Treatment	Mean	Std Dev	Min	Max	N	COV
Thinlay	6.8	0.4	6.1	7.7	522	5.2
Polymer Thinlay	6.8	0.4	6.1	7.9	521	5.4
Ultra-Thin Bonded Wearing Course	6.8	0.3	6.1	7.7	517	5.1
Control	6.8	0.3	6.2	7.6	519	3.9

Figure 4-52 shows the mean AUPP values of different treatment sections within the thinlays group compared to the control section at pretreatment, posttreatment and present time. The mean AUPP values indicate a slight increase of the mean AUPP values of the treated sections immediately after treatment while the mean AUPP of the control section decreased. At present time, the mean AUPP values of the treated sections are lower than the control section with lower variability.

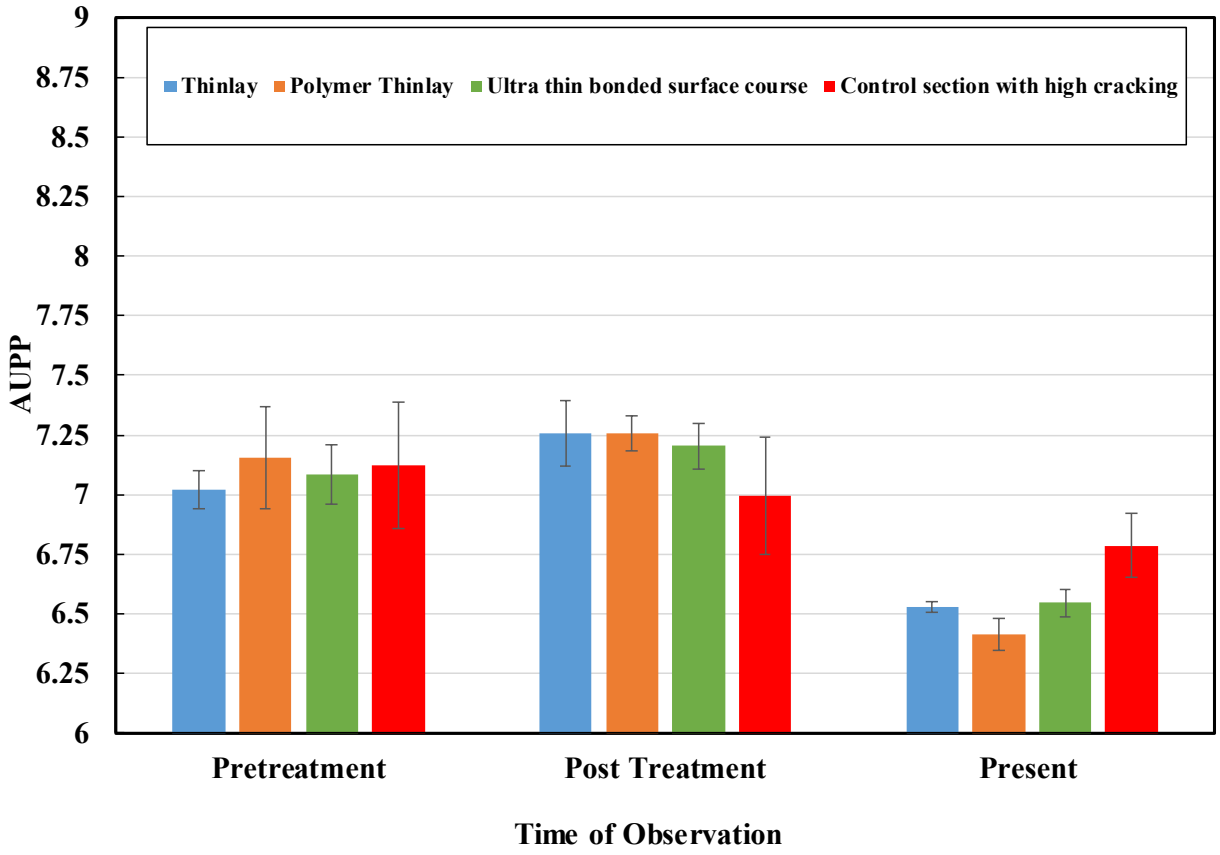

Figure 4-52: AUPP values for different treatments at different times within thinlay group

The trend of the mean AUPP values of the treated sections within thinlay groups are shown in **Figure 4-53**. Over the elapsed 77 months of service of the treated sections, the mean AUPP values decrease within a band of curves which is similar to the control section in magnitude. All the treated sections AUPP values decrease in a manner similar to the control section.

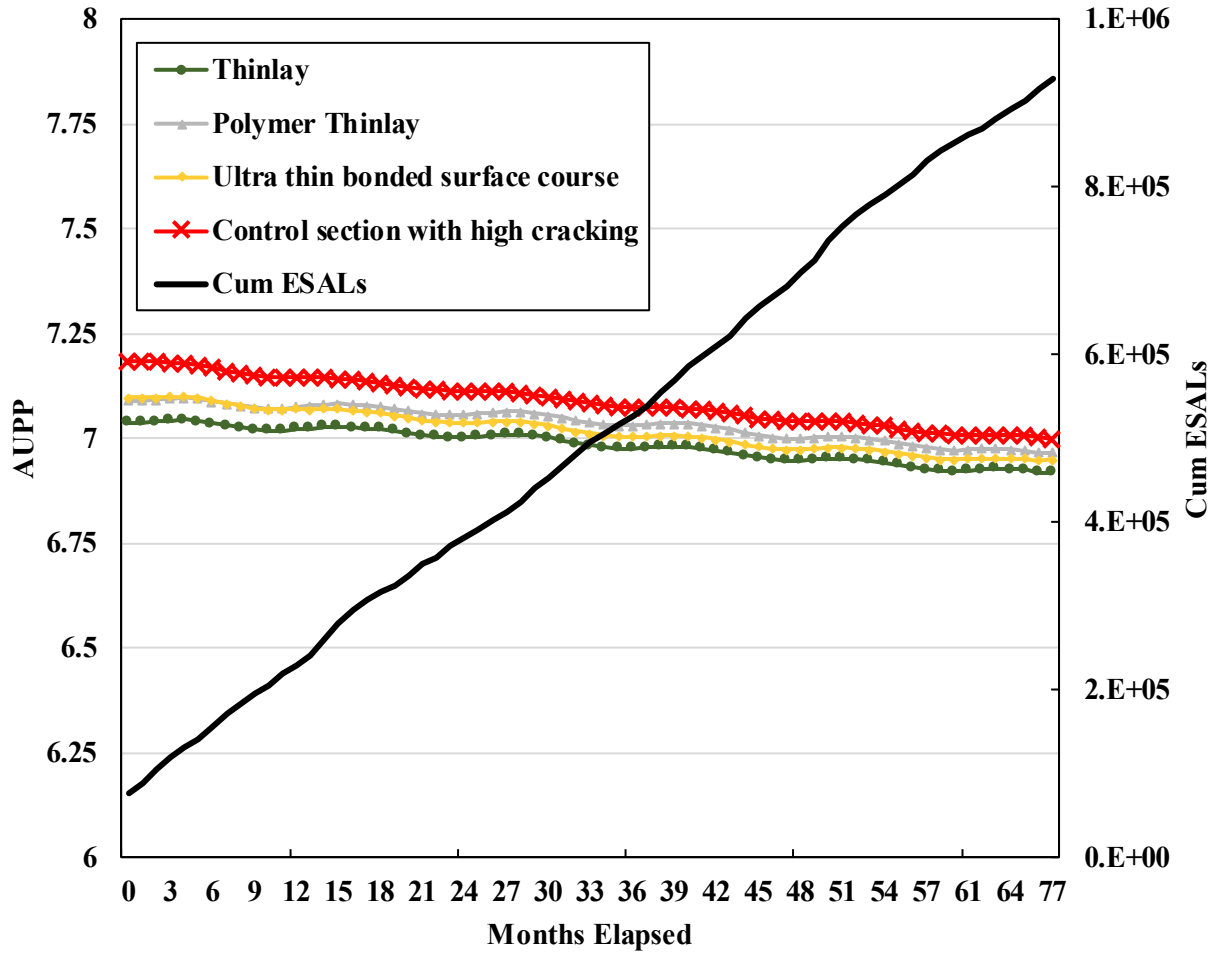

Figure 4-53: AUPP values over the elapsed service life for thinlay group

4.5 Overlay Thicknesses Requirement

Overlay thickness can be a very simple but effective representation of the structural requirement estimate, and therefore, the condition of the structural health of the pavement. Based on the monthly/quarterly collected FWD data, the effective structural number (SNeff) from each drop from each drop location from each treatment section were calculated. The required structural number (SNreq) was calculated in a similar fashion for each drop location for all magnitudes of load at each month using the AASHTO 1993 design method. The detailed methodology is explained in Chapter 3.5 of the document.

There is a presence of seasonality in the required overlay thickness data. As asphalt concrete is a temperature sensitive viscoelastic material, the AC layer exhibit more deflections during the summer high temperature resulting to a higher requirement of overlay thickness. To make a proper estimation and representative CDF curves, the years are chosen based on the availability of data over the complete yearly cycle. Therefore, the curves for 2012 and 2019 are not presented. In 2012 the data would show high thickness requirement as the available data are collected in post summer condition. In contrast, 2019 data were collected in post winter condition which also exhibit low overlay thickness requirement. To avoid bias and two extremes, the overlay thickness requirement for 2012 and 2019 were discarded.

Figure 4-54 shows the overall computed CDF plot of the computed required overlay thicknesses of the treatment sections over the years 2013 to 2018. Each of the curve represents around 5,400 overlay thickness requirement data points collected over all drop location for all magnitude of load for all 12 months within the specific year for all treatment section under the study. The required overlay thicknesses were rounded off to the next quarter inch. In the plot,

yearly average of the required thickness of the control sections are shown which varies from 4 in to 5 in based on the yearly high temperatures, duration of winter etc. variables. The plot indicates that at least 95% of the overlay thickness requirement from the treated sections are below the annual mean overlay thickness requirement of the control section at each year. The CDF curves are also shifting to the right over time, which also indicates the overall increase of structural requirement each year.

In all years, the vast majority of the sections (over 95%) are below the thickness requirement of the control section for that particular year. This emphasizes the effectiveness of the various treatments in preserving the structural integrity of the pavement sections.

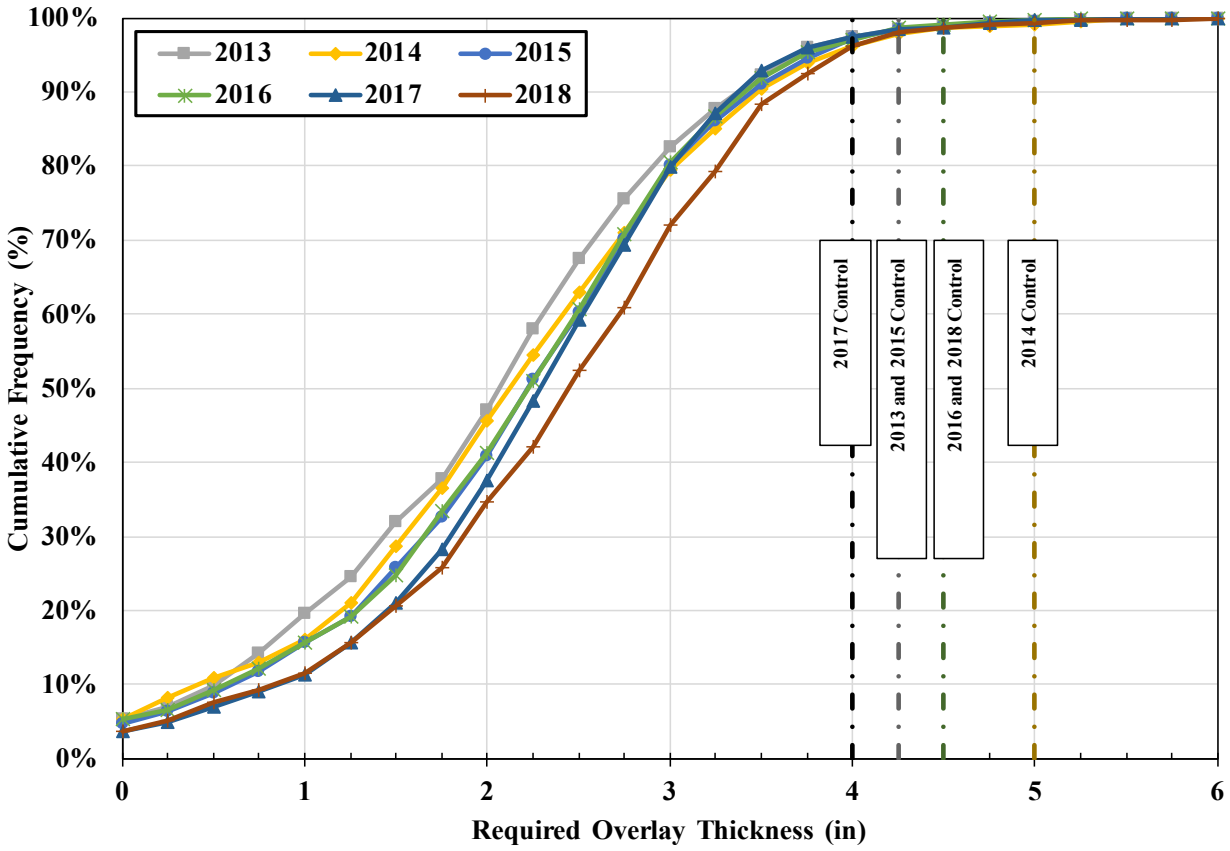

Figure 4-54: Required overlay thicknesses CDF plot for different years of service

5 SUMMARY AND CONCLUSIONS

This chapter summarizes the results to meet the objectives of the present study. The summary of the results follows the same sequence of the parameters being discussed from section 4.1 through 4.5. The observations for mean center deflection, BDI, BCI, AUPP, and required overlay thickness sections are be discussed in the following sections.

5.1 Center Deflection Under Loading Plate (D_0) Result Summary

At the end of analysis period of 77 months (spring 2013 to summer 2019), most of the mean D_0 values of the treated sections were lower than the control section, except for crack seal and double layer micro surfacing. This suggests that in general, the overall structural integrity of the pavement is in better condition for the treated sections after 77 months of service. In addition, less variability in the center deflection was observed in the treated sections compared to the control, especially for thinlays and combinations of treatments.

5.2 Base Damage Index (BDI) Result Summary

At the end of analysis period of 77 months most of the BDI values were lower than the control section except- crack seal, fog seal and double layer micro surfacing. Most of the treatment sections appeared to reduce the variability of the BDI values over the analysis period, especially combination and thinlay group treatments. The statistical analysis of the BDI values for the treated sections show the treatment effect was found significant over the sections within combination and thinlays group while the time effect was significant from the sections within chip seal and microsurfacing group. The ARIMA model forecast models indicate that the BDI values of the following treatment sections reach warning zone before 120 months of service- fog

seal, single layer chip seal, single layer micro surfacing with crack sealing and ultra-thin bonded wearing course.

5.3 Base Curvature Index (BCI) Result Summary

At the end of analysis period of 77 months most of the BCI values were lower than the control section except- crack seal and fog seal. All the treatment sections appeared to reduce the variability of the BCI values over the analysis period. The statistical analysis of the BCI values for the treated sections show that both the time and treatment effect were significant over the sections within combination and thinlays group. The ARIMA model forecast models indicate that none of the treatment sections BCI value reach warning zone before 120 months of service.

5.4 Area Under Pavement Profile (AUPP) Result Summary

Area Under Pavement Profile (AUPP) values of the treated sections did not exhibit significant difference between than that of the control section. As explained in the literature, the AUPP directly correlated with the tensile strain at the bottom of AC layer, the treatments were found to reduce the present day mean AUPP value of the treated sections to a varying percentage ranging up to 6% of the initial AUPP at posttreatment condition.

The summary table of the percent change of the parameters at present day compared to the posttreatment condition are summarized in Table 5-1. For the center deflection, BDI and BCI values, any increase in the percent changes are marked "Red", any percent changes between "No change" and up to 25% reduction are marked "Amber" and more than 25% reduction of the values are marked with "Green". For the AUPP values, reduction less than 5% are marked "Amber" while any more than 5% decrease in the values are marked "Green".

Table 5-1: Summary of the % Change of DBP values over 77 months of service (first measurement vs last measurement)

Group	Treatment Name	% Change D0	% Change BDI	% Change BCI	% Change AUPP
Standalone Group	Crack sealing only	16%	23%	-35%	-5%
	Rejuvenating fog seal	72%	77%	-21%	-10%
Chip Seal Group	Single layer chip seal	8%	16%	-40%	-6%
	FiberMat chip seal	1%	2%	-49%	-7%
	Single layer chip seal w/ CS	-8%	-6%	-56%	-8%
	Double layer chip seal	-7%	-5%	-42%	-4%
	Triple layer chip seal	2%	8%	-26%	-1%
	Scrub seal	9%	12%	-43%	-7%
Micro surfacing Group	Single layer micro surfacing	-14%	-11%	-54%	-6%
	Single layer micro surfacing w/ CS	-19%	-20%	-59%	-7%
	Double layer micro surfacing	-1%	-16%	-62%	-9%
Combination Group	Cape seal	-28%	-34%	-68%	-7%
	FiberMat Cape seal	-36%	-41%	-57%	0%
	Scrub Cape seal	-10%	-10%	-49%	-5%
	Thinlay on FiberMat	-33%	-32%	-51%	-1%
Thinlay Group	Thinlay	-37%	-39%	-57%	-2%
	Polymer Thinlay	-39%	-40%	-65%	-4%
	Ultra thin bonded surface course	-32%	-35%	-56%	-2%
Control	Control	16%	14%	-44%	-6%

The summary table represents that the micro surfacing, combination and thinlay group treatments improve the performance of the overall pavement and the base layer. The preservation treatments also found to add to the structural life of the subgrade layer as of from the present

study. The finally in can be commented that the preservation treatments are contributing to the long life of the pavement.

5.5 Recommendations

The following recommendations could be made from the author for the future scope of the study:

1. After 77 months of service, many of the preservation sections did not show any significant change over the analysis period. To capture any significant change of parameter over the service life, the analysis period should be extended until the sections reach to structural failure.
2. The integration of the traffic and seasonal variability to the study by incorporating the remaining test location data from the NCAT-Mn/ROAD partnership preservation study.
3. More reliable structural data can be collected from the test locations by performing destructive testing after the designed service life of the pavement sections.
4. Methodologies incorporating a variability component could be developed and adopted for the future projection of pavement performance.

REFERENCES

AASHTO. (1993). *AASHTO guide for design of pavement structure* (Vol. 1). AASHTO.

Arabali, P., Freeman, T. J., Sakhaeifar, M. S., Wilson, B. T., & Borowiec, J. D. (2017). Decision-Making Guideline for Preservation of Flexible Pavements in General Aviation Airport Management. *Journal of Transportation Engineering, Part B: Pavements*, *143*(2), 04017006. https://doi.org/10.1061/jpeodx.0000002

ASTM. (2008). Standard Guide for General Pavement Deflection Measurements, *03*(Reapproved), 1–7. https://doi.org/10.1520/D4695-03R08.2

ASTM. (2015). Standard Test Method for Deflections with a Falling-Weight-Type Impulse Load Device, *04*(April), 2–4. https://doi.org/10.1520/D4694-09R15.2

Bolander, P. W. (2005). Seal Coat Options. *Roadway Pavement Preservation*, 24.

Box, G. E. P., & Jenkins, G. M. (1994). *Time series analysis : forecasting and control.* Retrieved from https://www.wiley.com/en-us/Time+Series+Analysis%3A+Forecasting+and+Control%2C+5th+Edition-p-9781118675021

Chan, S., Lane, B., Kazmierowski, T., & Lee, W. (2011). Pavement Preservation. *Transportation Research Record: Journal of the Transportation Research Board*, *2235*, 36–42. https://doi.org/10.3141/2235-05

Cuelho, E., Mokawa, R., & Akin, R. (2006). Preventive Maintenance Treatments of Flexible Pavements: a Synthesis of Highway Practice. *Federal Highway Administration*, 161–169. https://doi.org/10.1163/_q3_SIM_00374

Fitzmaurice, G., Laird, N., & Ware, J. (2011). *Applied Longitudinal Analysis* (2nd ed.). Retrieved from https://content.sph.harvard.edu/fitzmaur/ala2e/

Hicks, R. G., Moulthtrop, J. S., & Daleiden, J. (1999). Selecting a Preventive Maintenance Treatment for Flexible Pavements. *Journal of the Transportation Research Board*, (1680), 1–12.

Highway Research Board. (1954). *The WASHO Road Test*. Retrieved from http://onlinepubs.trb.org/Onlinepubs/sr/sr18.pdf

Hoffman, M. S., & Thompson, M. R. (1982). Backcalculating nonlinear resilient moduli from deflection data. *Transportation Research Record*, *852*(852), 42–51. Retrieved from http://onlinepubs.trb.org/Onlinepubs/trr/1982/852/852-006.pdf

Horak, E. (2007). Surface moduli determined with the falling weight deflectometer used as benchmarking tool. *SATC 2007 - 26th Annual Southern African Transport Conference: The Challenges of Implementing Policy*, (July), 284–293. Retrieved from

http://www.scopus.com/inward/record.url?eid=2-s2.0-45149084713&partnerID=40

Horak, Emile. (2008). Benchmarking the Structural Condition of Flexible Pavements With Deflection Bowl Parameters. *Journal of the South African Institution of Civil Engineering*, *50*(2), 2–9. Retrieved from http://www.scielo.org.za/pdf/jsaice/v50n2/01.pdf

Horak, Emile, Hefer, A., Emery, S., & Maina, J. (2015). Flexible road pavement structural condition benchmark methodology incorporating structural condition indices derived from Falling Weight Deflectometer deflection bowls. *Journal of Civil Engineering and Construction*, *4*(1), 1–14.

Hossain, A. S. M. M., & Zaniewski, J. P. (1991). Characterization of Falling Weight Deflectometer Deflection Basin. *Transportation Research Record: Journal of the Transportation Research Board*, (1293).

Huang, Y. H. (2004). *Pavement design and analysis*. Pearson/Prentice Hall.

Irwin. (1989). Deflection Reading Accuracy and Layer Thickness Accuracy in Backcalculation of Pavement Layer Moduli. *Technology*.

Jahren, C. T., Nixon, W. A., Bergeson, K. L., Al-Hammadi, A., Celik, S., Chung, J. W., … Thorius, J. (2003). *Thin Maintenance Surfaces Phase Two Report with Guidelines for Winter Maintenance on Thin Maintenance Surfaces*.

Johnson, E., Wood, T., & Olson, R. (2007). Flexible Slurry-Microsurfacing System for Overlay Preparation: Construction and Seasonal Monitoring at Minnesota Road Research Project. *Transportation Research Record: Journal of the Transportation Research Board*, *1989*, 321–326. https://doi.org/10.3141/1989-79

Jung, F., & Stolle, F. E. D. (1992). *Nondestructive Deflection Testing and Backcalculation for Pavements*.

Kheradmandi, N., & Modarres, A. (2018). Precision of back-calculation analysis and independent parameters-based models in estimating the pavement layers modulus-Field and experimental study. *Construction and Building Materials*, *171*, 598–610. https://doi.org/10.1016/j.conbuildmat.2018.03.211

Kim, M., Kim, D., & Murphy, M. (2013). Improved Method for Evaluating the Pavement Structural Number with Falling Weight Deflectometer Deflections. *Transportation Research Record: Journal of the Transportation Research Board*, *2366*, 120–126. https://doi.org/10.3141/2366-14

Kim, Y R, Lee, Y., & Ranjithan, S. R. (2000). Y. Richard Kim, 1 Yung-Chien.

Kim, Y Richard, Hibbs, B. O., Lee, Y., Kim, Y. R., Lee, Y., Engineering, C., & Carolina, N. (1993). Strength and Deformation Characteristics of Pavement Sections and Pavement Rehabilitation Temperature Correction of Deflections and Backcalculated Asphalt Concrete Moduli.

Kim, Y Richard, & Park, H. (2002). USE OF FALLING WEIGHT DEFLECTOMETER MULTI-LOAD DATA FOR PAVEMENT STRENGTH ESTIMATION, (June).

Labi, S., Lamptey, G., & Kong, S.-H. (2007). Effectiveness of Microsurfacing Treatments. *Journal of Transportation Engineering*, *133*(5), 298–307. https://doi.org/10.1061/(ASCE)0733-947X(2007)133:5(298)

Labi, S., & Sinha, K. C. (2003). Measures of short-term effectiveness of highway pavement maintenance. *Journal of Transportation Engineering*, *129*(6), 673–683. https://doi.org/10.1061/(ASCE)0733-947X(2003)129:6(673)

Lee, Y.-C., Kim, Y. R., & Ranjithan, S. R. (1998). Dynamic Analysis-Based Approach To Determine Flexible Pavement Layer Moduli Using Deflection Basin Parameters. *Transportation Research Record: Journal of the Transportation Research Board*, *1639*(1), 36–42. https://doi.org/10.3141/1639-04

Montgomery, D. C. (2013). *Design and Analysis of Experiments* (5th ed.).

Mun Park, H., Kim, Y. R., & Park, S. (2007). Temperature Correction of Multiload-Level Falling Weight Deflectometer Deflections. *Transportation Research Record: Journal of the Transportation Research Board*, *1806*(1), 3–8. https://doi.org/10.3141/1806-01

Peshkin, D., Wolters, A., Smith, K. L., Krstulovich, J., Moulthrop, J., & Alvarado, C. (2011). *Guidelines for the Preservation of High-Traffic-Volume Roadways*. *Guidelines for the Preservation of High-Traffic-Volume Roadways*. https://doi.org/10.17226/14487

Pierce, L. M., Bruinsma, J. E., Kurt, D. S., Chatti, K., & Vandenbossche, J. M. (2017). Using Falling Weight Deflectometer Data with Mechanistic-Empirical Design and Analysis, Volume 2, *2*(November).

Pierce, L. M., Bruinsma, J. E., Smith, K. D., Wade, M. J., Chatti, K., & Vandenbossche, J. M. (2009). Using Falling Weight Deflectometer Data with Mechanistic-Empirical Design and Analysis, Volume 2, *2*(November).

Rijkswaterstaat. (2017). No Title. Retrieved April 12, 2019, from https://beeldbank.rws.nl/MediaObject/Details/Dynaflect_442203

Roesset, M., Ii, K. H. S., & Seng, C. (1995). Determination of Depth to Bedrock from Falling Weight Deflectometer Test Data, *2*, 68–78.

Rohde, G. T., & Van Wijk, A. J. (1996). A mechanistic procedure to determine basin parameter criteria. In *Southern African Transportation Conference, Pretoria*.

Rolt, J Parkman, C. (2000). CHARACTERISATION OF PAVEMENT STRENGTH IN HDM-III AND CHANGES ADOPTED FOR HDM-4 J Rolt. *10th International Conference of the Road Engineering Association of Asia and Australia. 2000.*, 1–11.

Schmalzer, P. N. (2006). Long-Term Pavement Performance Program Manual for Falling

Weight Deflectometer Measurements. *Long-Term Pavement Performance Program Manual for Falling Weight Deflectometer Measurements*, (December), 1–2.

Seo, J. W., Kim, S. Il, Choi, J. S., & Park, D. W. (2009). Evaluation of layer properties of flexible pavement using a pseudo-static analysis procedure of Falling Weight Deflectometer. *Construction and Building Materials*, *23*(10), 3206–3213. https://doi.org/10.1016/j.conbuildmat.2009.06.009

SHRP. (1993). *SHRP Procedure for Temperature Correction of Maximum Deflections*. Retrieved from http://onlinepubs.trb.org/onlinepubs/shrp/SHRP-P-654.pdf

Smith, K. D., Bruinsma, J. E., Wade, M. J., Chatti, K., Vandenbossche, J. M., & Yu, H. T. (2017). Using Falling Weight Deflectometer Data with Mechanistic-Empirical Design and Analysis, Volume I: Final Report. *Report No. FHWA-HRT-16-009. Federal Highway Administration*, *I*(March). https://doi.org/10.1520/STP104445

Talvik, O., & Aavik, A. (2009). Use of FWD Deflection Basin Parameters (SCI, BDI, BCI) for Pavement Condition Assessment. *The Baltic Journal of Road and Bridge Engineering*, *4*(4), 196–202. https://doi.org/10.3846/1822-427X.2009.4.196-202

Talvik, Ott. (2007). FWD mõõtmistulemuste alusel arvutatud parameetrite SCI, BDI ja BCI kasutamine teekatendi seisukorra hindamisel (Use of FWD deflection basin parameters (SCI, BDI, BCI) for pavement condition assessment). *Magistritöö. Tallinn: TTÜ Teedeinstituut*.

Thompson, M R. (1989). Area Under the Pavement Profile to Predict Strain. In *Informal Presentation at FWD Users Group Annual Meeting, Indianapolis, IN*.

Thompson, Marshall R, & Elliott, R. P. (1985). ILLI-PAVE based response algorithms for design of conventional flexible pavements. *Transportation Research Record*, *1043*, 50–57.

Ullidtz, P. (1987). *Pavement Analysis. Developments in Civil Engineering, 19*.

Vargas-Nordcbeck, A. (2018). Field Performance of Chip Seals for Pavement Preservation. *Transportation Research Record*. https://doi.org/10.1177/0361198118768531

Vrtis, M. C. (2017). Investigation of Deflection Basin to Identify Structural Destress Within Flexible Pavements.

Wade, M., R. DeSombre, and D. P. (2001). High Volume / High Speed Asphalt Roadway Preventive Maintenance Surface Treatments, (December).

Watanatada, T. (1987). *The Highway Design and Maintenance Standards Model: User's Manual for the HDM-III model* (Vol. 2). Johns Hopkins University Press.

Xu, B., Ranji Ranjithan, & Kim, Y. R. (2002). New Condition Assessment Procedure for Asphalt Pavement Layers, Using Falling Weight Deflectometer Deflections, *7*(02), 57–69.

Xu, B., Ranjithan, S. R., & Kim, Y. R. (2001). Development of relationships between FWD deflections and asphalt pavement layer condition indicators. In *81st Annual Meeting of the Transportation Research Board, Washington, DC*.

Xu, B., Ranjithan, S. R., & Kim, Y. R. (2007). New Relationships Between Falling Weight Deflectometer Deflections and Asphalt Pavement Layer Condition Indicators. *Transportation Research Record: Journal of the Transportation Research Board*, *1806*(02), 48–56. https://doi.org/10.3141/1806-06

Zubeck, H., Mullin, a., & Liu, J. (2012). Pavement Preservation Practices in Cold Regions. *Cold Regions Engineering 2012*, 134–143. https://doi.org/10.1061/9780784412473.014

APPENDIX A: CORE THICKNESSES

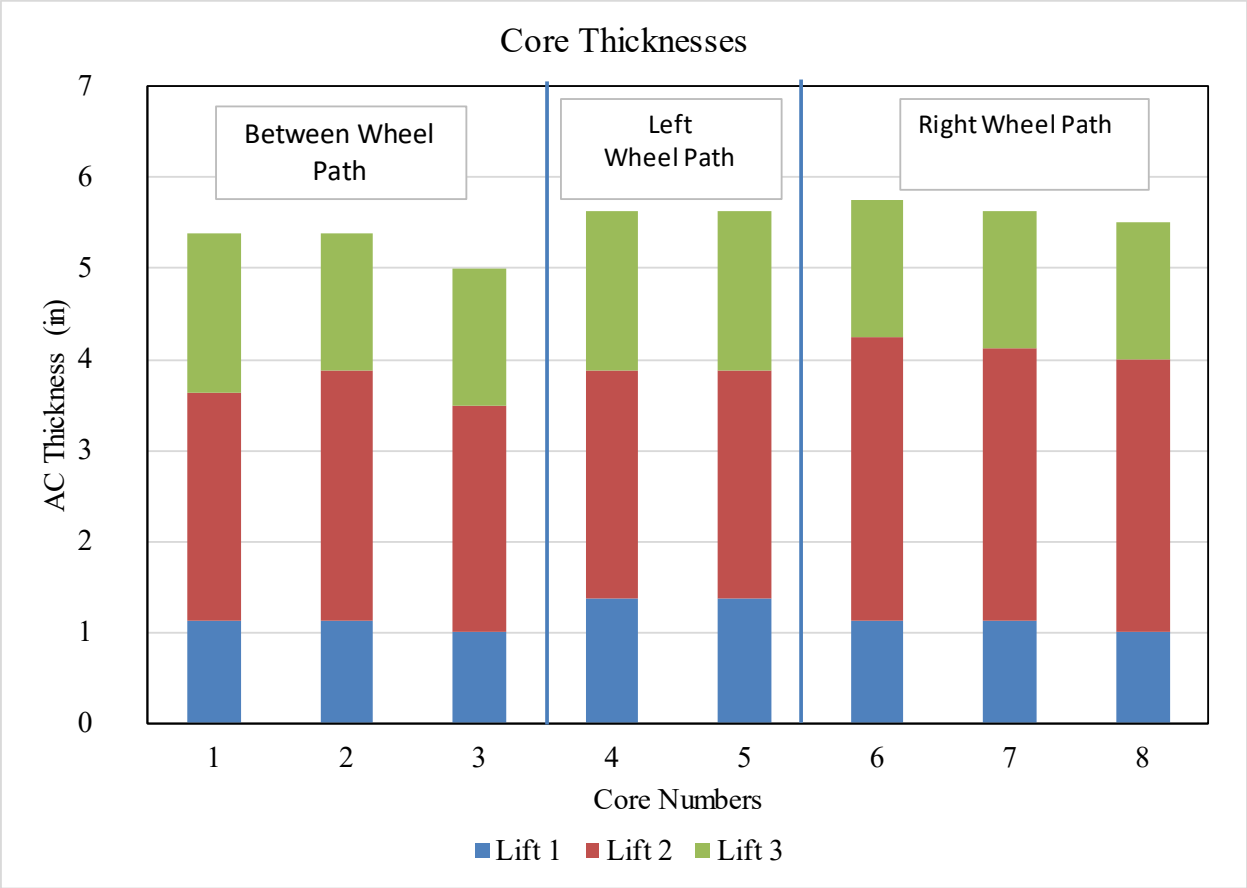

APPENDIX B: DROP LOCATIONS

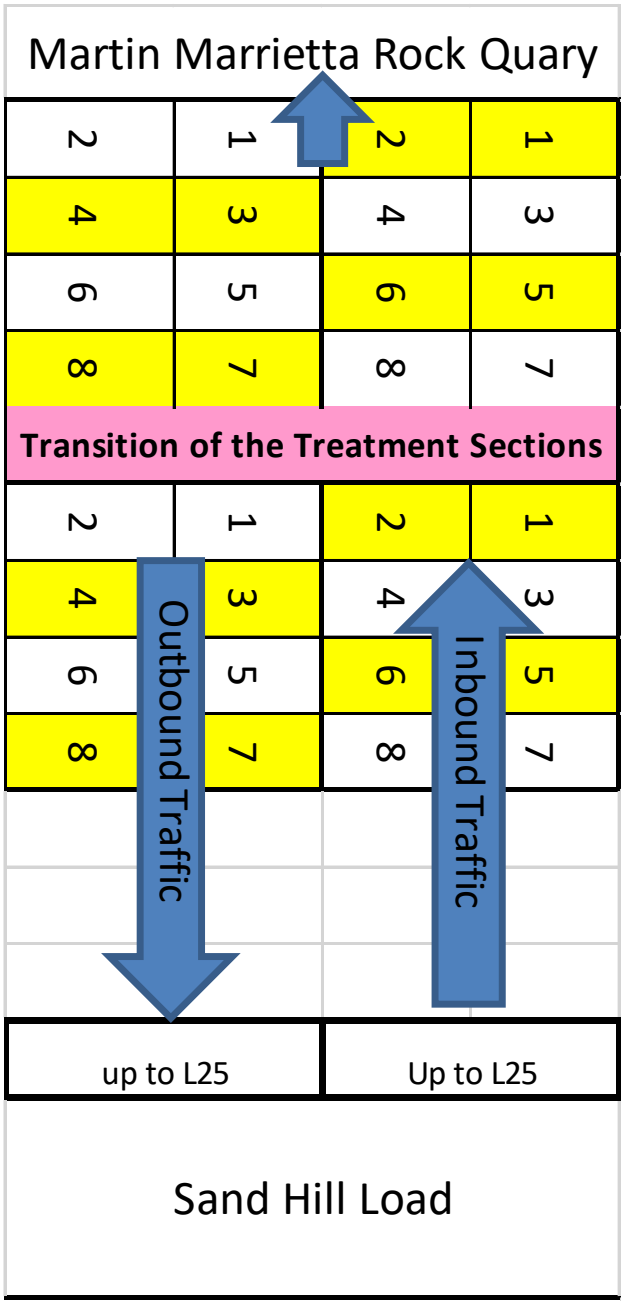

APPENDIX C: DISTRIBUTION TYPES FOR D_0 VALUES

Table C1: Distribution Parameters for the D_0 values

Slab	Treatment	Distribution	A-D	P-value	LRT-P
L10	Cape seal	Weibull	0.424	0.19	0.449
L11	Single layer micro surfacing	Weibull	0.2	0.25	0.449
L12	Single layer micro surfacing w/ CS	Weibull	0.295	0.25	0.556
L13	Double layer micro surfacing	Weibull	0.532	0.207	0.631
L14	FiberMat Cape seal	Weibull	0.481	0.12	0.56
L15	Scrub Cape seal	Weibull	0.788	0.015	0.363
L16	Scrub seal	Weibull	0.441	0.224	0.731
L17	FiberMat chip seal	Weibull	0.139	0.25	0.595
L18	HMA Cape seal	Weibull	1.103	0.01	0.554
L19	Virgin thinlay with PG67-22	Weibull	0.364	0.25	0.749
L2	FiberMat chip seal	Weibull	0.614	0.01	0.003
L20	Virgin thinlay with PG67-22 on Recycled Bases	Weibull	0.312	0.25	0.502
L21	Virgin thinlay with PG76-22	Weibull	0.637	0.144	0.738
L22	Ultra-thin bonded surface course	Weibull	0.256	0.25	0.584
L23	50% RAP thinlay	Weibull	0.554	0.21	0.684
L24	5% RAS Thinlay	Weibull	0.707	0.214	0.146
L25	HiMA Thinlay	Weibull	0.557	0.162	0.151
L3	Control section with low cracking	Logistic	0.181	0.25	0.815
L4	Control section with high cracking	Weibull	0.098	0.048	0.001
L5	Crack sealing only	Weibull	0.142	0.016	0
L6	Single layer chip seal	Normal	0.229	0.803	0.228
L7	Single layer chip seal w/ CS	Weibull	0.45	0.089	0.014
L8	Triple layer chip seal	Weibull	0.194	0.25	0.658
L9	Double layer chip seal	Weibull	0.167	0.25	0.326
L1	Rejuvenating fog seal	Weibull	0.619	0.01	0.003

APPENDIX D: STATISTICAL COMPARISON BEFORE AND AFTER TREATMENT

Table D1: Paired t-test results for the D0 values (pretreatment vs posttreatment)

Pre-treatment vs posttreatment				
Slab ID	**Treatment Name**	**DF**	**t Value**	**Pr > |t|**
L1	Rejuvenating fog seal	7	-7.15	0.0002
L2	FiberMat chip seal	7	-0.62	0.5552
L5	Crack sealing only	7	-0.84	0.429
L6	Single layer chip seal	6	-0.17	0.867
L7	Single layer chip seal w/ CS	7	0.34	0.7404
L8	Triple layer chip seal	6	1.39	0.2137
L9	Double layer chip seal	6	-0.2	0.8516
L10	Cape seal	7	2.79	0.0269
L11	Single layer micro surfacing	7	-0.43	0.6824
L12	Single layer micro surfacing with crack sealing	7	0.37	0.7215
L13	Double layer micro surfacing	6	-2.09	0.0816
L14	FiberMat Cape seal	7	3.17	0.0156
L15	Scrub Cape seal	7	0.28	0.7889
L16	Scrub seal	7	-1.17	0.2786
L18	HMA Cape seal	7	2.73	0.0295
L19	Virgin thinlay with PG67-22	7	2.63	0.0341
L21	Virgin thinlay with PG76-22	7	3.97	0.0054
L22	Ultra-thin bonded surface course	7	1.27	0.244
L4	Control section with high cracking	7	-2.52	0.0397

APPENDIX E: FORECASTED VS MEASURED BDI VALUES

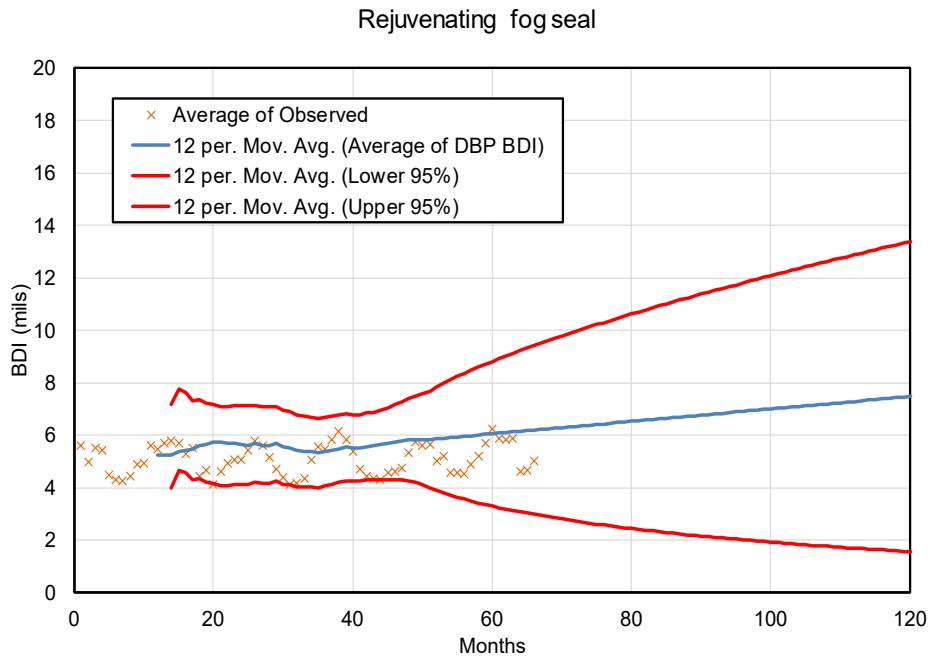

Figure E1: BDI projection model accuracy for Rejuvenating Fog Seal

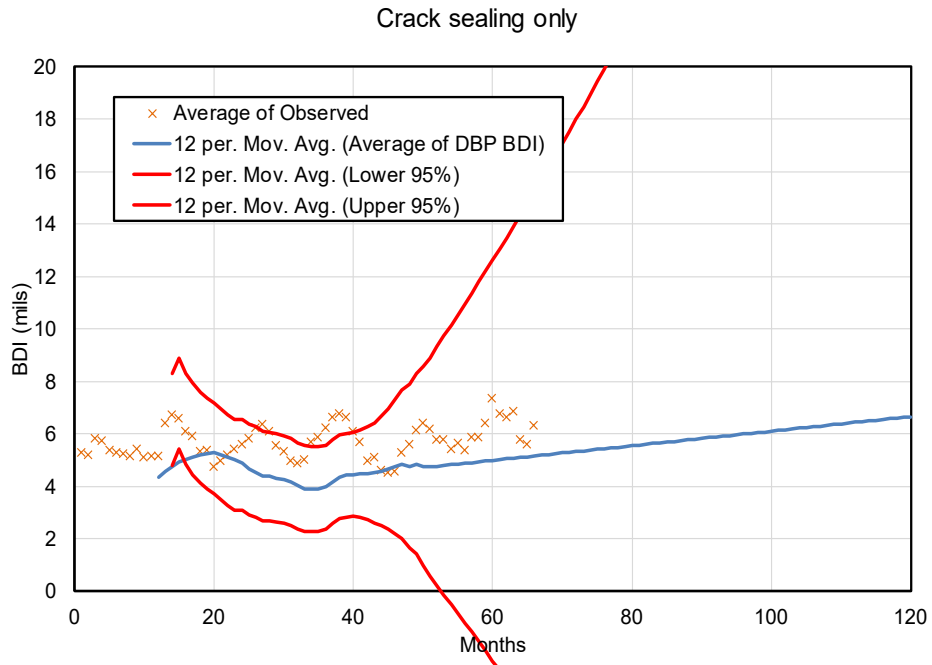

Figure E2: BDI projection model accuracy for Crack Sealing

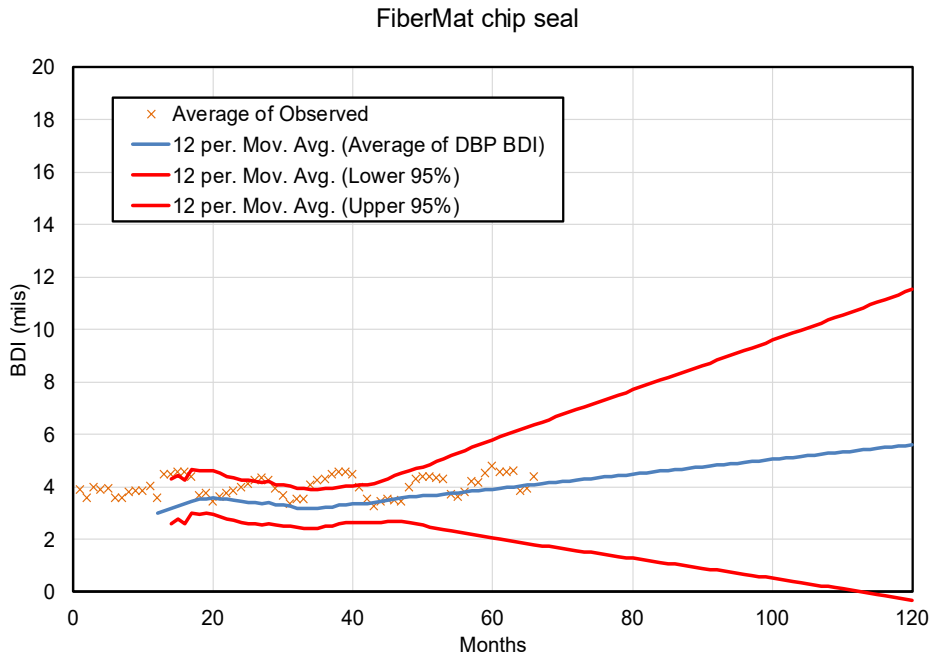

Figure E3: BDI projection model accuracy for FiberMat Chip Seal

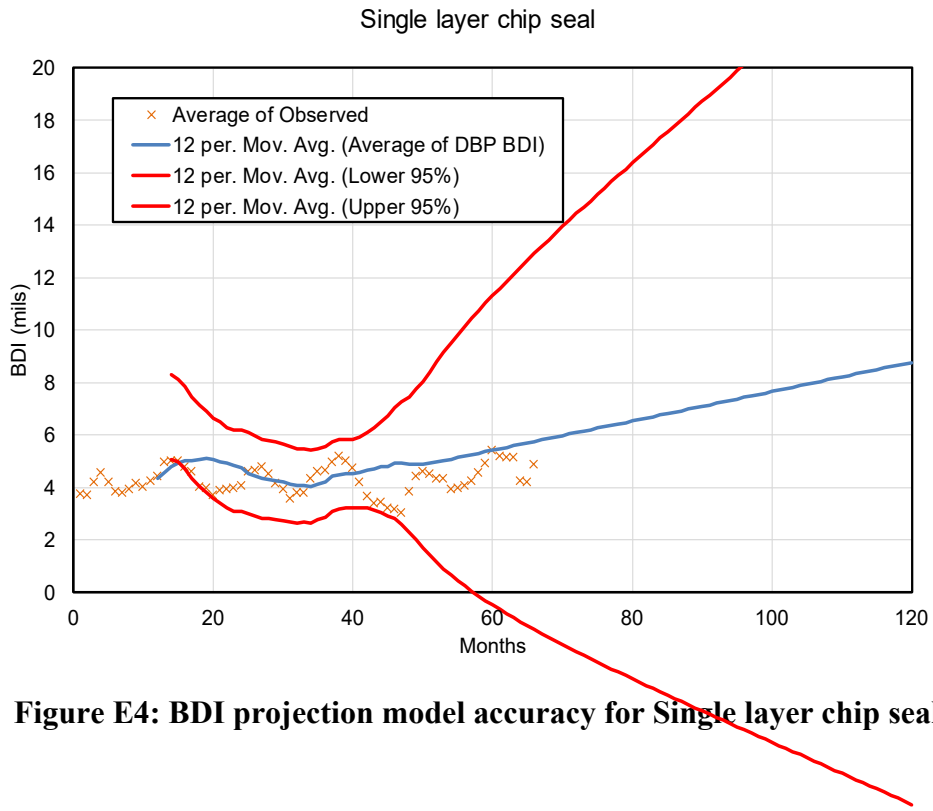

Figure E4: BDI projection model accuracy for Single layer chip seal

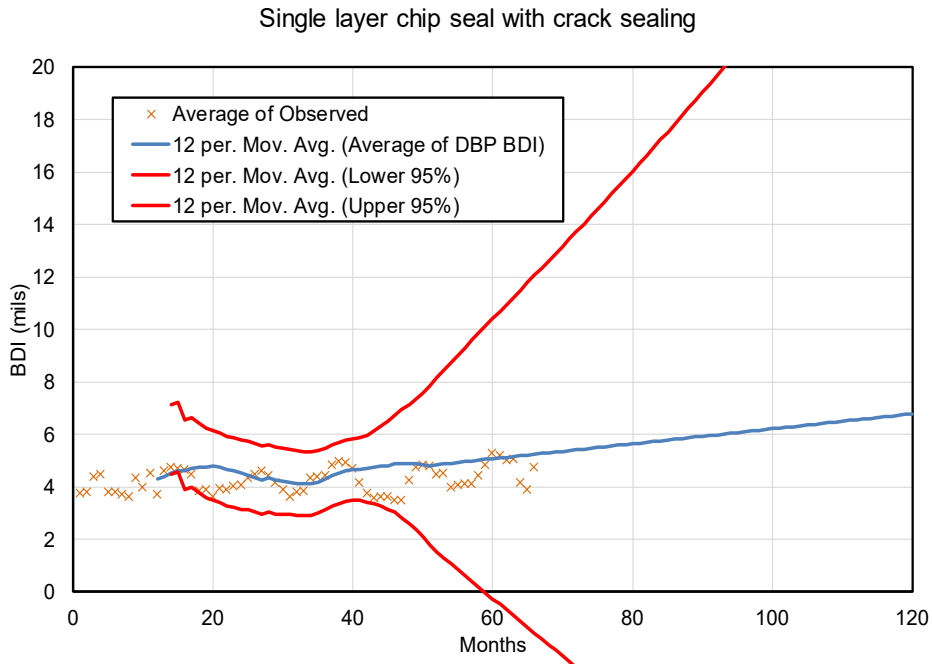

Figure E5: BDI projection model accuracy for single layer chip seal w/ crack seal

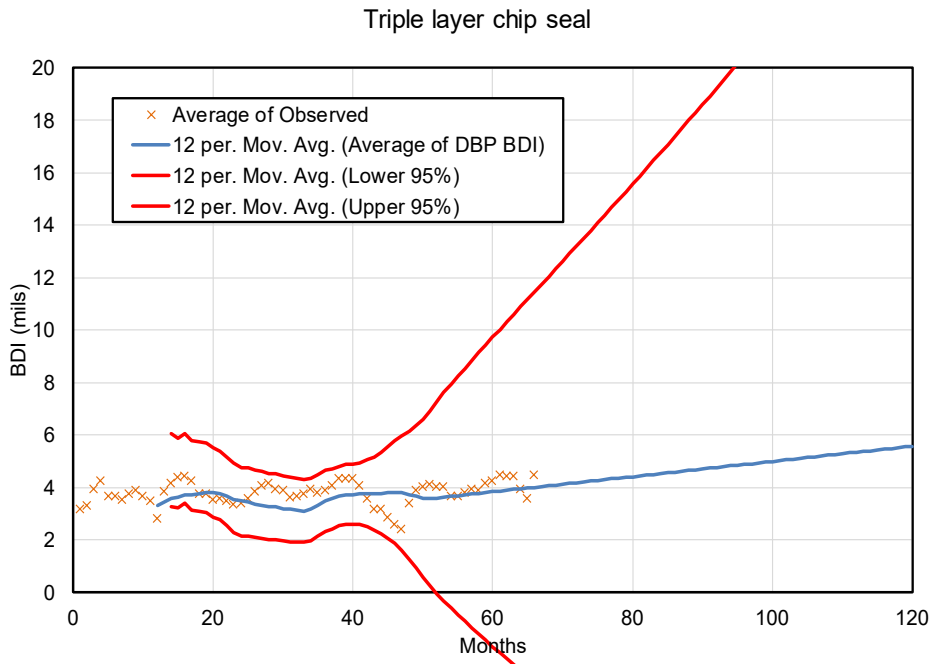

Figure E6: BDI projection model accuracy for triple layer chip seal

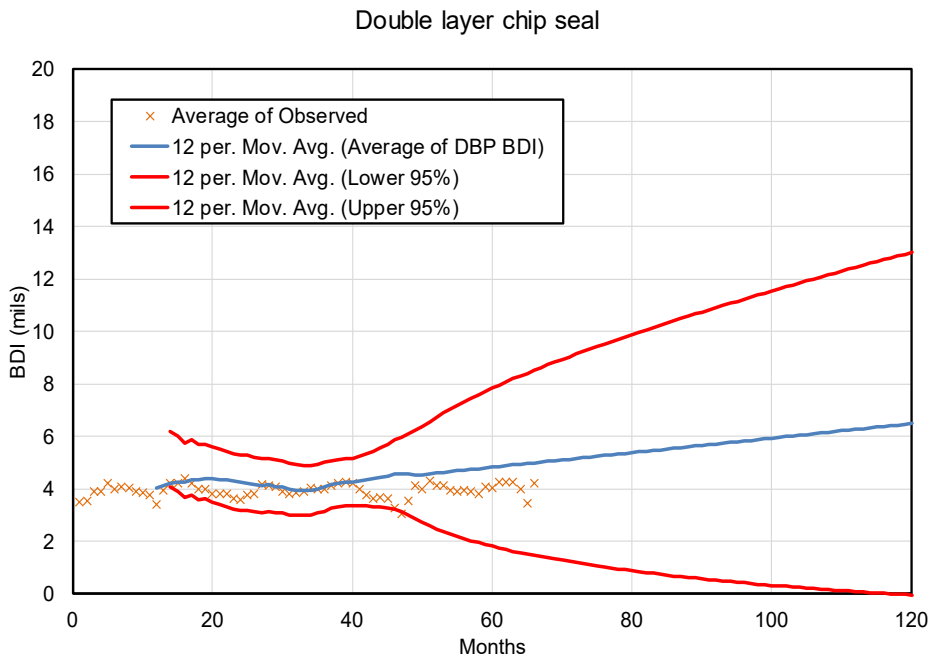

Figure E7: BDI projection model accuracy for double layer chip seal

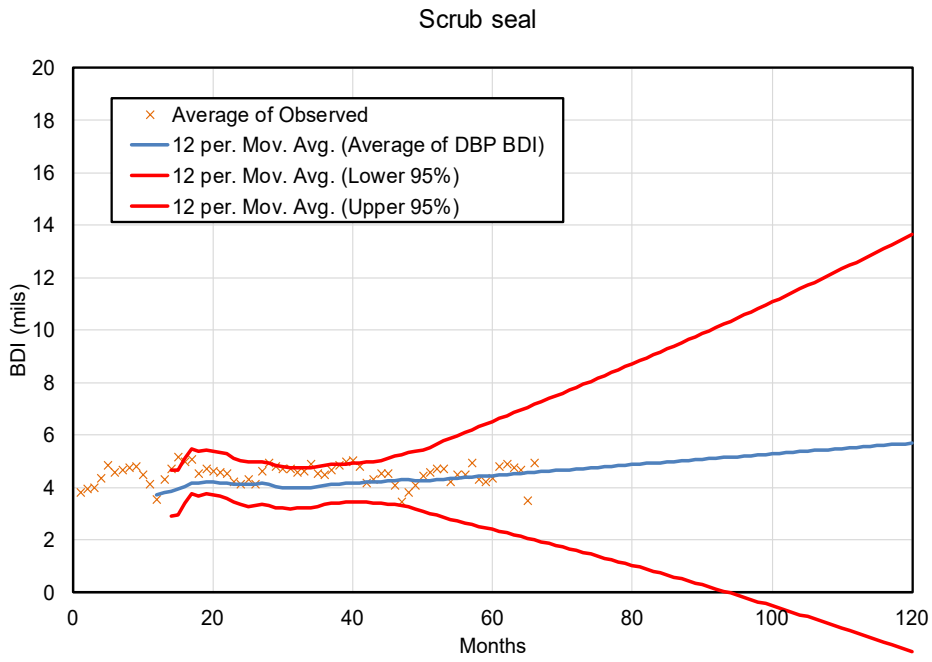

Figure E8: BDI projection model accuracy for scrub seal

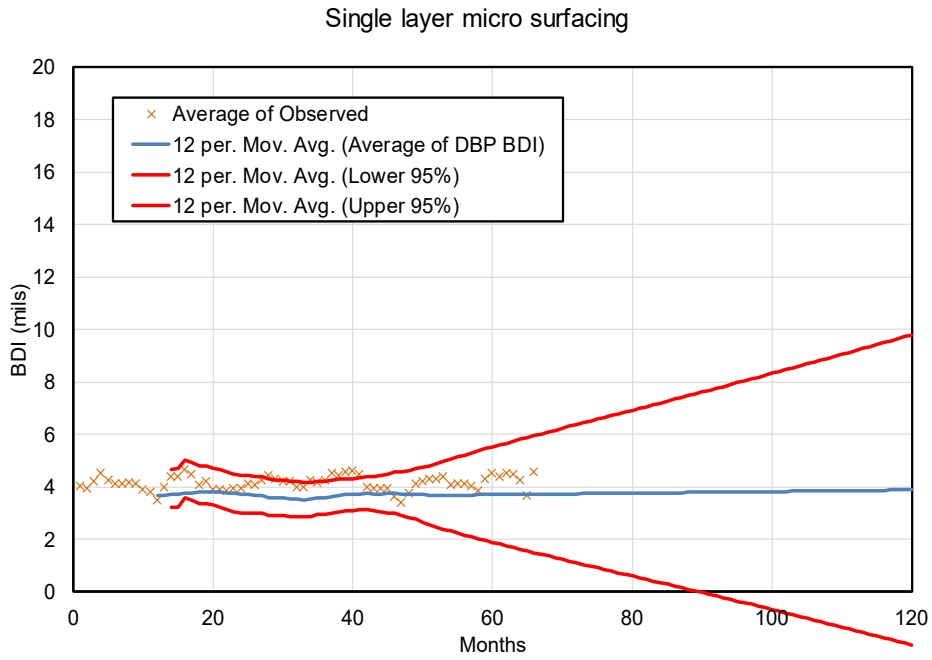

Figure E9: BDI projection model accuracy for single layer micro surfacing

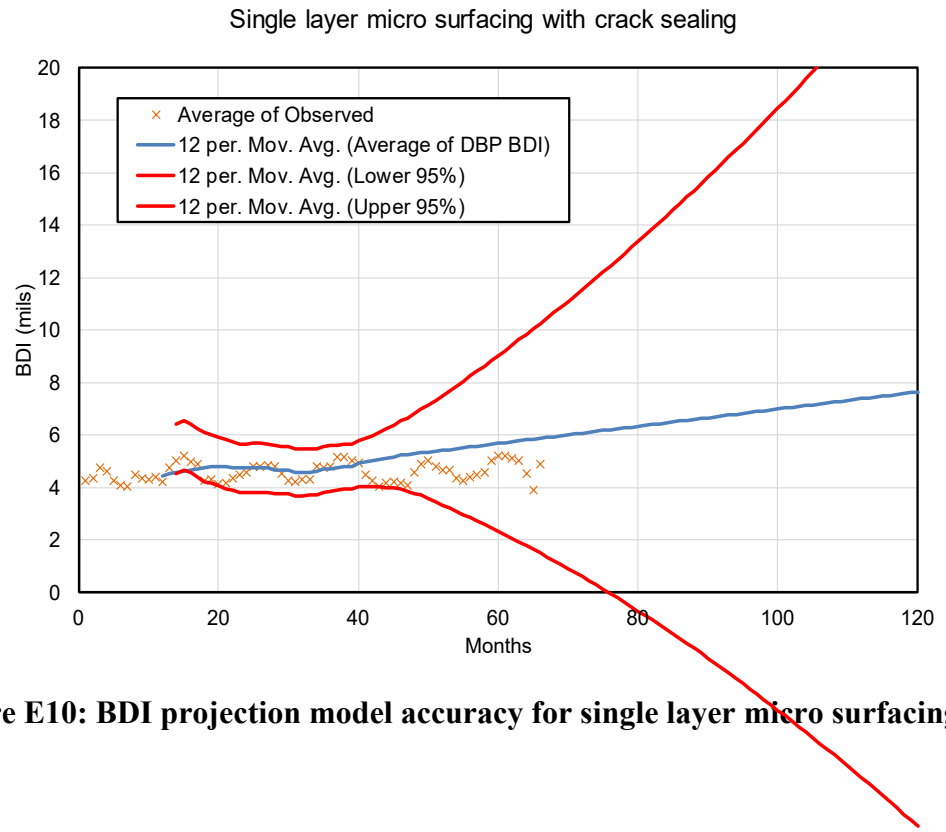

Figure E10: BDI projection model accuracy for single layer micro surfacing w/CS

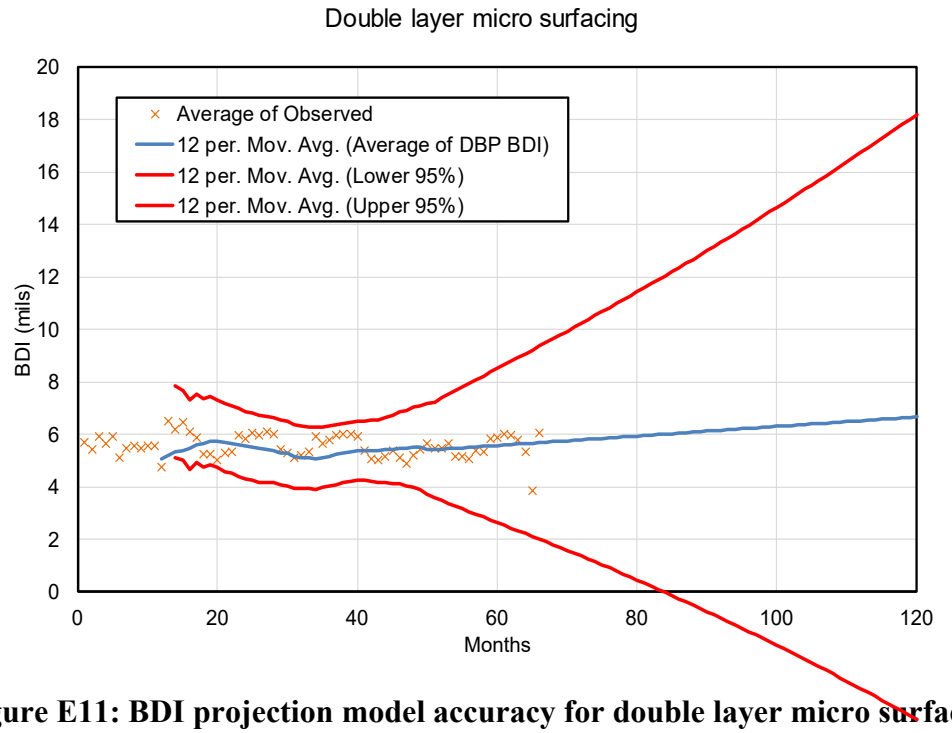

Figure E11: BDI projection model accuracy for double layer micro surfacing

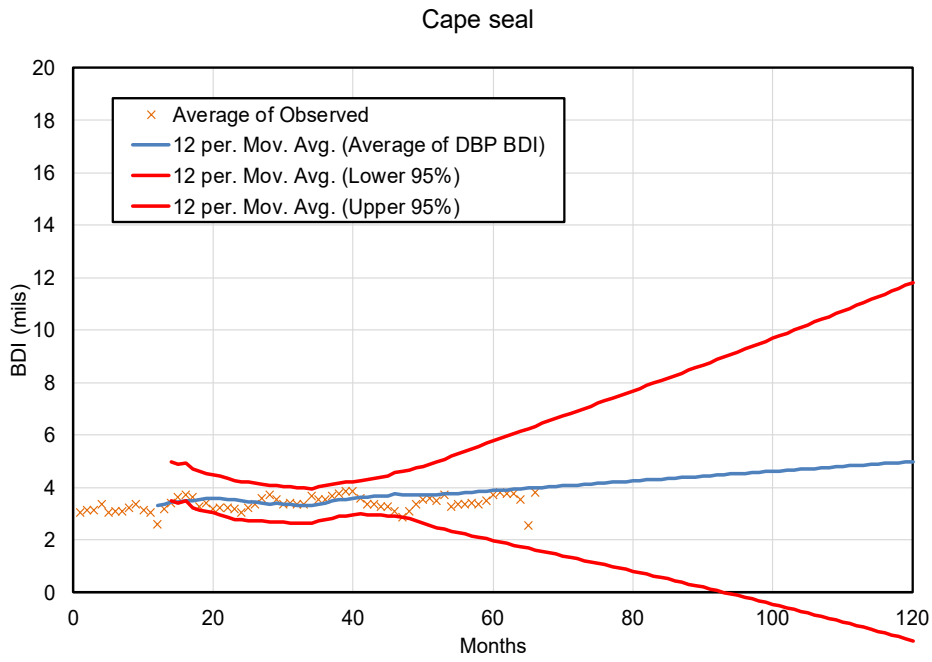

Figure E12: BDI projection model accuracy for cape seal

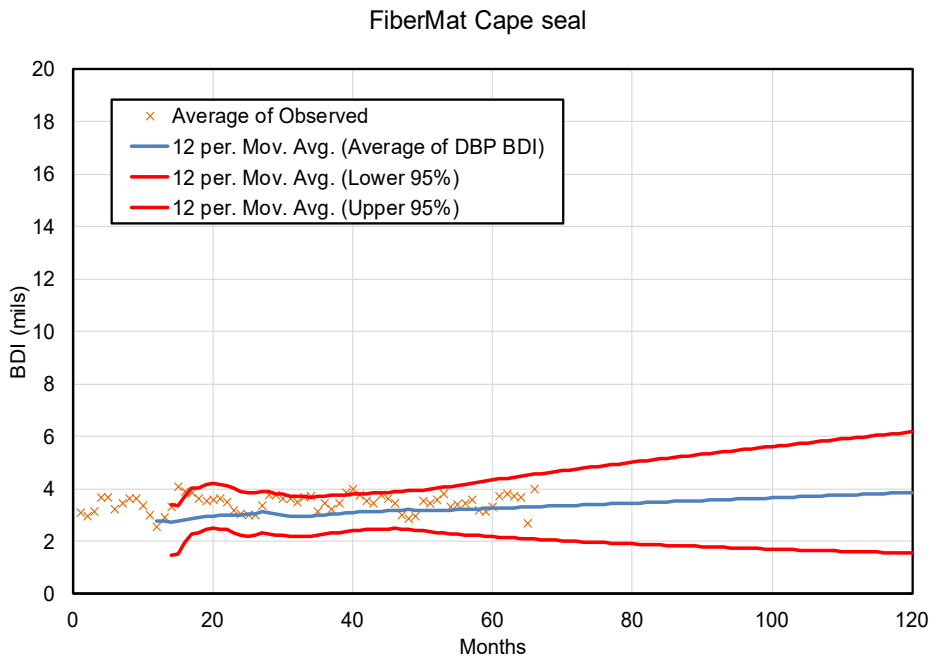

Figure E13: BDI projection model accuracy for FiberMat cape seal

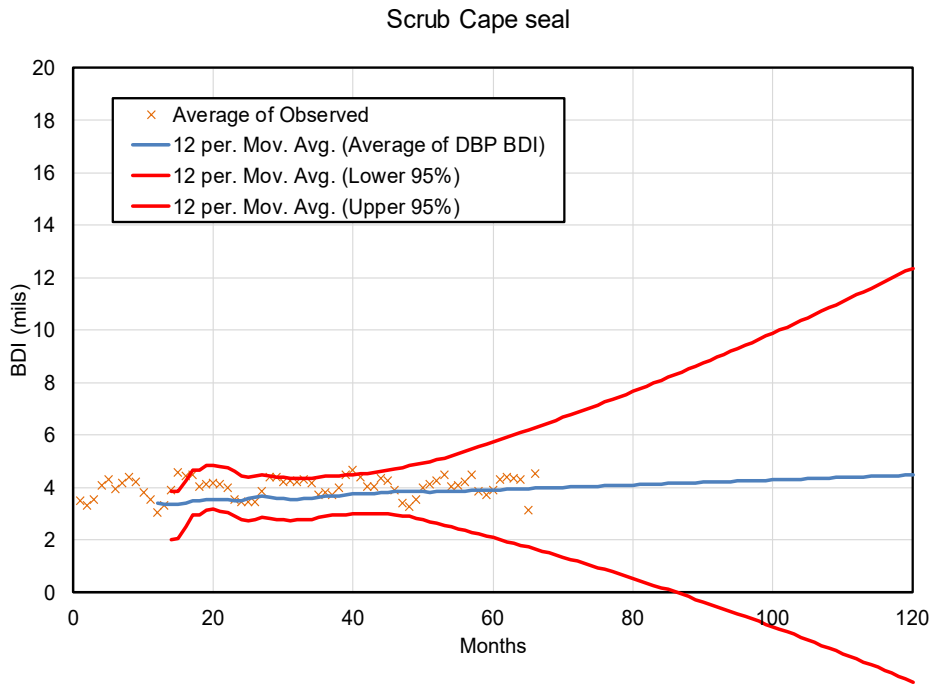

Figure E14: BDI projection model accuracy for scrub cape seal

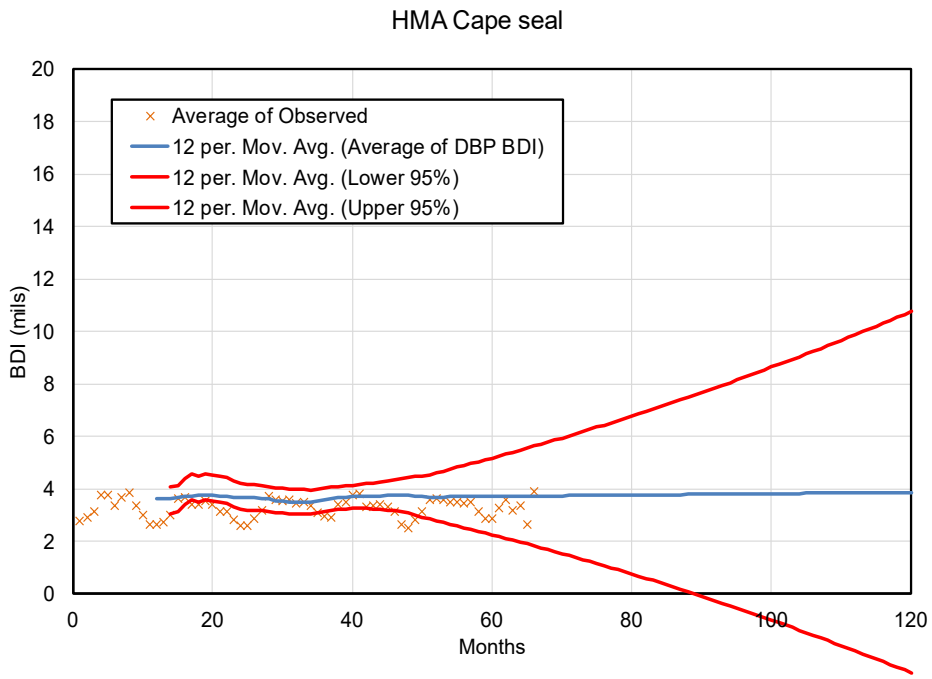

Figure E15: BDI projection model accuracy for thinlay on FiberMat

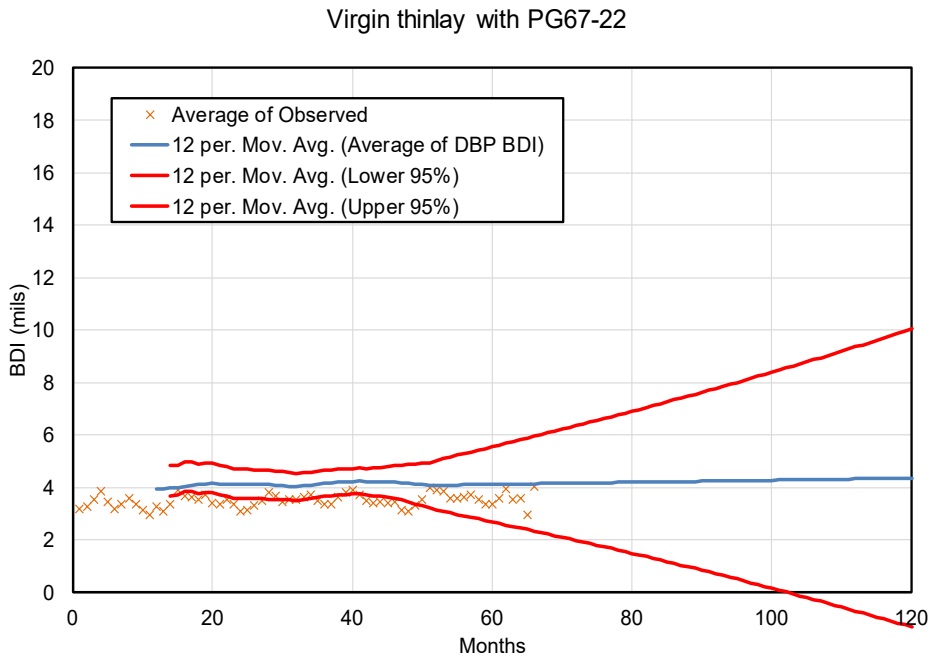

Figure E16: BDI projection model accuracy for thinlays

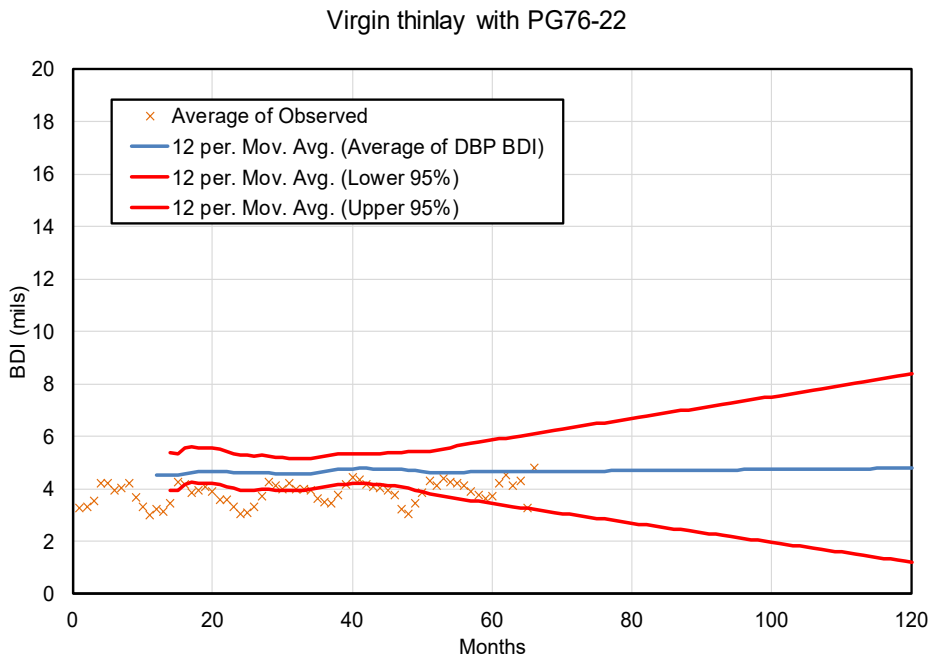

Figure E17: BDI projection model accuracy for polymer thinlay

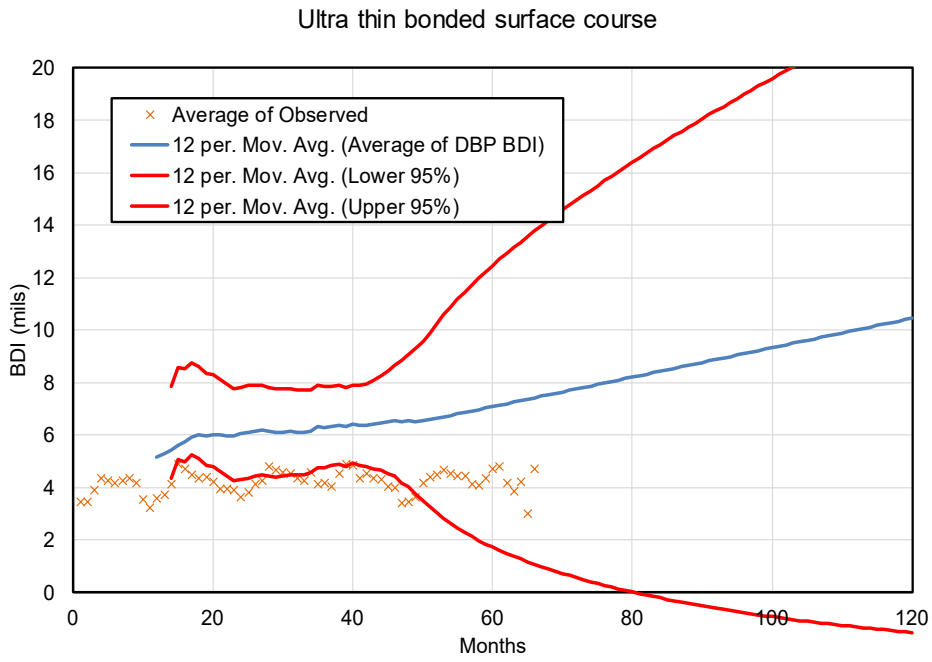

Figure E18: BDI projection model accuracy for ultra thin bonded thinlay